CATALYTIC FLUORINATION OF HALOETHANES

THESIS SUBMITTED TO THE UNIVERSITY OF GLASGOW IN FULFILMENT OF THE REQUIREMENT OF THE DEGREE OF DOCTOR OF PHILOSOPHY

BY

WILLIAM DUNCAN SEMION SCOTT Bsc.

DEPARTMENT OF CHEMISTRY

UNIVERSITY OF GLASGOW

FEBRUARY 1997

ACKNOWLEDGEMENTS.

I would like to thank my supervisors, Professors J. M. Winfield and G. Webb, for their support, encouragement, critical eye and guidance throughout the course of this work. At ICI Klea, the supervision and guidance I received from my industrial supervisors, Drs. D. W. Bonniface, J. D. Scott and M. J. Watson, was of invaluable for a successful research and I formally acknowledge ICI Klea for their generous contribution towards the funding of this project. I would also like to thank Dr. J. R. Fryer for assistance in the transmission electron microscopy study.

Technical assistance at Glasgow provided by Mr. R. R. Spence and Mr. L. McGhee was greatly appreciated, as was the assistance provided by Miss V. Yeats, who performed the transmission electron microscopy. The skills of technical staff from both the Glass Blowing and Mechanical workshops were also very much appreciated. At ICI Runcorn, Mr G. Ramsbottom and colleagues from the Fluorochemicals Laboratory were of enormous help. I would also like to thank the Analytical and Physical Sciences Group at ICI Runcorn who performed XPS, XRD and Micrometrics analysis. Dr. H. M. Banford and Mr. A. Wilson, from the SURRC in East Kilbride, were also of help during the [^{18}F] - fluorine radiotracer studies.

During my time as a postgraduate student at Glasgow I have been fortunate to have had some of the most pleasant colleagues that anyone could wish to work with. I would like to thank all of my friends and colleagues over these last few years from the Fluorine, Inorganic, Catalysis, Electron Microscopy groups, and other areas of the department, by name and deed, but unfortunately I would require another volume, therefore, from economic considerations, I will refrain from doing so. I would, however, like to make special mention of one such friend, Dr. Phil Landon, who has been my colleague on this project and acted as a mentor and as a responsible example on social occasions. He was more successful in the former role.

I would finally like to thank my family for the support I have received during this work. I have very much appreciated the love shown to me by my fiancee, Sonia, during my University career. The encouragement given to me by my parents has been unfailing during the whole of my education and I could not have done this without them. If I become as much a scholar as my father, a Glasgow man also, I will indeed be proud.

SUMMARY

A study has been made of the catalytic halogen exchange reaction to form the commercially important CFC alternative compound, CF_3CH_2F from CF_3CH_2Cl. This reaction is thermodynamically difficult to perform and requires temperatures in the region of 573K. The fluorinating agent is anhydrous HF and the presence of a fluorinated chromia catalyst is essential. The performance of this catalyst can be altered by the presence of zinc(II) chloride as a dopant, before catalyst fluorination. The influence of zinc(II) doping and crystallinity were studied to determine the effect of these parameters on catalytic performance. Catalyst activity testing, characterisation and radiotracer techniques were used to elucidate a catalytic mechanism.

Chromias were prepared by ICI via a controlled precipitation of chromium nitrate in aqueous ammonia, to yield a chromium hydroxide gel. Subsequent calcination of this gel yielded chromia which was then pelleted. This chromia was ground and sieved to the correct particle size. The chromia was then calcined, under an inert atmosphere, using differing parameters to induce varying degrees of α - Chromia phase. The crystallinity was determined by X - ray diffraction, which assessed the amounts of crystalline α - Chromia present. Wet impregnation with predetermined amounts of zinc(II) chloride in aqueous solution and fluorination with anhydrous HF under atmospheric pressure flow conditions at 573K for 17h, provided a working catalyst. Four differing crystallinities of chromia, ranging from amorphous to highly crystalline, were impregnated with differing amounts of zinc(II) and fluorinated. These formed the working catalysts.

Catalysts were tested in microreactor flow systems at atmospheric pressure over a temperature range of 523 - 623K. An anhydrous HF : CF_3CH_2Cl molar ratio of 4 : 1 was used to promote the fluorination reaction as this was thermodynamically unfavourable. Effluent from catalytic reactions was sampled at each reaction temperature and analysed by gas chromatography. This work indicated that chromias with lower crystallinity were superior catalysts in comparison to chromias of higher crystallinity. Small amounts of zinc(II) doping promoted the activity of chromia catalysts in comparison to undoped chromias, having a four fold increase in the percentage of CF_3CH_2F formed during the reaction, in some cases. Larger amounts of zinc(II) doping had an opposite effect on catalyst activity giving an apparent

'poisoning effect'. Using these catalysts the reaction was shown to be 98% selective towards CF_3CH_2F, the only other product of note being CF_2CHCl. From the percentage of CF_3CH_2F in the reaction effluent samples at different temperatures, apparent activation energies were calculated. These calculations revealed that zinc(II) doping lowered the apparent activation energy of chromia catalysts for this reaction in every case.

Selected fluorinated zinc(II) doped and undoped chromias were studied to determine surface species present using transmission electron microscopy and X - ray photoelectron spectroscopy. These studies determined that chromium species on the surface of these catalysts were nether in an unfluorinated of fully fluorinated state. This work indicated that some partially fluorinated state may be present, for example, as a chromium oxo - fluoride phase. Zinc(II) species on the surface of these catalysts were in a heavily fluorinated form and the most likely phase present was ZnF_2.

[^{18}F] - fluoride radiotracer studies have been used to examine the behaviour of fluoride species on these materials under flow conditions. This aspect of the work determined that a percentage of fluoride on the surface of the fluorinated chromia was labile to reaction with HF. A smaller percentage of fluoride on these fluorinated chromias was labile to reaction with both HF and CF_3CH_2Cl. This labile fluoride is believed to be responsible for the halogen exchange process. The amounts of fluoride which are labile are not effected by the amount of zinc(II) doped onto the chromia, but are, however, affected by the crystallinity of the chromia. Chromias of lower crystallinity have larger amounts of labile fluoride than chromias of higher crystallinity. The percentage of fluoride uptake which is labile is lower for lower crystallinity chromias.

[^{36}Cl] - chlorine labelled CF_3CH_2Cl was used to determine the interaction of CF_3CH_2Cl with fluorinated chromia surfaces. It is demonstrated that a large amount of surface [^{36}Cl] - chloride species is [^{36}Cl] - CF_3CH_2Cl, weakly bound to the surface of the fluorinated chromia. The remainder of this surface bound [^{36}Cl] - chlorine species is strongly bound to the surface and cannot be removed by dynamic vacuum. The quantities of both weakly bound and strongly bound [^{36}Cl] - chlorine species are effected by the amount of zinc(II) doping on the chromia and the temperature at which the experiment is performed. Larger amounts of zinc(II) doping and higher

temperatures give rise to larger amounts of both weakly and strongly bound [^{36}Cl] - chloride species.

TABLE OF CONTENTS.

1 INTRODUCTION

1.1 CFCs AND THE ENVIRONMENT

The history of fluorine and its compounds is relatively new in comparison to that of other halogens. Hydrogen fluoride was discovered in 1771 by Scheele and elemental fluorine was first isolated in 1886 by Moissan. Initial research into organofluorine compounds began around 1900 and was pioneered by F. Swarts (1). The American chemist Thomas Midgley (1889 - 1944) pioneered the development of chlorofluorocarbons and this work was further developed by A. L. Henne and E. C. Ladd, who carried out research on organofluorine chemistry in the 1930s performing fluorine for chlorine exchange on haloethanes using antimony trifluoride (2). At the same time General Motors research laboratories developed fluorinated chlorocarbons in a search for a non - toxic, non - flammable alternative refrigerant to the commonly used sulphur dioxide and ammonia (3). These developments led to a new wave in research concerned with the preparation and properties of chlorofluorocarbons (CFCs) and routes to their manufacture involving hydrogen fluoride and the development of new catalysts for fluorination reactions (4, 5).

In addition to their use as refrigerants, CFCs, favoured because of their chemical inertness, were valuable as aerosol propellants, foam blowing agents for plastics production and solvents. Large scale production of CFCs totalled over one million tonnes per annum and involved some of the worlds largest chemicals manufacturing companies such as the American company DuPont (trade name for CFCs - 'Freon') and the British company ICI (trade name for CFCs ' Arcton'). All CFC uses eventually lead to their atmospheric release, even 'hermetically sealed' refrigeration units and closed cell foams finally leak into the atmosphere. In 1973, Lovelock *et al.*, reported the presence of CFCs in the atmosphere in both the north and south Atlantic oceans (6). This report stated that quantities of CFCs present in the atmosphere were equal, within experimental error, to the amounts ever

manufactured and studies have suggested that 5/6 of CFCs released each year stay in the atmosphere. One year later, in 1974, Molina and Rowland reported a route to stratospheric ozone destruction by chlorine radicals derived from CFCs (7). Due to the inert nature of CFCs to reaction with most chemicals, it was predicted that these compounds would have a lifetime in the order of 40 - 150 years. This would allow CFCs to reach high concentrations in the stratosphere which could lead to the photodissociation of the C - Cl bond by ultraviolet light producing a chlorine radical (EQN. 1.1)

$$\text{initiation } CFCl_3 \xrightarrow{h\nu} CFCl_2^{*} + Cl^{*} \quad \text{EQN. 1.1}$$

The chlorine radical produced by this process could act as a catalyst for the destruction of stratospheric ozone (EQN. 1.2, 1.3)

$$Cl^{*} + O_3 \longrightarrow ClO + O_2 \quad \text{EQN. 1.2}$$

propagation

$$ClO + O \longrightarrow Cl + O_2 \quad \text{EQN. 1.3}$$

The chlorine radical chain reaction can involve the destruction of thousands of molecules of ozone before the chlorine radical joins with another radical and terminates the chain reaction. The main 'sink' for chlorine radicals is HCl which can be transported across the troposphere before being 'rained out'. This catalytic chain reaction is very efficient and was reported to be almost six times faster than the NO - NO_2 chain reaction which is believed to contribute to the destruction of ozone (8).

Ozone (O_3) exists in the stratosphere as a result of earth's atmosphere growing rich in oxygen through the advent of green plants (9). Ozone is a high energy form of oxygen formed by ultraviolet light photons which encounter O_2 in the stratosphere (EQN.s 1.4, 1.5)

$$O_2 \xrightarrow{h\nu} 2O^{*} \qquad \text{EQN 1.4}$$

$$O^{*} + O_2 \longrightarrow O_3 \qquad \text{EQN 1.5}$$

The ozone layer acts as a solar filter, screening out ultra violet rays which are, if particularly strong, harmful to life. It is a thermodynamically unstable compound, however in spite of this, its decomposition is slow and can only be accelerated by the catalytic action of chemicals which react with oxygen atoms. Since the mid 1950s ozone levels have been monitored above the Antarctic. One feature of these levels are the large seasonal fluctuations observed every year . However, since the mid - 1970s the reduction in ozone levels monitored by the British Antarctic Survey has been too great to be accounted for by seasonal fluctuation and this discrepancy could be explained by the catalytic destruction of ozone leading to the creation of a 'hole' in the ozone layer above the Antarctic.

Four years following Molina and Rowland's report, the United States Government banned the use of CFCs as propellants in aerosol cans. However, it was not until 1987 that the Montreal Protocol gave a commitment from governments around the world to cut back the production of CFCs to 50 % of the 1986 levels by 1999. This agreement was further strengthened by the London amendment in 1990, which agreed a complete phase out of CFCs by 2000 and the Copenhagen agreement which brought this deadline forward to 1996 (with a ten year grace period for developing countries).

This ban on ozone depleting substances requires their replacement by non - chlorine or bromine containing substances as alternatives and better conservation practices. A search for suitable alternatives was undertaken with unprecedented speed. Ideal replacements from an industrial view point would be 'drop in' replacements where little alteration to existing production methods or practical applications was necessary, so CFC alternatives require properties which are close

to those of the CFCs they replaced. The most feasible alternatives are hydrofluorocarbons (HFCs) and hydrochlorofluorocarbons (HCFCs), although the latter do contain chlorine.

CFCs, HCFCs and HFCs are coded for simplicity by the American Society of Heating, Refrigeration and Air Conditioning, Standard for Refrigerants (ASHRAE) Code (this code was last updated in 1978). The numerical nomenclature employed is from left to right, first digit = no. of C atoms minus 1 (not included for C_1 compounds where it = 0), second digit = no. of H atoms plus 1 and the third digit = no. of F atoms. Isomer rules; most symmetrical has no suffix, increasing asymmetry denoted by alphabetical suffixes a, b, c etc. (1). The alphabetical part of the nomenclature is based upon the mass difference between the sum of the substituents on each carbon. A new code has been devised by A. A. Woolf relating to HFCs. This code relies upon the number of fluorine atoms attached to each carbon and the number of hydrogens follow the requirement for saturation (10). However, the majority of workers in the halocarbons field continue to use the ASHRAE code which will be employed through out this text when required.

Trichlorofluoromethane (CFC 11) and dichlorodifluoromethane (CFC 12), the two CFC compounds, which accounted for the largest tonnages in production, have been replaced by 1,1 - dichloro - 2 - fluoroethane (HCFC 141b) and 1,1,1,2 - tetrafluoroethane (HFC 134a). For example, Table 1.1 compares physical properties of CF_2Cl_2 with its alternative replacement CF_3CH_2F (11, 12).

Table 1.1 Comparison of the Physical Properties of CF_2Cl_2 and CF_3CH_2F

	CF_2Cl_2	CF_3CH_2F
Molecular Weight (g)	120.93	102.03
Boiling Point (K)	243.2	246.078
Freezing Point (K)	115	165
Ozone Depletion Potential (arbratory units relative to CF_2Cl_2)	1.0	0.0
Atmospheric Lifetime (yr.)	116	15.6

The similarity in physical properties between CF_2Cl_2 and CF_3CH_2F make CF_3CH_2F an excellent replacement for CF_2Cl_2 as it is non - toxic, non - flammable and can be used as a refrigerant and foam blowing agent. The shorter atmospheric lifetime of CF_3CH_2F (15.6 years cf. 116 years for CF_2Cl_2) is a result of the carbon hydrogen bonds which will lead to its atmospheric breakdown prior to reaching the stratosphere by the reaction of the C-H bond with OH*. One disadvantage of the breakdown of CF_3CH_2F, which is common to CFCs also, is the production of CO_2 which acts as a greenhouse gas and contributes to global warming. A concept known as Total Equivalent Warming Impact (TEWI) was developed jointly by The Alternative Fluorocarbons Environmental Acceptability Study and the United States Department of Energy. TEWI is the sum of the emissions of refrigerant gases and total energy required to run equipment converted into equivalent amounts of CO_2. Thus the TEWI of a refrigerant can provide a measure of the effect of that compound towards global warming in comparison with other such compounds. On applying this concept to CF_3CH_2F, CF_3CH_2F has 1/3 TEWI of CF_2Cl_2 and a lower TEWI than hydrocarbon refrigerant alternatives such as propane. Thus the only foreseeable problem which HFCs may have is their contribution to global warming if amounts of HFCs released into the atmosphere become large.

1.2 CATALYSIS IN FLUORINE CHEMISTRY

Catalytic routes towards fluorine containing halocarbons and hydrohalocarbons have centred on two main pathways, fluorination catalysis and hydrogenation catalysis. Catalytic fluorination has been the more extensively studied of these two routes and it can be divided into two main areas, heterogeneous and homogeneous catalytic fluorination. Some early work to synthesise CFCs was by heterogeneous catalysis using chromium and aluminium containing compounds acting as catalysts and hydrogen fluoride gas acting as the fluorinating agent. The main route towards these compounds was homogeneous catalysis based on antimony pentachloride catalysts, with liquid hydrogen fluoride as the fluorination agent. Both the homogeneous and heterogeneous routes have hazards associated as the use of hydrogen fluoride has obvious associated problems of corrosion and toxicity.

The adsorption behaviour of HF has been studied in few systems although a two site model for HF adsorbed on CrF_3 has been reported (13). Little information also exists regarding the adsorption of fluoroorganics on heterogeneous catalysts. What information is available suggests that fluorochloromethanes adsorb weakly on aluminium(III), chromium(III) and iron(II) and (III) fluorides (14), on UO_2 (15) and on alumina (16). Infra red studies on lanthanide halides have shown that fluorocompounds, adsorbed on these halides, have very similar infrared spectra to their gas infrared spectra. The three routes to fluoroorganics are discussed below.

(i) HOMOGENEOUS CATALYTIC FLUORINATION

The preparation of fluorinated organic halogen compounds was pioneered by Swarts using antimony fluorides. These were not, however, true catalytic reactions, as SbF_3, the most commonly used of the antimony fluorides, was required in excess and could only be recovered after reaction by regeneration using hydrogen fluoride. Henne *et al.* used SbF_3 when fluorinating organic halogen compounds in

the 1930s (2). Antimony trifluoride is not a very efficient fluorinating agent on its own and its activity was increased by transforming the antimony from the trivalent state to a pentavalent state by addition of chlorine, bromine or $SbCl_5$. More recently, SbF_3 / Cl_2 was used to fluorinate pentachlorotrifluoropropane to yield tetrachlorotetrafluoropropane and trichloropentafluoropropane (17).

A more common antimony based fluorination catalyst, which is employed today, is $SbCl_5$. In fluorination reactions employing $SbCl_5$, hydrogen fluoride supplies the fluorine species and the antimony halide acts as a carrier for the fluoride. Thus $SbCl_5$ can be used in catalytic amounts during such reactions. Antimony pentachloride is a volatile compound which renders it unsuitable as a catalyst on its own. However, when impregnated onto activated charcoal, forming a supported heterogeneous catalyst, $SbCl_5$ can be used up to 473K.

Antimony pentachloride is believed to catalyse reactions by exchange of one or more of its chlorine atoms with a fluorine atom from HF. The lost chlorine becomes HCl, the catalyst being an antimony mixed halide. Chlorine on the organic halogen compound is exchanged with fluorine from the antimony mixed halide and the exchanged chlorine regenerates the $SbCl_5$, making this a true catalytic process. A mechanism for the fluorine for chlorine exchange was originally proposed by Kolditz *et al.* (18). This mechanism suggests that the reaction proceeds by the formation of fluorine bridges between the antimony mixed halide and the organic halogen compound. The formation of different antimony halide complexes in the system can influence and occasionally inhibit the exchange. This mechanism contradicts one suggested by Booth *et al.* (19) postulated during the 1930s which suggested that the chlorine atoms of the organic halogen compound could co-ordinate themselves to the antimony atom forming a reaction intermediate.

Santacesaria *et al.*(20) postulated that $SbCl_4F$ was the main fluorinating agent when HF and $SbCl_5$ were used in a ratio of 1:1. These workers made a kinetic study of this system for the fluorination of $CHCl_3$. Their studies determined that the fluorine for chlorine exchange between $SbCl_4F$ and $CHCl_3$ proceeded stepwise to

CHF_3, the relative rates of exchange reaction being 7:1:0.03 for each fluorination of $CHCl_3$ respectively. In contrast, the fluorine / chlorine exchange rate between HF and $SbCl_5$ relative to exchange on $CHCl_3$ was 150:1.

Blanchard *et al.*(21, 22, 23), studied the $SbCl_5$ / HF system extensively and discovered that the type of antimony mixed halide obtained was dependant on the reaction temperature. Antimony mixed halides were titrated with potassium permanganate to discover what type of mixed halide was formed at differing temperatures. When mixing $SbCl_5$ and HF at 333K it was found that $SbClF_4.4HF$ was the mixed halide formed. This proved to be an active fluorination agent for CCl_3CH_3 at this temperature. When $SbCl_5$ and HF were mixed at 233K the major mixed halide formed was $SbCl_5.4HF$. This proved to be the active species at 233K, however, when $SbClF_4.4HF$ was used to fluorinate CCl_3CH_3 at 233K no reaction occurred. Blanchard postulates that the fluorinating species in this reaction appears to be polymeric hydrogen fluoride bonded to antimony and that the fluorine atom taking part in halogen exchange is the terminal atom of an HF oligomer.

Another homogeneous fluorination catalyst, which was less frequently used, was BF_3. Henne and Arnold (5) report the use of BF_3 to catalyse fluorination across the double bond of halogenated olefins. The fluorination of halogenated olefins by HF was improved by addition of BF_3 to the reaction. This proved particularly advantageous when hydrofluorinating heavily halogenated olefins or olefins bearing a CF_3 group and difference in the ease of hydrofluorination was noted. The authors explain the action of BF_3 as the formation of a co-ordinated complex between HF and BF_3 enhancing the ionic character of the H - F bond which facilitates the separation of H as a proton.

A small number of major companies have examined methods of fluorinating haloethanes using processes involving non Al or Cr based catalysts. ICI (24) have patented the fluorination of alkyl halides containing at least one halogen other than F using transition metal fluorides. For example, CH_2Cl_2 was fluorinated by F_2 in the presence of UF_6 at 195 - 293K and $CHCl_2F$ was obtained. The reaction was 99.9 %

selective. Atochem (25) patented the synthesis of CCl_2FCF_3 using $SbCl_5$. Antimony pentachloride was mixed with HF to produce an antimony chloride fluoride catalyst *in situ* and the reactants used were CCl_3CF_3 or a mixture of CCl_3CF_3 / CCl_2FCClF_2. Atochem have also patented a non - catalytic process for the fluorination of chloroethanes using HF (26). The reactants used were CH_3CCl_3 and HF and the reaction was performed in the liquid phase. Products, such as CH_3CCl_2F and CH_3CClF_2 which were present in the vapour phase were removed and the reactants were constantly fed into the system. None of these processes are likely to be commercially viable in today's organofluorochemicals industry, as they have problems of product separability, energy costs and catalyst cost.

(ii) HETEROGENEOUS FLUORINATION CATALYSTS

Reactions to fluorinate organic halogen compounds have been studied using a number of heterogeneous catalytic systems (27, 28, 29). The most popular of these involve the use of aluminium - based catalysts and chromium - based catalysts. Many of the reaction systems studied have been explained mechanistically by three main routes :- fluorination (EQN. 1.6), isomerisation (EQN. 1.7) and dismutation (EQN. 1.8)

Fluorination $C_2Cl_2F_4 + HF \text{ -----> } C_2ClF_5 + HCl$ EQN. 1.6

Isomerisation $CClF_2CClF_2 \text{ -----> } CCl_2FCF_3$ EQN 1.7

Dismutation $2C_2Cl_2F_4 \text{ -----> } C_2Cl_3F_3 + C_2ClF_5$ EQN 1.8

Exchange of chlorine for fluorine was explained by a mechanism in which dissociation of a CFC molecule into a chloride ion and a carbocation occurred. This ionic dissociation was believed to occur on active catalytic acid sites which could

bond the chloride ion to the active site whilst halogen transfer occurred. Radiotracer techniques provided information to indicate that this was not the case and so a halogen exchange model was developed.

Halogen exchange involves the transfer of halogen from the catalyst surface to the reactant molecule. Early ideas of halogen exchange involved a concerted dismutation process in which halogen was transferred between molecules as opposed to between molecules and the surface. Labelling of catalyst surfaces with [^{18}F] - fluorine radiotracers has proved that the exchange occurs between the surface and the molecule by the incorporation of the [^{18}F] - fluorine label into the product. [^{36}Cl] - chlorine labelled organic halogen compounds proved that this exchange was a true surface - organic mechanism by labelling of catalyst surfaces with [^{36}Cl] - chlorine (30). Some of the chlorine species deposited on the catalyst surface remained as inactive material, however, the majority of [^{36}Cl] - chlorine species could be removed from the surface by exchange with fluoride from HF. This proved that Cl could partake in halogen exchange as a surface species and that the active site on the catalyst for exchange with fluorine was probably also the active site for exchange of chlorine. Thus catalytically active chlorine used in chlorine - for - fluorine exchange originates from a fluorine - for - chlorine exchange (FIG. 1.1)

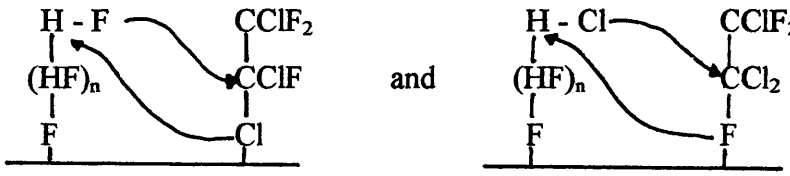

FIG. 1.1 Mechanistic Model for Fluorination and Chlorination Reactions

Work with radiotracers has supported the idea that isomerisation reactions are intramolecular by retaining [^{36}Cl] - chlorine labels in the isomers of the reactant molecule. However, recent ideas have suggested that an ionic dissociation may well occur on the surface such that the adsorbed fluorine species is not equivalent to any other species (FIG. 1.2).

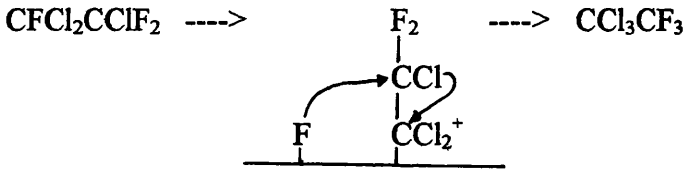

FIG. 1.2 Mechanistic Model for Isomerisation Reaction

Much work has been performed on alumina based systems. Kemnitz and co-workers have studied the reactions of C_1 organic halogen compounds over alumina catalysts (31). They used a γ - alumina catalyst which was activated by $CHClF_2$ flow producing a catalyst containing 13 w/w % fluorine and less than 0.05 w/w % chlorine. From the reaction of $CHClF_2$ on this activated alumina catalyst two products are obtained, CHF_3 and $CHClF_2$ in a ratio of 2:1. From this work two mechanistic proposals are suggested involving dismutation reaction mechanisms. The first proposal assumes that the adsorption / desorption equilibrium $CHCl_2F_{(ads)}$ $\Leftrightarrow$ CHCl2F is disturbed and slow when compared to dismutations (EQN. 1.9, 1.10).

$$CHClF_{2\,(ads)} + CHClF_{2\,(ads)} \text{-----} > CHCl_2F_{(ads)} + CHF_{3(ads)} \qquad \text{EQN. 1.9}$$

$$CHCl_2F_{(ads)} + CHClF_{2(ads)} \text{-----} > CHCl_{3\,(ads)} + CHF_{3\,(ads)} \qquad \text{EQN. 1.10}$$

In this case a certain amount of adsorbed species directly forms $CHCl_3$ instead of being desorbed. The second proposal assumes the opposite, i.e. adsorption / desorption equilibrium $CHCl_2F \Leftrightarrow CHCl_2F$ is established, not disturbed and is fast when compared to dismutation (EQN. 1.11)

$$3CHClF_{2\,(ads)} \text{-----} > CHCl_{3\,(ads)} + 2CHF_{3\,(ads)} \qquad \text{EQN. 1.11}$$

In both cases the fully chlorinated and fully fluorinated products desorb into the gas phase. However, in a further investigation of C_1 organic halogenated compounds (

32, 33) both dismutation and halogen exchange reactions are suggested. In other work performed by these same workers involving halogen exchange in C_1 and C_2 organic halogenated compounds, it was suggested that dismutation is an unimportant process with halogen exchange dominant. Thus, there is no generally accepted mechanism for these seemingly similar catalytic halogenation reactions.

Other well characterised catalyst systems involve the use of chromium compounds. The most popular of these are chromia catalysts in conjunction with hydrogen fluoride as a fluorination agent. The majority of chromia systems involve treatment of the catalyst with fluorinating agents such as HF, SF_4, BF_3 or a fluoroorganic prior to use of the chromia to catalyse fluorination reactions (29, 34, 35, 36). Such catalysts are very effective in the production of fluoroorganic compounds and can be found in many industrial systems. Often chromia catalysts are doped with other transition metals or transition metal halides in relatively small quantities in order to produce enhanced activity and selectivity. For example Kim *et al.* (37) employed a doped chromia catalyst in the vapour phase fluorination of CF_3CH_2Cl with hydrogen fluoride to produce CF_3CH_2F. Their work attempted to reduce the relatively quick deactivation of chromia due to the formation of large quantities of CF_2CHCl. By the addition of small quantities of MgF_2 and CrF_3 to the chromia, increases in activity, selectivity and lifetime were noted.

A small number of chromia - alumina mixed metal oxides have been used as catalysts for the fluorination of organic halogen compounds. The selective transformation of CCl_2F_2 to $CClF_3$ (38) was achieved via the dismutation of CCl_2F_2 over a chromia - alumina catalyst in the absence of HF. In this case it appears that partial fluorination of the catalyst occurs using the organic halogen compound as a fluorination agent. This reaction leaves large quantities of carbonaceous residues on the catalyst surface, which lead to deactivation over a short period of time. The extent of recent patent literature available demonstrates the importance of heterogeneous catalysts for the fluorination of organic halogen compounds. Alumina, AlF_3 or fluorinated alumina doped with transition metal

compounds such as Ti, V or Pb are catalysts used to provide an efficient process for the production of fluorinated halogenated hydrocarbons with HF (39) and $AlCl_xF_y$ (x = 0 - 1; y = 3 - 2)is used to fluorinate $CHClCCl_2$ with HF in the preparation of CF_3CH_2Cl (40).

Many major companies in the organic halogen compound manufacturing industry have shown an interest in Al based catalysts for fluorination. ICI have patented processes for manufacturing halogen exchange catalysts for the production of halohydrocarbons by reacting calcined γ - alumina with a halogenating agent such as SF_4, SOF_4, COF_2, COCl2 or CCl_4 to produce a halogenated γ - alumina which is subsequently reacted with a gaseous olefin or halohydrocarbon to deposit a halohydrocarbonaceous layer on the surface of the halogenated γ - alumina (41). Zn promoted alumina has been patented in both a halogenated or partially halogenated form as a fluorination catalyst by ICI for the production of fluorinated halogenated hydrocarbons (42).

Other heterogeneous fluorination catalysts studied include silica fluorinated by fluoroorganics such as CF_4 by cleavage of weaker C - F bonds (43) and cobalt trifluoride which was used in the monofluorination of $CH_3CF_2CH_3$ with HF (44). Patent literature relating to organic halogen compounds has been available for many years and early literature centred on catalysts containing CrF_3 and AlF_3. For example Benning and Park (45) patented a process for the manufacture of CFCs using CrF_3 impregnated on activated carbon. By mixing CH_4, Cl_2 and HF in a 40:60:30 ratio at 613K the major product was CCl_2F_2. At 548 - 573K 31 % of the product ratio was CCl_2F_2. DuPont also showed interest in this catalyst (46) for the manufacture of chlorofluoroethanes by mixing CCl_2CCl_2, Cl_2 and HF in a 1:1.2:4.3 ratio at 673K producing tri and tetrafluoroethane CFC compounds. AlF_3 was another compound used extensively in CFC production. It was generally prepared by fluorination with HF of a halogenated aluminium compound other than AlF_3 and could be used to catalyse reactions to produce CFCs in the presence of chlorinated halocarbons and HF (47). Often AlF_3 was doped with other transition metal

compounds such as $CrCl_3.6H_2O$ or $NiCl_2.6H_2O$ followed by fluorination with HF to produce a working catalyst for CFC production (48). Fluorinated alumina was used as a catalyst in reactions to produce CCl_3F and CCl_2F_2 when doped with 10 % ThF_4 and reacted with Cl_2, HF and CH_4 at 743K (49).

(iii) HYDROGENATION CATALYSTS

An alternative route to producing HFCs is the use of hydrogenation catalysts. Much activity in this area has centred on hydrogenolysis of C - Cl bonds over a Pd / charcoal catalyst. This presents problems of a lack of selectivity with the formation of unwanted isomers and catalyst deactivation by CFCs. Palladium mixed metal systems have been employed (50) such as PdK, PdFe, PdCo and PdAg supported on graphite with H_2 as the hydrogenation agent. However, unhydrogenated products can be produced as a side reaction emphasising difficulties in selectivity. Other systems previously studied include Pd supported on TiO_2 in the presence of hydrogen to convert CCl_2FCClF_2 to $C_2H_2F_3$ (51). Palladium supported on graphite and Al, Ti, and Zr oxides and fluorides was used to hydrogenate CF_2Cl_2 at 433 and 523K. The result, in most cases was low conversion to products which were 95 % CH_2F_2 and CH_4. Oxides used in the reaction were partially fluorinated by HF, released as a product from the reaction, thus the Lewis acidity of acid sites on the oxide surface was increased. It was suggested by infrared CO adsorption studies on catalyst surfaces that this increase in Lewis acidity influenced the electron availability of Pd at the catalyst surface. This in turn influenced the bond strength of CF_2 species which was believed responsible for product selectivity. Hydrogenation has been less favoured than fluorination as a method of manufacture due to difficulties in selectivity and subsequent product separation and therefore fewer examples of methods which use hydrogenation catalysis exist in the patent literature.

Platinum supported on activated charcoal has been patented for use as a hydrogenation catalyst for the production of fluorinated saturated hydrocarbons by

hydrogenating fluorinated unsaturated hydrocarbons (52). Other supports for Pt include alumina and zirconia as catalysts in the preparation of $CHCl_2CF_3$ by hydrogenation at 393K (53). Palladium supported on silica was used to hydrogenate halogenated hydrocarbons containing at least one chlorine and one fluorine atom. This catalyst was prepared by wet impregnation of $PdCl_2$ on silica followed by calcination and hydrogenation of the catalyst precursor (54). The other commonly used patented noble metal is ruthenium which was used as a hydrogenation catalyst when supported on activated carbon, alumina and zirconia for the preparation of HFCs (55) and HCFCs (56). Mixed Pd / Cu on activated carbon was a catalyst in the gas phase hydrogenation of $CHCl_2CCl_2F$ to form $CHClCF_2$ (57) and hydrogenation of HCFCs with H_2 to form HFCs by 2 % Pd on activated carbon, $CHClFCF_3$ reacted with H_2 in the presence of a Pd / Cu catalyst to produce CH_2FCF_3 (58).

Few industrial manufacturers have chosen to patent the hydrogenation route to produce HFCs and HCFCs. ICI, who use a fluorination route to produce HFC compounds have patented the hydrogenation of $XYCF_2$ (where X,Y = H, Cl or Br with at least one being Cl or Br) with hydrogen to form CH_2F_2 at 490K in the presence of a 10 % Pd catalyst supported on activated carbon (59). DuPont have perhaps examined hydrogenation catalysts for HFC manufacture more than most other companies, however they did not chose to patent any of these processes.

1.3 USE OF CHROMIA IN CATALYTIC HALOGENATION

1.3.1 CHROMIA AS A CATALYST

The catalytic properties of chromia merit considerable attention and more is known about chromia catalysts than any other metal oxide catalysts with the exception of group VIII metal oxides, silica and alumina. Catalytic properties of chromia were noted as far back as the mid 1800s when Wöhler (60) noted that at high temperatures, chromia catalysed the reaction $2SO_2 + O_2 \text{ -----> } 2SO_3$.

Preparation of chromia catalysts is normally by the slow hydrolysis of $[Cr(NO_3)_3].9H_2O$ (61) or by pyrolysis of $(NH_4)_2Cr_2O_7$ (62). Hydrolysis of $[Cr(NO_3)_3].9H_2O$ by addition of aqueous ammonia creates an hydrous chromia gel which can be calcined in an inert atmosphere to remove partially water and hydroxyl groups forming chromia. Chromia can exist in ether the crystalline or amorphous state, although X - ray diffraction studies have determined that most 'crystalline chromias' contain some amorphous phase. Crystalline or α - chromia has the corundum structure in which oxide ions are hexagonally close packed and chromium ions fill two thirds of the octahedral interstitial sites. α - Chromia has the idealised formula Cr_2O_3 with all Cr ions in the 3+ oxidation state. In contrast, there is evidence for amorphous chromia having chromium existing in the +4, +5 and +6 oxidation states as well as in the +3 oxidation state.

X - ray photoelectron studies have indicated the presence of large amounts of Cr(III), Cr(V) and Cr(VI) on the surface of alumina supported chromia catalysts in the proportions 35, 45 and 20 % respectively. On reduction under hydrogen the proportion of Cr(V) decreased and the proportion of Cr(III) increased. Crystallisation of chromia reduces the proportion of Cr(VI) evident on the surface. Further studies of chromium surface states on chromia catalysts (63) reveal that the conductivity of chromia is the result of a Cr(III) / Cr(IV) band which allows electrons to move through the lattice.

Infrared studies (64) indicate that uncalcined, newly prepared chromia contains large quantities of water and hydroxyl groups. Activation of such chromia involves a dehydration of the surface resulting in coordinativly unsaturated Cr(III) ions which are thought to be adsorption centres. α - Chromia also contains large amounts of hydroxyl groups prior to activation and coordinatively unsaturated Cr(III) is also observed.

To preserve electrical neutrality, water, adsorbing on coordinatively unsaturated chromium ions on the surface of chromia, would lose a proton which moves from the adsorbed water molecule to an adjacent oxide ion thus forming a

close packed layer of $[OH]^-$ ions on the surface of chromia. Fig. 1.3 shows an α - chromia surface in which the outer layer of OH^- ions has been left incomplete. To return to coordinatively unsaturated Cr^{3+} ions on the surface two hydroxyl ions can condense as described by Eqn. 1.12.

$$2OH^- = O^{2-} + H_2O \qquad \text{Eqn. 1.12}$$

From this a defect is generated, represented in Fig. 1.4 . In forming this defect two five co-ordinate surface Cr^{3+} ions and one two co-ordinate O^{2-} ion are formed (against four - co-ordinate O^{2-} ions in the bulk).

The possibility of active sites forming on chromia by reduction of Cr^{3+} to Cr^{2+} has been discussed by a number of workers in this field (65, 66, 67, 68). For α - chromia this is a difficult process to achieve other than at high temperatures. However, as amorphous chromia has a higher free energy than α - Chromia, this reduction reaction may be more facile. Experimentally, chromia, supported on alumina or silica, can be reduced to CrO by reducing agents such as hydrogen or carbon monoxide gas at 773K, however the reduction of Cr(III) to Cr(II) in bulk α - chromia will be an unfavourable process as it would change the coordination environment of this chromia thus requiring higher temperatures. As the coordination environment of amorphous chromia is unknown, but is believed to be irregular throughout the structure, this process is likely to be more favourable than it is in α - chromia.

Surface studies of chromia catalysts for the isomerisation of *n*-but-1-ene to *cis*-but-2-ene and *trans*-but-2-ene yield information regarding possible active sites on chromia. It was suggested that different active sites were present on chromias which had undergone differing pretreatments. The reaction of *n*-but-1-ene on chromias, subjected to a relatively low temperature pretreatment, is via a carbonium ion type mechanism and the site believed responsible for this was associated with surface hydroxyl groups. The active site associated with chromia which underwent

FIGURE 1.3

α - Chromia Surface. Thick Circles Are in an Unfinished Upper Layer.

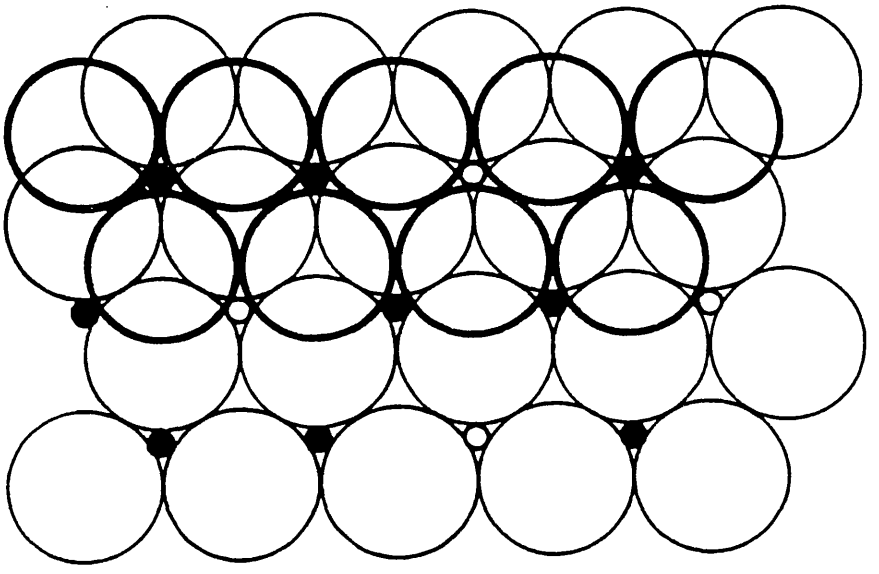

FIGURE 1.4

Defect in α - Chromia. Double Circles Are Sufrace Hydroxyl Ions. Thin Circles Are Oxide Ions in the Bulk Except For One at the Defect.

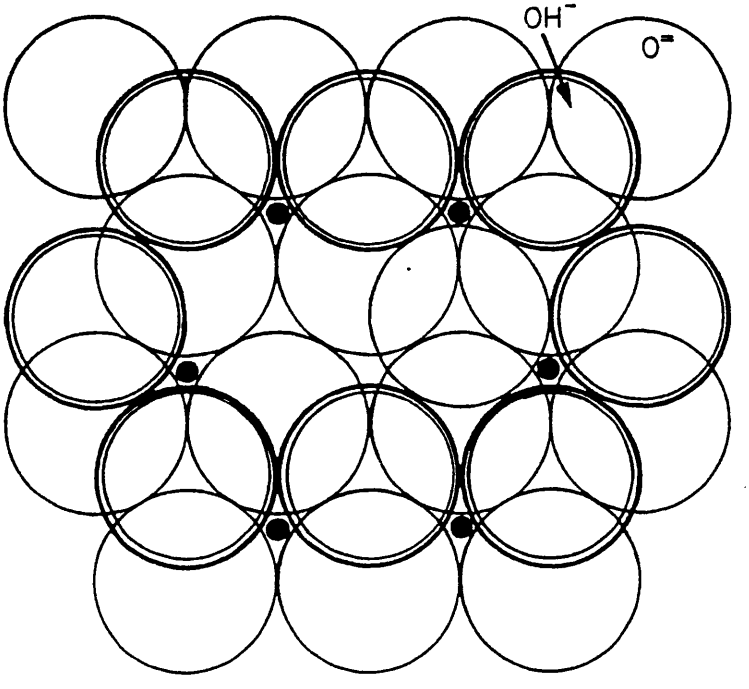

higher temperature pretreatment was a strained surface site created by the removal of water from two adjacent hydroxyl groups. Sites of this type cause the reaction to proceed via an allylic type intermediate (69). These findings were supported by deuterium isotope labelling studies performed on the C_3H_8 / C_3D_8 exchange on chromia which indicates a π - allyl mechanism for this reaction. Other catalytic mechanisms studied on both amorphous and crystalline forms of chromia were isomerisation of cyclopropane and hydrogenolysis of cyclopropane. Isomerisation of cyclopropane proceeded on both catalysts and was insensitive to surface structure. Hydrogenolysis also occurred on both catalysts. However crystalline chromias showed an improvement for this reaction (70).

Chromia has been used for a number of years as a heterogeneous halogen exchange catalyst in conjunction with HF. EPR studies from the early 1980s (63) suggest that catalytic activity of chromia in halogen exchanged is strongly linked to different oxidation states on the surface. Chromium(IV) and Cr(VI) are said to heavily influence the catalytic activity of Cr(III). More recently Blanchard *et al* (71) found that the catalytic activity of chromias for halogenation were directly proportional to the number of chromium atoms which were capable of being reversibly oxidised. The results of TPR and TPO studies between 293 and 653K when compared with catalytic activity, showed that the more sites capable of reversible oxidation on a chromia surface, the higher the catalytic activity.

1.3.2 CHROMIA AS A HALOGENATION CATALYST.

Chromia has long shown its worth as a heterogeneous catalyst for the fluorination of CFCs. Gaseous fluorination of CF_3CCl_2F to CF_3CClF_2 was performed over a chromia catalyst in the presence of HF and gave a yield of over 90 % CF_3CClF_2. However the catalytic fluorination activity of the chromia was adversely affected by the presence of traces of water (72). Recently chromia was used to catalyse the fluorination of CF_3CH_2Cl to CF_3CH_2F, an important CFC alternative. The chromia used was formed from the thermal decomposition of

(NH_4)$_2$ Cr_2O_7 and calcined at 673K before pretreatment with CH_2ClCCl_2F prior to reaction. XPS studies determined that this pretreatment partially fluorinated the chromia and surface area measurements indicated a small reduction in surface area between the calcined and pretreated chromias. CF_3CH_2Cl and HF were reacted in the presence of pretreated chromia to form CF_3CH_2F (34).

Labelling studies have often been employed to determine the mechanism of reaction such as those described above. Deuterium isotope labelling (36) was employed, using DF as the fluorinating agent to determine the mechanism for the fluorinated chromia catalysed reaction of CCl_2CCl_2 to form CF_3CH_2F. These small quantities of deuteriated products in the reaction effluent determined that a halogen exchange mechanism was occurring on the surface of the fluorinated chromia and that a hydrofluorination / dehydrochlorination mechanism was a side reaction. Other radiotracers used to study this system are [^{18}F] - fluorine and [^{36}Cl] - chlorine employed extensively in mechanistic studies by Webb, Winfield *et al* (73). A [^{18}F] - fluorine radiotracer study of the fluorination of CCl_2FCClF_2 or $C_2Cl_2F_4$ isomers by HF over a labelled chromia catalyst determined that fluoride incorporated into the reaction products came from the fluorinated surface of the chromia. [^{36}Cl] - chlorine labelled organic halogen compounds were fluorinated in another study using fluorinated chromia and HF. The label was retained on the surface of the chromia and exchange reactions on this labelled chromia determined that up to 85 % of the chlorine took part in further exchange. Studies (74) on pelleted chromia catalysts indicated that surface fluoride species were heavily involved in the fluorination of organic halogen compounds. Pretreatment of chromias with [^{18}F] - HF led to the incorporation of [^{18}F] - fluoride species into the reaction products of the interaction of $C_2Cl_2F_4$ or isomers of CCl_2FCClF_2 over pretreated chromia at 623K. Reactions were described as a series of F for Cl and Cl for F exchanges from the distribution of [^{18}F] - fluoride in the products.

Chromias have often been used mixed with trace amounts of other transition metals and transition metal fluorides to catalyse fluorination reactions. Catalyst

doping to produce bimetallic systems is well documented and can demonstrate considerable enhancement of activity and selectivity in comparison to monometalic systems. Nickel doped fluorinated chromias have been used to catalyse CFC production from chlorocarbons by reaction with HF. This system was examined by EPR and the results of the investigation indicate that different oxidation states of Ni and Cr lead to an electron exchange phenominum giving rise to a more effective catalyst for halogen exchange (75).

MgF_2 and CrF_3, present in small amounts on an unfluorinated chromia catalyst, have improved the activity, selectivity and catalyst lifetime of the vapour phase reaction of HF and CF_3CH_2Cl to produce CF_3CH_2F. Evidence from the reaction effluent indicates that these dopants limit a competing olefination reaction to form CF_2CHCl the presence of which can lead to the deactivation of the chromia surface (37). Blanchard *et al* (76) have compared chromia impregnated on activated charcoal with chromia impregnated on alumina for the transformation of CCl_2FCClF_2 on these catalysts. Their findings show that the C / Cr_2O_3 catalyst system gives a rapid dismutation reaction to $C_2Cl_4F_2$ and $C_2Cl_2F_4$ but a slow isomerisation to CCl_3CF_3. The Al_2O_3 / Cr_2O_3 system is more active than the C / Cr_2O_3 system however isomerisation is the more prominent reaction. Acid centres played a major role in both reaction pathways as poisoning experiments demonstrated.

Chromia fluorination catalysts have been patented by a number of companies during the last 6 years. Zn /chromia extensively fluorinated with HF at 573K for 24 h was used as a halogen exchange catalyst to prepare CH_2F_2 from CH_2Cl_2 at 523K (77). This catalyst was also used in the preparation of fluoroaromatic compounds such as fluorobenzene which is a useful agrochemicals intermediate compound (78) and undoped fluorinated chromia has been patented as a general fluorination catalyst for hydrochlorofluorocarbon compounds (79).

DuPont have patented HF fluorinated chromia as a catalyst in the gas phase fluorination of HCFCs with HF to produce C_2HF_5 (80) and as a general

hydrofluorination catalyst when the chromia is prepared by the pyrolosis of $(NH_4)_2Cr_2O_7$ and mixed with chromium acetate and 1 - 5 % graphite prior to pelleting (81). Atochem have patents for the fluorination of unsaturated alaphatic halogenated hydrocarbons with HF in the presence of chromia doped with an 'active' metal or metal oxide which is found to improve the catalyst lifetime (82).

1.4 HALOGENATION OF CHROMIA CATALYSTS FOR HALOGEN EXCHANGE REACTIONS

Halogenation of metal oxides has been studied extenisvely for many years and well documented examples can be found in the literature. Halogenation is an important pre - reaction conditioning process as it can increase the acidity of the surface acid sites and provide labile fluoride species for halogen exchange. Halogenation can also limit the extent of some unwanted competing reactions in halohydrocarbon manufacturing processes. The interaction of CCl_2F_2 with a TiO_2 catalyst (83) over a temperature range of 473 - 673K resulted in a considerable reduction in surface area (75 % reduction) over the first four days of reaction. Most of this surface area reduction occurred within the first 1.0 - 1.5 h of reaction and a considerable increase in the activity of the TiO_2 catalyst for the decomposition of CCl_2F_2 was noted during this period. The increase in activity was attributed to an increase in surface acidity as a result of the fluorination of TiO_2 by CCl_2F_2. The vapour phase fluorination of a silica surface was performed using chlorofluoromethanes and CF_4 as fluorinating agents (43). Fluorinations were performed at around 773K and the surface was examined using X - ray photoelectron spectroscopy both before and after fluorination. The most effective fluorination agents were CCl_3F and CF_4. The complete removal of all surface OH groups was achieved and replacement of Si - OH for Si - F occurred in some cases and the surface became more hydro - and lipophobic However the affinity of the surface towards perfluorocompounds increased. Much is known about the fluorination of alumina surfaces as fluorinated alumina is one of the most commonly

used fluorination catalysts for haloalkanes. Kemnitz *et al* (84) compared the adsorption and desorption behaviour of γ - alumina, which had been activated with $CHClF_3$, with the behaviour of non - activated γ - alumina. Fluorination of γ - alumina with $CHClF_2$ results in an increase in the catalytic activity for halogen exchange and the amount and strength of ammonia adsorption. Pyridine adsorption revealed that the sites responsible for catalytic activity are Lewis acid sites of a certain strength on the surface, the strength of which are increased by the fluorination process. Further studies on the nature of active sites on fluorinated γ - alumina were performed using ammonia, pyridine and 2,6 - dimethylpyridine (85). The γ - alumina in this case was fluorinated using aqueous ammonium fluoride solution before drying and calcination. Fluorination was found to affect the strength of Lewis acid sites, however the number of these sites decreased with increased fluorine content. In this study it was noted that the optimum acid strength of the sites was related to the fluorine content of the γ - alumina with 2 - 4 % fluorine content giving maximum acid site strength.

Halogenation of γ - alumina was studied by Webb, Winfield *et al* (86) in an effort to understand the role of these catalysts for the halogenation of organic halogen compounds. [^{36}Cl] - chlorine radiotracer studies were performed using [^{36}Cl] - CCl_4 and [^{36}Cl] - HCl as chlorinating agents. Two types of surface Cl species are formed when the surface is treated with CCl_4 One of these species is inert with respect to exchange of [^{36}Cl] - chloride species with unlabelled anhydrous HCl at 293K. The other type of surface species is labile and behaves in a similar manner to an HCl treated γ - alumina surface Cl species. Labelling studies, infrared spectroscopy and [^{27}Al] - MAS NMR spectroscopy point to Brønstead acid sites on alumina, with Al - OH replacement by Al - Cl (terminal Cl) as labile Cl sites and Lewis acid sites, with coordinatively unsaturated $AlCl_2$ groups in which both Cls bridge neighbouring Al(III) atoms as non - labile sites.

Fluorination of γ - alumina with SF_4, followed by conditioning with CCl_3CH_3, produces a catalyst for the room temperature fluorination of CH_3CCl_3

with anhydrous HF to produce a mixture of chlorofluorocarbons (87). Sulphur tetrafluoride fluorination does increase the acidity of Lewis acid sites on the surface and this fluorinated surface, in conjunction with HF, is a very good fluorination catalyst. SF_4 fluorinated alumina is also used to fluorinate $CH_3CCl_2CH_3$, CH_2ClCCl_3, $CHCl_2CHCl_2$ and $CHClCCl_2$ with HF (88). Other halogenating agents used to chlorinate or fluorinate γ - alumina include SOF_2, COF_2 and $COCl_2$ and these catalysts can all be used for fluorination of organic halogen compounds with HF.

Activation of fluorinated chromias is generally carried out using one of two fluorination agents. The most commonly used is HF and studies concerning the fluorination of chromia with HF will be discussed later. The other major type of fluorination agents are fluorine containing organic halogen compounds which undergo decomposition on the chromia surface. The chromia undergoes two different surface transformations in the presence of $CHClF_2$ before becoming catalytically active. The first involves a reductive deoxygenation of the high valent Cr surface species resulting in the formation of CO_2 and other oxidised products. The reduced surface then reacts with $CHClF_2$ to form CO and a halogenated catalytically active surface. Increases in Lewis acidity accompany each transformation step.

Another organic halogen compound used to fluorinate chromia surfaces is CH_2ClCCl_2F. Kemnitz *et al* (34) passed a constant flow of CH_2ClCCl_2F gas over a calcined chromia catalyst prepared from the thermal decomposition of $(NH_4)_2Cr_2O_7$. The period of fluorination was the length of time required for a constant product composition to appear in the effluent. This preconditioned catalyst did not provide fluoride species for the reaction of $C_2H_2ClF_3$ to form $C_2H_2F_4$ and HF was used as a fluorination agent. The suggested reaction mechanism was a dehydrochlorination / hydrofluorination mechanism which reverted to a halogen exchange mechanism as the reaction proceeded further. Evidence for the dehydrochlorination / hydrofluorination reaction comes from the presence of different olefins in the

effluent at the beginning of the reaction. X - ray photoelectron spectroscopy, X - ray diffraction and excited Auger electron spectroscopy have been employed to examine the surface of chromias fluorinated by CCl_2F_2 at 573K, $CHClF_2$ at 523K, CH_2ClCCl_2F at 673K and CHF_2CHF_2 at 673K. Partial halogenation of the chromia surface is observed as a result of these pretreatments. The total amounts of halogen present at the surface appear to be independent of the organic halogen compound used in the pretreatment. It is suggested that the catalytically active sites on fluorinated chromias are similar to β - CrF_3, which is catalytically active, as opposed to α - CrF_3, which is catalytically inactive. Both α - CrF_3 and β - CrF_3 contain $CrF_{6/2}$ octrahedra, however, they differ by the nature of the linking. In α - CrF_3 the fluoride ions are close packed with Cr cations situated in octrahedral holes. In β - CrF_3 the $CrF_{6/2}$ octrahedra are arranged in such a way that hexagonal channels are found in one direction only.

The second and most widely used fluorinating agent is anhydrous HF. Radiotracer studies involving [^{18}F] - HF have determined the presence of different fluoride species on the surface of catalysts (29). Chromia, prepared by the calcination of chromium hydroxide, was fluorinated with [^{18}F] - HF 623K and the labelled catalyst examined with unlabelled HF at various stages during the lifetime of the catalyst. These radiotracer studies together with temperature programmed reduction (TPR) and exchangeable hydrogen studies have been used to explain the nature of fluoride species present and the state of the chromia surface. Three different fluoride species are present on this chromia. The first type is consistent with the behaviour of HF molecules and oligomers present on the surface in a weakly adsorbed state. This accounts for a minor fraction of the total (around 15 %) and can be easily removed by inert gas flow at 623K. The industrial conditions under which these catalysts are normally used requires the constant flow of HF gas and hence replacement of lost HF molecules and oligomers would be continuous in these processes. The second type of fluoride species is inert to exchange or displacement with HF gas flow at 623K. The proportion of fluoride of this type

increases with catalyst lifetime until at some stage the catalyst is no longer catalytically active for fluorination. The behaviour of this type of fluoride towards HF is similar to that of α - CrF_3 and hence this fluoride is believed to be directly bonded to Cr(III) by the slow replacement of Cr(III) - O for Cr(III) - F. The third type of fluoride present is believed to be catalytically active and is the source of fluorine incorporated into chlorofluoroethanes. The exact nature of this catalytically active fluoride is unknown. TPR indicates that Cr(VI) and Cr(IV) are present in the catalyst initially, however Cr(IV) is no longer present following prolonged fluorination and Cr(VI) sites with HF weakly bonded to them may well be the active species. Radiotracer studies also suggest that hydrogen bonded $(HF)_n$ oligomers may be the source of catalytically active fluorine and that incorporation of HCl into those species as a result of halogen exchange may provide catalitically active chlorine species.

Studies of unfluorinated chromias and chromias fluorinated to differing degrees have been performed using CF_3CH_2Cl as a test reaction (35). In some cases HF was used to fluorinate $C_2H_2ClF_3$ and in other cases HF was absent. In the absence of HF the reaction of CF_3CH_2Cl over fluorinated chromia leads to large quantities of olefins in the effluent stream at 653K. The major olefin product present is CF_2CClH which appears from the beginning of the reaction. This suggests that dehydrofluorination is an important reaction when a hydrochlorofluorocarbon is reacted in the presence of an unfluorinated chromia. Fluorinated chromia greatly reduces the amount of olefin present in the effluent and leads to larger quantities of fluorinated hydrochlorofluorocarbons. It is known from X - ray photoelectron spectroscopy studies of chromias involved in this reaction that the initial olefination to form CF_2CClH results in HF which fluorinates the chromia surface and leads to the catalytic fluorination of CF_3CH_2Cl to form CF_3CH_2F. Therefore, the unfluorinated chromia undergoes an initial activation period during which it is fluorinated by HF produced as a result of the olefination of CF_3CH_2Cl. After a

certain period of time a critical, minimum level of fluorination allows the now partially fluorinated chromia to fluorinate CF_3CH_2Cl resulting in CF_3CH_2F.

The importance of catalyst fluorination can be further emphasised by the preparation of C_2HF_5 and by the reaction of C_2HClF_4 and HF in the presence of a Zn doped chromia catalyst prepared via the calcination of the mixed metal hydroxides (79). An extensive HF pretreatment of chromia was performed at 573K under atmospheric pressure. HF was passed over the chromia catalyst, pre - dried under nitrogen at 573K for 1 hour at a flow rate of 0.0537 mol h^{-1} for 24 h. The effluent mixture contained the fluorinated product and the unreacted starting material only. The high degree of fluorinated products and the lack of olefin at any stage of the reaction in the effluent were a direct result of the extensive fluorination and the large quantity of HF in the reactant stream. This is in direct contrast to the reaction of CF_3CH_2Cl without HF in the presence of an unfluorinated chromia catalyst as detailed previously and the reaction of chloroethanes over unfluorinated chromia which proceeds via a dehydrochlorination to produce olefin (89).

1.5 ROUTES TO THE PRODUCTION OF CF_3CH_2F (HFC 134a).

The production of CF_3CH_2F is difficult to perform and many different routes have been used to attain this product. To minimise costs, readily available and inexpensive starting materials are required and chloro- or hydrochloro-carbons are the most likely candidates with anhydrous HF or hydrogen as reagents to effect the exchange reactions C - Cl ----> C - F and C - Cl ----> C - H. This however opens the possibility of different routes to attaining CF_3CH_2Cl as fluorination and hydrogenolysis or indeed a combination of both are possible. The three most likely routes towards CF_3CH_2F are described in Fig 1.5 and below.

$$(\text{I})\ CCl_2CHCl \xrightarrow{HF} CClFCH_2Cl \xrightarrow{2HF} CF_3CH_2Cl \xrightarrow{HF} CF_3CH_2F$$

$$(\text{II})\ CCl_2CCl_2 \xrightarrow{Cl_2} C_2Cl_6 \xrightarrow{4HF} CClF_2CClF_2 + CF_3CCl_2F \xrightarrow{HF} CF_3CH_2F$$

$$(\text{III})\ CCl_2CCl_2 \xrightarrow{HF} CCl_2FCHCl_2 \xrightarrow{2HF} CF_3CHCl_2 \xrightarrow{HF} CF_3CHClF \xrightarrow{H_2} CF_3CH_2F$$

Figure 1.5 Three Possible Routes To CF_3CH_2F

The first route (I) involves catalytic fluorination beginning from CCl_2CHCl. This has the advantage of being a direct fluorination with hydrofluorination being the initial reaction and a fluorine for chlorine exchange occurring during subsequent stages. Unfortunately, the final stage in this reaction, CF_3CH_2Cl ----> CF_3CH_2F, is difficult thermodynamically and requires very forcing conditions. The second route (II) involves chlorination of CCl_2CCl_2 to form C_2Cl_6 followed by a series of halogen exchange steps with anhydrous HF to form a mixture of $CClF_2CClF_2$ and CF_3CCl_2F. Hydrogenolysis of CF_3CCl_2F with hydrogen then occurs to form CF_3CH_2F. This route uses similar chemistry to that described for route (I) above, however it is less direct and less selective in obtaining the required product at each stage thus separating products, such as $CClF_2CClF_2$ and CF_3CCl_2F, before the final stage in the reaction can occur presents a problem. The most direct route to the hydrogenolysis of CF_3CCl_2F is via a conventional hydrogenolysis catalyst such as Pd supported on charcoal, however it is known that such catalysts suffer rapid deactivation in the presence of halogen containing species and thus this is also a consideration. Route (III) uses CCl_2CCl_2 as a starting material which undergoes the same hydrofluorination / fluorination process as described in route (I). The final step in the fluorination of CF_3CH_2F is a hydrogenolysis as described above however only one C - Cl ----> C - H transformation need occur in route (III) as opposed to two transformations in route (II). The catalyst deactivation problems as described for route (II) also apply for route (III).

The fluorination and hydrogenolysis reagents used in these routes have problems associated with them. Anhydrous HF, the most obvious fluorination agent has problems associated with its toxic and corrosive nature and requires special handling techniques for both laboratory and plant scale synthesis. These problems are magnified by the temperature at which the reaction proceeds, therefore this is an added consideration in choosing routes to CF_3CH_2F. Hydrogen, while not particularly presenting a toxic or corrosive hazard is highly flammable and could present a problem of potential explosion. The majority of literature examples of processes used to form CF_3CH_2F have been patented and the majority of these patents describe the fluorination route (I) using chromia catalysts. These patents are discussed in 1.6, however some other routes, catalytic or otherwise, are described below.

Patent literature relating to processes for the manufacture of CF_3CH_2F has expanded greatly over the last 10 years. An example of a patented catalytic hydrogenation process for the manufacture of CF_3CH_2F was CCl_2FCF_3 hydrogenated at 393 - 473K with H_2 to produce CF_3CH_2F in the presence of 0.2 - 5 w/w % Pd on alumina. Solvay (90) have patented an AlF_3 catalyst used to produce CF_3CH_2F from the reaction of CF_2CHF and HF. A number of examples exist of Al / Cr containing catalysts used for the manufacture of organic halogen compounds, however few examples involve patents lodged by the major manufacturers. Many of these catalysts are mixed oxides with the Al compound acting as a support for the Cr compound. Alumina is the most common support with chromia impregnated onto it. For example, Sobolev (91) has patented an HF fluorinated chromia doped with a large quantity of $TiCl_3$ and supported on alumina for the vapour phase fluorination of haloethanes (containing Br or Cl) with HF to produce CF_3CH_2F. Other fluorination catalysts supported on alumina include chromia doped with Bi and In and fluorinated for up to 5 h with HF prior to use as a catalyst for the manufacture of HCFCs and HFCs (92, 93). AlF_3 is also mentioned in the patent literature as a support for chromia in the preparation of a fluorination catalyst for

the manufacture of HCFCs (94) and $CrCl_3$ supported on AlF_3 has been patented for similar reactions (95).

Patents lodged by industrial manufacturers include few of the major manufacturers in this area. Allied - Signal have a patent on a mixed chromia / alumina catalyst fluorinated and doped with a small quantity of metal salt such as 1.4 w/w % $CoCl_2$ used to catalyse the fluorination of organic halogen compounds to produce CFCs, HCFCs and HFCs (96). Ausimont have patented a process for the manufacture of CF_3CH_2F by reacting $CHClCCl_2$ and CF_3CH_2Cl with HF at 573 - 673K over a chromia catalyst supported on AlF_3. It is worth noting that this catalyst had a high selectivity, a long lifetime and it was used in plant scale operations to produce CF_3CH_2F (97). The Central Glass Company of Japan have also produced fluorination catalysts by supporting Cr salts on alumina and pretreating this with HF. These catalysts can be used to manufacture HCFCs (98). However, examination of the patent literature will reveal that most mixed Al / Cr containing catalysts were patented long before the major manufacturers considered plant scale operations to produce CFC alternative halohydrocarbons illustrating the limited use of these compounds as catalysts in fluorination processes.

A small number of patents (post 1987) exist concerning processes, catalytic or otherwise, for fluorinating haloethanes. The preparation of CF_3CH_2F has largely been performed by catalytic reactions involving alumina and chromia fluorination catalysts some of which were discussed previously, and hydrogenation catalysts. However one or two patents exist for the preparation of CF_3CH_2F using catalysts other than those mentioned above or non - catalytic processes. A Chinese patent (99) involves mixing CF_3CH_2Cl in water and heating this mixture to 503K for 2 h under high pressures to produce 88 % CF_3CH_2F. The catalyst used in this process is $Cl(CF_2CF_2)_4OCF_2CF_2SO_2F$. Other catalysts used for the same process can be prepared by exchanging the last halogen attached to the SO_2 group for chlorine or hydroxyl. A mixture of alkali metal fluorides and aprotic solvents has been patented as a catalyst for CF_3CH_2F production by reacting CF_3CH_2Cl with a catalyst such as

KF in sulfolane in an autoclave at 553K at 15.5 atmospheres, obtaining 67 % of the desired product (100). One non - catalytic process has also been patented by reacting C_2Cl_3 and HF to produce CF_3CH_2Cl and further reacting this with HF to produce CF_3CH_2F (101). Clearly none of the above processes are industrially viable and all of these patents were lodged by non - industrialists.

1.6 CATALYSIS IN THE REACTION TO FORM CF_3CH_2F FROM CF_3CH_2Cl AND HF.

As described in the previous section, the reaction to fluorinate CF_3CH_2Cl to form CF_3CH_2F is thermodynamically difficult. This process requires a high reaction temperature and the presence of a catalyst. Catalysts require for the fluorination route, to increase the activity of the reaction considerably as well as having high selectivity towards CF_3CH_2F. The most popular choice of fluorination catalyst is chromia or doped chromias which allow the reaction to occur under atmospheric pressure and at temperatures below 673K. Such a catalyst must be highly selective towards a halogen exchange process to form CF_3CH_2F as there is the possibility of dehydrofluorination occurring to form CF_2CHCl. Blanchard *et al* (35) have studied this system, both in the presence and absence of anhydrous HF, using chromia catalysts pretreated with differing amounts of HF. Their findings reveal that the formation of CF_2CHCl is an important process in the reaction, however the importance of this process diminishes with the increasing extent of HF pretreatment and the presence of HF in the reactant stream. Other workers who have studied this reaction in the presence of chromia catalysts have determined that CF_2CHCl formation is a factor contributing towards the deactivation of these chromia catalysts. Hence, not only does the formation of CF_2CHCl compete with the formation of CF_3CH_2F, it deactivates the chromia as a catalyst leading to reduced catalytic lifetime as well as reduced activity. To combat this problem divalent metal dopants were employed which allowed the activity of the chromia to remain

constant as the catalytic lifetime is increased by inhibiting the formation of CF_2CHCl (37).

The mechanism of the fluorination of CF_3CH_2Cl has been suggested as a chlorine for fluorine halogen exchange reaction. Deuterium isotope studies (36) of the fluorination of C_2Cl_4 with HF to give CF_3CH_2F suggested that a halogen exchange is the major pathway involved in these reactions with HF addition / HCl elimination also occouring as a minor reaction process. This suggestion was made from the observation of few intermediate compounds of an HF addition / HCl elimination process present in the reaction effluent suggesting that such a process is of little importance in the reaction. The halogen exchange process occurs via labile fluoride species present on the surface of the chromia as determined from studies described previously in this chapter. The work of Blanchard *et al* (61) suggests that active sites containing such species are chromia sites which are capable of being reversibly oxidised as demonstrated by TPR and TPO studies compared to catalytic activity which suggests that higher numbers of such sites are present on more active catalysts. Industry has developed catalysts for this reaction using existing available technology relating to halocarbon fluorination catalysts. Most of these processes have been patented and a number of these patents are described below.

Industrial interest in Al containing catalysts is quite extensive and DuPont has patented a number of processes involving AlF_3 to produce heavily fluorinated halogenated hydrocarbons (102). The manufacture of CF_3CH_2F as a drop in replacement for the refrigerant CCl_2F_2 was performed by the reaction of CH_2ClCX_3 (where X = Cl, F) with HF vapour at 548 - 773K in the presence of an AlF_3 catalyst doped with 18 % ZnF_2. DuPont also chose to patent the manufacture of CF_3CH_2F by using fluorinated doped Al_2O_3 as a catalyst in the vapour phase reaction of CF_3CH_2Cl and HF (103) and processes to manufacture other higher fluorinated organic halogen compounds such as CF_3CHF_2 using fluorinated alumina doped with transition metals in oxidation states greater than 0 as fluorination catalysts with HF and tetrahaloethanes (104) and HF and tetrahaloethenes (105).

Other major companies who have patents on Al containing compounds as fluorination catalysts include Atochem (106) who have patented a process for the manufacture of CF_3CH_2F from CF_3CH_2Cl and HF with Cr or Ni doped AlF_3 or an AlF_3 / alumina mixed catalyst.

CF_3CH_2F manufacture based on chromium containing catalyst manufacturing processes have been the biggest growth areas in fluorination catalyst patents over the last eight years. The production of hydrofluorocarbons, in particular CF_3CH_2F, via chromium containing fluorination catalysts and processes has been widely reported and many patents exist in this area, some of which are described here. Fluorinated Zn doped chromium prepared by coprecipitation of the respective nitrates with ammonia followed by calcination and fluorination with HF at 673K was used to fluorinate CF_3CH_2Cl with HF at 593K giving 95 % selectivity and 22.2 % conversion of CF_3CH_2Cl (107). Chromia doped with Cd and fluorinated with HF was also patented for use as a fluorination catalyst in this reaction with 18.8 % conversion of CF_3CH_2Cl at 593K and 95 % selectivity (108). Other fluorinated chromia dopants reported in patent literature include In, which can also produce a good fluorination catalyst (109).

Industrial patents have been lodged by all of the large chemical companies involved in HFC manufacture. In particular, ICI have patented a number of chromium containing catalysts for HFC manufacture (110). The reaction of HF and CF_3CH_2Cl to form CF_3CH_2F was carried out in the presence of a fluorinated Zn / chromia catalyst prepared by the wet impregnation of chromia with $ZnCl_{2(aq)}$ solution. Recent Atochem patents include chromia / V fluorination catalysts (111). and chromia on active carbon (112) which is used to catalyse the fluorination of $C_2HX_{2-n}F_{3-n}$ (where X = Cl or Br, n = 0, 1) with HF to form CF_3CH_2F and CF_3CHF_2. The Japanese manufacturer Daikin Industries has patented an amorphous chromia catalyst (113) of surface area 170 $m^2 g^{-1}$ pretreated to at least 8 % fluoride with HF for the production of CF_3CH_2F by reaction of CF_3CH_2Cl with HF over this catalyst at 623K and a Ru and / or Pt promoted partially fluorinated

chromia for the same reaction (114). Allied - Signal have a recent patent on a Ni, Pd or Pt doped chromia for this reaction and other similar reactions using HF as the fluorination agent (115).

1.7 AIMS OF THE PRESENT WORK

As discussed, the development of effective routes for the production of alternatives to chlorofluorocarbons such as CF_3CH_2F is an urgent requirement for industry in view of international regulations requiring the introduction of more environmentally friendly compounds and public demand for the introduction of such compounds. The commercial interest in manufacturing technologies for CF_3CH_2F production has been great and intense world wide competition to improve chemical process efficiency has determined the size and share of the market won by various manufacturing companies. The commercialisation of CF_3CH_2F production, as discussed in 1.5 and 1.6, has proved to be very difficult and was largely influenced by the catalyst systems employed. The British company ICI is at the forefront of these developments and has captured 30 - 40 % of the world market following the development of advanced and new halogen exchange catalysts.

1,1,1,2 - tetrafluoroethane (HFC 134a)is currently employed as the 'drop in' replacement for the refrigerant and foam blowing agent dichlorodifluoromethane (CFC 12). 1,1,1,2 - tetrafluoroethane is manufactured by ICI using a process, described in 1.5, in which $CHCl_2CCl_2$ is hydrofluorinated and then undergoes halogen exchange using anhydrous HF vapour as the hydrofluorination and fluorination agent with catalysis required at all stages (EQN. 1.13)

$$CHClCCl_2 \xrightarrow{HF} CH_2ClCF_3 \xrightarrow{HF} CH_2FCF_3 \qquad \text{EQN. 1.13}$$

Fluorination of a - CCl_2F group is achieved more readily than is replacement of Cl by F in - CH_2Cl and hence 1,1,1 - trifluoro - 2 - chloroethane (HCFC 133a) is a

key intermediate in EQN. 1.13. Operationally the process is divided into two reactions from which the products are CF_3CH_2Cl and CF_3CH_2F, the formation of these compounds requires temperatures in the ranges 423 - 573K.

Commercial production of CF_3CH_2F via halogen exchange is based on the use of chromium containing catalysts and chromia has proved to be the most active catalyst for this type of reaction. Various supported and unsupported chromium containing catalysts were evaluated, however, all proved to have problems with activity, selectivity or lifetime. A new generation of fluorinated catalysts based on divalent metal chromites, M(II)O - Cr_2O_3 where M(II) = Mg, Mn, Co, Ni or Zn was developed by ICI Klea and ICI Katalco. Zinc(II) / chromia catalyst systems show significant advantages over chromia for CF_3CH_2F production, requiring operating temperatures in the lower end of the ranges described previously, having high selectivity and activities up to 5 times greater than conventional chromia catalysts. These chromias are amorphous but X - ray photoelectron studies suggest that the active surface, developed during use, has an oxo - fluoride composition and that heavy depths of fluorination may occur with extended usage.

An understanding of the mechanism of halogen exchange on these new Zn(II) doped chromias could lead to further catalyst improvement in this and similar systems and this was the overall aim of this project. Model chromias were prepared from ICI commercial chromia to produce differing degrees of crystallinity and these chromias were doped with differing amounts of Zn(II). These catalyst precursors then underwent an extensive (17 h) fluorination with anhydrous HF at 573K to produce the working catalyst. The reaction to produce CF_3CH_2F from CF_3CH_2Cl and anhydrous HF was used as a test reaction for the catalysts prepared (EQN 1.14).

$$CF_3CH_2Cl + HF \text{ -----> } CF_3CH_2F + HCl \qquad \text{EQN 1.14}$$

In order to gain the greatest understanding of a catalyst there is a need to ensure that the preparation and operating conditions of the catalyst are appropriate to generate a 'true' working catalyst. Microreactor testing rigs at ICI Runcorn, which were proven to mimic full scale plant performance, were used to condition catalysts *in situ* under industrial conditions. Comparisons of catalyst performance were determined by controlled sampling and testing by gas chromatography at various key temperatures in the range 623 - 523K. Determination of the effects of crystallinity and zinc(II) doping on the activity and selectivity of chromias tested in this temperature range is one of the aims of this work.

Various characterisation techniques have been employed to determine the bulk and surface structures of these materials both before and after fluorination and following reaction as an understanding of the catalyst structure was essential to understanding its catalytic behaviour. Determination of how the bulk and surface structures of these materials control the activity and selectivity of the catalysts is a key element to understanding these chromia's catalytic performance. Another project, performed in conjunction with this work to examine divalent metal dopants other than Zn(II), will allow comparison to be made, enabling the effects of the radius of the divalent metal and its electronic properties on the performance of these halogen exchange catalysts to be determined. Thus determination of the effects of crystallinity and Zn(II) doping, in comparison with other divalent metal dopants, on catalytic behaviour were another aim of this project.

Achievement of the overall objectives of this work was heavily dependant on the use of the radiotracer [^{18}F] - fluorine (γ - emitter, $t_{1/2}$ = 110 min.) and [^{36}Cl] - chlorine (β^- emitter, $t_{1/2} = 3 \times 10^5$ yr.). *In situ* studies using these radiotracers have been performed previously at Glasgow and the facilities in which to study heterogeneous catalytic systems, such as the one described above, are readily available. Interactions involving [^{18}F] - HF with the catalyst have allowed the catalyst fluorination process to be studied in detail by scintillation counting, revealing information about fluoride species on the surface of the catalyst and

determining the effects of crystallinity and Zn(II) doping on fluorinated chromias. The interaction of CF_3CH_2Cl on fluorinated chromias was studied using [^{36}Cl] - labelled CF_3CH_2Cl by the direct monitoring Geiger - Müller counting technique under static conditions. These techniques have allowed the interaction of the reactants of EQN. 1.14 on fluorinated chromias to be examined revealing information regarding the interaction of the reactants with the working catalyst, a major part of the overall objective of this project. The behaviour of the reactants is compared with information obtained from catalyst testing and characterisation to draw conclusions regarding of the catalytic mechanism of this reaction.

Observations from this study are compared with observations and conclusions from similar studies by other workers. Differences in catalyst preparation and treatment between this and other studies are examined and comparisons are drawn between conclusions from this work and the work of other workers. This project aimed to increase the understanding of the mechanism for this catalytic reaction and the mechanistic effects of differing catalyst preparations and pretreatments on the transformation of CF_3CH_2Cl to CF_3CH_2F over chromia catalysts.

2 EXPERIMENTAL

Due to the hygroscopic nature of the calcined and halogenated materials used during the course of this work, it was important to ensure that air and moisture were excluded from the reactions under examination. All work was therefore carried out under vacuum (10^{-4} Torr), under enclosed flow conditions or in an inert (N_2) atmosphere box with an H_2O level < 5.0ppm.

2.1 EQUIPMENT.

2.1.1 THE VACUUM SYSTEMS

Two separate types of vacuum system were used to manipulate volatile materials - a Pyrex glass system for handling organic materials and a Monel metal system for handling anhydrous hydrogen fluoride and hydrogen chloride. Monel is an alloy of nickel and copper which was used because of its resistance to corrosive chemicals.

Rotary pumps (Edwards or Genevac) were used to evacuate both systems. A series of waste traps, cooled with liquid nitrogen, protected the pump from any volatile materials in the system. The pump and the waste traps could be isolated from other parts of the line.

2.1.2. PYREX GLASS VACUUM LINE.

This was an enclosed Pyrex glass structure consisting of a manifold, a Heise Bourdon Gauge or manometer and a mercury Vacustat (Fig. 2.1). A water cooled mercury diffusion pump was used in conjunction with the rotary pump to achieve a vacuum of 10^{-4} Torr. The Vacustat measured the vacuum achieved by the pumps. The Heise Bourdon gauge or the manometer was used to measure pressures of gases in the line to pressures of $\pm$ 0.5 Torr. The manifold had several B14 sockets which could be isolated from the line by means of high vacuum stopcocks (J. Young or Rotaflow). Vacuum flasks and ampoules equipped with high vacuum

FIGURE 2.1 Pyrex Glass Vacuum Line

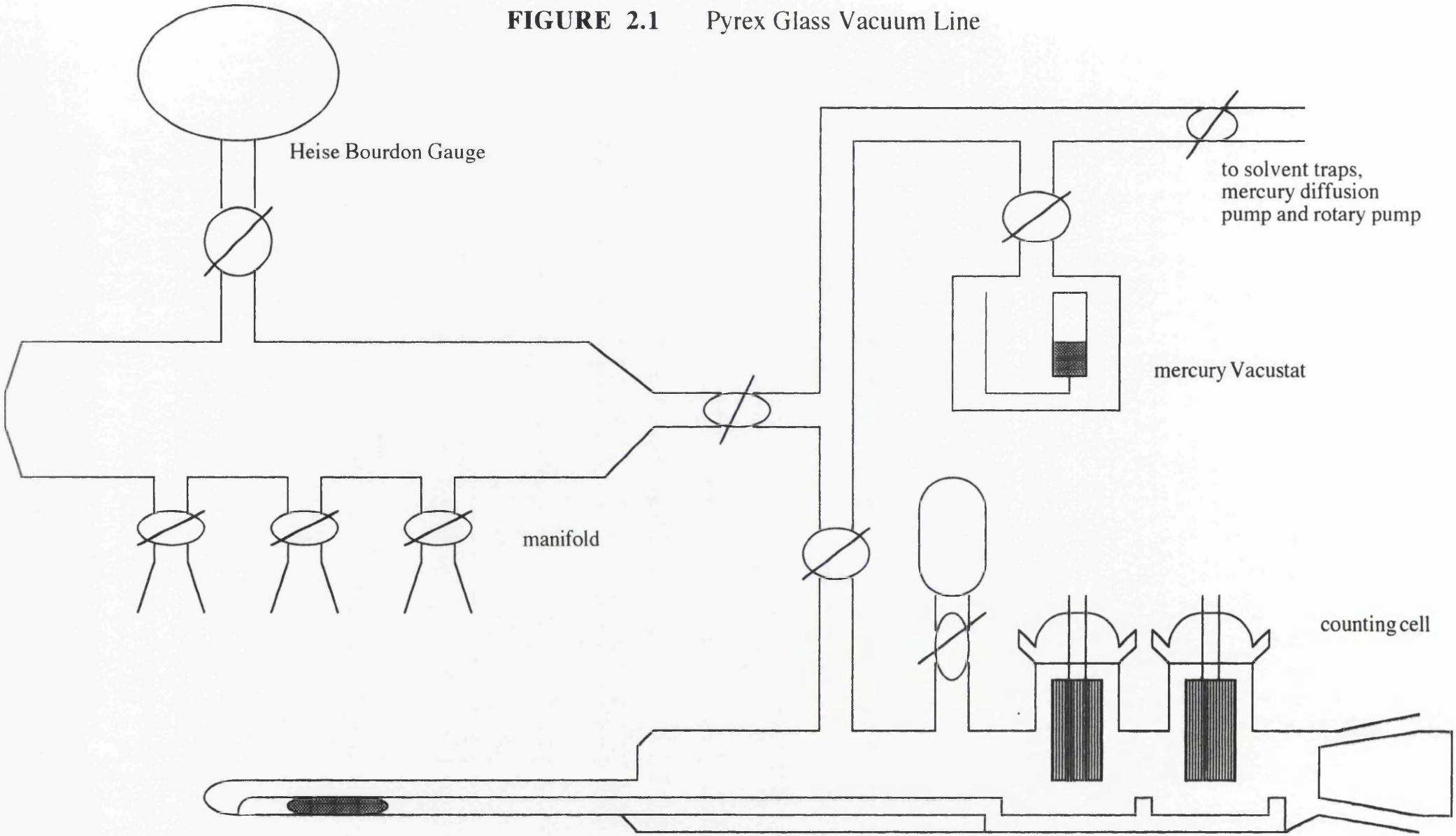

stopcocks and B14 cones were attached to the manifold to introduce and withdraw reactants. All vessels and the line itself were flamed out, in order to reduce the amount of moisture adsorbed on the surface of the glass (116).

2.1.3. MONEL METAL VACUUM LINE

This was similar to the Pyrex system but was constructed using 2/5 inch o.d. Monel tubing and Monel metal valves (Autoclave Engineers). Monel metal or stainless steel pressure bombs were connected to the line via nipple and collar screw couplings (Autoclave Engineers). A cylinder of anhydrous hydrogen fluoride (Air Products) and a Monel metal waste trap was also connected to the HF - line. Pressure in the line was determined using a Budenberg gauge (Fig. 2.2). The Monel section of the line was connected to the rotary pump through a 0.25 inch glass - metal joint and two glass waste traps.

The line was calibrated using a Pyrex glass bulb of known volume, equipped with a B14 cone and a ground glass socket and key tap, attached to the line via a B14 brass socket. The pressure was recorded on the Budenbourg gauge as various sections of the line were opened. Volumes were calculated using the ideal gas equation (EQN. 2.1) :-

$$PV = nRT \qquad \text{EQN. 2.1}$$

where P = pressure (atmospheres); V = volume (litres); n = amount of gas (moles); R = gas constant (8.314 $JK^{-1}mol^{-1}$) and T = absolute temperature (K).The calibration was repeated several times to calculate the error on the volume. The volume of the bulb was stamped on it and this was checked by subtracting the accurately weighed mass of the evacuated bulb from the accurately weighed mass of the bulb filled with distilled water.

FIGURE 2.2 Monel Metal Vacuum Line

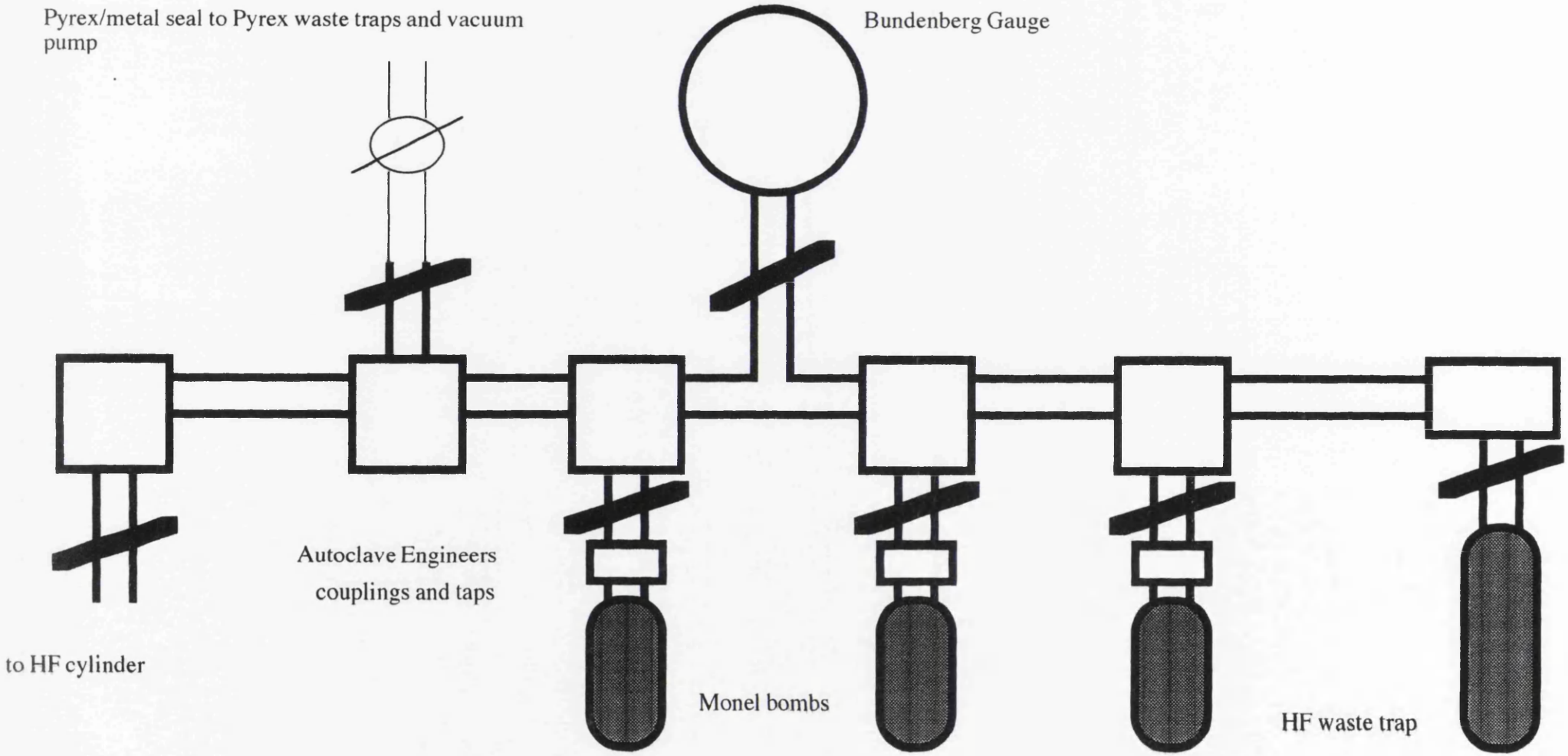

2.1.4 FLOW SYSTEMS.

Three separate flow systems were used to perform reactions over catalysts :- a Monel and polytetrafluoroethene (PTFE) catalyst microreactor rig, to fluorinate precursor catalysts *in situ* before testing their activity at ICI, Runcorn, a Monel catalyst fluorination rig, to fluorinate precursor catalysts for future studies and a Monel radiochemical catalyst testing rig to perform radiochemical studies on catalysts. All three of these systems were operated at atmospheric pressure. Alkaline waste traps were used to collect rig off gases (ROG) and neutralise anhydrous hydrogen fluoride gas leaving the system. The catalyst microreactor rig and the catalyst fluorination rig were both housed within large fumehoods, the radiochemical catalyst testing rig was housed under an overhead air extraction system.

2.1.5. CATALYST MICROREACTOR RIG.

A Monel and PTFE catalyst microreactor rig at ICI, Runcorn, was used to dry and fluorinate catalyst precursors *in situ* as well as to react catalysts under flow conditions -that is where the reactants pass through the reactor as a continuous flow - to emulate an industrial system and allow comparisons between catalysts for the reaction under study (Fig. 2.3)

The main constituents of the rig were a hydrogen fluoride reservoir, a CF_3CH_2Cl reservoir and a catalytic reaction vessel. The hydrogen fluoride reservoir was a Monel double ended sample cylinder, housed in an insulated bath and cooled between 281 - 276K by means of a chiller unit fitted with a temperature controller, to allow greater control over the HF flow. The tubing leading into the reservoir was 1/4 inch Monel and the tubing leading from the reservoir was 1/8 inch PTFE. The HF reservoir could be filled via the main HF cylinder through the HF fill valve. Excess HF resulting from over pressurisation of the rig was neutralised by a scrubber (K_2CO_3) positioned just after the reservoir.

FIGURE 2.3 Catalyst Microreactor Rig

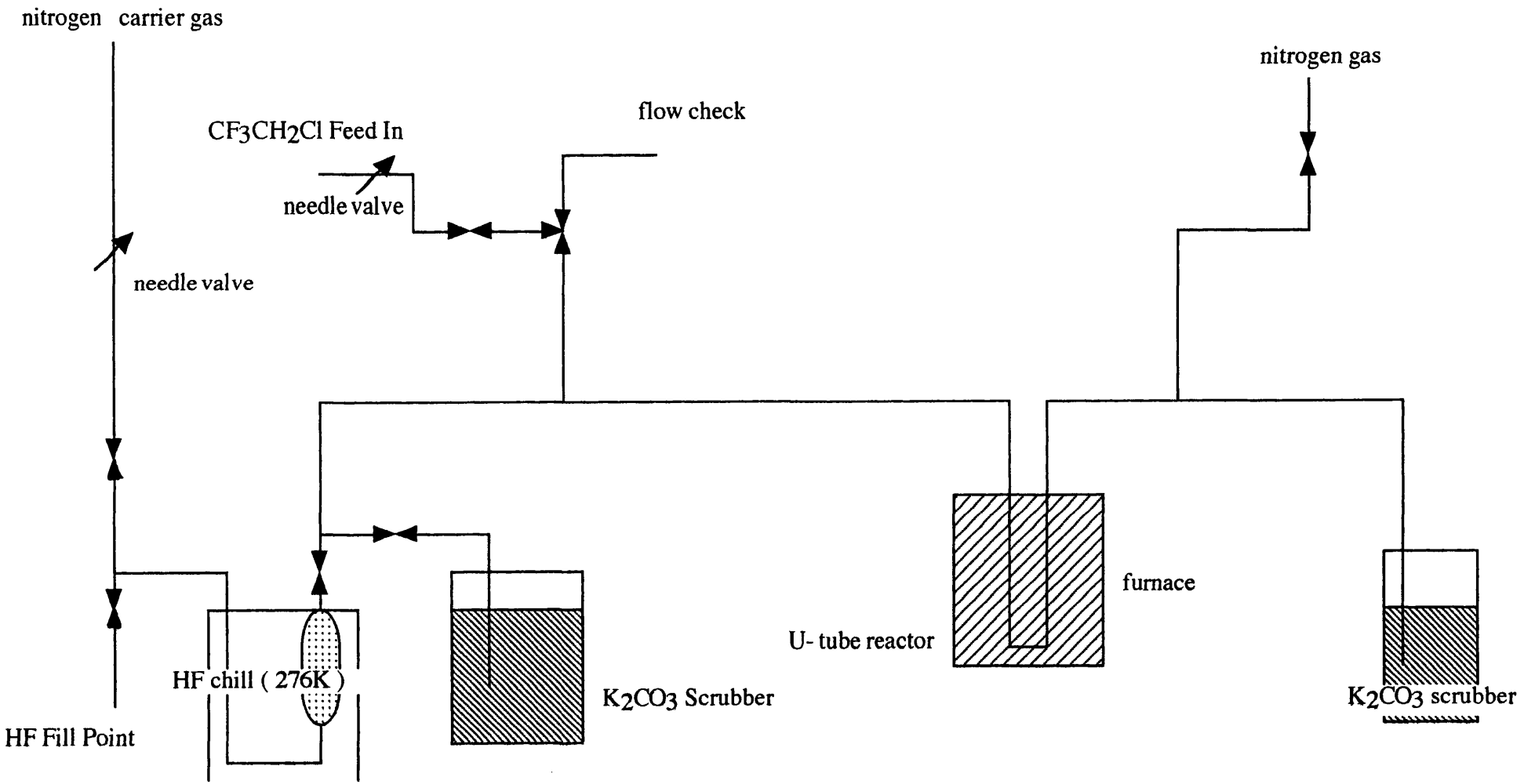

The CF_3CH_2Cl reservoir was a cylinder of CF_3CH_2Cl (ICI) controlled by a series of valves and a gauge. The CF_3CH_2Cl flow was controlled using a needle valve and a pressure regulator. Separate feed lines for HF and CF_3CH_2Cl allowed the catalyst to be treated with HF alone for the fluorination reaction or with HF and CF_3CH_2Cl for the catalytic reaction. A nitrogen carrier gas was used to flow HF over the catalyst.

The catalytic reactor was a Monel 1/4 inch U - shaped vessel with catalyst charged into it. The catalytic reactor was housed in an oven allowing heating of the reactor. A diluent nitrogen flow was incorporated into the rig after the reactor to allow clear flow of products and unused reactants from the ROG tubing.

The ROG could be passed through the main scrubber (K_2CO_3) to remove excess HF. From the ROG a sampling tube allowed sampling of the reaction products for testing by gas chromatography. Details of a typical catalyst testing run can be found in chapter 3.

2.1.6. FLOW LINE FOR CATALYST FLUORINATION.

A Monel metal flow system was used to fluorinate catalysts with anhydrous hydrogen fluoride under flow conditions - to provide samples of fluorinated catalysts for further studies (Fig. 2.4).

The main constituents of the fluorination rig were a hydrogen fluoride reservoir and a catalyst fluorination vessel. The hydrogen fluoride reservoir was a double ended sample cylinder, housed in an insulated bath and cooled to 276 -273K by means of a chiller unit fitted with a temperature controller to allow greater control of HF flow. A reactor bypass line allowed the flow of HF to be measured by timed titration with NaOH solution. A nitrogen carrier gas, controlled via a mass flow controller (Brooks Instrument B.V.), was used to flow HF gas over the catalyst.

The catalytic reactor was a U - shaped vessel, with catalyst loaded into the larger left hand side, so that HF gas flowed from the bottom to the top of the

FIGURE 2.4 Catalyst Fluorination Rig

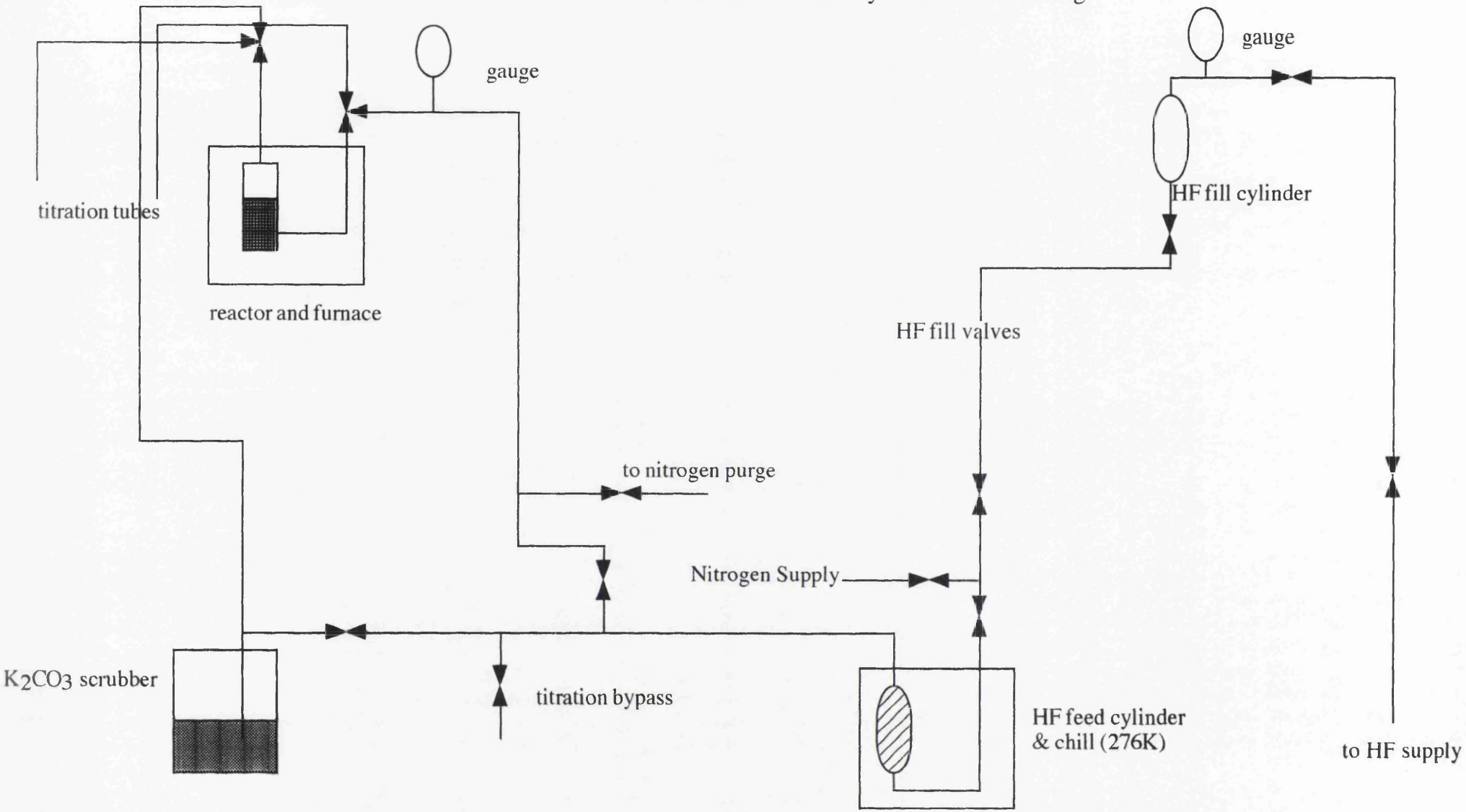

reactor. The reactor was housed in an oven allowing it to be heated. The ROG could be passed through the main scrubber (K_2CO_3) to remove excess HF. Details of a typical fluorination can be found in chapter 3.

2.1.7. FLOW LINE FOR RADIOCHEMICAL CATALYST TESTING.

A Monel metal flow system was used to study catalysts with radiolabelled gases under flow conditions - to provide information about the behaviour of different catalysts with specific radiolabelled gases (Fig 2.5).

The main constituents of the radio chemical catalyst testing rig were a radiolabelled hydrogen fluoride gas reservoir, a CF_3CH_2Cl gas inlet and a catalytic reaction vessel. The radiolabelled hydrogen fluoride gas reservoir was a Monel metal bomb (Whitey) attached to the line. The bomb was housed in an oven connected to a Variac transformer allowing the bomb to be heated. The temperature was controlled by varying the voltage on the Variac and measuring temperatures attained with a digital ratemeter connected to a thermocouple wire inserted into the oven. This ensured that most of the radiolabelled HF gas left the bomb to flow over the catalyst. A controlled flow of radiolabelled HF gas was difficult to achieve therefore, the oven was heated to 373K to ensure that most of the HF gas would pass into the rig. The point of attachment of the radiolabelled HF reservoir to the rig also served as a point of attachment for a non - labelled HF reservoir during fluoride liability studies.

The CF_3CH_2Cl gas inlet allowed for the attachment of a CF_3CH_2Cl gas cylinder to the radiochemical catalyst testing rig. The flow of CF_3CH_2Cl was controlled using Monel metal valves (Whitey), a needle valve, and a flow meter.

The catalytic reaction vessel was a length of Monel tubing with a FEP (a fluorinated ethene propene copolymer) side arm attached. A Monel mesh bung was placed half way down the length of the tube. This prevented catalyst charged into the reactor from falling through the reactor into the line while at the same time allowing the free flow of gases through the reactor and catalyst bed. The FEP side

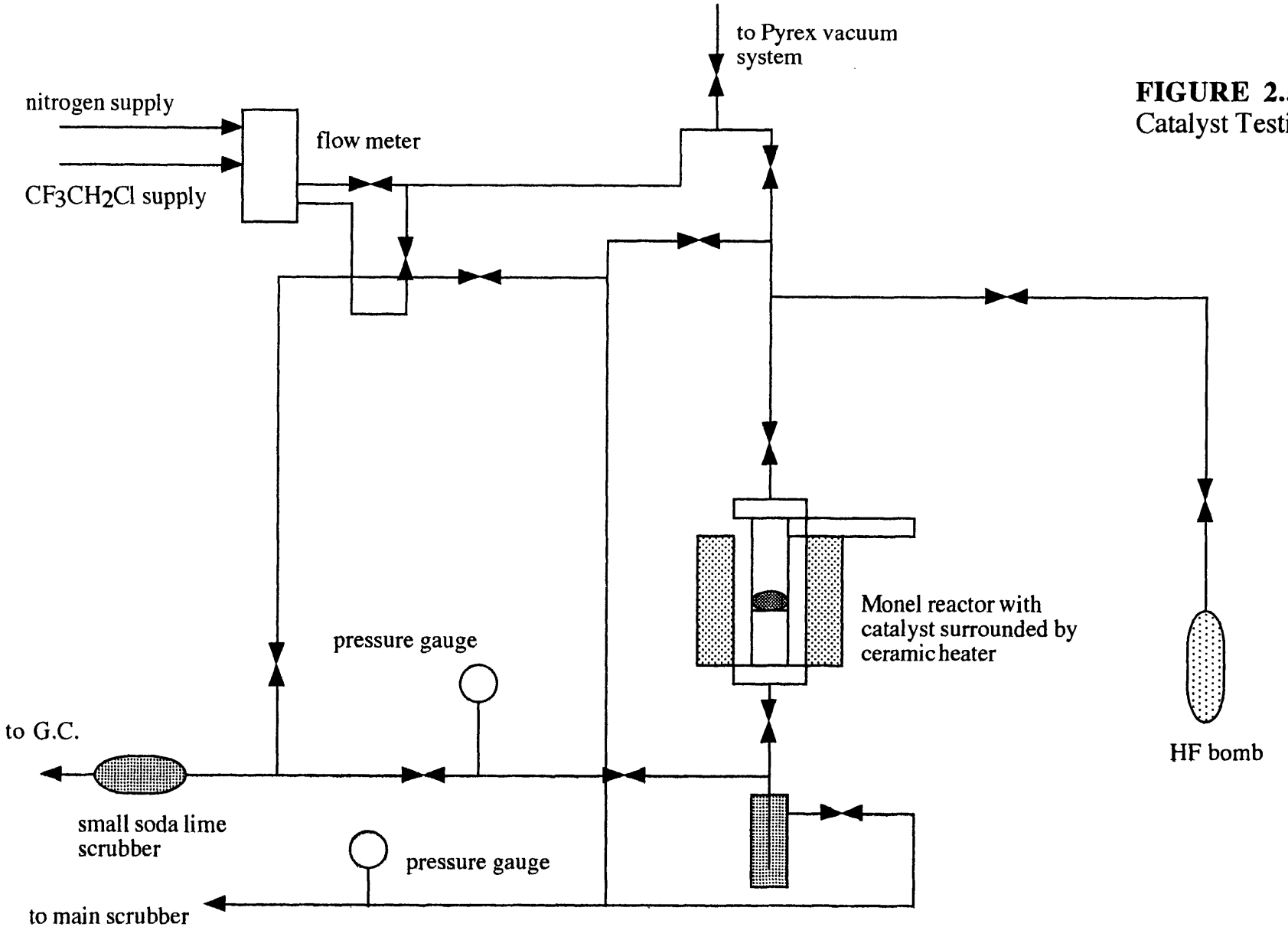

FIGURE 2.5 Radiochemical Catalyst Testing Rig

arm was used to count radiolabelled catalysts in a scintillation counter by tipping the catalyst into this arm after removal of the reaction vessel from the rig. A typical reaction is described in section 4.2..

Separate feed lines for radiolabelled HF and CF_3CH_2Cl allowed the catalyst to be treated with radiolabelled HF alone for catalyst labelling or CF_3CH_2Cl alone for fluoride liability experiments. A nitrogen flow was used to dry catalysts prior to reaction and clear the line of residual HF and CF_3CH_2Cl prior to removing the reactor for radiochemical counting.

The ROG could be passed through the main scrubber (soda lime) to remove any excess HF and was then vented into a fumehood. Alternatively ROG could be passed through a small scrubber to remove excess HF and into a gas chromatograph to monitor the products.

2.1.8. INERT ATMOSPHERE BOX.

A nitrogen atmosphere glove box (Lintott) (H_2O = 1 - 3 ppm typically) was used when handling and storing all samples. Glass vessels were evacuated and flamed out before being transferred to the box. The box contained an analytical balance allowing samples to be weighed precisely in a dry, inert atmosphere. Samples were placed into a transfer port prior to entering the box which could be evacuated with a rotary pump before being filled with nitrogen.

2.1.9. FLOW RIG FOR SURFACE AREA ANALYSIS.

A PTFE flow system at ICI, Runcorn, was used to measure the surface area of catalysts with nitrogen.

The main constituents of this flow system were the nitrogen flow line, the catalyst adsorption vessel and a gas chromatograph detector. The nitrogen flow line lead directly from the main nitrogen cylinder to the catalyst adsorption vessel. The flow rate of nitrogen was controlled via a pressure regulator (Norgren Ltd.) and a

needle valve. A three way tap (Whitey) allowed the flow of nitrogen to be measured prior to passing over the catalyst.

The catalyst adsorption vessel was a U - shaped vessel made from 1/4 inch copper tubing, into which catalyst was charged. During the experiment the U - shaped vessel was cooled in a flask of liquid nitrogen.

A helium gas flow which passed through the system via the nitrogen flow line, was used to dry catalyst in an oven prior to reaction and to determine the free flow of gases through the adsorption vessel as it was cooled in liquid nitrogen.

The ROG could be passed through a gas chromatograph linked to a chart recorder to record the presence of nitrogen gas coming from the catalyst adsorption vessel over the time of the experiment.

2.1.10. FLOW RIG FOR CATALYST CALCINATION.

An inert gas flow rig for calcining catalyst samples was used to induce degrees of crystallinity into amorphous chromia samples for future study.

The flow rig for catalyst calcination had three main features, a stainless steel catalyst reaction vessel, an inert gas flow system and a ceramic fibre heater. The inert gas flow system consisted of a nitrogen flow from the main cylinder into the stainless steel catalyst reaction vessel and from the catalytic reaction vessel into a scavenger waste system.

The stainless steel catalyst reaction vessel was a tube of 1/4 inch stainless steel with a central stainless steel body with a volume in excess of 100 cm^3 . Catalyst was charged into the central body of the vessel and one end of the 1/4 inch stainless steel tubing was blocked with 1/8 inch stainless steel rod.

The main body of the catalyst reaction vessel was housed in the centre of a ceramic fibre heater (Watlow Ltd.). This heater was capable of reaching temperatures of up to 1273K and the temperature was controlled by a programmable temperature control unit. A typical calcination is described in section 2.3.1.

2.2. PREPARATION AND PURIFICATION OF REAGENTS.

2.2.1. RADIOISOTOPES.

Extensive use was made of radiotracer techniques in this work. The radioisotopes used were :-

(I) [^{18}F] - FLUORINE

The isotope [^{18}F] - fluorine is a β^+ emitter. Annihilation of β^+ particles with negative electrons releases energy in the form of γ - radiation, which can be detected from both the surface and bulk of the material. The γ - emission energy is 0.51 MeV and the half life is 109.72 $\pm$ 0.6 min. (117).

This relatively short half life requires the completion of experimental work within one day. After 11 hours (6 half - lives) less than 2 % of the original activity remains.

(II) [^{36}Cl] - CHLORINE

The [^{36}Cl] - isotope has a half life of 3 x 10^5 years (118) and decays by β^- - emission. Although moderately energetic, self - adsorption, which is the interaction of emissions with the surrounding matter, will dictate that emission from the solid is limited to that from the surface. The isotope was supplied as a solution of $Na^{36}Cl$ (aq.) (Amersham International plc.). The 1 ml sample of $Na^{36}Cl$ (aq.) was removed from the suraseal bottle in which it was contained by withdrawing the solution from the cap of the bottle using a syringe. The $Na^{36}Cl$ (aq.) solution was injected into a graduated ampoule equipped with a B14 cone and high vacuum stopcock (J. Young). Concentrated hydrochloric acid was decanted into a beaker and a syringe was used to withdraw 9 ml of concentrated hydrochloric acid. The concentrated hydrochloric acid was injected into the ampoule containing the $Na^{36}Cl$ solution. This dilution with concentrated hydrochloric acid gave a solution with a specific [^{36}Cl] - chlorine activity of ca. 25μ Ci cm^{-3}. The above procedure was

performed in a fumehood contained in a secure area designated for radiochemical work. The bottom of the fume hood was covered with spillage trays lined with absorbent laboratory tissue. Apparatus used in this procedure was soaked in Decon 90 after use and thoroughly washed with water followed by storage in an oven designated for radiochemical use at 393K.

2.2.2 PREPARATION OF [^{18}F] - FLUORINE LABELLED CAESIUM FLUORIDE.

[^{18}F] - fluorine was prepared by the neutron activation of lithium carbonate (ca. 2g.) in the central core of the S.U.R.R.C. reactor at East Kilbride. This method used the sequence (EQN. 2.2):-

$$^{6}Li\ (\ n,\alpha\ )\ ^{3}H,\quad ^{16}O\ (\ ^{3}H,n\ )\ ^{18}F \qquad \text{EQN. 2.2}$$

The irradiation conditions were typically 50 min. at a flux of $3.6 \times 10^{1/2}$ neutrons $cm^{-2}\ s^{-1}$. The [^{18}F] - LiF produced from the irradiation was converted to [^{18}F] - HF by reaction with sulphuric acid (conc. H_2SO_4 : H_2O 1 : 1 by volume) in a specially designed round bottomed Pyrex reaction vessel. The vessel had a long neck and had an air compressor fitted to the top of the neck through a B14 glass socket. A large side arm with a dip tube attached to the end protruded from the side of the neck. This step was required to liberate the [^{18}F] - fluorine from the Li^{18}F and obtain it in a form from which it could easily be converted to CsF. The [^{18}F] - HF gas formed from the acid hydrolysis passed down the side arm, carried by the air flow created by the air compressor and was distilled into a solution of caesium hydroxide (aq.) contained in a PTFE test tube cooled at 273K in an ice bath. This solution was neutralised by addition of aqueous hydrogen fluoride in a Pyrex crystallising dish which was followed by evaporation to dryness on a hot plate to give [^{18}F] - CsF as a finely divided white powder.

2.2.3. PREPARATION OF [^{18}F] - FLUORINE LABELLED ANHYDROUS HYDROGEN FLUORIDE.

Simple isotopic exchange between $Cs^{18}F$ and HF will produce sufficient activity in $H^{18}F$ to carry out subsequent reactions. The procedure used in this work was developed previously in Glasgow (119) and involves the following exchange reaction (EQN. 2.3) :-

$$Cs^{18}F + HF \longrightarrow Cs^{+}[HF^{18}F]^{-} \longrightarrow H^{18}F + CsF \quad \text{EQN. 2.3}$$

This reaction was performed in a Monel bomb (100 ml volume) attached to the Monel vacuum system. In a typical preparation, $Cs^{18}F$ (2.00g) was heated with HF (12 mmol)at 523K for 60 minutes. During this time [^{18}F] - fluorine was exchanged between the $Cs^{18}F$ and HF forming $H^{18}F$. The [^{18}F] - fluorine labelled HF was distilled into a second Monel bomb for use in subsequent reactions. An aliquot of the labelled vapour (1 mmol), was distilled onto CsF powder (0.5g) charged into a single limb PTFE/FEP counting vessel and evacuated at 293K overnight. HF readily absorbs onto CsF powder and this was used to determine the specific count rate of $H^{18}F$ by counting the aliquot on a solid.

2.2.4. PREPARATION AND PURIFICATION OF [^{36}Cl] - CHLORINE LABELLED HYDROGEN CHLORIDE.

[^{36}Cl] - chlorine labelled hydrogen chloride (120, 121)was generated in an apparatus consisting of a reaction vessel with a dropping funnel and a pressure equilibrating arm, to which a series of cooled traps were attached (Fig 2.6).

Traps (I), (II) and (IV) contained phosphorus pentoxide as a drying agent. Traps (I) and (II) were cooled to 213K in dichloromethane / dry ice baths. The collection vessel (III) was equipped with high vacuum stopcocks to isolate it from the rest of the apparatus and this vessel was cooled in an isopentane / liquid N_2 bath.

FIGURE 2.6 $H^{36}Cl$ Preparation Apparatus

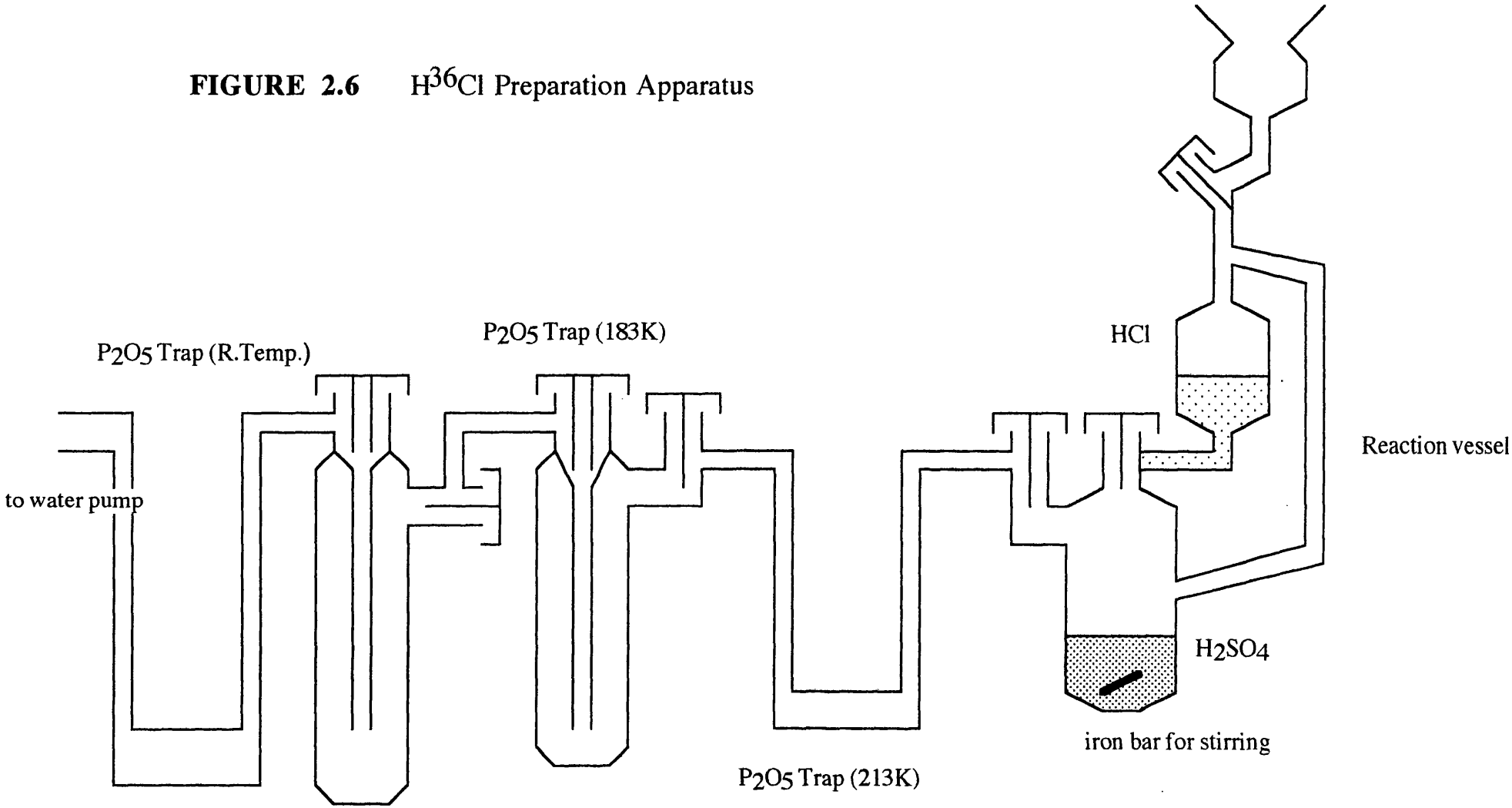

Aqueous [^{36}Cl] - chlorine labelled sodium chloride (1.0 ml, 250 μCi, Ammersham International plc.) was diluted with conc. HCl (9.0 ml), as described in section 2.2.1 and this solution was added dropwise to concentrated sulphuric acid. The [^{36}Cl] - chlorine labelled hydrogen chloride generated was distilled through traps (I) and (II) and collected in the collection vessel (III), then transferred to a vacuum line where the [^{36}Cl] - HCl was degassed and vacuum distilled into a Monel bomb containing phosphorus pentoxide. The yield of [^{36}Cl] - HCl from this preparation was 40 mmol and this [^{36}Cl] - HCl had a typical ^{36}Cl count rate of 1144 count min^{-1}.

DETERMINATION OF SPECIFIC COUNT RATE OF [^{36}Cl] - HCl.

[^{36}Cl] - HCl was vacuum distilled onto an excess of frozen aqueous NaOH solution and both were allowed to warm and react in a closed vessel at room temperature for at leased three hours. The resultant solution was decanted into a beaker. The vessel was washed out with distilled water and the washings were added to the solution in the beaker. The solution was acidified with ten drops of concentrated nitric acid.

Under subdued light a solution of silver nitrate (0.22 mol. L^{-1}, > 98% pure, Johnson Matthey) was added with stirring until precipitation of AgCl was judged to be complete. The precipitate was allowed to settle and a few more drops of silver nitrate were added. The suspension was heated on a hot plate nearly to boiling with occasional stirring and digested until the precipitate coagulated. The beaker was removed from the hot plate and allowed to settle. The beaker was then set aside in a dark cupboard for at least one hour.

A sintered glass crucible (porosity 4) was dried to constant weight at 423K. The precipitate was filtered with very dilute nitric acid (approximately one part concentrated nitric acid to one thousand parts distilled water) and washed in the crucible with very dilute nitric acid until 3 ml of the washings gave no turgidity

with dilute hydrochloric acid. The crucible and precipitate were dried to constant weight at 423K. [^{36}Cl] - HCl was converted to [^{36}Cl] - AgCl with an efficiency > 85%. Accurately weighed portions of [^{36}Cl] - AgCl obtained were counted using a Geiger - Müller tube in a lead castle for periods of time sufficient to accumulate significant (10^4) counts.

2.2.5. PREPARATION AND PURIFICATION OF [^{36}Cl] - CHLORINE LABELLED CF_3CH_2Cl.

[^{36}Cl] - chlorine labelled CF_3CH_2Cl was prepared by halogen exchange with CF_3CH_2F and [^{36}Cl] - HCl over a chromia catalyst which was amorphous by XRD (Eqn. 2.4).

$$FCH_2CF_3 + H^{36}Cl \xrightarrow[\text{chromia}]{673K} [^{36}Cl]CH_2CF_3 + HF \qquad \text{Eqn. 2.4}$$

Amorphous chromia (ICI ref. TR176, prepared from chromium hydroxide) was loaded into a Monel bomb and attached to a Monel vacuum line. The bomb was heated to 523K under vacuum for 3 h. Using a ceramic fibre heater (Watlow), temperature was monitored using a thermocouple wire connected to a ratemeter and the temperature was controlled with a Variac transformer. The bomb was cooled in liquid nitrogen and CF_3CH_2F (6.1 mmol., ICI) and [^{36}Cl] - HCl (6.0 mmol.) were distilled into the bomb which was then heated to 673K.

Sampling and subsequent analysis of samples by gas chromatography revealed that 95 % of the CF_3CH_2F was converted to CF_3CH_2Cl after one hour.

Removal of [^{36}Cl] - HCl and HF from the reaction effluent was achieved by distillation of the reaction products into a vessel containing moist NaOH pellets. The products were allowed to warm to room temperature in the presence of the moist NaOH pellets to remove unreacted $H^{36}Cl$ and HF and an infrared spectrum of

the gas phase was taken using the procedure detailed in section 2.4. This procedure was repeated until $H^{36}Cl$ and HF were absent from the infrared spectra.

2.3. PREPARATION OF CATALYSTS.

Chromia catalyst prepared industrially by ICI Chemicals and Polymers Ltd. (ICI ref. TR176) was used to prepare all catalysts under study. The industrial chromia catalyst was prepared by ICI, Runcorn by slow addition of aqueous ammonia to a solution of aqueous chromium(III) nitrate (122). The chromium hydroxide obtained was dried in air at 373K and then calcined in an inert atmosphere at 500 - 700K. XRD analysis determined that this chromia was amorphous.

The catalyst was received in the form of pellets which were ground before use. The required particle size of the catalyst (0.5 mm - 1.4 mm) was obtained using laboratory test sieves.

2.3.1. CALCINATION OF CHROMIAS.

Industrial chromia was calcined under various conditions to produce differing percentages of α - chromia phase. Calcinaton of ground industrial chromia was performed under a nitrogen atmosphere. The required quantity of catalyst (typically 40.0g) was charged into the stainless steel reaction vessel, plugged with 1/8 inch stainless steel rod, in the catalyst calcination rig and the reaction vessel was placed into the centre of the ceramic fibre heater. The nitrogen gas flow system was attached to allow the flow of nitrogen through the catalyst bed from top to bottom and then into the scavenger waste system. A thermocouple rod, connected to the temperature programmer, was inserted half way into the ceramic fibre heater central core touching the outside wall of the central body of the stainless steel reactor.

The degree of calcination was determined by the temperature ramping rate, the final temperature and the length of time that the catalyst was held at the final

temperature ('dwell time'). These parameters were programmed using the temperature programmer associated with the ceramic fibre heater.

2.3.2. ZINC DOPING OF CHROMIAS WITH ZINC(II) CHLORIDE.

The method used was a wet impregnation with aqueous zinc(II) chloride solution. The required amounts of zinc(II) chloride and chromia were weighed accurately into 100 cm^3 Pyrex beakers and the zinc(II) chloride was dissolved in distilled water (5 - 15 cm^3.). The preweighed ground and calcined chromia was poured carefully into the aqueous zinc chloride solution and the mixture was allowed to stand for two hours.

Following the standing period the chromia / aqueous zinc(II) chloride mixture was heated on a hot plate to drive off water and this process was assisted using a hot air gun mounted on a retort stand directed towards the top of the beaker. When all visible traces of water were driven from the mixture the catalyst was stored in a labelled glass sample jar.

Four different chromias were each impregnated with differing amounts of zinc(II). Chromias calcined to a maximum temperature of 973, 873 and 723K were impregnated with 0, 0.25 and 4 w/w % Zn(II). Amorphous chromia was impregnated with 0, 1, 3, 5 and 15 w/w % Zn. The mass of $ZnCl_2$ and chromia to be used in each impregnation was determined using EQN. 2.5 :-

$$\text{w/w \%} = \frac{(\text{mol } ZnCl_2 \times \text{Atomic mass Zn})}{(\text{mass } Cr_2O_3 + \text{mass } ZnCl_2)} \qquad \text{EQN 2.5}$$

Where mass Cr_2O_3 + mass $ZnCl_2$ = Total mass of catalyst required and atomic mass Zn = 65.38g

This equation can be rearranged to give EQN 2.6 :-

$$\text{mass } ZnCl_2 = \text{RMM } ZnCl_2 \times \frac{(\text{mass } Cr_2O_3 + ZnCl_2) \times w/w\ \%}{\text{atomic mass Zn}} \quad \text{EQN 2.6}$$

Where relative molecular mass (RMM) $ZnCl_2$ = 136.286g

The required mass of chromia and $ZnCl_2$ used in each impregnation was weighed accurately to 4 figures using an analytical balance.

2.3.3. FLUORINATION OF CHROMIAS.

The catalyst (typically 10g) was loaded into the large left arm of the U - shaped Monel catalyst fluorination vessel. The vessel was attached to the flow line for catalyst fluorination inside of the oven. A nitrogen gas flow of 0.0537 mol h^{-1} was passed through the catalyst bed, from bottom to top, and the oven was heated to 573K for 40 minutes. This drying period served to remove water and hydroxyl groups from the surface.

During the drying period a steady HF flow of 0.0537 mol h^{-1} was established through the reactor bypass using a nitrogen carrier gas flow of around 0.0134 mol h^{-1}. When the drying period was over the nitrogen passing through the catalyst bed was discontinued and the HF flow passing through the reactor bypass was diverted to flow through the reactor.

Following the diversion of the HF flow through the reactor the ROG was constantly monitored for any trace of HF gas. When HF was detected at the ROG outlet the oven temperature was increased to 623K and the reaction proceeded for 17 h..

At the end of the 17 h. period the HF flow was discontinued and the oven temperature reduced to 293K. Nitrogen was passed through the system for 2 h. To remove HF remaining in the rig. The Monel valves at the two ends of the reactor were closed and the reactor was removed from the flow rig. The fluorinated samples were stored under nitrogen in the dry box.

2.4. INFRARED SPECTROSCOPY.

2.4.1. TRANSMISSION INFRARED SPECTROSCOPY OF GASES.

Infrared spectroscopic analysis of reactants and products from the reaction to produce [^{36}Cl] - chlorine labelled CF_3CH_2Cl were performed using a gas IR. cell (Fig. 2.7) which could be attached to the vacuum system. The IR. cell was fitted with AgCl windows and had path length 10 cm.. A B14 cone and high vacuum stopcock (J. Young) allowed attachment to a Pyrex glass vacuum system and a Monel metal vacuum system, through a brass socket, for convenient gas handling.

Vapour was expanded into the gas cell to the desired pressure (usually 25 Torr). The gas cell was then fitted to the spectrometer, using a specially designed holder to ensure reproducible positioning of the cell in the spectrometer beam.

IDENTIFICATION OF GASEOUS SAMPLES.

In all infrared spectroscopic analysis species were assigned by comparison with standard vapour phase spectra obtained from the Aldrich Library of Infrared Spectroscopy or vapour phase spectra of pure standard samples. Analytically useful peak positions are presented in Table 2.1.

Table 2.1 Principal IR. Peaks for Possible Reaction Products

Compound	**Wavelength (cm^{-1})**
HCl	2900 - 2800
HF	3962
CF_3CH_2F	1464, 1428, 1300, 1188, 1104, 972, 842, 666, 550
CF_3CH_2Cl	1440, 1338, 1280, 1158, 1112, 856, 800, 638

FIGURE 2.7 Pyrex Glass Gas Infrared Cell

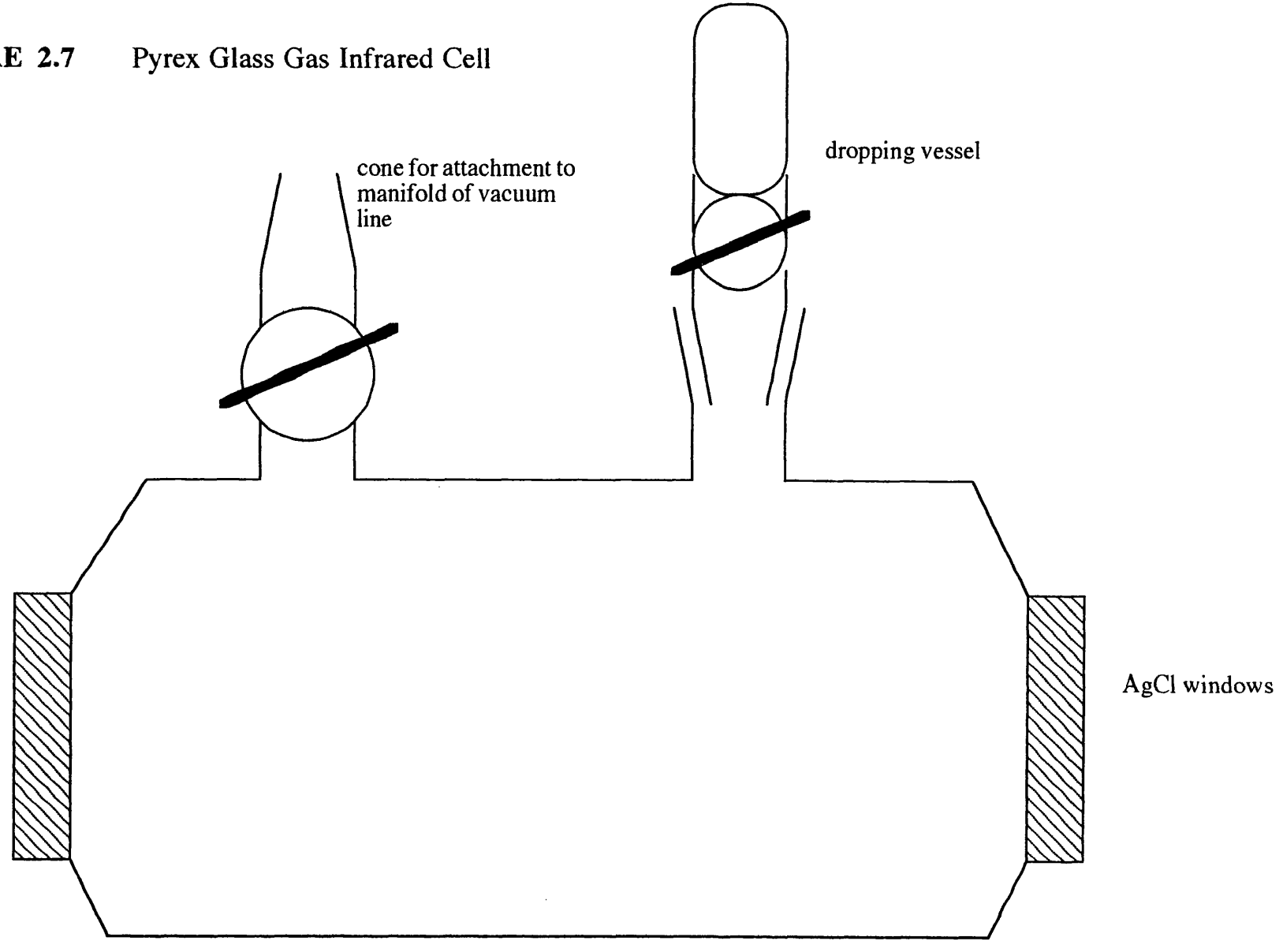

2.5. GAS CHROMATOGRAPHY.

Samples were analysed by gas chromatography using a Varian 3400 G.C. fitted with a F.I.D., a 50 m capillary column with injection via gas sampling valve onto the column. Helium was used as a carrier gas with a flow rate of 8 cm^3 min^{-1}. Identification of species present was by analysis of pure standard samples.

ANALYSIS METHOD

Initial Column Temp. : 35°C. ; Column Hold Time : 7.5 min. ; Final Temp : 150°C ; Hold time : 2.2 min. ; Ramp Rate : 50°C min^{-1} ; Injector Temp. : 200°C; Detector Temp : 250°C; Sensitivity Factor : ± 5 %; Response Factor : linear response, CF_3CH_2Cl : CF_3CH_2F ratio of 1 : 1.08; Retention Times : CF_3CH_2Cl : 0.84 min., CF_3CH_2F : 0.64 min, CF_2CHCl : 0.72 min.

2.6. X - RAY PHOTOELECTRON SPECTROSCOPY.

X - ray photoelectron spectroscopy(XPS) is a surface technique which probes approximately the top 5 nm of a sample surface. All elements, with the exception of hydrogen and helium are detectable by XPS.

XSP analysis of samples was performed by the Analytical and Physical sciences Group, Surface science Team at ICI, Runcorn. Samples were prepared for analysis using Analytical and Physical sciences Standard Operating Procedure. Samples were analysed in a VG ESCALAB 200 - D X - ray photoelectron spectrometer.

2.7 TRANSMISSION ELECTRON MICROSCOPY

Transmission electron microscopy is a technique which can be used to determine crystallites on solid surfaces. Transmission electron microscopy was performed by the Electron Microscopy Group in the Department of Chemistry in the University of Glasgow on samples prepared during the course of this work.

Micrographs and diffraction patterns from the samples were obtained and analysed with the aid of the Electron Microscopy Group. 'd' Spacings were calculated from micrographs and diffraction patterns with the aid of an eye piece. Calculated 'd' spacings were compared to 'd' spacings for various compounds listed in the Joint Committee on Powder Diffraction Standards (JCPDS) Powder Diffraction File.

2.8 X - RAY DIFFRACTION

X - ray diffraction (XRD) is designed to give information on phases present, the degree of crystallinity and the crystallite size of samples. The Analytical and Physical sciences Group at ICI, Runcorn performed XRD on catalyst samples. Samples were prepared using Standard Operating Procedures which involved grinding using an agate pestle and mortar and loading samples into a standard Phillips deep pack, stationary, XRD specimen holder. Catalysts were examined using a Phillips Automatic Powder Diffraction Unit, with PW 1800 generator. This operates at 50KV and 40ma using a long fine focus copper tube. The ganiometer is fitted with a graphite monochromator and proportional counter.

Chromia samples were examined using a method based on a standard α chromia sample which was used for comparison with chromia present in the samples. Reference data used in this interpretation was obtained from the Joint Committee on Powder Diffraction Standards. The standard used for each determination was a National Institute of Standards and Technology (NIST) α - chromia. Previous work carried out at Runcorn, by the Analytical and Physical Sciences Group, on this sample, indicated that the chromia present in the sample was not a true α - chromia in crystallographic terms as it contained traces of non α - chromia. Selected reflections, the 012, 104, 110 and 113 reflections, of the sample were directly compared to the standard by the Analytical and Physical Sciences Group and a percentage of "crystallinity" was calculated for each reflection from this comparison.

A full scan of the sample from 2 - 70° 2θ was carried out over the range of interest, to assess phases present, counting for four seconds per point and 50 points per degree. To estimate crystallinity both the standard and the unknown were examined in duplicate to assess the relative areas of the four reflections (i.e. the 012, 104, 110 and 113). These areas are 23.2 - 26.0, 32.5 - 35.0, 35.0 - 37.5 and 40.6 - 42.5° 2θ respectively. For example an industrial chromia sample calcined to a maximum temperature of 723K for 12 h. was estimated to have <5 % α - chromia from the 012 reflection and 5 - 15 % α - chromia from the 110 reflection..

2.9 RADIOCHEMICAL COUNTING.

2.9.1. GEIGER MÜLLER COUNTERS.

A Geiger - Müller tube (123, 124) consists of an earthed metal tube with a thin gas tight mica window at one end and a gas tight central support for a central wire at the other (Fig. 2.8). The tube is filled with a gas mixture. An example of a typical gas mixture was 90 % argon and 10 % methane, which becomes partially ionised when radiation enters the detector producing positive ions and free electrons. The inside wall of the tube forms an enclosed cylindrical cathode with the central wire forming the anode, which is held at a high positive potential with respect to the wall cathode. Hence the electrons which formed move rapidly towards the central wire and the positive ions drift relatively slowly towards the wall.

As the potential difference between the wall and wire is increased, electrons gain sufficient energy to cause further ionisations as they collide with gas molecules. Hence the number of electrons collected on the wire becomes greater than the number created by the passage of radiation through the detector gas. This is called ion multiplication.

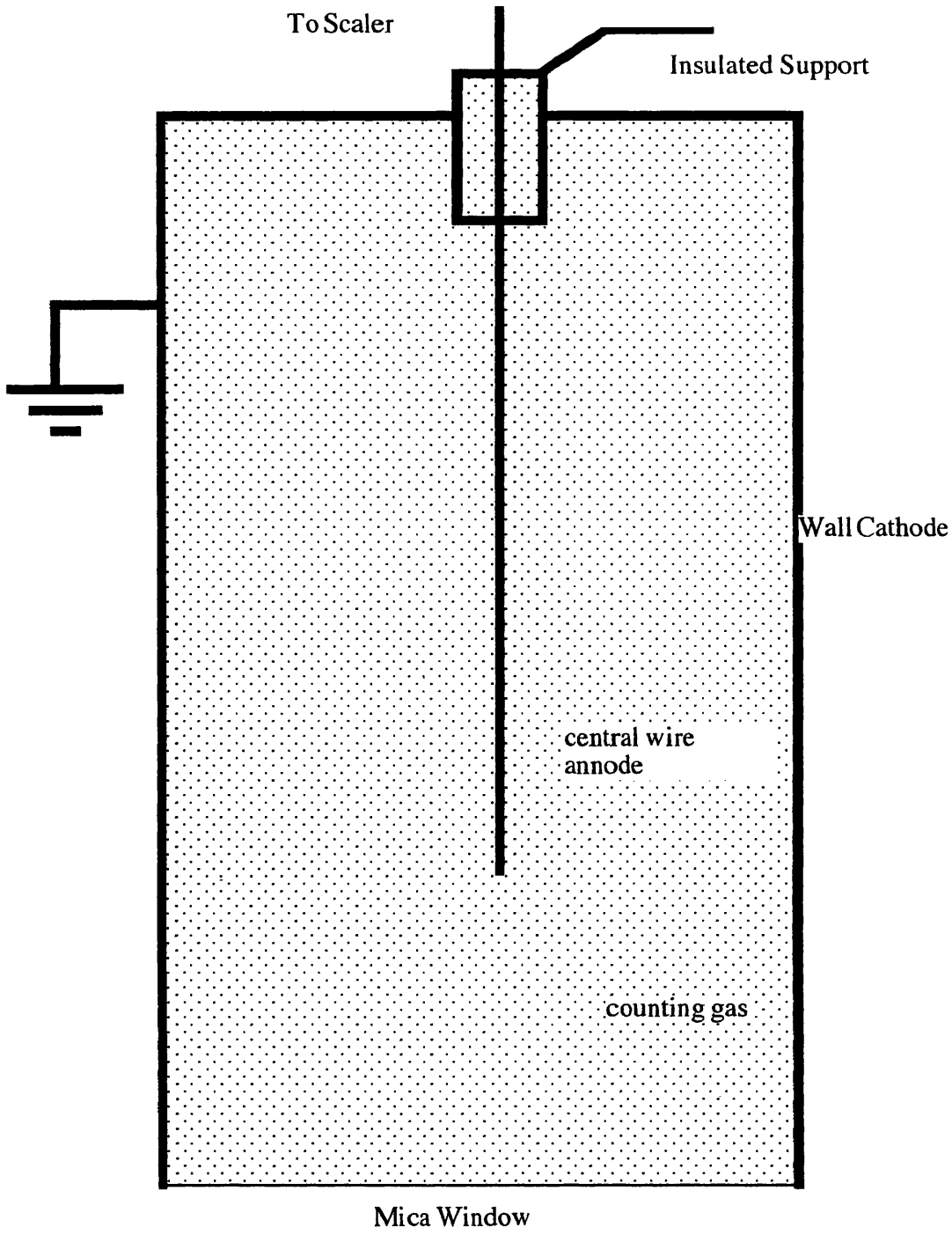

FIGURE 2.8 Geiger - Muller Tube

Increasing the wire voltage further increases the extent of ion multiplication until a finite limit is reached, known as the Geiger region, where the number of electrons produced by radiation becomes so great that this "electron avalanche" effect which is created spreads along the entire anode wire. In this state the detector is said to be saturated. The number of electrons detected on the wire and hence the magnitude of the resultant voltage pulse is independent of the number of electrons created by the passage of radiation through the detector.

Methane (or alcohol or ether vapour) is present in the tube to act as a "quench gas". When positive ions formed by ion multiplication reach the cathode they can cause secondary emission from the wall surface which can lead to a spurious discharge of the counter. This undesirable effect is suppressed by the quench gas which reacts by electron transfer with the positive ions to yield ultimately unstable products.

2.9.2. DEAD TIME

The electrons formed in a Geiger - Müller tube reach the central wire very quickly, typically in about 5×10^{-7} s.. However, the positive ions formed from ion multiplication remain in the vicinity of the wire for a short time. This sheath of positive ions reduces the voltage gradient below the value necessary for ion multiplication (Vo), and an other event cannot be recorded until the positive ions reach the cathode, which typically takes about 3×10^{-4} s.. The insensitive period is called the dead time and it is important that a correction is made for counts lost during the dead time in counting experiments, particularly at high counting rates.

Dead times of Geiger - Müller tubes were determined by counting samples of [^{18}F] - CsF for > 330 min.. Equation 2.7 is general for radioisotopes.

$$A_t = A_0 e^{-\lambda t} \qquad \text{Eqn. 2.7}$$

Where

λ = decay constant in s^{-1}

A_t = activity of sample at time t

A_0 = activity of sample at time 0

Thus a plot of $\ln A_t$ vs. time should be linear with gradient $-\lambda$ and intercept $\ln A_0$. Plots of this type were constructed for [^{18}F] - CsF counts. Plots obtained were near linear at $t > 1.5 \times 10^4$ s., but showed curvature at $t < 1.5 \times 10^4$ s. which was due to the effect of dead time at higher counting rates (Fig. 2.9). The linear portion of the plot was extrapolated to t = 0. This gave N_t the calculated true count rate at any time t which is related to N_0 the observed count rate at any time t, by equation 2.8, where τ is the dead time.

$$N_t = N_0 / (1 - N_0 \tau) \qquad \text{Eqn. 2.8}$$

τ can be calculated from N_t and N_0 by rearranging Eqn. 2.8 to give Eqn. 2.9

$$\tau = 1 / N_0 - 1 / N_t \qquad \text{Eqn. 2.9}$$

Hence the calculated dead time from Fig. 2.9 is 6.49×10^{-4} s..

2.9.3. PLATEAU REGIONS.

The voltage plateau of a Geiger - Müller counter is a region in which the counting rate caused by a given radiation source is approximately independent of the applied voltage. It is desirable to work at a voltage which is in the middle of the plateau region. The plateau region was determined for each Geiger - MÜller counter used by constructing a plot of counts obtained from a solid β^- source vs. applied voltage. Fig. 2.10 shows a typical plateau curve obtained. As the applied voltage was increased above the minimum voltage required to produce ion multiplication,

FIGURE 2.9 Plot of $\ln A_t$ vs. Time for [^{18}F] - CsF

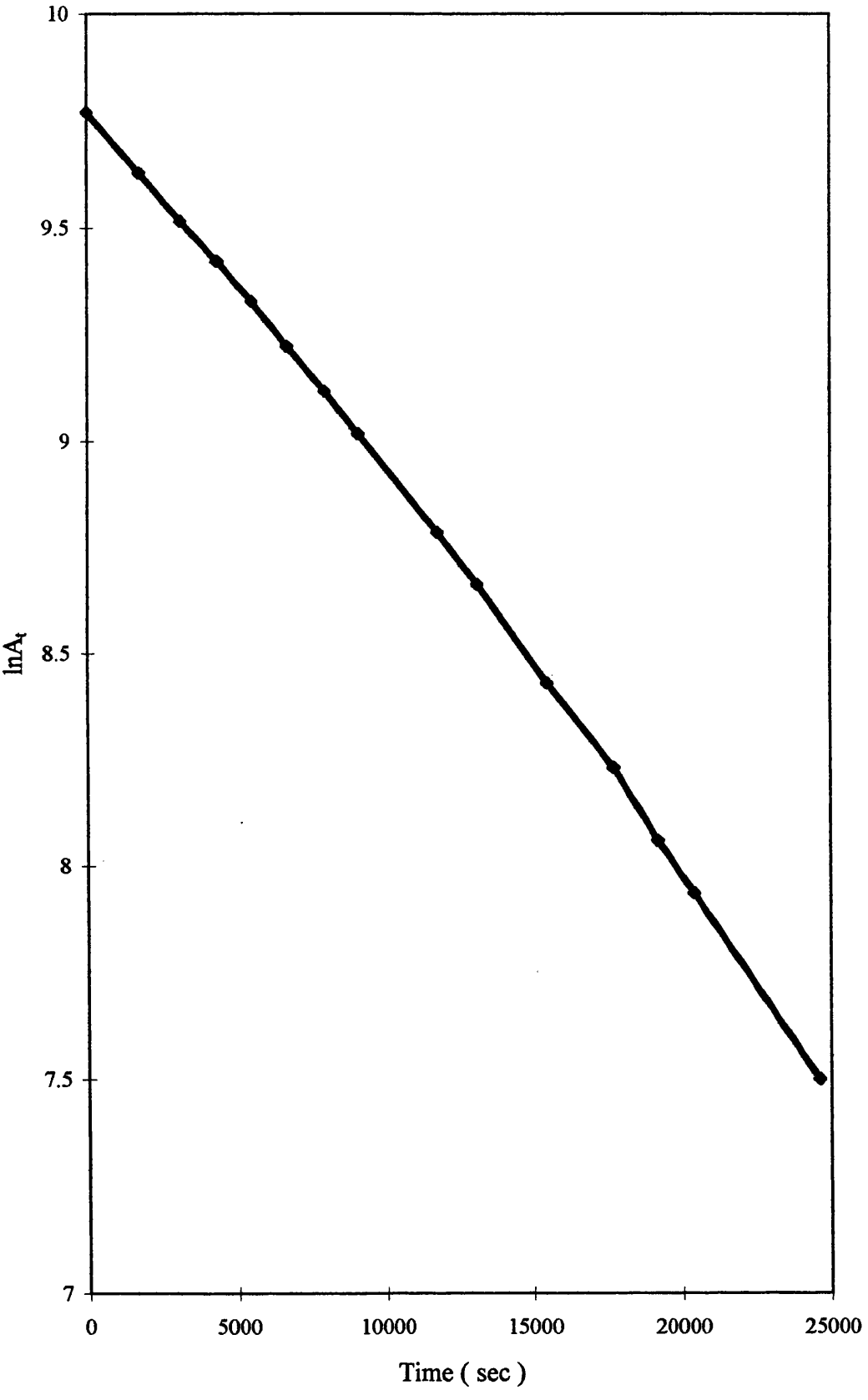

FIGURE 2.10 Plot of Counts From [226Ra] - Radon Source vs. Applied Voltage

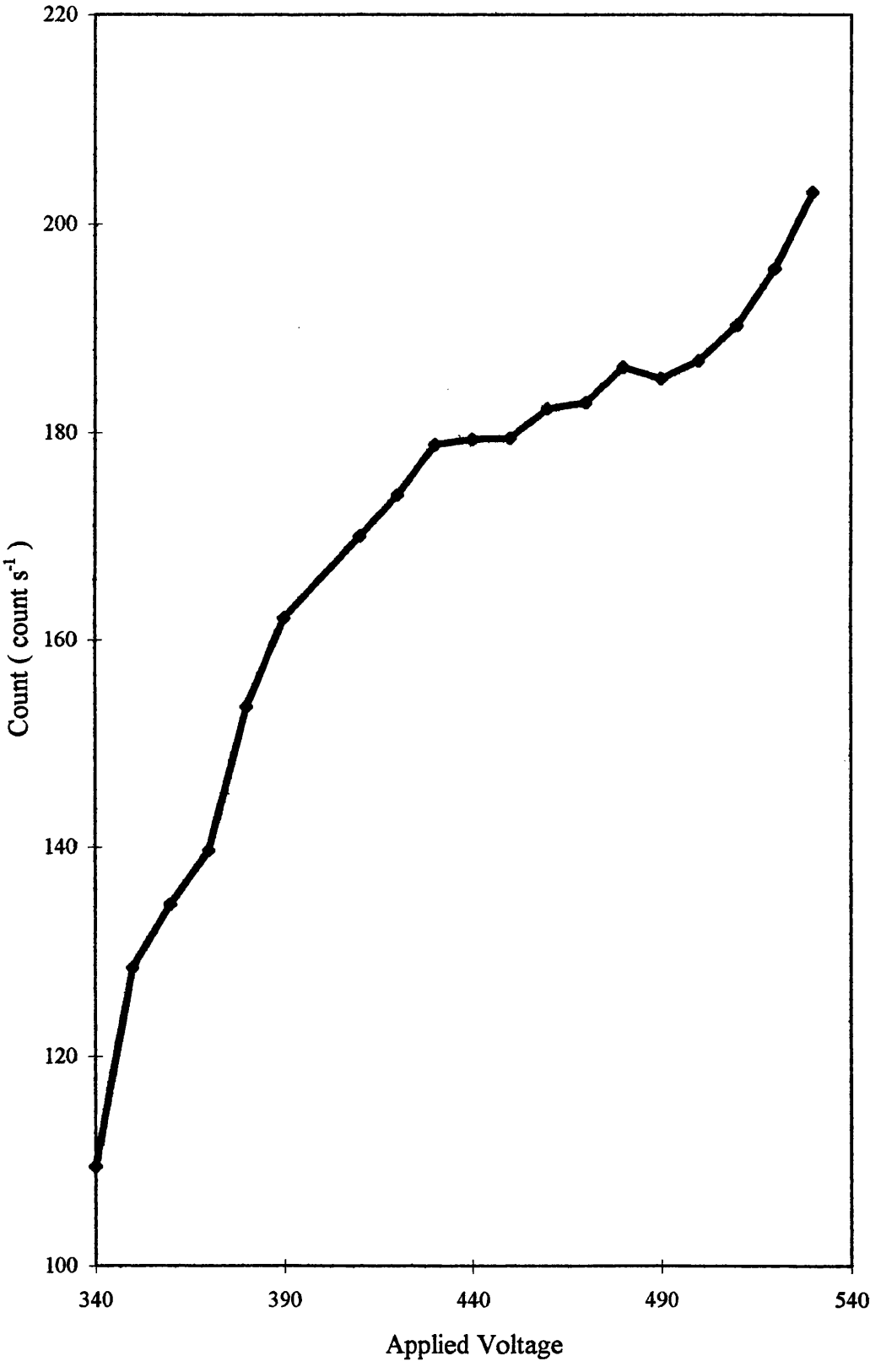

Vo, the count rate increased until the plateau region was reached. As the applied voltage was increased towards the end of the plateau region the count rate began to increase and then increased very steeply. This effect is due to the counter beginning to discharge as the quench gas becomes unable to suppress secondary electron emission at the cathode wall. A working plateau region was typically 380 to 460 V and an operating voltage in the region of 440 V was employed.

2.9.4. BACKGROUND.

Since Geiger - Müller counters detect individual ionising events, they register some counts in the absence of a radioactive source, for example, from naturally occurring radioisotopes in the environment such as materials used in the construction of the laboratory and cosmic radiation. An average background count must be subtracted from all counts in radiochemical counting to correct for this effect. Typical background count rates were 20 - 30 count min^{-1}.

2.10 DIRECT MONITORING GEIGER - MÜLLER COUNTING TECHNIQUE.

This method was developed by Thomson and modified by Al - Ammar and Webb (125) (126) to determine surface radioactivity on solids exposed to radiolabelled gases. The technique has proved useful in the determination of adsorption mechanisms in heterogeneous catalysis allowing *in situ* monitoring of the reaction between solid surfaces and radiolabelled gases.

2.10.1. EQUIPMENT.

The counting vessel consisted of an evacuable Pyrex reaction vessel (Fig. 2.11) containing two Geiger - Müller counters and connected via a manifold to a constant volume manometer and gas handling facilities. A Pyrex "boat" with two sections, was placed inside the counting vessel and this could be moved along the

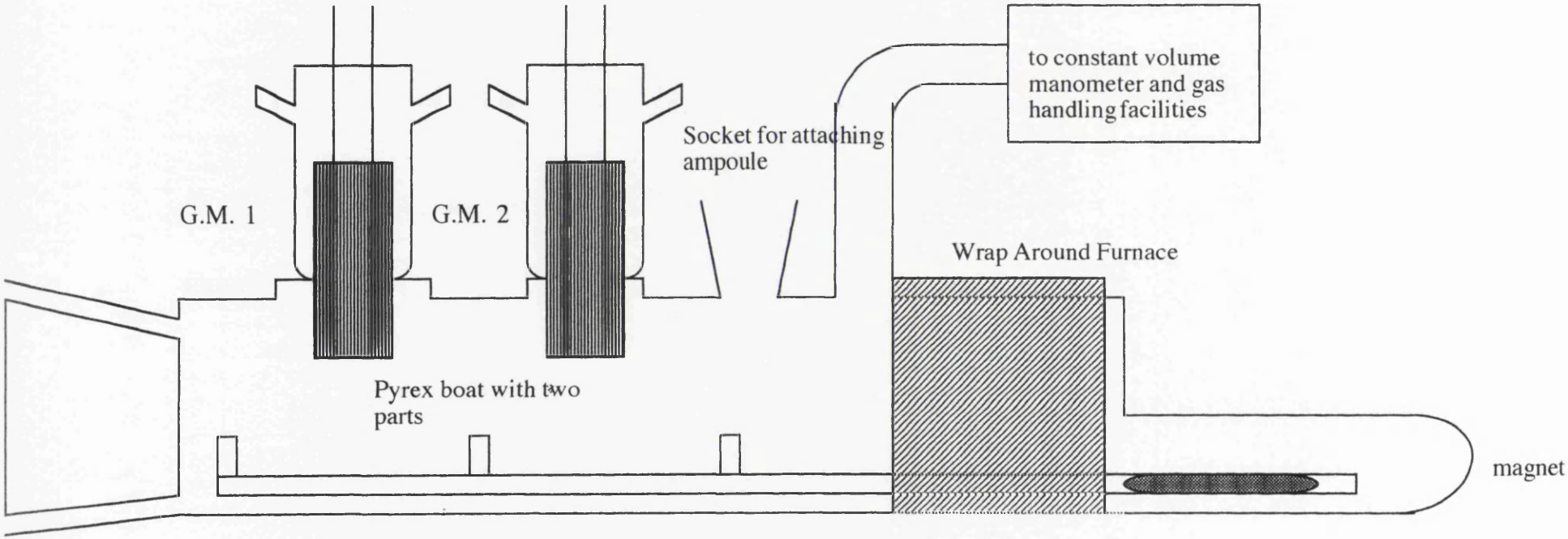

FIGURE 2.11 Counting Cell

length of the vessel using a magnet. The counting vessel was fitted with a B14 socket for the attachment of an ampoule containing the solid to be studied, thus enabling an air or moisture sensitive solid to be introduced into the counting vessel under vacuum. The apparatus was calibrated prior to use. The Geiger - Müller counters were calibrated by monitoring counts using varying pressures of radioactive gas. A plot of pressure against counts should give a straight line which passes through the origin. Fig. 2.12 shows a typical calibration. When counts from the two Geiger - Müller tubes were plotted against each other (Fig. 2.13) a straight line was obtained. The gradient of this line is equal to the counting ratio of the two tubes. The counting ratio should remain constant and was usually in the region of 0.85.

2.10.2. EXPERIMENTAL METHOD.

A sample of catalyst (1.0g) was transferred to a small dropping ampoule in the dry box, degassed and attached to the evacuated, flamed out counting vessel. The solid was dropped from the ampoule into the left hand section of the "boat", which was positioned so that the left hand section of the boat was directly under Geiger - Müller 1 and the right hand section of the boat was directly under Geiger - Müller 2. Thus, G.M.1 recorded counts from gas plus solid and G.M.2 recorded counts from gas alone.

Radioactive gas was introduced to the counting vessel at a desired initial pressure. The reaction vessel was then isolated from the rest of the system and counts were taken from both Geiger - Müller tubes for a measured time. All counts were corrected for background, dead time, and intercalibration. The counts from G.M.2, gas alone, were subtracted from the counts from G.M.1, gas plus solid, to give values for surface counts alone.

FIGURE 2.12 Plot of Count From Geiger - Muller Counter vs. Pressure (atm.) of $CF_3CH_2{}^{36}Cl$ Gas

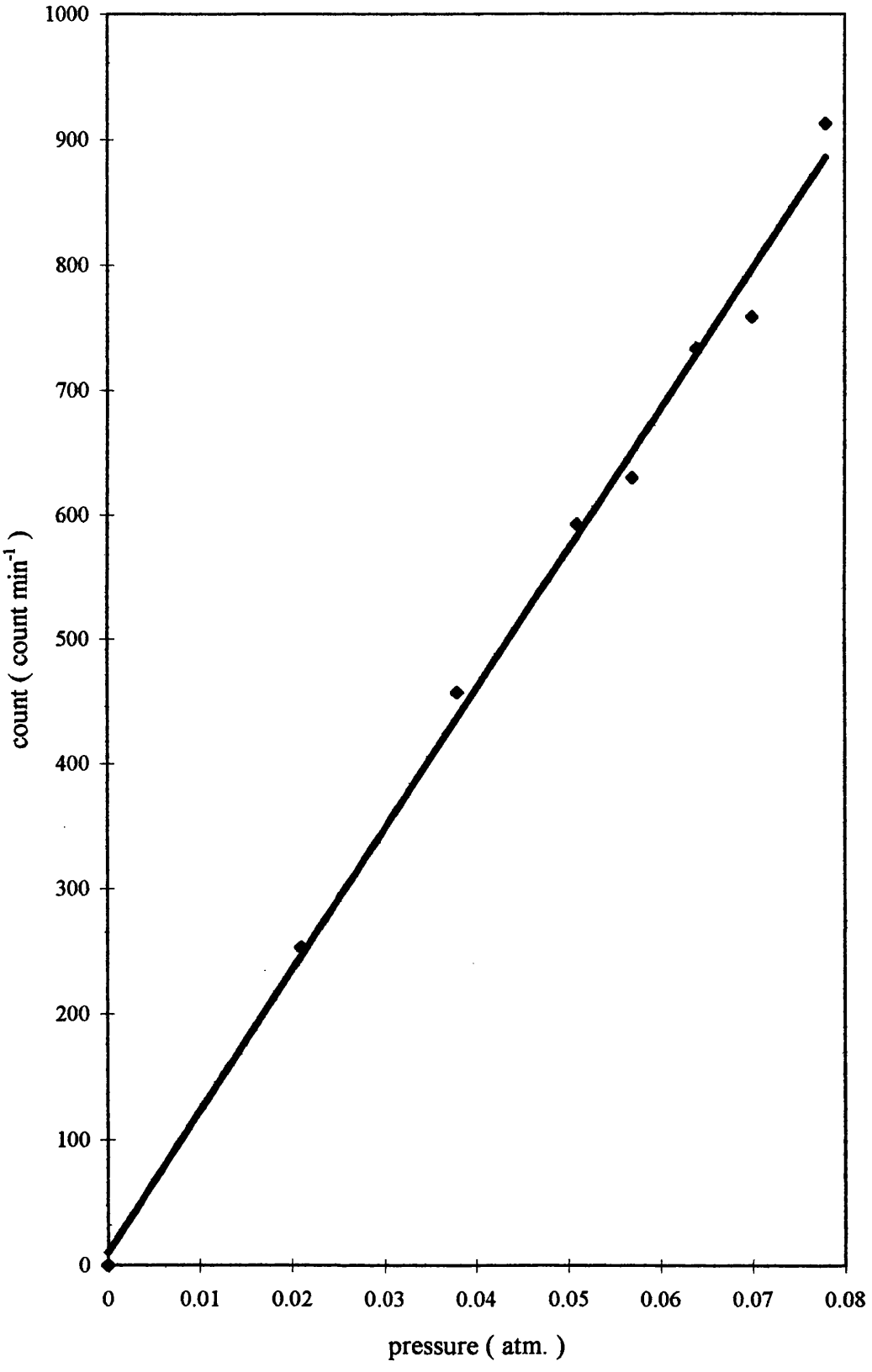

FIGURE 2.13 Plot of Count of Geiger - Muller Counter 1 vs. Geiger - Muller Counter 2 for Increasing Pressures of $CF_3CH_2{}^{36}Cl$

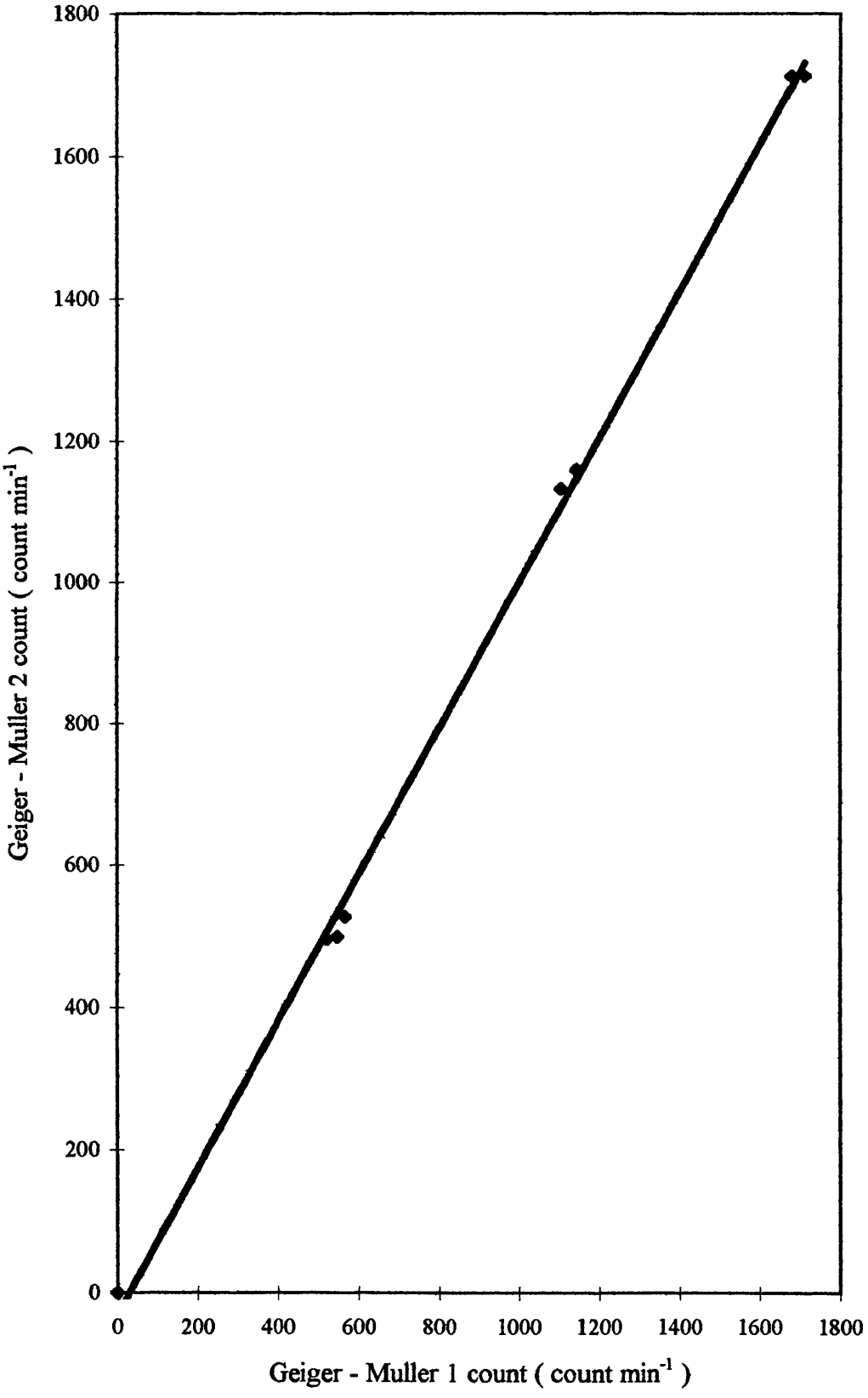

2.11 SCINTILLATION COUNTERS

When energetic photons enter certain crystals, short duration flashes, known as scintillations, are observed (124). This phenomena forms the basis of the technique used for detecting γ - radiation. The most widely used crystal for γ - detection is sodium iodide containing small quantities of thallium (I) iodide (0.1 - 0.2 %). The high density of NaI (3.7 gcm^3) and the high Z value of iodine make this a very efficient γ - ray detector. Thus the problem of detecting γ - photons is reduced to the problem of detecting visible light scintillations.

A photomultiplier tube (PMT), which essentially converts light flashes into electrical impulses, is used as the standard device for detecting small numbers of photons. When a γ - photon interacts with Na / Tl crystal a scintillation, which consists of several visible light photons, is detected by the photomultiplier which converts it into a shower of electrons by accelerating them by an electrical potential gradient to an electrode producing an approximately fourfold increase. These secondary electrons are similarly accelerated so that in a ten stage photomultiplier tube there is a gain of 10^4. The electrons are collected on the anode of the tube producing a negative pulse of short duration on the anode. The pulses are amplified and passed to a scaler ratemeter, where they are recorded. The magnitude of the voltage pulses is proportional to the energy of the γ - photons which give rise to scintillations.

To achieve a maximum pulse the scintillation crystal is surrounded by a reflector. The space between the crystal and the photomultiplier is filled with high viscosity paraffin or silicone oil, to improve light transmission. The scintillation counter and the scaler were calibrated before use using a [^{60}Co] source which emits γ - rays of energy 1.33 MeV. The γ - ray spectrum obtained by monitoring counts from a $Cs^{18}F$ source while varying the applied threshold is shown in Fig. 2.14.

FIGURE 2.14 Gamma Ray Spectrum of $Cs^{18}F$

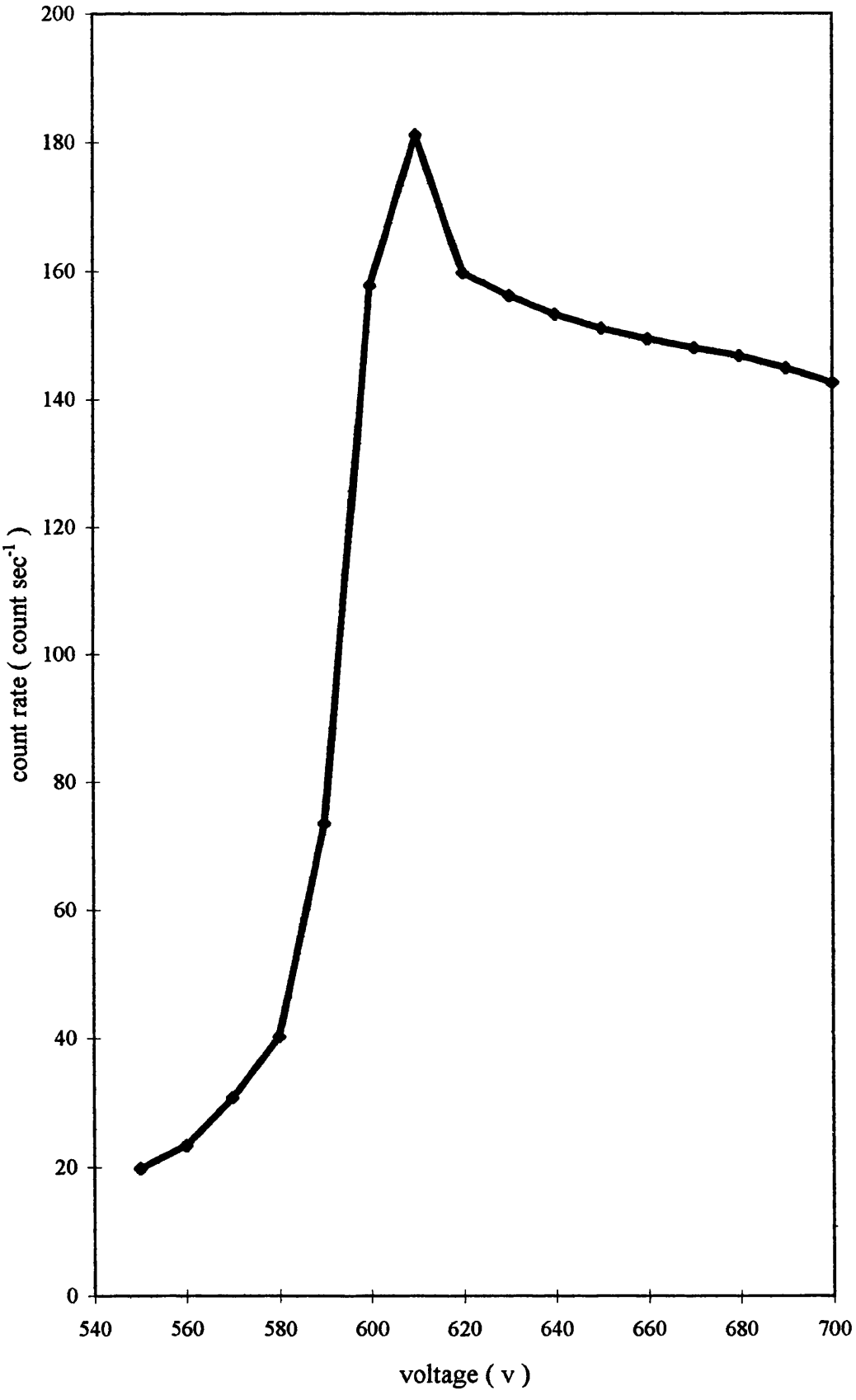

2.12 COUNTING VESSELS.

Reactions involving [^{18}F] - fluorine were monitored using single limbed PTFE and FEP counting vessels (Fig. 2.15). The specific count rate of [^{18}F] - hydrogen fluoride was determined by introducing an aliquot (1 mmol) of the labelled vapour contained in a measured volume to a single limbed counting vessel containing ceasium fluoride (0.5g). The efficiency of [^{18}F] - fluorine counting is dependent on the state of the sample; solid > liquid > gas, so by absorbing the gaseous [^{18}F] - hydrogen fluoride sample onto ceasium fluoride the counting is more efficient.

To follow uptake and lability experiments between solids and [^{18}F] - hydrogen fluoride, a Monel reactor with an FEP sidearm was used (Fig. 2.16). Catalyst labelled during these experiments was tipped into the FEP sidearm which could be conveniently inserted into the well of the scintillation counter.

2.13 STATISTICAL ERRORS

Decay of a radioisotope is a random process and therefore subject to fluctuations due to the nature of the process. The number of disintegrations observed during a fixed time when a source is measured repeatedly will not remain constant, even when half - life decay is taken into consideration. The probability W(m) of obtaining m disintegrations in time t from N_o original radioactive atoms is given by the binomial expression (Eqn. 2.10)

$$W(m) = \{ N_o / (N_o - m) ! \, m ! \} \, p^m (1 - p)^{No - m} \qquad \text{Eqn. 2.10}$$

where p is the probability that a disintegration will occur within the time of observation.

It can be shown from this expression (127, 128, 129) that the expected standard deviation for radioactive disintegration, σ, is given by equation 2.11.

FIGURE 2.15 PTFE/FEP Counting Vessels

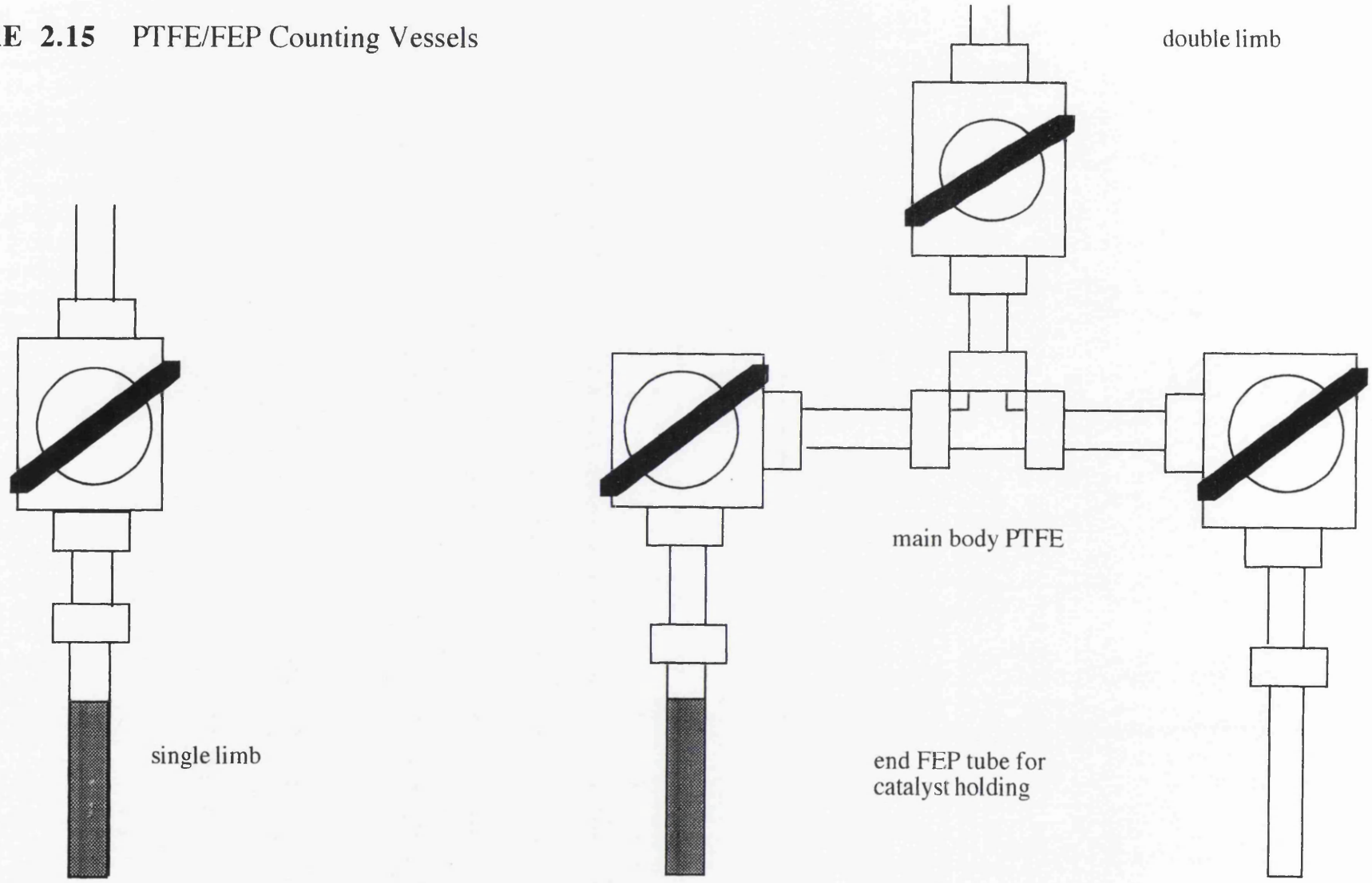

FIGURE 2.16 Monel Counting Vessel With Side Arm

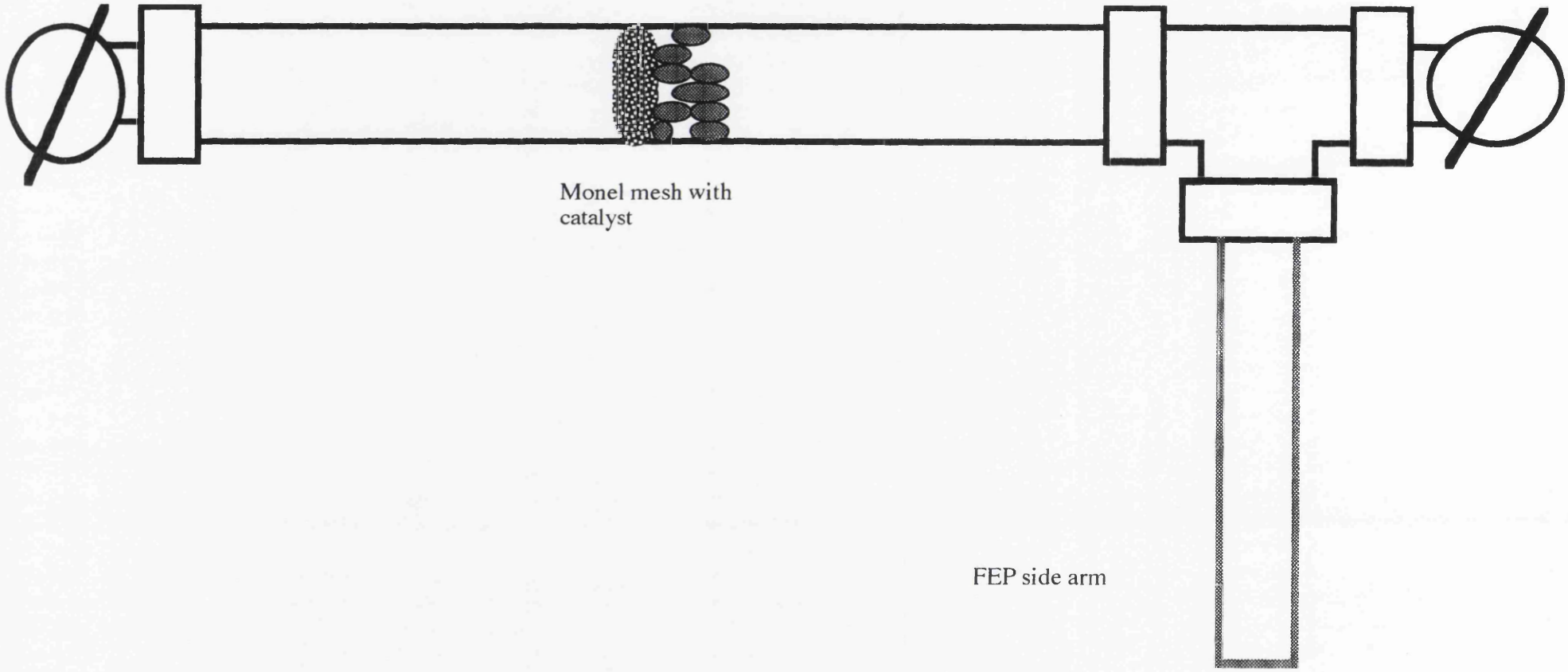

$$\sigma = \sqrt{m}e^{-\lambda t} \qquad \text{Eqn. 2.11}$$

In practice the observation time t is short in comparison to the half - life so equation 2.11 is reduced to :-

$$\sigma = \sqrt{m} \qquad \text{Eqn. 2.12}$$

where m is the number of counts obtained.

In this work all errors quoted on radiochemical measurements are a combination of the uncertainty in the physical measurement, such as mass of sample and pressure of gas, and the uncertainty in the count obtained.

2.14 DECAY CORRECTIONS

As radioactive decay is a random process it is impossible to predict when a single atom will decay. However the characteristic rate of decay can be expressed in terms of the half - life, $t_{1/2}$, which is defined as the time required for the measured activity, A, to decrease by one half of its original value. The half life can be conveniently determined from a plot of lnA against time.

The decay constant, λ, is related to the half - life by the equation

$$t_{1/2} = \ln 2/\lambda \qquad \text{Eqn. 2.13}$$

The activity of a sample, A, is the number of events per second occurring within the sample. The decay process is described by the equation :-

$$A_t = A_0 e^{-\lambda t} \qquad \text{Eqn. 2.7}$$

Where A_t is the count rate of the sample at time t, A_0 is the count rate of the sample at time 0 and λ is the decay constant.

Where significant decay occurred in the time taken to complete an experiment (i.e. when using short lived isotopes such as [^{18}F] - fluorine) all data collected were corrected to zero time using a computer programme before analysis.

3 CATALYST MICROREACTOR STUDIES, CHARACTERISATION AND ANALYSIS.

3.1 INTRODUCTION

This chapter describes the parameters used to prepare test and characterise catalysts. Catalysts were prepared via the method detailed in 2.3 and fluorinated in the catalyst flow rig described in 2.1.6. The activities of different catalysts were determined using the reaction of CF_3CH_2Cl and HF as a test reaction and analysing samples of reaction effluent by gas chromatography. Characterisation of the catalysts was performed at Runcorn using BET - Surface area analysis, X - ray diffraction and mercury porosymmetry. There were three main aims of this work. First, determining the effects of calcination on crystallinity. Second, the effect of chromia crystallinity and zinc doping on catalyst activity. Finally, determination of the effects of zinc doping, fluorination and reaction on chromia structure and surface area.

3.2 CALCINATION OF AMORPHOUS CHROMIA

Amorphous chromia was calcined in the calcination rig using the procedure described in 2.3.1. Parameters programmed into the temperature control unit and the nitrogen gas flow used to calcine chromias are detailed in Table 3.1.

Table 3.1 Parameters Programmed Into Temperature Control Unit and Nitrogen Flow Used to Calcine Chromias

Chromia Sample	Start Temp. (K)	Ramp Rate ($Kmin^{-1}$)	Maximum Temp. (K)	Dwell Time (h.)	Nitrogen Flow ($molh^{-1}$)
1	573	1	723	12	0.107
2	573	1	873	12	0.107
3	573	1	973	12	0.107

3.3 ZINC DOPING OF CHROMIA

Chromias were doped with aqueous zinc chloride by wet impregnation according to the procedure described in 2.3.2. Masses and calculated w/w % Zn appear in Tables 3.2 - 3.5

Table 3.2 Masses of Chromia and $ZnCl_2$ and calculated w/w % Zn for Impregnation on Chromia Calcined to 973K

Mass Chromia	Mass $ZnCl_2$	w/w % Zn
10.0	0.0	0.0
9.9483	0.0523	0.251
9.7915	0.2077	0.9965
7.3336	0.6675	4.002

Table 3.3. Masses of Chromia and $ZnCl_2$ and calculated w/w % Zn for Impregnation on Chromia Calcined to 873K

Mass Chromia	Mass $ZnCl_2$	w/w % Zn
10.0	0.0	0.0
7.9583	0.0429	0.257
7.8336	0.1668	1.00
7.3330	0.6670	3.999

Table 3.4 Masses of Chromia and $ZnCl_2$ and calculated w/w % Zn for Impregnation on Chromia Calcined to 723K

Mass Chromia	Mass $ZnCl_2$	w/w % Zn
10.0	0.0	0.0
9.9479	0.0521	0.2509
9.7915	0.2085	1.001
9.3330	0.6670	4.0017

Table 3.5 Masses of Chromia and $ZnCl_2$ and calculated w/w % Zn for Impregnation on amorphous Chromia.

Mass Chromia	Mass $ZnCl_2$	w/w % Zn
10.0	0.0	0.0
2.9369	0.0633	1.01
2.8184	0.1877	3.00
2.6873	0.3127	5.00
4.8114	2.1875	14.99

3.4 X - RAY DIFFRACTION ANALYSIS.

Samples of chromias prepared under varying calcination parameters and doped with differing levels of zinc were analysed by the Analytical and Physical Sciences X - ray Diffraction Group at ICI Runcorn as described in 2.7. The aim of the analysis was to determine phases present in samples, the degree of crystallinity in chromias with differing calcination parameters and the effect that zinc doping would have on these factors. A sample (ca. 3g) was analysed by X - ray diffraction. Samples were ground using an agate pestle and mortar and loaded into a standard Phillips deep pack, stationary X - ray diffraction specimen holder. The sample was analysed with a Phillips Automatic Powder Diffraction Unit. To estimate the crystallinity both a standard NIST alpha chromia and the sample were examined in duplicate to assess the relative areas of the four reflections examined i.e. the 012, 104, 110 and 113. A goniometer was programmed to search for the peak maximum and adjust data collected and counts accumulated over the areas of interest. The collection and processing of data is performed using a MICROVAX 3400 computer to produce a plot of the profile for the range covered, calculate the percentage of crystallinity, based upon a straight line model, and calculate an apparent average crystallite size, based upon peak width at half height after deconvolution to remove instrumental broadening.

RESULTS

Chromias, calcined under differing parameters and doped with differing amounts of zinc, were examined by X - ray diffraction at ICI Runcorn as described in sections 2.7. The phases present and degree of crystallinity were determined. The results of this work are shown in Tables 3.6 - 3.7.

Table 3.6 Levels of Crystalline α - chromia Present in Amorphous Chromia Calcined Under Differing Conditions.

Calcination Temperature Maximum	% α - chromia			
	012	104	110	113
723K	<5	<5	5 - 15	<5
873K	70 - 80	70 - 80	75 - 85	70 - 80
973K	75 - 85	75 - 85	85 - 95	80 - 90

Table 3.7 Level of Crystallinity of 70 - 85 % α - Chromia Doped with Differing w / w % of $ZnCl_2$

w/w % Zn Doping	% α - Chromia			
	012	104	110	113
0	70 - 80	70 - 80	75 -85	70 - 80
0.25	70 - 80	70 - 80	70 - 80	70 - 80
1	75 - 85	70 - 80	75 - 85	75 - 85
4	70 - 80	65 - 75	70 - 80	70 - 80

From Table 3.6 we can deduce the amounts of α - chromia formed from the calcination of amorphous industrial chromias in section 3.2.1. In each case a small

amount of highly crystalline graphite was present. Graphite is mixed with chromia to aid the pelleting process and it was therefore present in the catalysts presented for X - ray diffraction analysis. Chromia heated to a maximum of 723K for 12 h had a small amount of α - chromia phase present. Of the four reflections examined, only one reflection showed an α - chromia level greater than 5 %. The majority of this material was amorphous, thus this chromia was referred to as 'low crystallinity' chromia. In contrast, the chromias calcined at higher temperatures had greater amounts of α - chromia present in their X - ray diffraction spectra. Chromia calcined at 873K for 12 h contained some non - crystalline material. The major crystalline phase detected was α - chromia with crystalline graphite being the only other phase detected. All four reflections had at least 70 % α - chromia phase and the 110 reflection has a maximum of 85 % α - chromia. This chromia is referred to as 'medium crystalline' chromia. Chromia calcined at 973K for 12 h also contained some non - crystalline material. α - Chromia was again the major crystalline phase present with small amounts of crystalline graphite as the only phase detected. In this instance the four reflections had a minimum of at least 75 % α - chromia phase with the 110 reflection having a maximum of 95 % α - chromia phase. This chromia was referred to as 'high crystalline' chromia

These results demonstrate that there is a very narrow temperature range between the formation of small and large amounts of α - chromia from amorphous chromia. As the temperature of the calcination process is gradually increased it approaches a 'critical' temperature at which the formation of α - chromia phase becomes favourable. The reaction to form α - chromia from amorphous chromia is highly exothermic and heat generated from the reaction can cause amorphous chromia close to the newly formed α - chromia to reach the 'critical' temperature. This results in large amounts of α - chromia phase forming at the same time and therefore it was difficult to attain a percentage of α - chromia between the two extremes of large and small quantities of α - chromia. This reaction was monitored

with a thermocouple linked to a chart recorder to plot temperature increase during the reaction. The temperature rise was noted by the increasing gradient of the plot and the formation of α - chromia at the 'critical' temperature was noted by a sharp peak on the chart recording.

Table 3.7 compared chromia, calcined at 873K and having 70 - 85 % α - chromia present (medium crystalline), loaded with different levels of w/w % Zn. The data obtained for these samples was very similar in each case. Differences between chromias doped with 0.25, 1 and 4 w/w % Zn were not significant in terms of their crystallinity over the four reflections. The 4 w/w % Zn chromia had slightly less α - chromia for each reflection than the other chromias.

All of the chromias examined contained some non - crystalline material. The major crystalline phase detected was α - chromia and a small amount of highly crystalline graphite was present. The level of graphite in the undoped chromia was higher than it appeared to be in the doped chromia. A comparison of these zinc doped chromias with other zinc doped chromias previously examined at Runcorn, derived from projects other than this study, yielded no information regarding the presence and state of zinc in these chromias and it is believed that the amount of zinc present in chromias examined is below the detection limit of this technique.

3.5 FLUORINATION OF CHROMIAS IN ATMOSPHERIC PRESSURE FLOW RIG FOR CATALYST FLUORINATION AND CATALYST TESTING.

A sample (2.00g) of ground chromia catalyst, sieved using 0.8 mm sieves, was charged into a 1/4 inch Monel metal U - tube reactor via a plastic funnel, the process being performed within a dust cabinet. The reactor was then attached to the flow rig for catalyst testing and placed inside of the oven controlled with a temperature programmer. A nitrogen flow was passed through the reactor at a flow rate of 20 cm^3min^{-1} and the oven was heated to 573K. A ceramic fibre lid, with an opening large enough to allow the Monel U - tube reactor to fit through, was placed

on top of the oven and gaps in the hole were plugged with glass fibre to conserve heat and allow greater temperature control. Rig off gas was passed into a scrubber ($K_2CO_{3\,(aq)}$). This process dried the chromia prior to fluorination with HF vapour.

During the drying period a consistent HF mass flow was established of $0.015 gmin^{-1}$. A nitrogen carrier gas was bled via a series of valves into a Monel HF storage bomb housed in a chiller unit controlled via temperature control apparatus and containing mildly alkaline solution ($K_2CO_{3\,(aq)}$) at 276 - 281K. The nitrogen carrier gas flow of approximately $5cm^3min^{-1}$ was controlled with a pressure regulator and a needle valve from the main nitrogen cylinder. The approximate flow of $5cm^3min^{-1}$ gave an HF mass flow of $0.015gmin^{-1}$. However, the HF flow was dependent upon the exact temperature of the chill bath in which the HF storage bomb was immersed and small adjustments to the nitrogen carrier gas flow, using the pressure regulator and needle valve, were required to obtain the desired HF flow each time the rig was used. The exact HF flow was measured by timed titration using NaOH solution. Sodium hydroxide solution (25 cm^3; 0.1 mol dm^{-3}) was delivered into a 50 cm^3 graduated measuring cylinder using a 30 cm^3 syringe. To this were added 2 drops of a phenolphaline indicator solution made from phenolphaline mixed in a 40 : 60 ethanol : water solution. The end of the PTFE HF gas flow line was placed into the measuring cylinder ensuring that the end of the line reached the bottom of the cylinder which would force bubbles of nitrogen, saturated with HF vapour, to travel up through the NaOH solution. The reaction of HF vapour and the NaOH solution was timed by stopwatch until the phenolphaline indicator solution changed colour from its customary purple in alkaline solution to colourless in acidic or neutral solutions. A reproducible time of 3 min $\pm$ 10 s gave an HF mass flow of around $0.015gmin^{-1}$ and delicate adjustment to the nitrogen carrier gas flow were made to achieve this flow rate.

After a period of 40 min drying, to remove water from the catalyst, the connection between the Monel U - tube reactor and the rig off gas tubing was checked for condensation by holding a cold glass mirror close to the connection. If

condensation was observed the drying period was continued until no condensation was observed. When no condensation was observed, the PTFE HF flow line was attached to the top of the Monel U - tube reactor and the diluent nitrogen flow was removed from the top of the reactor and attached to the PTFE rig off gas line via a Monel three way connecting 'T' junction. The rig off gas line was attached to the gas out end of the Monel U - tube reactor and the end of the rig off gas line was placed into the alkaline scrubber solution.

The effluent of the rig off gas was monitored every ten minutes for traces of HF vapour by blowing air, heavily saturated with concentrated ammonia, over the end of the rig off gas line using a squeeze bottle containing cotton soaked in concentrated ammonia. When HF vapour was detected in the effluent, the initial period of HF uptake was at an end and the oven temperature was increased to 623K. The reaction was left to continue overnight for 17 h.

3.6 SURFACE AREA DETERMINATION.

Surface areas of chromias were examined using a BET surface area rig at ICI Runcorn described in 2.1.9 . The sample (1g) was charged into a copper U - tube reactor charged into a PTFE He flow line. The catalyst U - tube reactor was placed into an oven at 523K and dried in a stream of He at a flow rate of 20 cm^3min^{-1}. This process was used to dry the catalyst prior to analysis. The system was checked for leaks by closing a two way tap positioned in the reactor out gas line and watching pressure build up on a gauge connected to the He flow line entering the reactor. A detergent solution was used to detect leaks at the connections between the reactor and the He flow line. Leaks detected were resolved by tightening these connections. The drying process lasted 30 min. and this was timed using a digital stopwatch.

The reactor out gas was passed through a gas chromatograph, linked to a chart recorder, to note the presence of gases from the reactor out gas. After the 30 min drying period, the chart recorder was switched on and the catalyst U - tube was

cooled in liquid nitrogen. A bubble flow meter, connected to the end of the rig, was used to measure the flow of gases through the reactor and could control the cooling process by watching the progress of the bubble in the flow meter and checking for 'suck back' of the He gas as the reactor cooled. When the U - tube was cooled to 80K and the chart recorder had attained a steady base line an N_2 flow, checked using a digital flow meter to be $2cm^3min^{-1}$, was passed through the rig and the He flow was discontinued. The start of the N_2 flow through the rig was marked on the chart recorder paper. When a 'break through' of N_2 flow from the catalyst U - tube was attained, the nitrogen flow was discontinued. This break through followed adsorption of nitrogen on the surface of the chromia and was noted by the recording of a peak by the chart recorder. The reactor was disconnected from the rig and removed from the bath of liquid nitrogen. The catalyst was discharged from the reactor and the reactor was washed thoroughly with water and cleaned in a sonic bath before storage in an oven heated to 393K in preparation for the next analysis. This process was repeated using an empty U - tube reactor.

The surface area of chromias examined was calculated by obtaining the length of time for nitrogen flow to achieve 'break through' from the chart recording subtracted from the length of time taken for nitrogen to pass through an empty U - tube reactor. These parameters, together with other measured parameters such as the mass of sample and the exact nitrogen flow rate, were collated in a computer programme to calculate the surface area in m^2g^{-1}. This calculation relies upon the amount of nitrogen adsorbed onto the catalyst surface being equivalent to a monolayer coverage. From this assumption we can say (EQN. 3.1):-

Surface Area = moles N_2 adsorbed x Avogadro no. x N_2 area EQN. 3.1

Where moles N_2 adsorbed = moles N_2 per gram of catalyst, Avogadro no. = 6.023×10^{23} and N_2 area = 16.2 $angstroms^2$.

To calculate the number of moles of N_2 adsorbed, the time for N_2 to peak on the chart recorder when passed through a blank U - tube (e.g. 1.9 min.) was subtracted from the time for N_2 to peak on the chart recorder when passed through a U - tube containing catalyst (e.g. 15.9 min.). The mass of catalyst was known and hence the number of moles of N_2 adsorbed could be obtained from (EQN. 3.2):-

$$(15.9 - 1.9 / 22{,}400) \times (2 / \text{mass cat}) = \text{no. moles } N_2 \text{ ads/g} \qquad \text{EQN 3.2}$$

Where 24,000 = the no. of cm^3 N_2 in one mole and 2 = the flow of N_2 in cm^3min^{-1}.

RESULTS

Surface area analysis of all catalysts tested in the catalyst testing rigs at ICI Runcorn was performed using the surface area analysis rig at ICI Runcorn as described in section 2.1.9. Selected catalyst precursors and fluorinated catalysts prior to reaction were also analysed at Runcorn to determine their surface areas. The results of this work are shown in Tables 3.8 - 3.11.

Table 3.8 Surface Areas of High Crystalline Chromia (Various Pretreatments)

CATALYST	SURFACE AREA (m^2g^{-1})
undoped precursor	33.49
,, reacted	32.04
0.25 w/w % Zn precursor	31.51
,, reacted	28.42
1 w/w % Zn precursor	33.97
,, reacted	29.48
4 w/w % Zn precursor	19.45
,, reacted	28.49

Table 3.8 illustrates the effects of Zn doping on chromias. At higher levels of Zn doping a significant reduction in surface area is observed in comparison to undoped chromias. Undoped chromias (0.25 and 1 w/w % Zn) have no significant difference in surface area. Upon reaction undoped and lightly doped chromias all reduce in surface area. However, heavily doped chromia increases in surface area. The net result is that all of these chromias have similar surface areas after reaction.

Table 3.9 Surface Areas of 70 - 85 % α - Chromias (Various Pretreatments)

CATALYST	SURFACE AREA (m^2g^{-1})
undoped precursor	42 46
„ fluorinated	33.49
„ reacted	40.74
0.25 w/w % Zn precursor	46.08
„ fluorinated	37.61
„ reacted	43.65
1 w/w % Zn precursor	45.89
„ fluorinated	38.17
„ reacted	32.65
4 w/w % Zn precursor	27.7
„ fluorinated	35.2
„ reacted	35.29

Table 3.9 illustrates similar effects to those observed in Table 3.8 for medium crystalline chromia. In Table 3.8 however, only precursor and reacted catalysts have their surface areas reported. Table 3.9 reports surface areas of fluorinated chromias along with precursor and reacted catalysts. The reduction in surface area for undoped and lightly doped (0.25 and 1 w/w % Zn) chromias was more dramatic upon fluorination. Subsequent reaction of these fluorinated chromias causes an increase in surface area between fluorinated and reacted states of the chromias

analysed, however the reacted state surface areas are lower than the precursor surface areas. The heavily doped chromia again has an increased surface area in comparison to its precursor upon both reaction and fluorination. The difference between this chromia's reacted and fluorinated state surface areas was negligible in this instance. Comparison of surface areas of fluorinated and reacted chromias in Table 3.9 show a larger range of surface area for catalysts in these states.

Table 3.10 Surface Areas of Low Crystalline Chromias (Various Pretreatments)

CATALYST	SURFACE AREA (m^2g^{-1})
undoped precursor	136.25
„ reacted	68.36
0.25 w/w % Zn precursor	155.66
„ reacted	58.64
1 w/w % Zn precursor	176.74
„ reacted	66.37
4 w/w % Zn precursor	72.29
„ reacted	32.89

Table 3.10 shows the same trend as Tables 3.8 and 3.9. A reduction in surface area is observed between precursor and reacted catalysts. In this instance the reduction is very marked in comparison to the data presented in Tables 3.8 and 3.9. The increase in surface area observed in 4 w/w % Zn chromias in Tables 3.8 and 3.9 is not evident here and the 4 w/w % Zn chromia in the low crystallinity chromia series follows the trend of the other catalysts in the series. The reduction in surface area between the 4 w/w % Zn precursor catalyst and the other precursor catalyst in this series can also be seen.

Table 3.11 reports the effects of zinc doping and reaction on surface areas of chromias. The same general trends are observed on these chromias as were observed on the previous Tables 3.8 - 3.10. Fluorinated chromias, which were only

analysed for undoped and 15 w/w % Zn doped chromia in the amorphous chromia series, shows an initial reduction followed by an increase in surface area upon reaction in comparison to the precursor.

Table 3.11 Surface Areas of Amorphous Chromias (Various Pretreatments)

CATALYST	SURFACE AREA (m^2g^{-1})
undoped precursor	179.02
,, fluorinated	60.84
,, reacted	52.72
1 w/w % Zn precursor	169.13
,, reacted	47.20
3 w/w % Zn precursor	140.25
,, reacted	41.27
5 w/w % Zn precursor	81.37
,, reacted	34.58
15 w/w % Zn precursor	24.43
,, fluorinated	11.59
,, reacted	35.84

Examination of all tables presented reveals a number of general trends. First the surface area of chromias increases with decreasing crystallinity (crystallinity being determined by the amount of α - chromia present as reported in section 3.3.1) Highly crystalline chromias have greatly reduced surface areas in comparison to low crystalline chromias. This is clear when undoped and precursor chromias from Tables 3.8 and 3.11 are compared and an increase in surface area can be seen when precursor catalysts are examined between Tables 3.8 - 3.11. Second, the general trends mentioned above such as reduction in surface area between precursor and reacted undoped and lightly doped chromias, appear through out the range of chromia surface areas determined. Finally, when the surface areas of all reacted

chromias are examined the range of surface area results is far smaller than those for precursor surface areas. Reacted surface area results all appear to be ca. 40 m^2g^{-1} ± 20 m^2g^{-1}, which is in contrast to precursor surface areas which range from 24.43 m^2g^{-1} to 179.02 m^2g^{-1}

3.7 PORE VOLUME ANALYSIS BY MERCURY POROSIMETRY.

Pore volume analysis was performed by the Analytical and Physical Sciences Group, Micrometrics Section at ICI Runcorn. Samples (ca.3g) were presented for analysis to determine the pore size / volume and surface area by N_2 adsorption and pore size, pore volume distribution by the mercury porosimetry technique. Samples were outgassed at 423K under vacuum overnight prior to analysis. For N_2 adsorption the analysis was performed using a Micrometrics ASAP 2400 Gas Adsorption Analyser and for mercury intrusion. Sample analysis was performed using a Micrometerics Autopore 9220 Mercury Porosimeter.

Mercury porosimetry indicates the volume of liquid mercury (non - wetting) forced under pressure into the pores on the surface of a catalyst and the volume of liquid mercury extruded from the pores as the pressure was released. Mercury intrudes pores in response to their size and applied pressure. The applied pressure must overcome the surface tension of mercury which opposes its intrusion into the pores. Mercury has a contact angle of > 90° with most materials, which causes it to resist wetting the solid and entering into pore spaces in the absence of an external applied pressure. A series of pore volume readings for a given applied pressure can be used to derive the pore size distribution for samples by virtue of the Young - Laplace equation (EQN. 3.3) (130):-

$$p = (4 \gamma \cos. \theta) / d \quad \text{EQN. 3.3}$$

Where θ = the contact angle (140° for mercury); d = the pore diameter (m); γ = the surface tension of the penetrating liquid (Nm^{-1}) and p = pressure (Pa).

Pore volume (cm^3g^{-1}) can be plotted against log_{10} (pore diameter). The plot is cumulative, hence at any given pressure the pore volume will be equivalent to the total number of pores filled.

The mercury porosimetry technique involved subjecting samples to a pressure cycle starting at a pressure of approximately 1.5 pound $inch^2$ $angstrom^{-1}$ (psia) (equivalent to a pore size of 140 microns diameter) increasing to 60000 psia (equivalent to a pore size of 30 angstrom diameter pores) in predefined steps to give pore size and pore volume information and a final stepwise reduction back down to atmospheric pressure (equivalent to a pore size of 15 micron diameter pores) to give an indication of how mercury was expelled from pores during the depressurisation stage.

RESULTS

Pore volume analysis was performed by Analytical and Physical Sciences Group, Micrometrics Section at ICI Runcorn. The analysis procedure is outlined in section 3.2.5. Chromias examined for pore size and volume by Mercury Porosimetery were medium crystallinity chromia with 4 w/w % Zn doping, unfluorinated and reacted samples. These samples were chosen because as heavily Zn doped chromias they showed anomalous surface area trends to undoped and lightly Zn doped chromias. Undoped and lightly Zn doped chromias decrease surface area upon fluorination and reaction, heavily Zn doped catalysts have low surface areas however these increase with fluorination and reaction. It was speculated that heavier Zn doping was blocking pores on the surface of chromias resulting in low surface areas and fluorination was unblocking these pores. The results of this analysis appear in the Table 3.12.

Table 3.12 Parameters and Results of Mercury Pore Volume Analysis of Reacted and Unreacted 4 w/w % Zn Medium Crystalline Chromias.

PARAMETER	UNREACTED CHROMIA	REACTED CHROMIA
sample weight	0.3116g	0.3352 g
total intrusion volume	0.3376 cm^3g^{-1}	0.3317 cm^3g^{-1}
total pore area	28.744 m^2g^{-1}	33.491 m^2g^{-1}
median pore diameter (volume)	0.0678 μm	0.0426 μm
median pore diameter (area)	0.0399 μm	0.0338 μm
average pore diameter (4V/A)	0.0470 μm	0.0396 μm
total intrusion volume (less contribution from interparticulate space)	0.31 cm^3g^{-1}	0.31 cm^3g^{-1}
% mercury remaining in pore volume after depressurisation	98 %	11 %

Intrusion up to pressures of 25 psia (pores > 10 μm diameter) is believed to be the result of the filling of interparticulate space, that is space in between particles as they pack into the mercury penetrometers and the filling of large cracks on the surface of the particles. Intrusion at higher pressures is the filling of any remaining structure. The total intrusion volume (30 angstrom to 100 μm range) of both catalysts is very similar namely 0.3376 cm^3g^{-1} and 0.3317 cm^3g^{-1}. When the contribution believed to be due to interparticulate space is removed from this the intrusion volumes are the same (0.31 cm^3g^{-1}). This suggests that pores are not filled with zinc or zinc chloride in the unreacted chromia, as both the reacted and

unreacted chromias have the same intrusion volume. Information regarding the depressurisation process and hence the extrusion of mercury from these pores was more interesting. A mercury extrusion curve was intended to give information about how mercury was expelled or entrapped upon depressurisation following the pressurised intrusion. The percentage of mercury remaining within the pore structure at the end of depressurisation was 98 % for the unreacted chromia and 11 % for the reacted chromia. This information suggests that there was blockage over the outer opening to these pores. Mercury intrusion data did not reveal this as the pressure at which mercury was forced into the pores was great enough to over come the resistance of the blockage and allow relatively easy access of mercury into the partially blocked pores of unreacted chromias. However upon depressurisation the pressure of mercury from within the pores was not great enough to force mercury back out from the pores and hence 98 % of mercury forced into the pores of this unreacted chromia remains in the pores. Fluorination of this chromia unblocks pores and thus allowed the majority of mercury forced in to extrude from the pores leaving 11 % remaining.

3.8 REACTIONS OF CF_3CH_2Cl IN THE PRESENCE OF CHROMIA CATALYSTS

The reaction of CF_3CH_2Cl catalysed by chromia can lead to two competing reactions. First, in the presence of HF the fluorination of CF_3CH_2Cl to form CF_3CH_2F can occur. The second reaction is the elimination of HF to form CF_2CHCl. The reaction equilibria are presented in Fig 3.1

$$(I)\quad CF_3CH_2Cl + HF \rightleftharpoons CF_3CH_2F + HCl$$

$$(II)\quad CF_3CH_2Cl \rightleftharpoons CF_2CHCl + HF$$

Fig. 3.1 Equilibria of Fluorination and Elimination Reactions of CF_3CH_2Cl on Chromia

Table 3.13 Reports ΔH° and ΔS° at 298K for all of the reactants and products mentioned in Fig 3.1.

Table 3.13 ΔH° and ΔS° at 298K for Various Compounds

Compound	ΔH°_{298} ($kJmol^{-1}$)	ΔS°_{298} ($Jmol^{-1}K^{-1}$)
CF_3CH_2Cl	-732.3	327.1
CF_3CH_2F	-878.8	317.0
$CHClCF_2$	-329.5	73.7
HF	-268.4	173.3
HCl	-92.2	186.5

For the fluorination of CF_3CH_2Cl with HF, in an open flow system, (Fig. 3. (I)) ΔH°_{298} of the reaction is 29.7 $kJmol^{-1}$ and ΔS°_{298} of the reaction is 3.1 $Jmol^{-1}K^{-1}$. ΔG for this reaction at 298K is 28.8 $kJmol^{-1}$ and under standard operating conditions at around 573K ΔG is 27.9 $kJmol^{-1}$. The reaction is weakly endothermic and ΔG is little influenced by temperature as ΔS° is low. The equilibrium constant (Kp) of this reaction at 573K can be calculated using Eqn. 3.4.

$$Kp = e^{-\Delta G / RT} \qquad \text{Eqn. 3.4}$$

where R = the gas constant. Thus at 573K Kp = 2.85×10^{-3}. If varying ratios of CF_3CH_2Cl : HF are used the theoretical conversion of CF_3CH_2Cl to products can be calculated using Eqn. 3.5

$$Kp = x^2 / (1-x)(y-x) \qquad \text{Eqn. 3.5}$$

where x = the % conversion of CF_3CH_2Cl to CF_3CH_2F and y = the ratio of CF_3CH_2Cl : HF. Thus Eqn. 3.5 can be rearranged to yield x using the quadratic formula.

Results at temperatures of 523, 553, 573 and 593K of ΔG° at equilibrium, Kp and % conversion of CF_3CH_2Cl for various HF : CF_3CH_2Cl molar ratios are given in Table 3.14.

Table 3.14 Values of ΔG°, Kp and % Conversion to CF_3CH_2F at equilibrium (With Differing Molar Ratios of CF_3CH_2Cl) for Temperatures at 523, 553, 573 and 593K

T (K)	ΔG°_r ($kJmol^{-1}$)	K_p (10^{-3})	CF_3CH_2Cl : HF			
			1:1	1:2	1:3	1:4
523	28.08	1.57	3.8	5.4	6.6	7.5
553	27.99	2.27	4.5	6.4	7.8	9.0
573	27.92	2.85	5.1	7.1	8.7	10.0
593	27.86	3.51	5.6	7.9	9.6	11.0

The competing reaction of dehydrofluorination presented in Fig. 3.1 (II) has $\Delta H^\circ_{298} = 131.9 kJmol^{-1}$ and $\Delta S^\circ_{298} = 151.7 Jmol^{-1}K^{-1}$. This reaction is also endothermic with $\Delta G^\circ = 34.4 kJmol^{-1}$. In order to form the desired fluorinated product an excess of HF is preferable. Typical reaction conditions employ an HF ; CF_3CH_2Cl ratio of 4 : 1 favouring the formation of CF_3CH_2F and the % of CF_2CHCl present in reaction products was always less than 2 %.

A typical reaction, performed using a fluorinated chromia catalyst and a CF_3CH_2Cl ratio of 1 : 4 within an open system, such as the microreactor described in this chapter, had a % of CF_3CH_2F, in the reactor effluent at 523K, of < 1 %. This was considerably less than the maximum % of CF_3CH_2F allowed by the reaction thermodynamics at equilibrium. The reaction would not, however, be at equilibrium and kinetic considerations would be important during the reaction. At 553K the typical % of CF_3CH_2F in the reaction effluent was 3 % and at 573K the typical % of

CF_3CH_2F was 7 %, both values being less than the maximum allowed by the reaction thermodynamics.

At 593K a typical % of CF_3CH_2F in reaction effluents was 12 %. This value was greater than the value of 11 % calculated, at equilibrium, from thermodynamic considerations. As kinetic considerations were of importance in the reactions studied, and the reaction was not at equilibrium, it is believed that the reaction kinetics played a major role in determining the % of CF_3CH_2F formed, particularly at higher reaction temperatures. The conversion to CF_3CH_2F was influenced also by the thermodynamics and, inspite of the influence of the reaction kinetics, the conversion to products was limited in every reaction studied, even when the kinetics allowed the % conversion to exceed the maximum allowed at equilibrium by thermodynamics.

3.9 CATALYST TESTING OF CHROMIAS ON MICROREACTOR FLOW FIG FOR CATALYST TESTING.

Following the 17 h fluorination period at 623K, the sample of chromia was heavily fluorinated and could be used to catalyse halogen exchange in the vapour phase reaction of CF_3CH_2Cl and HF. Hydrogen fluoride vapour, coming from the rig off gas effluent, was titrated using the method described 3.2.1 and adjustments were made to the nitrogen carrier gas flow to allow for temperature changes to the chill bath over the course of the 17 h fluorination. An HF mass flow of $0.015 gmin^{-1}$ was required for the vapour phase reaction of HF and CF_3CH_2Cl.

The flow of CF_3CH_2Cl was controlled using a needle valve, a pressure regulator and a Monel two way valve. The flow originated directly from the CF_3CH_2Cl cylinder, which had a control valve attached to it. A CF_3CH_2Cl flow of $0.015 gmin^{-1}$ was required for testing of catalysts as this would mimic plant conditions. The flow of CF_3CH_2Cl was tested using a bubble flow meter until the desired flow was achieved from adjustment of the pressure regulator and needle valve.

When the desired HF and CF_3CH_2Cl flows were achieved the HF gas line was removed from the top of the Monel U - tube reactor and together with the CF_3CH_2Cl gas line it was attached to a PTFE line leading into the rig via a Monel three way connecting 'T' junction. This PTFE line was attached to the top of the Monel U - tube reactor allowing HF and CF_3CH_2Cl to flow over the catalyst simultaneously at 623K. The reaction remained at a temperature of 623K for 30 min, with reactor effluent passing into the alkaline scrubber.

After 30 min of reaction the rig off gas effluent was sampled for gas chromatographic analysis. A specially designed Pyrex glass vessel was used for sampling. The vessel had a 300 cm^3 volume cylindrical shaped central body with outlets at both ends controlled with two way PTFE taps. The internal diameter of the outlet and the through holes in the PTFE 2 way taps were large enough to push comfortably a 1/8 inch length of PTFE tubing through. An opening, with a subaseal attached, protruded from the side of the central body of the sampling vessel.

Samples of effluent were taken by placing the end of the rig off gas tubing into the Pyrex sampling vessel containing a small (ca. 10 cm^3) amount of tap water to contain HF vapour from the effluent and allowing effluent gas to flow into the sampling vessel. The sampling was timed by stopwatch starting when the PTFE rig off gas tubing entered the vessel and finishing 30 s later when the tubing was removed. The tap at the end of the vessel, through which the tubing was passed, was closed and the vessel was removed for gas chromatography analysis of its contents. After gas chromatography the water at the bottom of the vessel was poured into an alkaline solution and a stream of air was blown through the vessel inside a fumehood to remove any remaining effluent gas. The vessel was filled with tap water and the water was then poured from the vessel by opening both taps. When only ca. 10 cm^3 of water remained in the vessel one tap was closed to prevent the loss of more water and the vessel was used to collect another sample.

Following sampling of effluent at 623K the temperature programmer was adjusted to lower the temperature of the oven by 10K and the reaction remained at

the lower temperature for 20 min. Sampling of the reaction at the lower temperature was performed, using the process described above and the temperature was lowered by another 10K. This process was repeated until a temperature of 523K was reached, after which the reaction was stopped. At the end of the reaction the HF and CF_3CH_2Cl flows were discontinued and the reactor was removed from the oven to allow cooling. A nitrogen flow ($20cm^3min^{-1}$) was passed through the reactor during the cooling process to remove residual HF and CF_3CH_2Cl from the line. The catalyst was discharged from the cooled reactor and stored for further analysis. The reactor was washed through with tap water and cleaned in a sonic bath before being stored in an oven set at 393K prior to use in further test reactions.

GAS CHROMATOGRAPHIC ANALYSIS OF SAMPLES

Gas chromatography analysis of effluent catalyst microreactor studies was performed using a Varian 3400 gas chromatograph described in (2.2.4). The gas chromatograph was calibrated by injecting samples of CF_3CH_2Cl, CF_3CH_2F and mixtures of CF_3CH_2Cl and CF_3CH_2F of increasing concentration and plotting the peak areas against concentration. A linear correlation was obtained for various pressures of CF_3CH_2Cl and CF_3CH_2F and a linear correlation was obtained when peak areas of CF_3CH_2Cl and CF_3CH_2F were plotted against each other when the sample was injected as a mixture of CF_3CH_2Cl and CF_3CH_2F (Figs 3.2 - 3.3). Samples were obtained by removing 5 cm^3 of gas through the suba seal of a Pyrex glass gas sampling vessel and injecting the sample through the septum cap injection port on the gas chromatograph onto the 50 m capillary column. A typical result, at 573K, was CF_3CH_2Cl (retention time = 0.84 min) = 10.0 %; CF_3CH_2F (retention time = 0.64 min) = 89.99 %; CF_2CHCl (retention time = 0.72 min) = 0.01 %.

Figure 3.2 Plot of Area Count From Gas Chromatograph VS Pressure For CF_3CH_2Cl

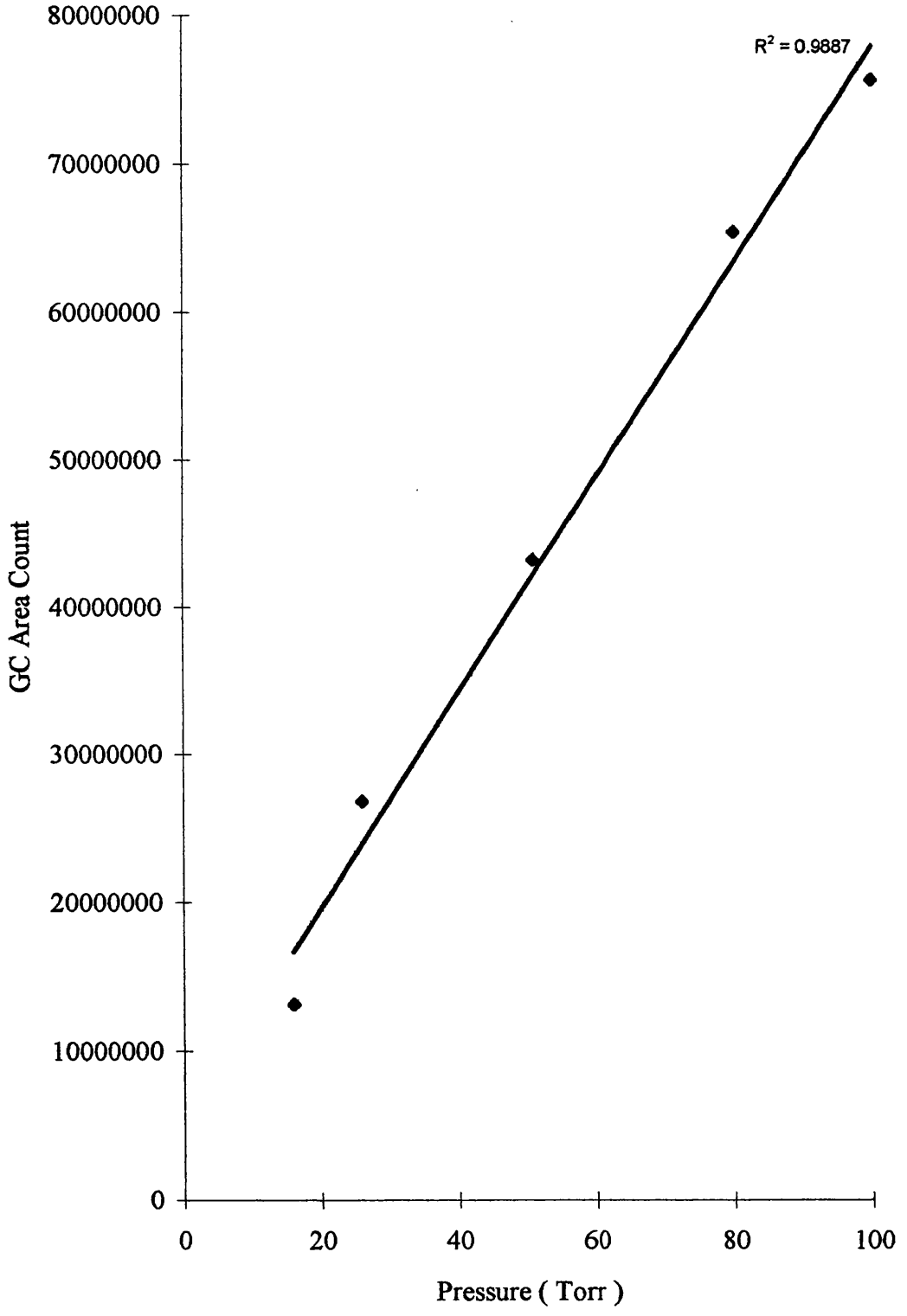

Figure 3.3 Plot Of Area Count From Gas Chromatograph VS Pressure For CF_3CH_2F

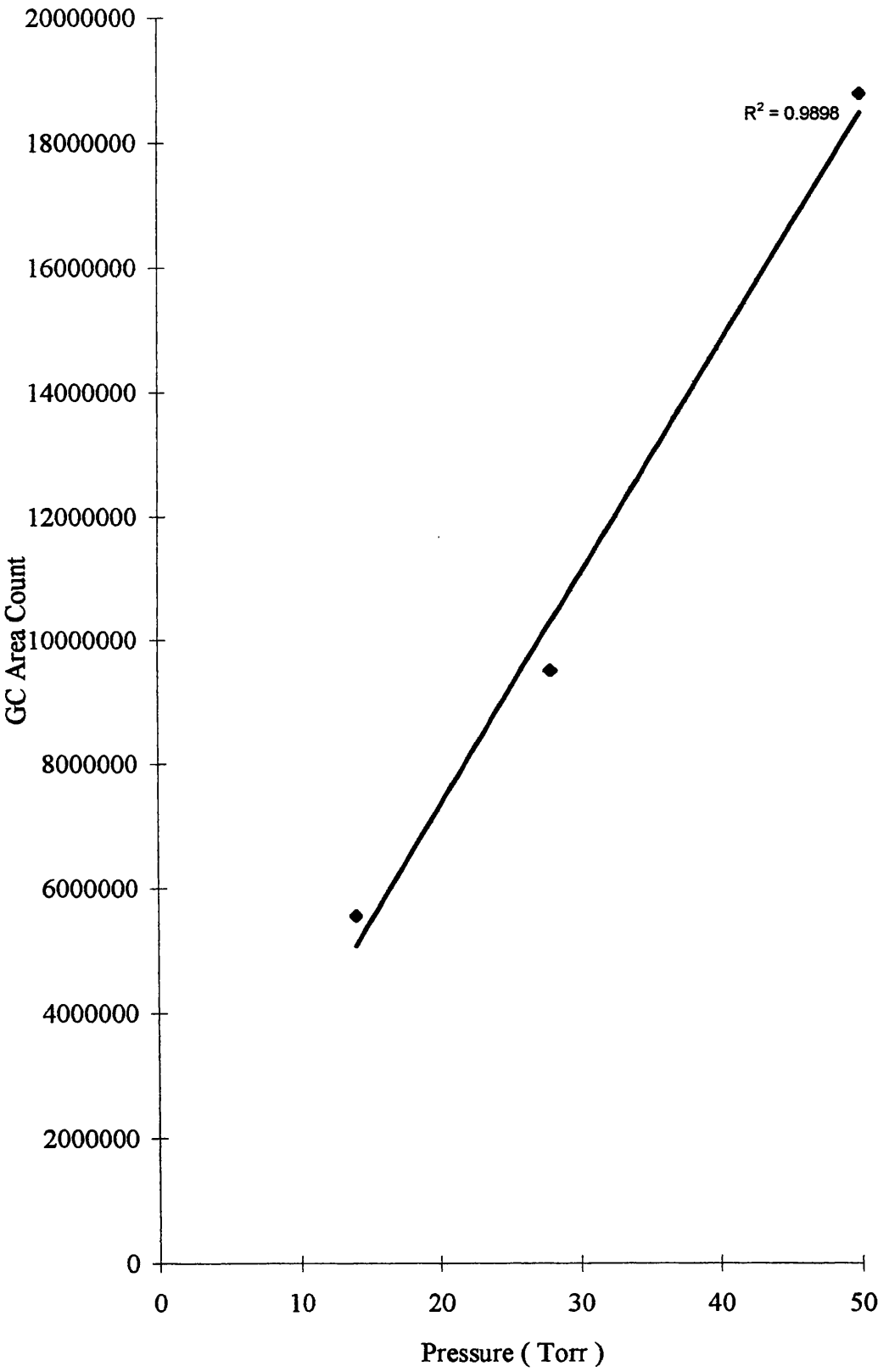

RESULTS

All catalysts described in sections 3.3 - 3.5 were tested using the flow rig for catalyst testing (2.1.5) as described above and analysed by gas chromatography. The results of gas chromatography analysis are shown in Tables 3.15 - 3.18 and Fig 3.4 - 3.8. Catalysts are grouped in each table according to the crystallinity of the undoped precursor chromia. Therefore, high crystallinity chromia catalysts, doped with varying amounts of zinc, are grouped together. The % of CF_3CH_2F present in the total effluent stream, determined from gas chromatography, is reported in each table between the temperature range 593 - 543K. Above 593K the reaction approaches the thermodynamic limit and below 543K the conversion of CF_3CH_2Cl is too low with all catalysts tested to obtain reliable results for % of CF_3CH_2F.

Table 3.15 % CF_3CH_2F In Effluent For High Crystallinity Chromias of Various Zn Doping as Catalysts in Reaction of CF_3CH_2Cl and HF Between 593 - 543K

TEMP (K)	UNDOPED	0.25 w/w % Zn	1 w/w % Zn	4 w/w % Zn
593	12.95	15.37	9.41	4.79
583	11.89	12.23	6.13	3.86
573	6.12	7.68	4.69	2.81
563	3.33	4.65	3.41	2.27
553	2.77	3.44	2.40	1.55
543	.54	2.60	1.65	1.11

FIGURE 3.4 % CF_3CH_2F in Effluent From Reaction of CF_3CH_2Cl with HF Over Chromia Catalysts of Different Crystallinity

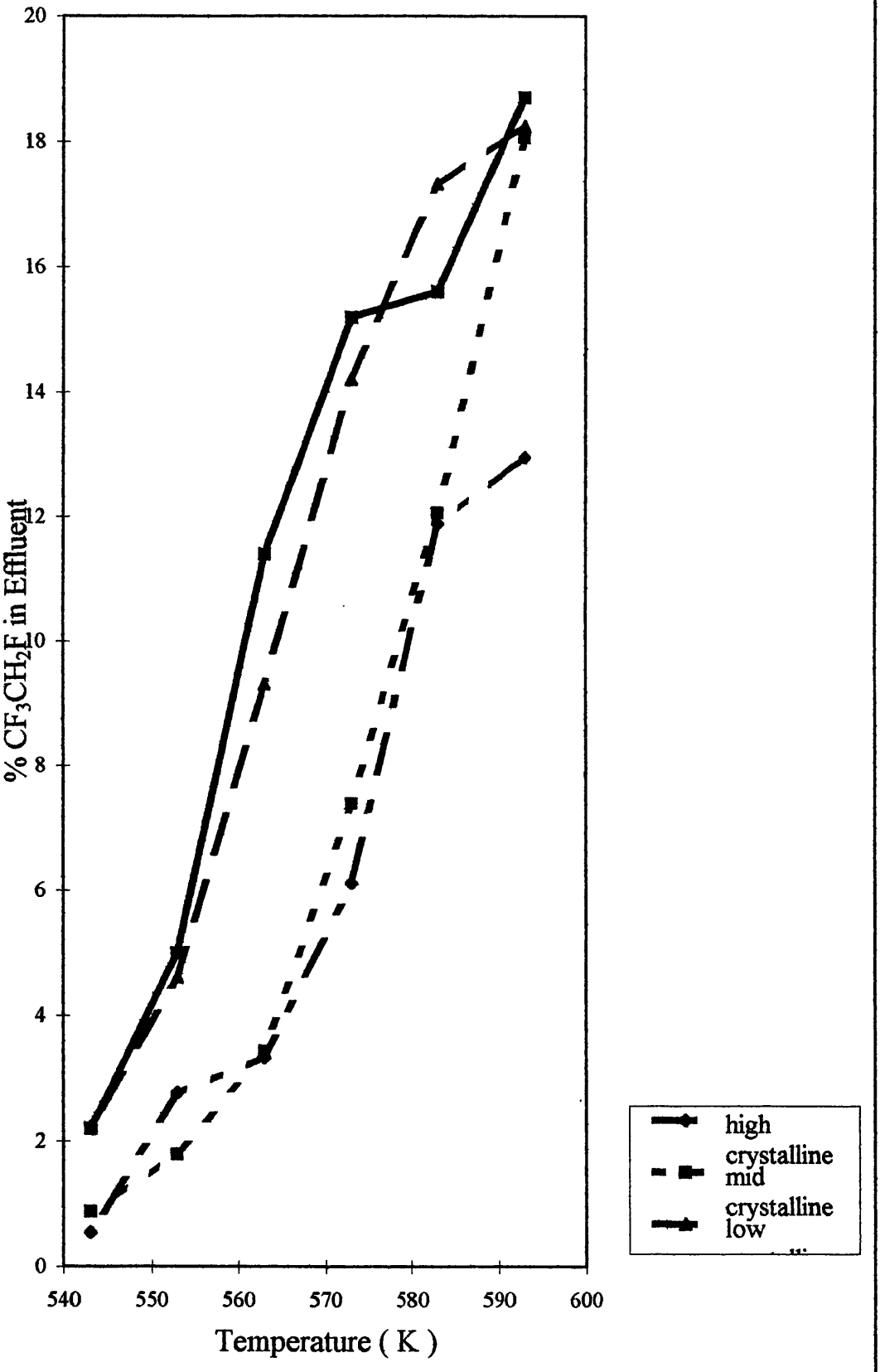

FIGURE 3.5 % CF_3CH_2F in Effluent From Reaction of CF_3CH_2Cl With HF Over High Crystalline Chromia Catalysts With Various Levels of Zinc

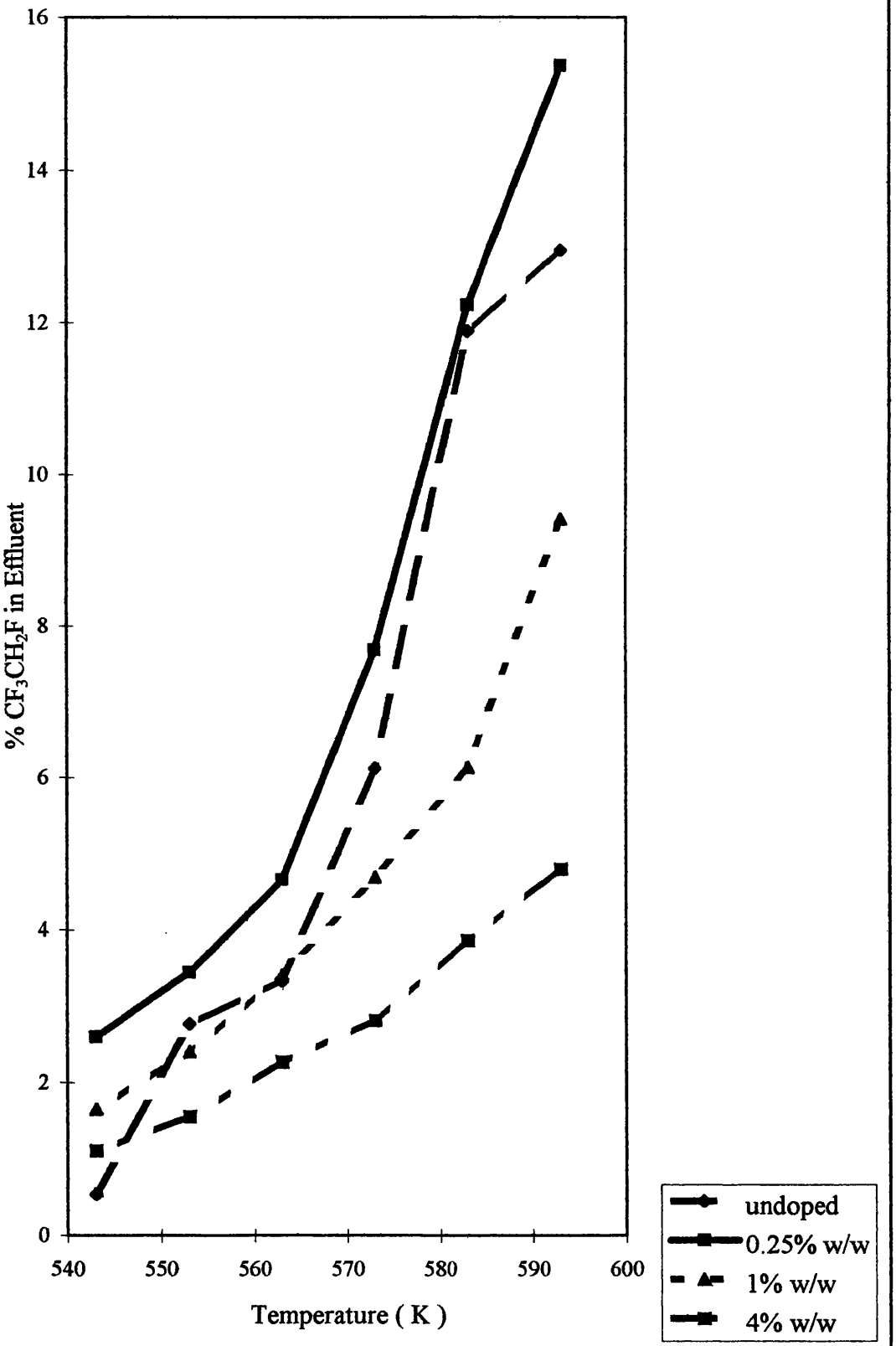

Table 3.16 % CF_3CH_2F in Effluent For Medium Crystallinity Chromias of Various Zn Doping as Catalysts in Reaction of CF_3CH_2Cl and HF Between 593 - 543K

TEMP (K)	UNDOPED	0.25 w/w % Zn	1 w/w % Zn	4 w/w % Zn
593	18.06	18.51	15.72	6.99
583	12.06	16.09	12.13	5.28
573	7.39	11.87	8.53	3.87
563	3.43	9.10	5.76	2.89
553	1.79	5.71	3.82	2.07
543	0.87	3.63	2.45	1.25

Table 3.17 % CF_3CH_2F in Effluent for Low Crystallinity Chromias of Various Zn Doping as Catalysts in Reaction of CF_3CH_2Cl and HF Between 593 - 543K

TEMP (K)	UNDOPED	0.25 w/w % Zn	1 w/w % Zn	4 w/w % Zn
593	18.25	16.98	18.16	13.90
583	17.32	16.65	15.20	11.90
573	14.21	14.92	13.80	7.90
563	9.3	10.91	8.20	5.10
553	4.61	7.51	6.60	3.50
543	2.23	4.01	3.50	2.40

FIGURE 3.6 % CF_3CH_2F in Effluent From Reaction of CF_3CH_2Cl With HF Over Mid Crystalline Chromia Catalysts Doped With Various Levels of Zinc

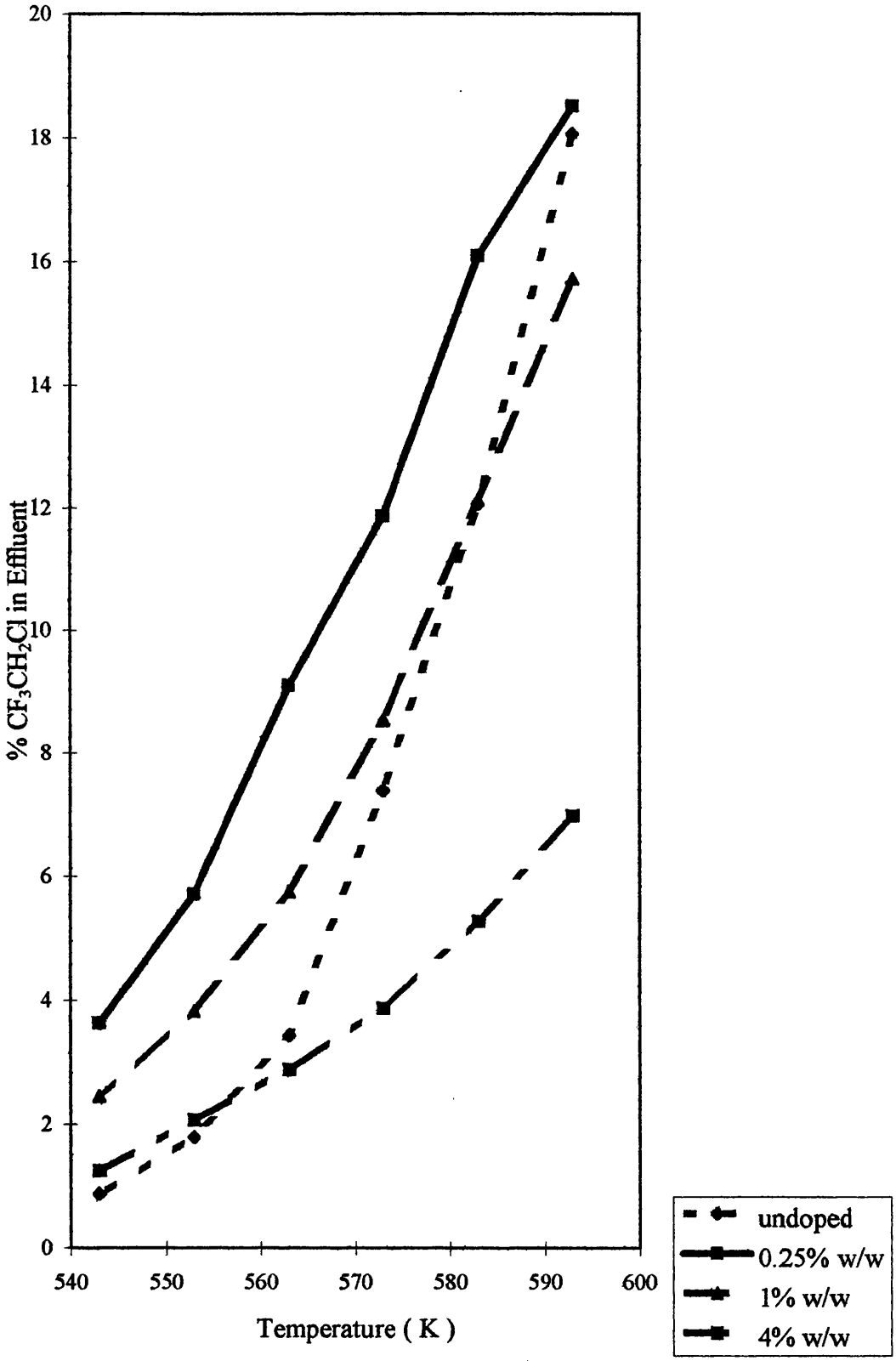

FIGURE 3.7 % CF_3CH_2F in Effluent From Reaction of CF_3CH_2Cl With HF Over Low Crystalline Chromia Catalysts Doped With Various Levels of Zinc

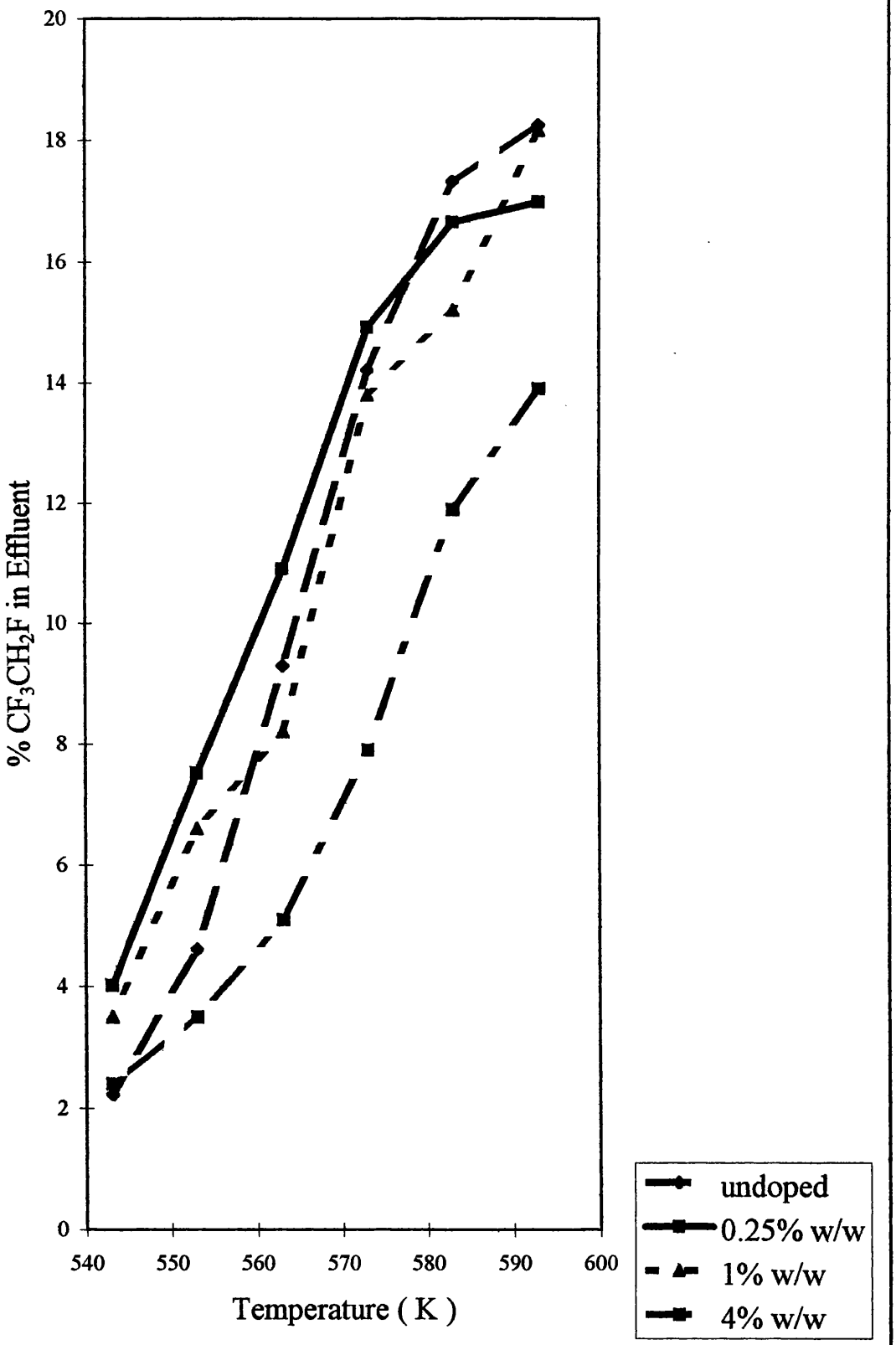

FIGURE 3.8 % CF_3CH_2F in Effluent From Reaction of CF_3CH_2Cl With HF Over Amorphous Chromia Catalysts Doped With Various Levels of Zinc

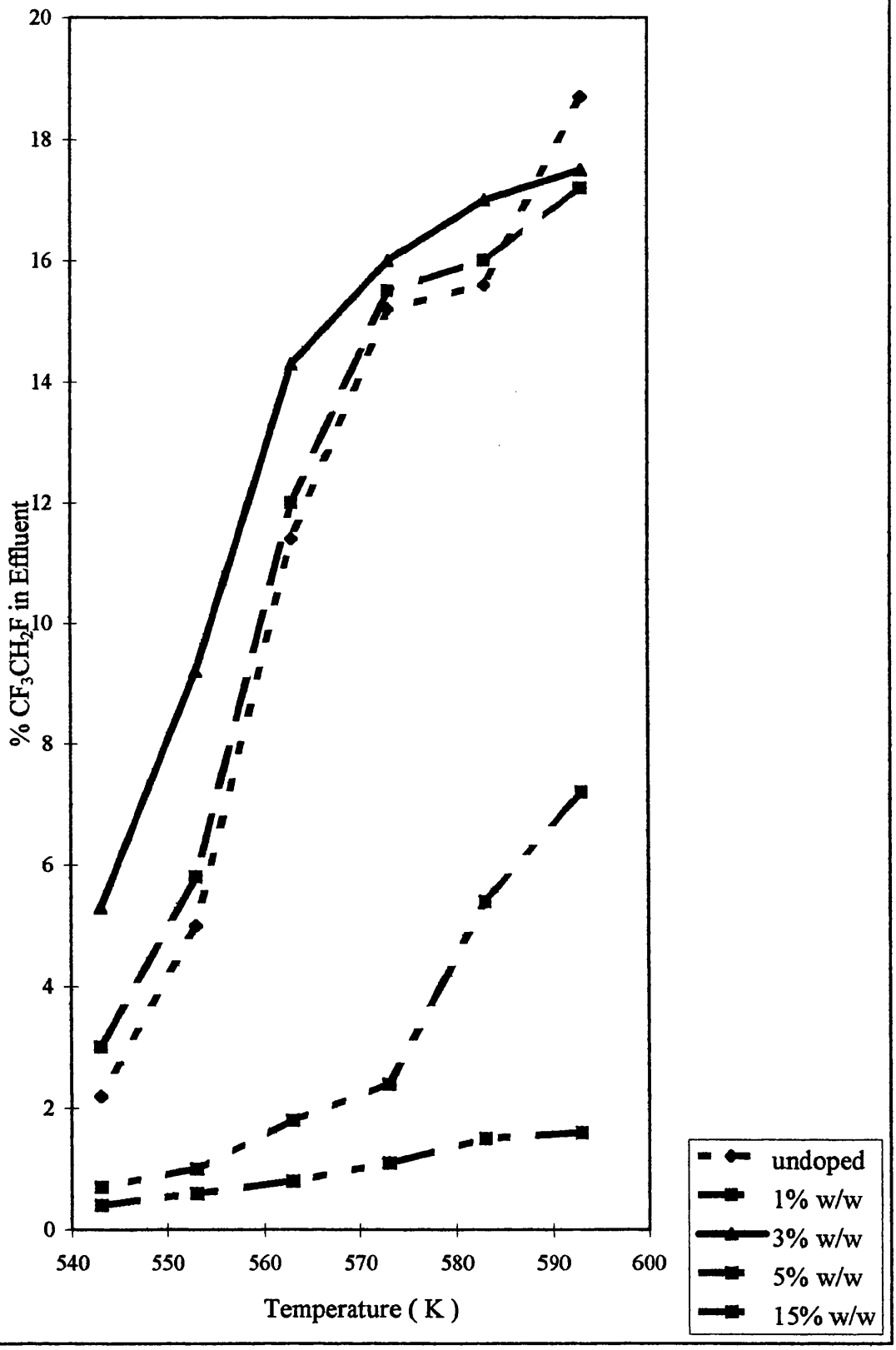

Table 3.18 % CF_3CH_2F in Effluent for Amorphous Chromias of Various Zn w/w Doping as Catalysts in the Reaction of CF_3CH_2Cl and HF Between 593 - 543K

TEMP (K)	UNDOPED	1 w/w % Zn	3 w/w % Zn	5 w/w % Zn	15 w/w % Zn
593	18.70	17.2	17.5	7.2	1.6
583	15.6	16.0	17.0	5.4	1.5
573	15.2	15.5	16.0	2.4	1.1
563	11.4	12.0	14.3	1.8	0.8
553	5.0	5.8	9.2	1.0	0.6
543	2.2	3.0	5.3	0.7	0.4

The results shown in Tables 3.15 - 3.18 are presented in Figs 3.4 - 3.8. One method for making direct comparison between chromia catalysts is to compare relative reaction rates which can be derived from EQN. 3.6 :-

Reaction Rate = F x (%conversion -> desired product) / wA EQN. 3.6

Where F = flow rate, w = weight of catalyst and A = surface area.
As the weight and flow rate remained constant for all catalysts tested EQN. 3.4 can be reduced to a relative reaction rate obtained from EQN. 3.7 : -

Relative Reaction Rate = (%conversion -> desired product) / A EQN 3.7

Relative rates of reaction derived from EQN. 3.7, using % conversion 134a at 573K are reported for all catalysts studied in Table 3.19.

Table 3.19 Relative Rates of Reaction for Chromias Used to Catalyse the Reaction of CF_3CH_2Cl With HF to Form CF_3CH_2F at 573K (Arbratory Units)

CATALYST	RELATIVE RATE	CATALYST	RELATIVE RATE
High Crystallinity chromia undoped	0.19	Low Crystallinity chromia undoped	0.21
0.25 w/w % Zn	0.27	0.25 w/w % Zn	0.25
1 w/w % Zn	0.16	1 w/w % Zn	0.21
4 w/w % Zn	0.10	4 w/w % Zn	0.24
Medium Crystallinity chromia undoped	0.18	Amorphous chromia undoped	0.29
0.25 w/w % Zn	0.272	1 w/w % Zn	0.34
1 w/w % Zn	0.26	3 w/w % Zn	0.41
4 w/w % Zn	0.11	5 w/w % Zn	0.16

In all of the reactions studied conversion of $CF_3CH_2Cl \rightarrow CF_3CH_2F$ was 98 % selective. The only other product detected during catalyst test runs was CF_2CHCl (HCFC 1122) which was present as < 2 % of the total reaction effluent. The total area under the peaks representing CF_2CHCl were small enough to make errors in percentages of CF_2CHCl present in the product mixture significant.

From Fig 3.4 the results of chromias of different crystallinities (catalyst crystallinity being determined by the amount of α - chromia phase present from X - ray diffraction analysis) illustrate that catalyst activity increases with decreasing crystallinity. Thus when undoped chromias are tested, the poorest catalyst has the highest crystallinity. This effect is clearly illustrated by comparison of the relative rates of reaction, at 573K, of undoped chromias with differing crystallinity. Clearly crystallinity is an important factor affecting catalyst activity.

Zinc doping effects are evident from Figs 3.5- 3.8. Large amounts of zinc doped onto chromias poisons the catalytic activity of these chromias for the reaction under study. Small amounts of zinc have a promotional effect on the activity. For example when medium crystallinity chromias are doped with varying amounts of zinc a comparison of zinc doped chromias with undoped chromia, comparing the % CF_3CH_2F in the reaction effluent at 573K, illustrates zinc acting as both a promoter and a poison. The 0.25 w/w % zinc doped chromia has 11.9 % CF_3CH_2F in the effluent stream at 573K, which compares favourably with 7.4 % CF_3CH_2F in the effluent of undoped chromia testing at 573K. In this instance zinc is acting as a promoter. The promotional effect of zinc is also evident in the 1 w/w % zinc doped chromia at 573K which had 8.5 % CF_3CH_2F in the effluent compared with 7.39 % CF_3CH_2F in the effluent of undoped chromia. Clearly the promotional effect of zinc in this instance is less evident and 0.25 w/w % Zn is closer to an optimum loading for zinc promotion. A zinc poisoning effect is apparent, in comparison to undoped chromia, when 4 w/w % zinc doped chromia is examined. At 573K the effluent from the reaction contained only 3.9 % CF_3CH_2F demonstrating that zinc had acted as a poison with respect to catalytic activity of the undoped chromia for this reaction.

The effect of differing amounts of zinc doping is illustrated by the relative reaction rates at 573K of different zinc doped medium crystalline chromias. Undoped chromia has a relative reaction rate of 0.18 which is poorer than the relative reaction rate of 0.25 w/w % Zn doped chromia, 0.272, and 1 w/w % Zn doped chromia, 0.26. Clearly 0.25 w/w % Zn doped chromia is the most active catalyst prepared in this series. 4 w/w % Zn doped chromia, with a relative reaction rate of 0.11 at 573K, is obviously a poisoned catalyst in comparison to undoped chromia.

These zinc poisoning and promotion effects were evident throughout the range of doped chromias examined, when compared with undoped chromias from which they were derived. The low crystallinity chromia range appears to be

anomalous with other series of catalyst studied as the 4 w/w % Zn doped chromia has a higher relative reaction rate in comparison to undoped chromia. When the % CF_3CH_2F in reaction effluent at 573K is compared between undoped and 4 w/w % Zn doped chromia (3.3.2) it is considerably lower. However, this doped chromia has a very low surface area in comparison to all of the other chromias in the same series. The relative reaction rate of this chromia is higher than that of undoped chromia, despite the doped chromia having a lower % CF_3CH_2F in the reactor effluent at 573K.

By examination of zinc poisoning and promotion throughout the range of chromias examined, it is clear that crystallinity plays a major role in determining the amount of zinc chloride required to obtain these different effects. If the medium crystallinity chromia series is taken as a 'model' series for determining zinc poisoning and promotion, in comparison to undoped chromia at 573K, comparisons between chromia series derived from chromias containing different amounts of crystalline chromia can be made. This can be a useful comparison for determining the w/w % Zn required to promote and poison their catalytic activity for the CF_3CH_2Cl - CF_3CH_2F reaction. When catalysts were prepared using high crystallinity chromia the promotional effect of 0.25 w/w % Zn is less marked in comparison to the effect of the equivalent doping of the medium crystallinity chromia series. 1 w/w % Zn, which was a mildly promoting zinc loading in medium crystallinity chromia is enough to poison high crystallinity chromia and 4 w/w % Zn is heavily poisoned.

When lower crystalline chromia catalysts were examined in comparison to medium crystallinity chromia at 573K the promotional effects of 0.25 w/w % Zn are less evident in the low crystallinity chromia series than in the medium crystallinity chromia series. Poisoning effects of larger amounts of zinc are not as dramatic for the low crystallinity chromia series as they are in the medium crystallinity chromia series. 1 w/w % Zn in the low crystallinity chromia series was a mild poison. Amorphous chromia was doped with different amounts of zinc in comparison to

chromias containing some crystalline chromia phase. 1 % w/w Zn was the only zinc doping level common between amorphous chromia and the other chromia series. 1 w/w % Zn was a mild promoter of amorphous chromia. 3 w/w % Zn, which poisoned other chromias, showed a strong promotional effect with amorphous chromia and 5 w/w % Zn was poisoned.

The relative reaction rates of reaction on chromia catalysts gave an indication of catalyst performance and could be used to identify factors contributing to good and bad catalysts throughout the range. From Table 3.5 catalysts can be grouped into three broad classes. Poor catalysts are those with relative reaction rates of 0.17 or below. Included in this class are the 4 w/w % Zn doped chromias of higher and medium crystallinity, the 1 w/w % Zn highly crystalline chromia and the 5 w/w % Zn amorphous chromia. All of these catalysts are poisoned with respect to the undoped chromias of the same series. The second classification is that of 'average' performance chromia catalysts. These chromias have relative reaction rates of between 0.18 - 0.24 and include undoped chromias containing some crystalline chromia phase and poisoned chromias in the low crystallinity chromia series. The final classification are 'good' catalysts. These chromias have relative rates of > 0.25. This is a very wide range and includes 3 w/w % Zn doped amorphous chromia, which has a relative rate of 0.41, and is easily the best catalyst tested and promoted 0.25 w/w % Zn doped chromias of higher and medium crystallinities. Undoped amorphous chromia is also in this class, illustrating the effect of low crystallinity on the catalytic performance of chromias for this reaction. The promotional effect of zinc can be best illustrated by comparing the relative rates of the 0.25 w/w % Zn and undoped medium crystallinity chromia with undoped amorphous chromia. When comparing 0.25 w/w % Zn doped medium crystallinity chromia, with undoped amorphous chromia the relative rates of these two chromias are similar (0.018 difference). However, comparison of the two undoped chromias reveals a relative rate difference of 0.11 illustrating the promotional effect of 0.25 w/w % Zn on medium crystallinity chromia.

3.10 APPARENT ACTIVATION ENERGY CALCULATIONS FOR CHROMIA CATALYSTS.

The rate constant for a reaction can be found from the Arrhenius equation (EQN. 3.8) :-

$$\ln K = \ln A - E_a / RT \quad \text{EQN. 3.8}$$

Where R = gas constant (8.314 $kJ^{-1}mol^{-1}$); T = the absolute temperature; k = rate constant; A = pre - exponential factor and Ea = the activation energy.

Hence a plot of lnK vs. 1 / T will have intercept lnA and slope - Ea / R and from this the activation energy can be derived :-

$$Ea\ (kJmol^{-1}) = -\text{slope} \times R \quad \text{EQN. 3.9}$$

As the rate is unknown, the activation energy (Ea) for these reactions cannot be calculated. An 'apparent' activation energy for each chromia catalyst tested can, however, be calculated. By substituting K, the rate constant, for % 134a, from gas chromatography analysis of samples results, the 'apparent' activation energy of catalysts tested is obtained. Therefore, by calculating the ln[% CF_3CH_2F] and 1 / T (K) using the results of catalyst testing, from 3.9, a graph of ln[% CF_3CH_2F] vs. 1 / T was plotted and the slope was obtained which can be multiplied by the gas constant (R) to obtain the apparent activation energy in $kJmol^{-1}$. It should be noted that only % CF_3CH_2F of 12% or less were used in this calculation. Results appear in table 3.20.

It is evident that the apparent activation energy of chromia catalysts in general decreases with increasing amounts of zinc doping. This relationship is not linear, however, comparison of undoped to 0.25 w/w % Zn doped apparent activation energies illustrates that the decrease in activation energy is substantial. Comparison of 0.25 w/w % Zn to 4 w/w % Zn chromias illustrates a far smaller

decrease in activation energy. The effect of even small amounts of Zn doping on apparent activation energies is quite dramatic.

Table 3.20 Calculated Apparent Activation Energies of Chromias Tested

CHROMIA	APPARENT ACTIVATION ENERGY ($kJmol^{-1}$)
High Crystallinity chromia	
undoped	211.691
0.25 w/w % Zn	101.474
1 w/w % Zn	105.17
4 w/w % Zn	75.765
Medium Crystalline chromia	
undoped	179.175
0.25 w/w % Zn	113.154
1 w/w % Zn	107.026
4 w/w % Zn	91.720
Low Crystalline chromia	
undoped	193.101
0.25 w/w % Zn	145.877
1 w/w % Zn	116.920
4 w/w % Zn	144.281
amorphous chromia	
undoped	202.105
1 w/w % Zn	162.505
3 w/w % Zn	118.159
5 w/w % Zn	118.824
15 w/w % Zn	89.018

4 SURFACE STUDIES OF FLUORINATED CHROMIAS

4.1 INTRODUCTION

This chapter is concerned with studies to determine species present on the surface of fluorinated chromias. As it is believed that the reaction of HF and CF_3CH_2Cl to form CF_3CH_2F and HCl occurs at the surface of the fluorinated chromia catalyst, identification of the surface species present was an important aspect of this study. X - ray photoelectron spectroscopy was performed by the Analytical and Physical Sciences Group at ICI Runcorn using fluorinated chromias prepared at Glasgow as described in chapters 2 and 3 to obtain data regarding surface species. Data analysis of the results of the XPS analysis was subsequently performed at Glasgow. This work intended to reveal the different surface species present on the catalyst surface. Undoped, heavily and lightly zinc doped fluorinated chromias were examined to identify differences between surface species. It was hoped that this would give an indication as to the difference in performance of these chromias during micro reactor studies.

Transmission electron microscopy of fluorinated chromias was performed at Glasgow University by the Electron Microscopy Centre in the Department of Chemistry using samples prepared as described in chapters 2 and 3. Lightly and heavily zinc doped fluorinated chromia samples were chosen for examination as it was hoped that differences between the micro reactor test results of these chromias would yield significant differences in the surface species present on these catalysts. Fluorinated chromia samples used in both X - ray photoelectron spectroscopic analysis and electron microscopy were taken from the same batch of fluorinated chromias. Experimental procedures and results of this work are described below.

4.2 X - RAY PHOTOELECTRON SPECTROSCOPY.

Various samples of fluorinated chromias with differing zinc dopings, prepared at Glasgow, were presented to the Analytical and Physical Sciences Group, Surface Science Team at ICI Runcorn as described in section 2.6. Samples (2g) were presented for analysis to determine the state of various key elements on the surface of catalysts. Samples were ground using an agate mortar and pestle and loaded onto disks using adhesive tape placed between the catalyst and disk, this work was performed in a dust cabinet as there was no facility for sample preparation under an inert atmosphere and unfortunately it was necessary to expose the samples to air. Disks loaded with catalyst were positioned on a sample holder before being examined in a VG ESCALAB 200 - D X - Ray Photoelectron Spectrometer.

Three chromia samples were submitted along with three standards for X - ray photoelectron spectroscopic analysis at ICI Runcorn. Chromias submitted were all reacted samples from the medium crystallinity chromia series and were undoped, 0.25 w/w % Zn doped and 4 w/w % Zn doped. Standards submitted were ZnF_2 (BDH Optran, 99.9 % pure), ZnO (Hopkin and Williams, 99.7 % pure) and $ZnCr_2O_4$ spinel (determined by X- ray diffraction). Cr_2O_3 and CrF_3 spectra held in an XPS data base at Runcorn were also used for comparison. The $ZnCr_2O_4$ spinel was prepared by coprecipitation of zinc and chromium nitrates with ammonia in a 1 : 2 zinc : chromium ratio and the product obtained was calcined within a muffel furnace for 24 h.. Results of XPS analysis appear in Tables 4.1 - 4.3 and spectra are shown in Figs 4. 1 - 4.6.

Table 4.1 Binding Energy Values / eV Obtained From XPS Results of Standards and Reacted Medium Crystallinity Chromias (error ± 0.2 eV).

	Cr 2p	Zn 2p	F 1s
ZnO		1022.4	
ZnF_2		1023.4	685.7
Zn / Cr SPINEL	576.9	1021.6	
UNDOPED	577.8		685.6
0.25 w/w % Zn	577.8	1023.1	685.4
4 w/w % Zn	577.7	1023.2	685.4
Cr_2O_3	576.9		
CrF_3	580.0		685.4

Table 4.2 Atom % Obtained From XPS Results of Zn / Cr Spinel and Reacted Medium Crystallinity Chromias.

	Zn / Cr SPINEL	UNDOPED	0.25 W/W % Zn DOPED	4 W/W % Zn DOPED
Cr 2p	27.95	25.46	30.48	26.88
Zn 2p	6.35		0.41	1.09
F 1s		10.37	10.77	9.00
C 1s	17.95	30.98	20.59	26.69
O 1s	47.75	32.57	37.44	35.77
N 1s		0.62	0.32	0.57

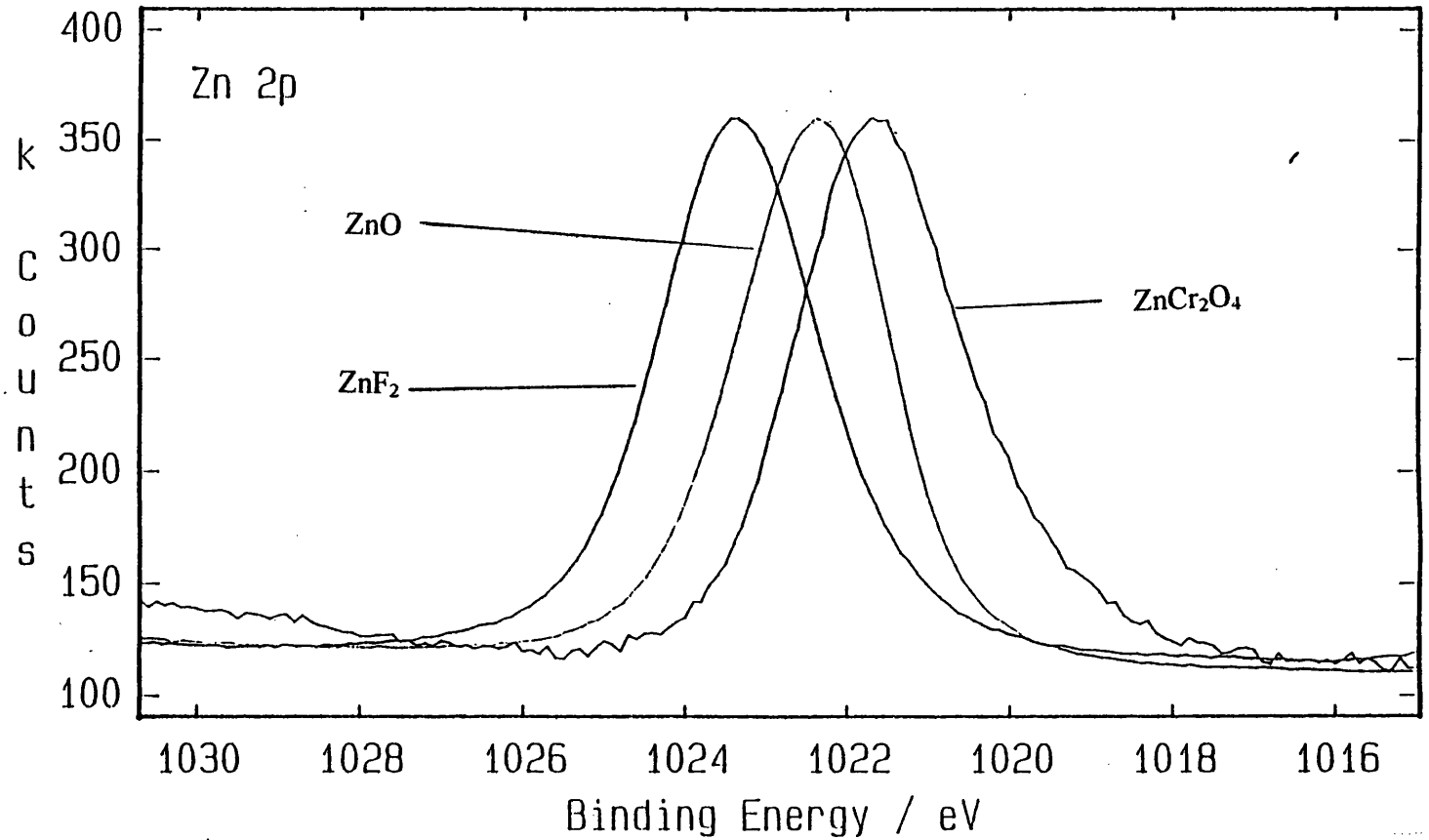

Fig 4.1 Zn 2p X - Ray Photoelectron Spectra of ZnF_2, ZnO and $ZnCr_2O_4$

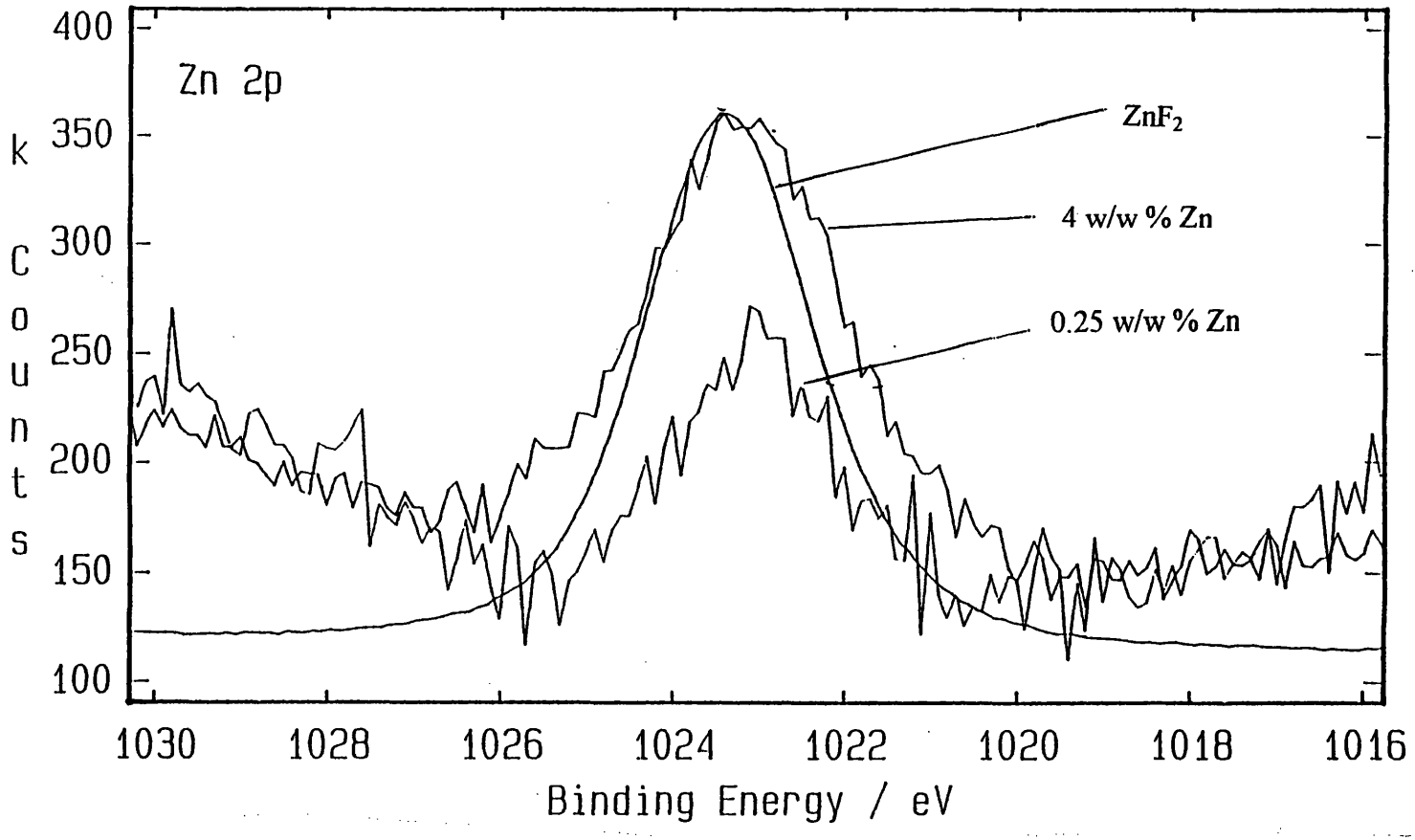

Fig 4.2 Zn 2p X - Ray Photoelectron Spectra of ZnF_2, 0.25 and 4 w/w% Zinc Doped, Fluorinated Chromias

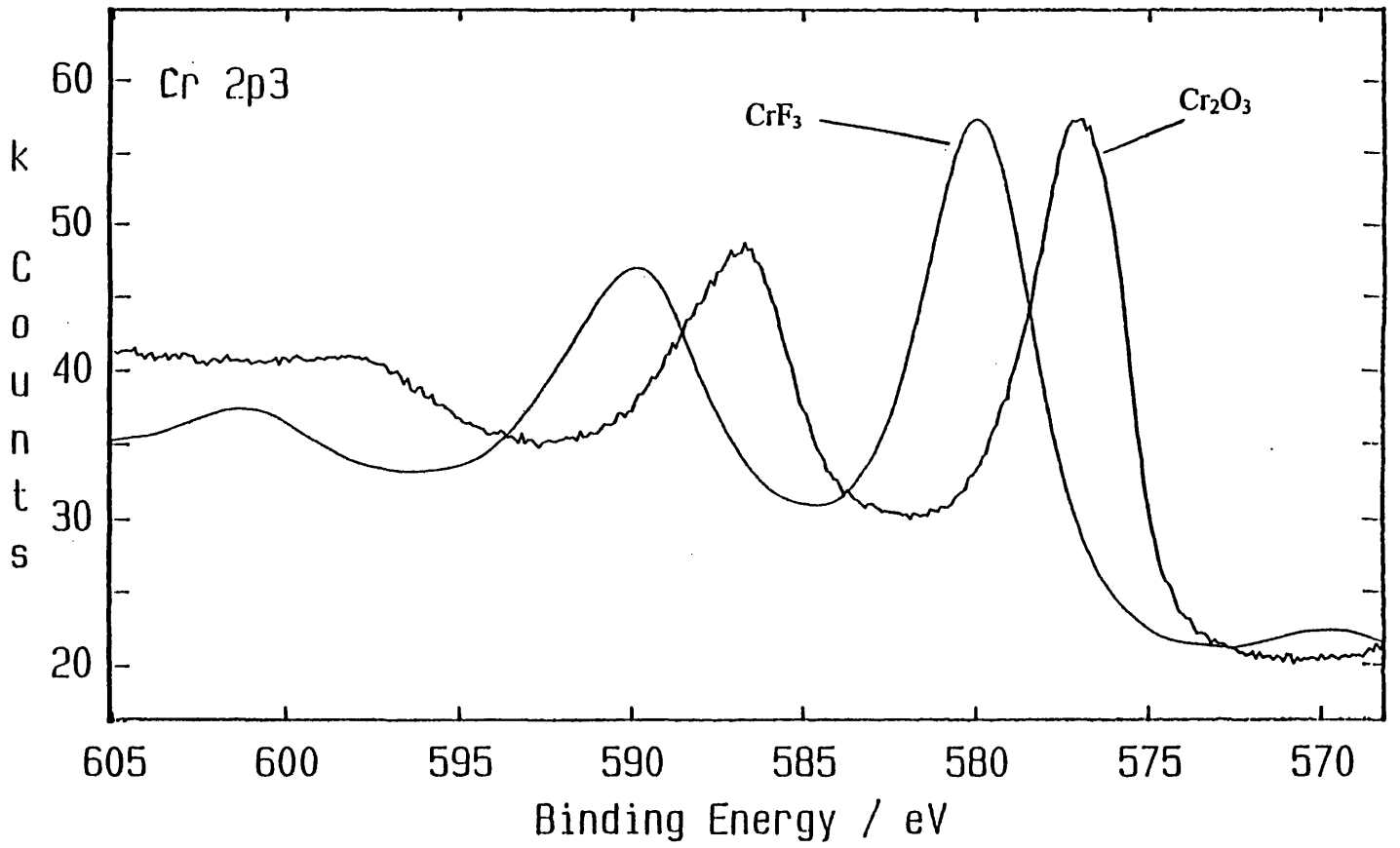

Fig 4.3 Cr 2p3 X - Ray Photoelectron Spectra of Cr_2O_3 and CrF_3

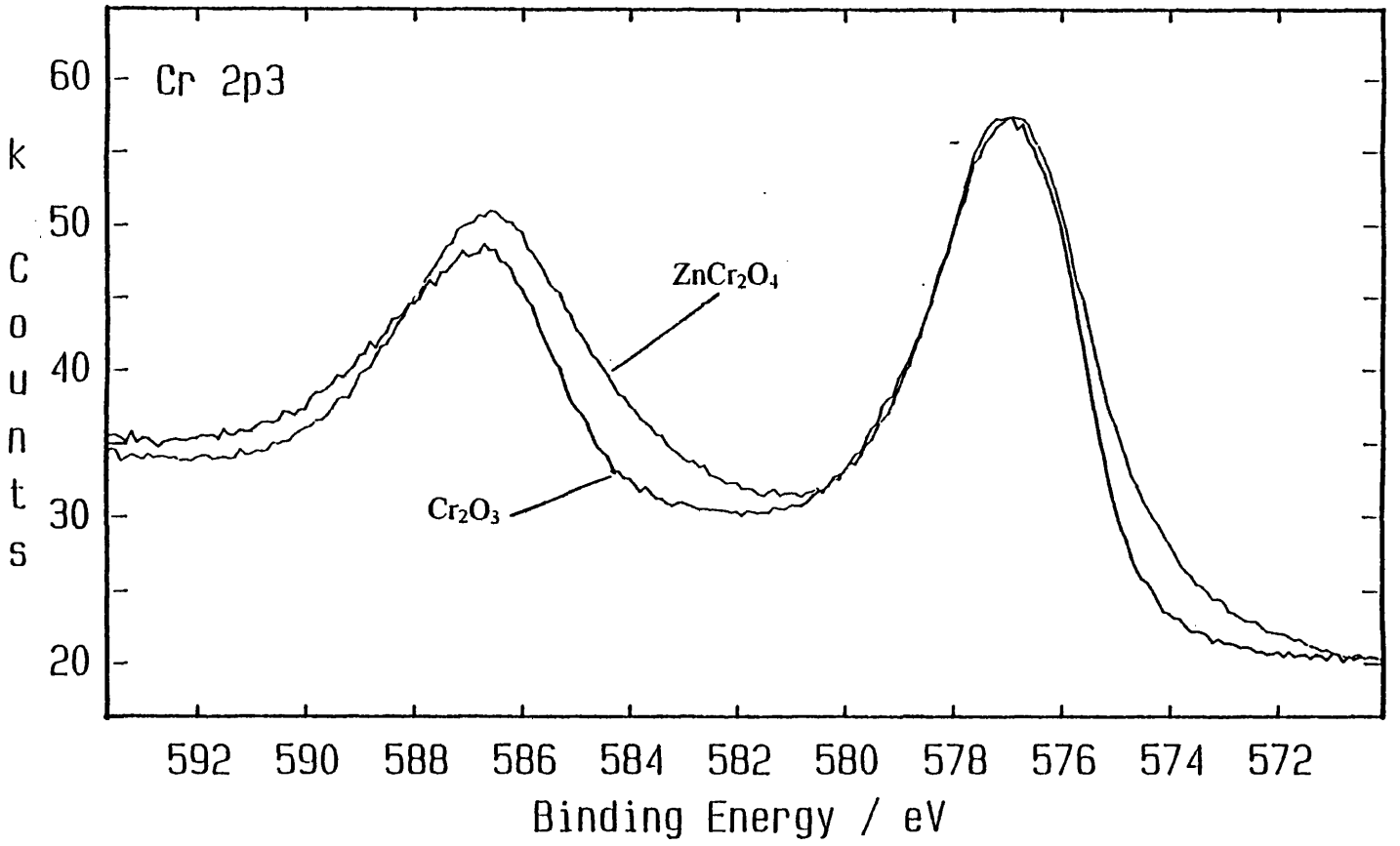

Fig 4.4 Cr 2p3 X - Ray Photoelectron Spectra of Cr_2O_3 and $ZnCr_2O_4$

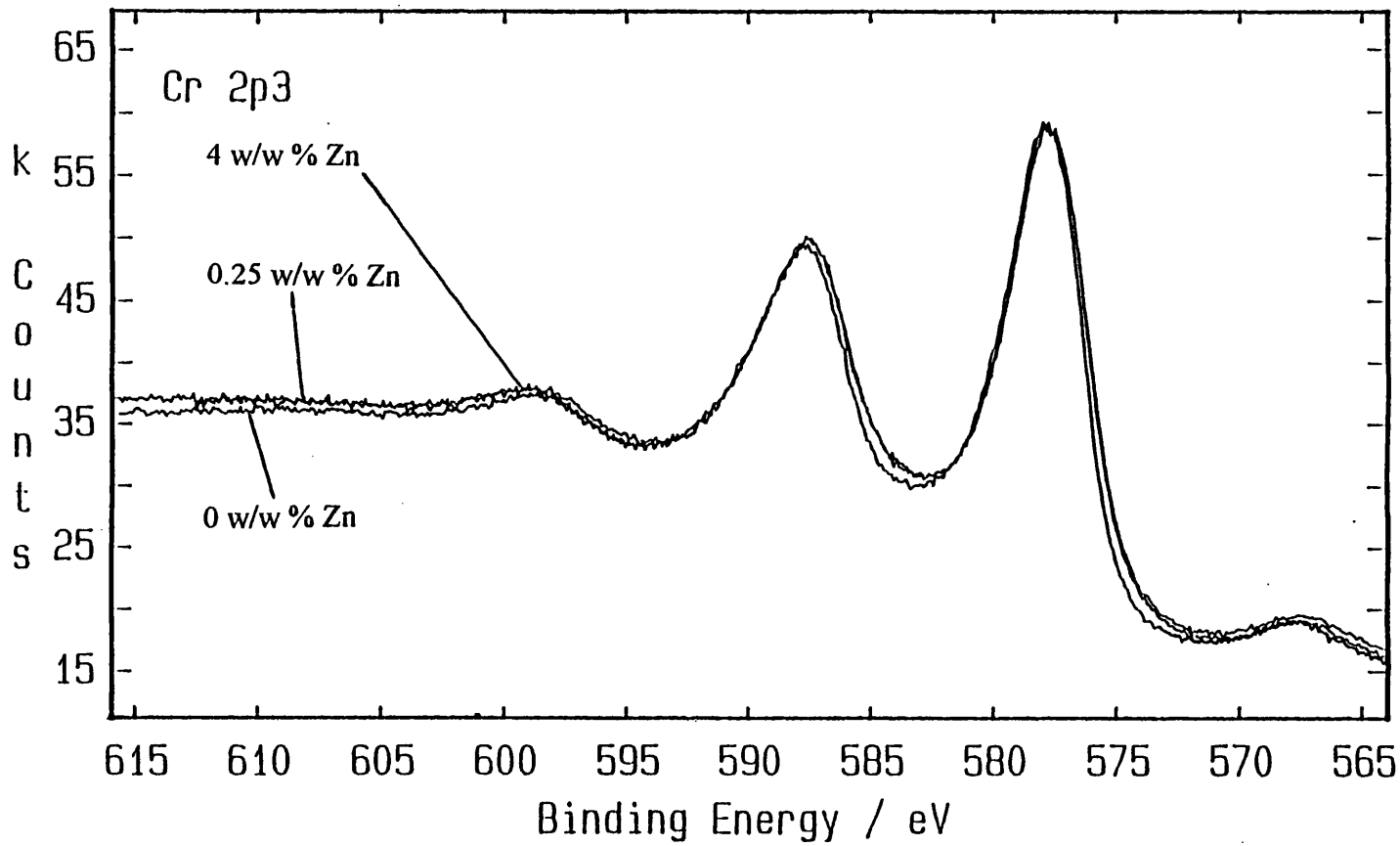

Fig 4.5 Cr 2p3 X - Ray Photoelectron Spectra of Undoped, 0.25 and 4 w/w % Zinc Doped, Fluorinated Chromias

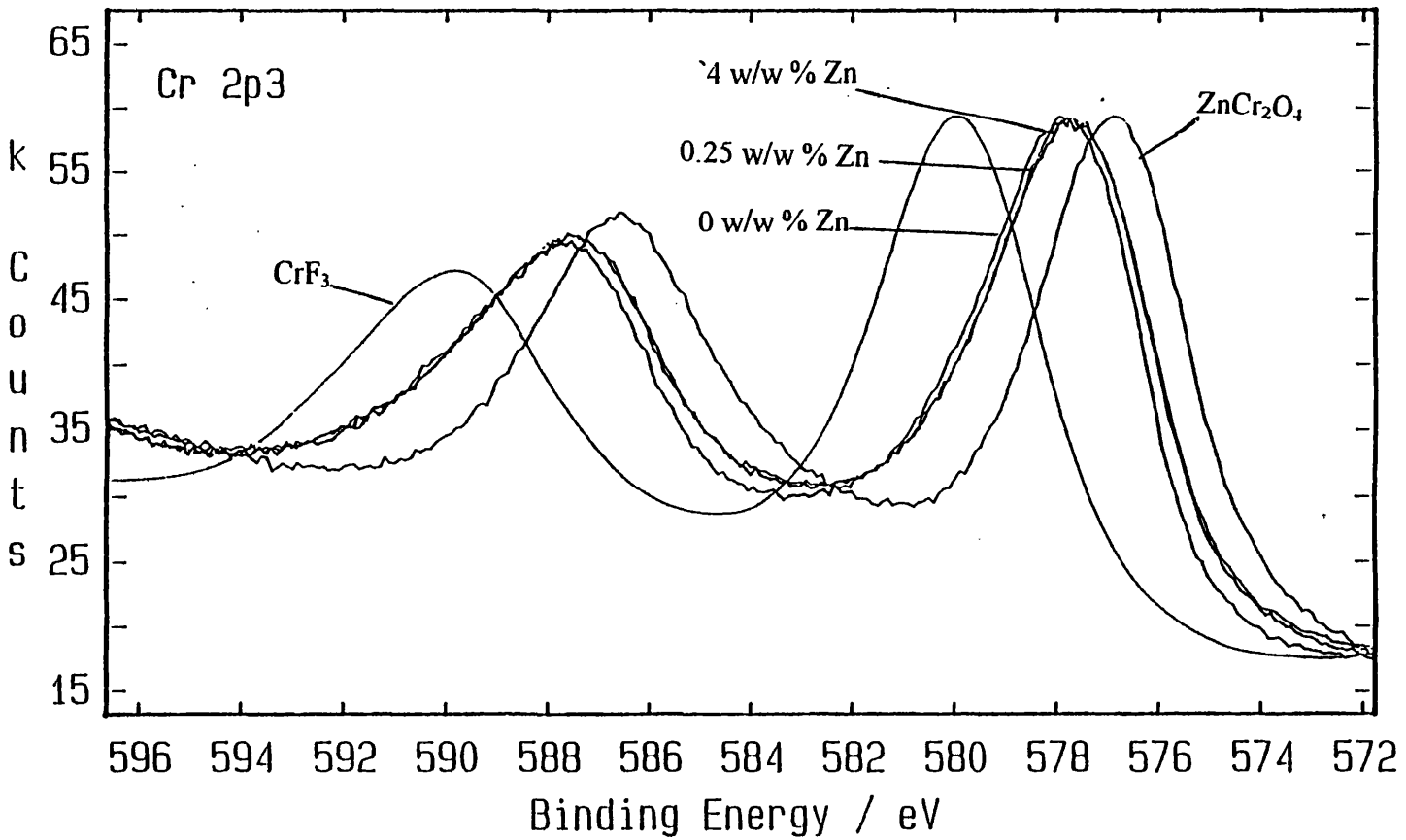

Fig 4.6 Cr 2p3 X - Ray Photoelectron Spectra of CrF_3, $ZnCr_2O_4$ and Undoped, 0.25 and 4 w/w % Zinc Doped, Fluorinated Chromias

Table 4.3 Atom Ratio Obtained From XPS Results of Zn / Cr Spinel and Reacted Medium Crystallinity Chromias.

	Zn / Cr SPINEL	UNDOPED	0.25 W/W % Zn DOPED	4 W/W % Zn DOPED
Cr 2p	1.00	1.00	1.00	1.00
Zn 2p	0.23		0.01	0.04
F 1s		0.41	0.35	0.34
C 1s	0.64	1.22	0.68	0.99
O 1s	1.71	1.28	1.23	1.33
N 1s		0.02	0.01	0.02

(I) Zn 2p SPECTRA

Zn 2p spectra allow this technique to give chemical information regarding different Zn environments. ZnO, ZnF_2 and $ZnCr_2O_4$ spinel are distinguished easily from Fig. 4.1 as each have different binding energies. Fig. 4.2 is the Zn 2p spectra of the two chromias containing zinc compared with the spectrum of ZnF_2. Both chromias exhibit spectra with large amounts of noise due to the relatively small amounts of zinc present. However, it is clear from the spectra that zinc on the 0.25 and 4 w/w % Zn doped chromias is highly fluorinated and exhibits a binding energy on Table 4.1 very close to that of ZnF_2. The binding energy of zinc in both of these chromias is too large in comparison to the binding energies of zinc in ZnO and $ZnCr_2O_4$ spinel standards to be in a similar environment to zinc in these compounds. The binding energy of zinc in both of these chromias, accounting for an error of ± 0.2 eV, is close enough to the zinc binding energy for ZnF_2 to suggest that the vast majority of zinc present on the surface of the chromias is ZnF_2.

Surface atomic composition was obtained, by Analytical and Physical Sciences at ICI Runcorn, on the basis of peak - area intensities by employing the following equation (131):

$$I_A / I_B = (n_A \sigma_A \lambda_A T_A) / (n_B \sigma_B \lambda_B T_B) \qquad \text{Eqn 4.1}$$

Where A and B are the atoms to analyse, n is the atomic concentration, σ represents the photoelectron cross - section of core levels taken from Scofield tables, λ is the escape depth of the photoelectron and T is the transmission factor of the analyser. T is proportional to the kinetic energy E_k and λ to $E_k^{0.75}$.

Tables 4.2 and 4.3 show very interesting results if the relative amounts of Zn : Cr are examined in the two Zn doped chromias and when the relative amounts of zinc are examined and compared for these chromias in consideration of the amounts of $ZnCl_2$ impregnated onto each chromia during catalyst preparation. The initial w/w % of zinc doped onto the chromias was 0.25 % and 4 % respectively. The atom % obtained reveals little information about zinc on the chromias following impregnation and reaction as some zinc may have gone into the chromia and fluorination has added large quantities of fluoride onto the surface which alters the relative % of elements on the surface between the unfluorinated and reacted states. However comparison of the relative amounts of zinc present on the surface between the two zinc doped chromias suggests that some considerable loss of zinc has occurred following the initial impregnation. The w/w % of zinc ratio between the two chromias in question was 1 : 16, however from these tables the surface ratio is 1 : 3 -4. This would suggest that zinc has ether gone into the bulk of the chromia or has been lost from the surface. $ZnCl_2$ has a melting point of 563K and a boiling point of 1005K and its heat of vaporisation is 126kJmol^{-1}, in comparison to that of ZnF_2 (190.1kJmol^{-1}) (118). This may account for some loss of zinc during fluorination and reaction particularly from the heavily doped chromia.

(II) Cr 2p SPECTRA

Information regarding different chromium environments can be obtained from Cr 2p spectra. Comparison plots of CrF_3 and Cr_2O_3 appear in Fig. 4.3. These show clear differences in the XPS spectra of the two compounds and hence enable comparisons to be made. Fig. 4.4 shows a comparison of the Zn / Cr spinel and

Cr_2O_3. The Cr 2p maxima are the same for $ZnCr_2O_4$ spinel and Cr_2O_3, however the peak shape is clearly different. Fig 4.5 compares the Cr 2p spectra of the undoped, 0.25 and 4 w/w % Zn doped chromias. There is very little difference between the chromium states in these three chromias as shown by their Cr 2p spectra and Table 4.3 shows the Cr 2p binding energy for undoped and 0.25 w/w % Zn doped chromia to be exactly the same with the binding energy for 4 w/w % Zn doped having a difference of 0.1 eV from the other two samples.

Comparison of these three chromias with spectra for CrF_3 and Cr_2O_3 show that these chromias are neither in the state associated with Cr_2O_3 or that associated with CrF_3 (Fig. 3.11). The chromium on the surface of these chromias is in a state somewhere in between CrF_3 and Cr_2O_3. This suggests that the chromia surface is fluorinated to some extent. However, the fluorination is not extensive enough to produce CrF_3 in significant quantities on the surface. Such a change in α - Cr_2O_3 to form α - CrF_3 would result in significant structural alterations on the surface as α - Cr_2O_3 has a hexagonal close packed arrangement of atoms and α - CrF_3 has an orthorhomboidal arrangement of atoms. The majority of fluorine associated with chromium in the chromias examined is probably bound to terminal and uncoordinated chromium or as an oxyfluoride bound to chromium. The binding energies in Table 4.3 clearly illustrate that the majority of the chromium is present in neither a fully oxygenated or fully fluorinated form.

(III) F 1s Spectra.

The F 1s binding energy values in Table 4.3 are typical of inorganic fluorides. Interestingly, the F 1s binding energy of undoped chromia is closer to that of the ZnF_2 inspite of this chromia containing no zinc. The F 1s binding energies of the 0.25 and 4 w/w % Zn doped chromias are both the same as that of CrF_3. Taken together with information gained from Cr 2p and Zn 2p spectra it is difficult to state the exact nature of fluoride species on these chromias from XPS other than to say

that the binding energies are typical for those found for first row transition metal fluorides.

4.2 TRANSMISSION ELECTRON MICROSCOPY

Transmission electron microscopy (TEM) was used as another method to determine surface species present and it was hoped that the results of this work would complement and enhance results obtained from X - ray photoelectron spectroscopy. Chromias examined were fluorinated 0.25 w/w % zinc doped and fluorinated 4 w/w % zinc doped. Prints obtained were examined with the aid of an eye piece and the spacing between lattice lines of individual crystals was measured in m x 10^{-3}. Typically, 10 lines were measured and the average spacing between all 10 lines was used to determine the line spacing of a crystal. The actual 'd' spacings were calculated by division of the average line spacing (in m) by the magnification factor and the results are reported in Å. A diffraction pattern was also obtained and 'd' spacings were determined by measuring the ring diameters in (m x 10^{-3}) with a ruler and dividing the camera constant by the result obtained. 'd' Spacings of certain crystals on micrographs may be 'distorted' depending upon the angle of the crystal in the photograph. Calculated 'd' spacings may, as a result of this, not match the actual 'd' spacing. Results of this work were also reported in Å. Measured 'd' spacings for each material (likely errors ± 0.07 Å) are shown in Tables 4.4 and 4.5 and micrograph prints for both samples appear in Figs 4.7 and 4.8.

Figure 4.7 Micrograph of 0.25 w/w % Zinc Doped Fluorinated Chromia

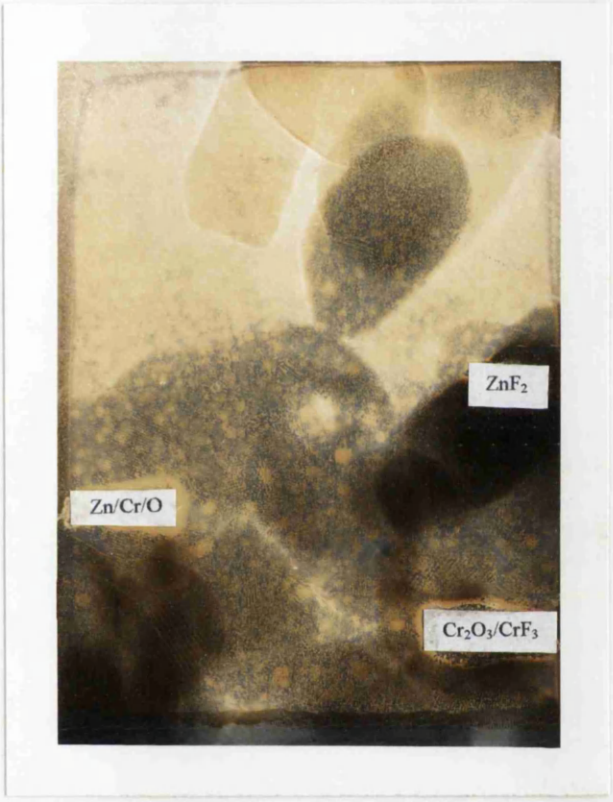

Figure 4.8 Micrograph of 4 w/w % Zinc Doped Fluorinated Chromia

Table 4.4 Observed 'd' Spacings (Å) for Materials From TEM Analysis of Micrograph Prints (numbers in superscript denote number of times 'd' spacing was found)

0.25 w/w % Zinc Doped Fluorinated Chromia	4 w/w % Zinc Doped Fluorinated Chromia
4.74^{1}	4.17^{1}
3.88^{1}	3.85^{1}
3.66^{4}	3.53^{7}
3.45^{3}	3.21^{6}
0.90^{1}	3.13^{1}
0.88^{1}	2.72^{2}
0.77^{1}	2.56^{3}
	2.31^{1}
	1.00^{1}
	0.93^{1}
	0.88^{6}

Table 4.5 Observed 'd' Spacings (Å) for 0.25 w/w % Zinc Doped Fluorinated Chromia Diffraction Pattern Analysis

'd' Spacing	'd' Spacing
3.67	1.24
2.65	1.18
2.45	1.14
2.12	1.07
2.03	1.03
1.80	0.94
1.64	0.88
1.56	0.86
1.40	0.82
1.27	0.79

The values of 'd' spacings obtained for crystals on each material can be compared with data from the Joint Committee on Powder Diffraction Standards (JCPDS) powder diffraction file. Tables 4.6 - 4.11 list 'd' spacings, taken from this file, of the species most likely to be present.

Table 4.6 JCPDS Powder Diffraction File Data for α - CrF_3

d (Å)	hkl	I/I_0
3.60	110	100
2.614	211	20
2.488	101	8
2.165	210	30
2.050	200	6
1.806	220	20
1.649	320	30
1.619	201	6
1.584	211	2
1.540	332	16
1.463	310	10
1.440	211	16

Table 4.7 JCPDS Powder Diffraction File Data for α - Cr_2O_3

d (Å)	hkl	I/I_0
3.633	012	75
2.666	104	100
2480	110	95
2.264	006	12
2.176	113	40
2.048	202	10
1.8156	024	40
1.672	116	90
1.579	122	14
1.465	214	25
1.4314	300	40
1.2961	1.0.10	20
1.2398	220	18

Table 4.8 JCPDS Powder Diffraction File Data for ZnF_2

d (Å)	hkl	I/I_0	d (Å)	hkl	I/I_0	d (Å)	hkl	I/I_0
3.33	110	100	1.2567	212	4	0.9239	510	4
2.608	101	95	1.2057	321	6	0.9056	332	4
2.356	200	18	1.1778	400	8	0.9022	501	6
2.285	111	25	1.1423	410	4	0.8740	422	4
2.108	210	10	1.1413	222	6	0.8693	303	6
1.748	211	80	1.1104	330	4	0.8424	521	6
1.666	220	25	1.0794	312	12	0.8329	440	2
1.565	002	18	1.0734	411	6	0.8156	323	2
1.490	310	14	1.0532	420	2	0.7957	512	4
1.4172	112	12	1.0102	103	2	0.7851	600	2
1.4039	301	20	0.9961	113	<1			
1.3451	311	2	0.9413	402	6			
1.3039	202	6	0.9354	213	8			

Table 4.9 JCPDS Powder Diffraction File Data for ZnO

d (Å)	hkl	I/I_0	d (Å)	hkl	I/I_0
2.816	100	71	1.0422	211	10
2.602	002	56	1.0158	114	5
2.476	101	100	0.9848	212	4
1.911	102	29	0.9764	105	7
1.626	110	40	0.9555	204	1
1.477	103	35	0.9382	300	4
1.407	200	6	0.9069	213	12
1.379	112	28	0.8826	302	6
1.359	201	14	0.8675	006	1
1.301	004	3	0.8369	205	6
1.238	202	5	0.8290	106	2
1.1812	104	3	0.8237	214	2
1.0929	203	10	0.8125	220	5
1.0639	210	4			

Table 4.10 JCPDS Powder Diffraction File Data for $ZnCrO_4$ (no data available of hkl for this compound)

d (Å)	I/I_0	d (Å)	I/I_0
4.63	12	1.762	10
4.25	20	1.623	12
3.78	35	1.580	16
3.55	30	1.550	4
2.97	4	1.488	60
2.78	25	1.390	4
2.62	100	1.373	4
2.53	60	1.340	8
2.18	8	1.105	8
2.11	4	1.090	4
2.08	8	1.072	2
1.882	16	1.040	4

Table 4.11 JCPDS Powder Diffraction File Data for $ZnCr_2O_4$

d (Å)	hkl	I/I_0
4.80	111	10
2.90	220	50
2.51	311	100
2.41	222	10
2.05	400	20
1.70	422	30
1.60	333	40
1.47	440	50

Various phases can be assigned to all three fluorinated chromias but most are assigned without a great degree of certainty. For 0.25 w/w % zinc doped fluorinated chromia results obtained from the diffraction pattern indicate that there is evidence for ZnF_2 crystals on the surface of the chromia. Distinguishing between Cr_2O_3 and CrF_3 phases was difficult as many of the characteristic 'd' spacings are common. It was noted that these phases are less in abundance than phases of zinc species. The diffraction pattern also indicated that some ZnO may be present. However, many of the ZnO 'd' spacings can also be attributed to ZnF_2. It is likely that most, or possibly all, of the ZnO / ZnF_2 overlap in 'd' spacing was ZnF_2 as the X - ray photoelectron spectroscopy results would indicate. The micrograph obtained for 0.25 w/w % zinc doped fluorinated chromia also contained 'd' spacings which can be attributed to $ZnCrO_4$ and $ZnCr_2O_4$. Some of these 'd' spacings can also be assigned to the powder diffraction file data for ZnO and ZnF_2 but the same conclusions can be drawn from the micrograph print, regarding zinc phases present, as were drawn from the diffraction pattern. No clear evidence for chromium species resulted from the micrograph examination, hence the major chromium phase present was probably neither α - Cr_2O_3 or α - CrF_3. This idea is supported by X - ray photo electron spectroscopy data, which indicated that binding energies for chromium species were indicative of nether α - Cr_2O_3 or α - CrF_3.

Fluorinated chromia with 4 w/w % zinc present had neither evidence for α - Cr_2O_3 or α - CrF_3. There was a strong possibility that ZnF_2 was present on this chromia and a number of crystals examined from the micrograph had 'd' spacings which could be attributed to ZnF_2. Some of the 'd' spacings attributed to ZnF_2 were also attributed to ZnO but, as discussed, the presence of ZnO was less likely. This would agree with X - ray photoelectron spectroscopy data, which suggested strongly that there was a heavily fluorided zinc phase, probably ZnF_2 on the surface of this chromia. Large 'd' spacings on both micrographs could be attributed to zinc chromates, $ZnCrO_4$ and $ZnCr_2O_4$. The micrograph of 4 w/w % zinc doped fluorinated chromia has a large 'd' spacing of 4.17Å, which agrees with the Powder

Diffraction File data for $ZnCr_2O_4$. The presence of such species is not evident from XPS analysis. However, transmission electron microscopy indicates the presence of these species on the surface of the catalyst. Table 4.12 attempts to make some comparative assignments between results obtained and Powder Diffraction File data. Few of the assignments are made with a degree of certainty. These results, together with X - ray photoelectron spectroscopy, do provide some information regarding the surface species on these catalysts. Further discussion of this work appears in chapter 7.

Table 4.12 Assignment of Certain 'd' Spacings for Micrograph and Diffraction Patterns to 'd' Spacings for Various Compounds From JCPDS Powder Diffraction File Data (✠ denotes a good assignment i.e. with some certainty)

Source	'd' Spacing	Cr_2O_3	CrF_3	ZnF_2	ZnO	$ZnCrO_4$	$ZnCr_2O_4$
Diff. Pat.	3.67	*	*				
0.25 w/w%	1.27			*			
Zn	✠1.18			*			
	1.14			*		*	
	1.07			*	*		*
	1.03				*	*	
	0.94			*	*		
	0.88			*	*		
	0.82			*	*		
	0.79			*	*		
Micro.	✠4.74						*
0.25 w/w%	✠3.88					*	
Zn	3.66	*	*				
	3.45					*	
	0.90			*	*		
	0.88			*	*		
	0.77			*	*		
Micro.	✠4.17					*	
4 w/w%	3.85					*	
Zn	3.53					*	
	3.21			*			
	1.0			*	*	*	
	0.93			*	*		
	0.88			*	*		

5 [^{18}F] - FLUORIDE LABELLED HF INTERACTION WITH CHROMIA

5.1 INTRODUCTION

This chapter describes work performed on fluorinated chromias using [^{18}F] - fluorine labelled hydrogen fluoride. Labelled hydrogen fluoride was prepared by the exchange of fluoride from unlabelled hydrogen fluoride with fluoride from [^{18}F] - fluorine CsF. The labelling of chromias with [^{18}F] - fluoride was used to determine the lability of fluoride species on the fluorinated chromia catalysts used in the reaction of CF_3CH_2Cl with HF. Fluoride labilities were used to compare chromias with different w/w % zinc and differing crystallinities. The interaction of labelled chromias with unlabelled HF and CF_3CH_2Cl determined lability of fluoride species with these compounds.

5.2 EXPERIMENTAL

5.2.1 PRETREATMENT OF CHROMIAS BEFORE REACTION.

All chromia catalysts studied were fluorinated with anhydrous HF according to the procedure described in 3.2.1 and fluorination was performed using the catalyst fluorination rig described in 2.1.6. Following fluorination, chromia samples were stored in sealed containers under a dry nitrogen atmosphere within an inert atmosphere box ($H_2O < 3$ ppm). A fluorinated chromia sample (ca. 1g) was weighed accurately into a beaker using the digital balance contained within the inert atmosphere box. The Monel reactor associated with the rig for radiochemical catalyst testing was removed to the inert atmosphere box and the weighed sample of fluorinated chromia was charged into the reactor. Valves on the reactor were closed and the reactor was removed from the inert atmosphere box and attached to the radiochemical rig for catalyst testing described in 2.1.7.

A nitrogen flow (0.0537 $molh^{-1}$) was passed through the rig and over the catalyst bed by opening the valves on the reactor and from the nitrogen inlet to the

scrubber and adjusting a needle valve attached to a flow meter to control the flow of nitrogen from the main cylinder. A ceramic fibre heater consisting of two semi - circular components (Watlow Ltd.) was positioned around the central straight length Monel piping which formed the central, catalyst holding, section of the reactor and the two components were held together with tie bands. Electrical connectors, protruding from the sides of the ceramic fibre heater, were connected to a Variac transformer and a thermocouple wire, attached to a multimeter, was placed into the centre of the heater to monitor the temperature of the reactor. Gaps between the reactor and the openings of the heater were plugged with glass wool to aid temperature control. The catalyst was heated under a nitrogen atmosphere at 573K for 1h before reaction.

5.2.2 LABELLING OF CHROMIA WITH [^{18}F] - FLUORIDE.

[^{18}F] - HF was prepared as described in 2.2.3. The Monel storage bomb containing 11 mmol of [^{18}F] - HF was removed from the Monel vacuum line used to prepare the [^{18}F] - HF and attached to the radiochemical flow rig. This acted as an [^{18}F] - HF reservoir for chromia labelling experiments. A specially designed furnace, temperature controlled using a Variac transformer, was positioned around the [^{18}F] - HF reservoir. A thermocouple attached to a ratemeter was inserted into the furnace and the opening of the furnace was plugged with glass wool. The furnace was heated to 393K for 30 min to ensure that [^{18}F] - HF boiled from the reservoir into the rig. Nitrogen flowing over the catalyst was discontinued and valves from the nitrogen inlet to the reactor were closed. Valves from the [^{18}F] - HF reservoir to the reactor were opened and [^{18}F] - HF was boiled from the reservoir through the rig and the reactor. Reactor out gas was neutralised with a soda lime scrubber. A Bundenberg gauge attached to the rig between the reactor and scrubber indicated that the majority of [^{18}F] - HF passed from the reservoir through the reactor within the first 30 seconds of reaction indicating an initial flow rate of 1 - 1.5 mol h^{-1}.

These reaction conditions were maintained for a further 40 min to ensure that the majority of [^{18}F] - HF had boiled into the rig. Following this 40 min boiling period, heating of the reactor was discontinued. Valves between the nitrogen inlet and the reactor were opened and a nitrogen flow (0.0537 molh^{-1}) was passed through the rig. This nitrogen flow was designed to clear residual [^{18}F] - HF from the reservoir and rig and to remove any [^{18}F] - HF adsorbed weakly on the fluorinated chromia before analysis.

Following the labelling process described above, the nitrogen flow was discontinued. A vacuum pump with a Pyrex manifold and two Pyrex traps cooled with liquid nitrogen, was connected to the Monel radiochemical flow rig through a glass to metal seal. The pump and gas handling system could be isolated from the flow rig using a Monel valve on the Monel part of the line and a ground glass socket and key tap on the Pyrex part of the line. The valves on the reactor were closed and the rig was opened to the vacuum to remove any traces of [^{18}F] - HF remaining. The valves leading to and from the reactor were closed and the rig was isolated from the vacuum. The reactor was then removed from the rig to the scintillation counter. [^{18}F] - fluorine labelled chromia, which was within the central body of the Monel reactor, was tipped into the FEP side arm of the reactor and the reactor remained in a horizontal position throughout the counting process.

5.2.3 EXCHANGE OF LABELLED FLUORINATED CHROMIA WITH NON - LABELLED HF.

In order to determine the lability of a labelled fluoride species on a labelled fluorinated chromia, non - labelled HF was passed over the labelled chromia and the count rate of [^{18}F] - fluoride remaining on the chromia was determined. Fluorinated labelled chromia was then tipped back into the central section of the Monel reactor from the FEP side arm. The reactor was reattached to the radiochemical flow rig and the ceramic fibre heater was reassembled around the reactor. The reactor was

warmed to 573K for 30 min before reaction and nitrogen (0.0537 mol h^{-1}) was passed over the catalyst.

Hydrogen fluoride (12 mmol) was distilled into a Monel bomb from the HF cylinder connected to the Monel vacuum line. The Monel bomb was removed from the vacuum line and attached to the radiochemical catalyst testing rig in the same position as the [^{18}F] - HF reservoir had previously been attached. The reservoir heating furnace was placed around the non - labelled HF reservoir and heated to 393K for 30 min. The nitrogen flow was discontinued and valves from the reservoir to the reactor, and from the reactor to the scrubber, were opened and HF was boiled from the reservoir into the rig for 40 min. The Bundenberg gauge indicated that the majority of the HF had boiled over within the first 30 s of reaction and the estimated flow rate was 1 - 1.5 $molh^{-1}$.

Following reaction, the heater was removed and a nitrogen flow (0.0537 $molh^{-1}$) was passed through the rig for 40 min to clear residual HF. Valves on the reactor were closed and the rig was opened to the vacuum to remove the remaining traces of HF. The rig was isolated from the vacuum and the reactor was removed. The fluorine exchanged chromia was tipped into the FEP side arm and the catalyst was counted in the scintillation counter.

5.2.4 REMOVAL OF [^{18}F] - FLUORINE ON CHROMIA WITH CF_3CH_2Cl.

In order to determine the interaction of fluoride species on the surface of [^{18}F] - fluorine labelled fluorinated chromia with CF_3CH_2Cl a flow of CF_3CH_2Cl was passed over the labelled chromia and counted. A CF_3CH_2Cl feed line was attached to the rig, the source of CF_3CH_2Cl coming from the main cylinder of CF_3CH_2Cl (ICI Klea) attached to the end of the rig and controlled via a valve at the cylinder head. Secondary controls of the CF_3CH_2Cl were a needle valve and a two way valve between the cylinder and the rig. A catalyst sample was prepared by labelling with [^{18}F] - HF according to the procedure detailed in 4.2.2 and heating under nitrogen flow (0.0537 $molh^{-1}$), employing the heater described above. The

nitrogen was discontinued and valves to the reactor were opened allowing a CF_3CH_2Cl flow (0.0537 $molh^{-1}$) to be passed over the labelled chromia for 40 min. Following treatment with CF_3CH_2Cl, nitrogen was passed through the rig and the rig was evacuated as described in 4.2.3. The reactor was removed from the rig and the catalyst was counted in the FEP side arm using a scintillation counter.

5.2.5 SPECIFIC ACTIVITY MEASUREMENTS AND RADIOCHEMICAL COUNT DETERMINATION.

Measured samples of [^{18}F] - HF used to determine the specific activity of a known amount (1 mmol) of HF were distilled onto CsF in a single limb PTFE / FEP counting vessel as described in 2.11. The vessel was removed from the Monel vacuum line and the FEP limb containing the active sample absorbed onto CsF was positioned in the bottom of the well of the scintillation counter. Counts were recorded until a sufficient number of counts ($< 10^4$) were accumulated. This procedure was repeated every half hour during the duration of a fluoride lability study with [^{18}F] - HF on fluorinated chromia. When the first set of counts was recorded, a stopwatch was started to record the time elapsed during the duration of the experiment from this set of counts which were recorded as having time = 0 min.

DECAY CORRECTION

All counts were recorded in count min^{-1} and the time elapsed from time = 0, at which the count was taken, was noted. A background count, taken as an average over 5 separate counts during the course of the experiment, was also recorded. Data accumulated throughout the course of the experiment were processed using a microcomputer programme based upon decay correction considerations, as described in section 2.13, to correct for decay and background. The amounts of fluoride uptaken and the percentage of this fluoride which was labile, were determined using the specific count rate of the known amount of [^{18}F] - HF on CsF.

Errors for the experiment were calculated using the radiochemical error calculation detailed in section 2.12 (Eqn 2.12).

5.3 RESULTS.

5.3.1 UPTAKE OF FLUORIDE ON CHROMIAS.

In order to determine the effect of zinc doping and crystallinity on fluoride uptake, two series of catalysts, one based on amorphous chromia and the other based on medium crystallinity chromia, were examined. These chromias were all prefluorinated according to the procedure detailed in 3.2.1 on the catalyst fluorination rig, described in section 2.1.6. Chromias displaying zinc promoted and zinc poisoned characteristics from catalyst testing, as detailed in section 3.3.1, were compared with undoped chromia in each series tested. Thus for the amorphous chromia series undoped, 3 w/w % zinc doped and 15 w/w % zinc doped chromias were examined and for the medium crystallinity chromia range undoped, 0.25 w/w % zinc doped and 4 w/w % zinc doped chromias were examined. Results of these experiments appear in Tables 5.1 and 5.2.

Table 5.1 Uptake of [^{18}F] - HF on Medium Crystalline Chromia (same sample used during each run)

w/w % Zn	$H^{18}F$ ads. (mmol) RUN 1	RUN 2	RUN 3
0	0.29 ± 0.00319	0.19 ± 0.00266	0.44 ± 0.00528
0.25	0.47 ± 0.0047	0.32 ± 0.004672	0.27 ± 0.00648
4	0.60 ±- 0.0096	0.52 ± 0.0065	0.71 ± 0.00938

From this data it is clear that the quantities of $H^{18}F$ adsorbed by the undoped and 0.25 w/w % zinc doped chromias are quite small and this results in a considerable scatter of data throughout the three runs. The small uptake of [^{18}F] -

HF was probably due to the extensively fluorinated surface onto which the [^{18}F] - HF was adsorbing and this [^{18}F] - HF was interacting with labile fluoride species on this surface. This uptake was a small fraction of that previously reported (28) for the uptake of HF on unfluorinated chromias and it illustrates the heavily fluorided nature of the catalyst. Taking into account this small uptake and the resultant scatter in the data, there were no significant differences between undoped and 0.25 w/w % zinc doped chromias in this series suggesting that low levels of zinc had no effect on the extent of fluoride uptake on chromia. The 4 w/w % zinc doped chromia had a significantly higher (ca. 80 - 90 %) uptake than the undoped and 0.25 w/w % zinc doped chromias. These uptakes were also subject to scatter. However, this was less significant with this chromia as the uptakes observed in all three runs were considerably higher than those of the undoped and 0.25 w/w % zinc doped chromias. In this case the heavily zinc doped nature of the catalyst was affecting the amount of fluoride uptake on this chromia.

Table 5.2 Uptake of [^{18}F] - HF on Amorphous Chromias.

% w/w Zn	H^{18}F ads. (mmol)
0	1.74 ± 0.0174
3	1.27 ± 0.0127
15	2.32 ± 0.0232

Unfortunately, due to the closure of the nuclear reactor at SURRC in East Kilbride very few experiments involving amorphous chromias could be performed. The results of these are reported in Table 5.2. Uptake on amorphous chromias were very large in comparison to crystalline chromia and hence data reliability in relation to these chromias is very high. There was a significant difference between the undoped and 3 w/w % doped and 15 w/w % doped chromia and a similar pattern of [^{18}F] - HF uptake was repeated in comparison to the medium crystalline chromia series. The larger uptake of fluoride in these amorphous chromias is almost

certainly due to their larger surface areas resulting in more exchangeable fluoride species.

5.3.2 LABILITY OF FLUORIDE ON CHROMIAS USING HF

The lability of fluoride species on various [^{18}F] - fluorine labelled chromias was determined according to the procedure detailed in 5.2.3. The effects of crystallinity and zinc doping on the lability of fluoride species were studied by examining the medium crystallinity chromia series and the amorphous chromia series. The results of fluoride lability are compared with catalyst microreactor studies on these chromias and are reported in Tables 5.3 and 5.4

Table 5.3 Lability of [^{18}F] - Fluorine Species on [^{18}F] - Fluorine Labelled Medium Crystallinity Chromias Towards HF In Relation to Uptakes From Table 5.1(All Runs on Same Sample)

w/w % Zn	H^{18}F removed (mmol)	% H^{18}F removed cf. uptake from table 5.1
0 RUN 1	0.2 ± 0.008	69
RUN 2	0.13 ± 0.003	62.2
RUN 3	0.33 ± 0.008	74.8
0.25 RUN 1	0.22 ± 0.004	71.3
RUN 2	0.33 ± 0.009	72.5
RUN 3	0.23 ± 0.008	73
4 RUN 1	0.2 ± 0.01	53
RUN 2	0.32 ± 0.009	22
RUN 3	0.11 ± 0.002	30.6

Data scatter as a result of small amounts of [^{18}F] - fluorine was a consideration in the results shown in this table. Taking account of this, the amounts of labile fluoride removed from the chromia were similar for all three chromias

examined. This suggests that, in terms of the actual amounts of labile fluoride, zinc doping has little effect. Therefore, undoped, lightly zinc doped and heavily zinc doped chromias all have similar amounts of labile fluoride species available for exchange. The column on the far right of Table 5.3 indicates the percentage of [^{18}F] - fluoride lost by comparison with the initial uptake of [^{18}F] - fluoride for each chromia, reported in Table 5.1. Undoped and 0.25 w/w % zinc doped chromia have similar percentages of [^{18}F] - fluoride removal. 4 w/w % zinc doped chromia has a far smaller percentage of [^{18}F] - fluoride removal. As the amounts of [^{18}F] - fluoride removal are similar for all three chromias this difference in percentages was the result of the larger uptake of [^{18}F] - fluoride observed on 4 w/w % zinc doped fluorinated chromia in Table 5.1. The reason for this anomaly can be attributed to the effects of heavy zinc doping on the pore structure of the zinc doped chromia. In chapter 3 it was reported that pores on the surface of 4 w/w % zinc doped chromia were partially blocked as determined by the mercury extrusion curve obtained from mercury porosymmetry analysis. Fluorination of this chromia resulted in the unblocking of these pores and larger uptakes of [^{18}F] - HF on 4 w/w % zinc in Table 5.1 can be attributed to this unblocking process.

As nitrogen was passed over the catalyst before reaction at 573K the removal of weakly bonded HF oligomers and molecules could be assumed to be complete before passing non - labelled HF over the labelled chromia. Thus the amounts of [^{18}F] - fluoride removed from these labelled chromias could be attributed to the labile 'type III' species noted by Webb, Winfield *et al* (28) in earlier work. [^{18}F] - fluoride which reacts with unblocked pores on 4 w/w % zinc doped chromias is permanently retained suggesting that labile fluoride species does not originate from within these pores.

Amorphous chromias with various zinc dopings were examined for the lability of fluoride species and compared to [^{18}F] - fluoride uptakes from chromias in Table 5.2 and the results from Table 5.3. Results of these experiments are presented in Table 5.4.

Table 5.4 Lability of [^{18}F] - Fluoride Species on [^{18}F] - Labelled Amorphous Chromias Towards HF In Relation to Uptakes From Table 5.2

% w/w Zn	H^{18}F Removed (mmol)	%^{18}F Removed cf. Uptake From Table 5.2
0	0.78 ± 0.008	44
3	0.58 ± 0.007	45
15	1.16 ± 0.0116	46

The size of the pool of labile [^{18}F] - fluoride on these chromias reflects the large uptakes of [^{18}F] - HF as a result of the surface area of amorphous chromias. The undoped and 3 w/w % Zinc doped chromias have comparable sizes of labile fluoride, however the 15 w/w % zinc doped chromia has a notably larger pool of labile fluoride. This catalyst had a very large level of zinc doping, considerably larger than that of others tested, and its activity was the poorest of those examined. XPS evidence from poisoned chromias displays evidence for the presence of heavily fluorided zinc species on the surface of these chromias and which could be explained by the exchange of fluoride on the heavily fluorided zinc species as opposed to exchange of fluoride on active sites. The % of [^{18}F] - fluoride removed from these chromias was far smaller than that removed from medium crystallinity chromias. Thus, in terms of fluoride uptakes on chromias of differing crystallinity, those with low crystallinity have larger pools of labile fluoride species, larger quantities of retained fluoride and a greater percentage of [^{18}F] - HF uptake on lower crystalline chromias was of 'type II' fluoride species as described by Webb, Winfield *et al* (28). Unlike the medium crystallinity chromias, the amorphous chromias all have similar percentages of [^{18}F] - fluoride labile.

5.3.3 LABILITY OF FLUORIDE ON MEDIUM CRYSTALLINITY CHROMIAS USING CF_3CH_2Cl

To determine differences in fluoride lability between fluorinated chromias HF was passed over these fluorinated chromias and the results were reported in the preceding section 5.3.2. 1,1,1-trifluoro-2-chloroethane was also passed over these fluorinated chromias to determine differences between them and also to make comparison with HF treatments in 5.3.2. The closure of the nuclear reactor at SURRC limited the number of these experiments and only medium crystalline chromias were examined. The results of uptakes agreed with those reported previously and are detailed in Table 5.5 for comparison to lability data.

Table 5.5 $H^{18}F$ Uptake and Lability on Medium Crystallinity Chromias With CF_3CH_2Cl In Relation to Uptakes From Table 5.1 (All Runs on Same Sample)

w / w % Zn	$H^{18}F$ Ads. (mmol)	^{18}F Removed (mmol)	% ^{18}F Removed
0 RUN 1	0.56 ± 0.007	0.28 ± 0.007	50.1
RUN 2	0.23 ± 0.003	0.08 ± 0.0018	35
RUN 3	0.33 ± 0.008	0.11 ± 0.004	34.3
0.25 RUN 1	0.3 ± 0.006	0.09 ± 0.007	28.2
RUN 2	0.3 ± 0.006	0.12 ± 0.007	40
RUN 3	0.46 ± 0.011	0.25 ± 0.006	53
4 RUN 1	0.3 ± 0.006	0.19 ± 0.006	38
RUN 2	0.64 ± 0.010	0.32 ± 0.010	50.6

The quantities of [^{18}F] - fluoride removed are similar for all three chromias, which is similar to the finding reported in 5.3.2. However, the quantities of fluoride removed were considerably less than those removed when HF was used for lability experiments. Thus the percentage of [^{18}F] - fluoride removed was far lower. In this case the percentages of fluoride removed from the three fluorinated chromias examined were similar to each other regardless of the percentage zinc doping. This

indicated that there was more than one type of labile fluoride species present on these chromias. Hydrogen fluoride will displace or exchange with labile fluoride species on chromia as described in Fig 5.1.

Fig 5.1 HF Possible Interactions With Fluoride Species on Chromia

$$HF + Cr(^{18}F) \rightarrow H^{18}F + Cr(F) \qquad \text{exchange}$$

$$HF + Cr(H^{18}F) \rightarrow H^{18}F + Cr(HF) \qquad \text{displacement}$$

The interaction of CF_3CH_2Cl with labile fluoride species on chromia is unlikely to be an exchange or displacement as CF_3CH_2Cl adsorbs weakly on fluorinated chromia as described in Chapter 6. Thus the removal of [^{18}F] - fluoride species from the surface of fluorinated chromia by CF_3CH_2Cl was more likely to be a result of reaction. Therefore it can be concluded that only a certain percentage of labile fluoride species on chromias will react with CF_3CH_2Cl.

6 INTERACTION OF [^{36}Cl] - CHLORINE LABELLED CF_3CH_2Cl WITH FLUORINATED CHROMIAS

6.1 INTRODUCTION

This chapter is concerned with the interaction of fluorinated chromias with [^{36}Cl] - chlorine labelled CF_3CH_2Cl. This interaction was of interest in this work as an halogen exchange model relies upon exchangeable chloride species in the CF_3CH_2Cl molecule. Chapter 5 showed that the fluorinated chromia catalysts under examination have labile fluoride species which could be used to exchange with chloride in the CF_3CH_2Cl. The presence of the catalyst in this reaction may require the involvement of an adsorption of CF_3CH_2Cl on the surface of the catalyst to cause reaction. Therefore, investigation of the adsorption behaviour of CF_3CH_2Cl on fluorinated chromias using the Geiger - Müller direct monitoring method was an important feature of this work. The role of zinc dopant in the interaction of CF_3CH_2Cl with fluorinated chromia was also investigated.

6.2 EXPERIMENTAL

6.2.1 PRETREATMENT OF FLUORINATED CHROMIAS

Chromias (1.0g) fluorinated in the manner detailed in 3.2.1 were weighed accurately in a Pyrex beaker within the inert atmosphere box ($H_2O < 3$ ppm). The weighed sample was charged into the Monel metal reactor used to perform fluorine uptake and liability experiments and the reactor was sealed before removal from the inert (N_2) atmosphere box. The Monel reactor was removed to the radiochemical flow rig for catalyst testing, described in section 2.1.7, and attached to the rig with the two section ceramic fibre heater positioned around the central section of the reactor. Nitrogen (0.0537 mol h^{-1}) was flowed through the rig and the reactor outgas was passed through a soda lime scrubber. The reactor was heated to 673K and the reaction was allowed to proceed for 4 h. The purpose of this step was to

remove weakly adsorbed HF oligomers and molecules from the surface of the fluorinated chromia prior to the interaction.

When the 4 h reaction period was over, the reactor was sealed and the nitrogen flow and heating were discontinued. The reactor and a small Pyrex dropping vessel equipped with a high vacuum stopcock (J. Young) and B14 cone were removed to the inert (N_2) atmosphere box. The treated, fluorinated chromia was transferred into the dropping vessel through a FEP funnel and the vessel was sealed. The dropping vessel was removed to a Pyrex vacuum line, with direct monitoring apparatus, within which the experiment would be performed. The dropping vessel was attached to the manifold of the vacuum line with the B14 cone greased with Kel - F high vacuum grease and evacuated overnight. After overnight evacuation a ceramic fibre heater was positioned around the dropping vessel containing the evacuated fluorinated chromia and the temperature was raised to 523K under vacuum for 2 h. Following heating, the dropping vessel was sealed and removed from the manifold. The dropping vessel was then inverted and attached to the direct monitoring apparatus before interaction of the catalyst with [^{36}Cl] - chlorine labelled CF_3CH_2Cl. This completed the pretreatment process.

6.2.2 INTERACTION OF FLUORINATED CHROMIAS WITH [^{36}Cl] - CF_3CH_2Cl AT ROOM TEMPERATURE.

The direct monitoring apparatus, described in 2.9, with the dropping vessel containing a pretreated sample of chromia attached, was opened to the vacuum and evacuated slowly to avoid damage to the thin mica windows of the Geiger - Müller tubes. The counting boat was manoeuvred to position the left hand side of the boat directly under the opening to the dropping vessel by dragging the small magnet encapsulated within the Pyrex stem of the boat to the left, using a large hand held magnet. When the boat was in position, the stopcock of the dropping vessel was carefully opened and the fluorinated chromia was dropped slowly into the boat with gentle tapping of the dropping vessel. A slow controlled dropping of fluorinated

chromia reduced the tendency for the sample to scatter upon landing in the Pyrex boat and hence improved reproducibility of data. When all of the fluorinated chromia had left the dropping vessel, the stopcock was closed and the boat was manoeuvred forwards and backwards in the counting cell using the magnet in order to obtain an even distribution of fluorinated chromia in the left hand side of the boat.

The vessel used to contain [^{36}Cl]- chlorine labelled CF_3CH_2Cl was a Monel bomb (100 ml) attached to a Monel Vacuum line. To perform experiments using [^{36}Cl] - CF_3CH_2Cl, the vessel was removed from the Monel line and a B14 brass cone adapter was attached to the top of the bomb after the valve. The Monel bomb was attached to the manifold of the Pyrex vacuum line by greasing the brass B14 cone with Kel - F high vacuum grease and the tap between the manifold and the counting cell was opened. The pump was isolated from the counting cell and manifold by closing the stopcock between the traps and the manifold. The valve on the bomb was gently opened and [^{36}Cl] - chlorine labelled CF_3CH_2Cl was introduced into the line to a pressure of 10 Torr. The counting cell was isolated from the rest of the line and [^{36}Cl] - chlorine labelled CF_3CH_2Cl was left to interact with fluorinated chromia for 40 min. During this time, the remaining [^{36}Cl] - chlorine labelled CF_3CH_2Cl was distilled back into the bomb from the manifold. After 40 min the Pyrex boat was positioned under the two Geiger - Müller tubes using the magnet. The left hand side of the boat, containing the fluorinated chromia sample, was positioned under the left hand Geiger - Müller tube, G.M.1, and the empty right hand side of the boat was positioned under the right hand Geiger - Müller tube, G.M.2. Counts were recorded from both tubes simultaneously on the scaler timers connected to each tube, for a sufficient length of time to accumulate > 10,000 counts. G.M.1 recorded counts from the surface of the fluorinated chromia and the gas phase and G.M.2 recorded counts from the gas phase alone. After the counting process was complete, the pressure of [^{36}Cl] - chlorine labelled CF_3CH_2Cl in the counting cell was increased to 20 Torr by introducing more [^{36}Cl] - chlorine

labelled CF_3CH_2Cl from the bomb through the manifold and the interaction and counting process was repeated. Further pressures of [^{36}Cl] - chlorine labelled CF_3CH_2Cl were introduced in increments of 10 - 15 Torr up to a maximum of 100 Torr at which point the experiment was ended.

6.2.3 INTERACTION OF FLUORINATED CHROMIAS WITH [^{36}Cl] - CF_3CH_2Cl ABOVE ROOM TEMPERATURE.

A resistance wire furnace, controlled using a Variac, was constructed, using insulating cloth, around the counting cell on the left hand side between the dropping ampoule socket and the section used to manoeuvre the stem of the boat with a bar magnet. The construction was further protected with insulating cloth tied back with copper wire. Before reaction the furnace was calibrated by measuring the temperature within the heated area of the counting cell. A thermocouple wire was connected to a multimeter and was placed into the counting cell within the heated area and the temperature was noted at various voltages on the Variac.

A sample of fluorinated chromia (1.0g) was pretreated as described in 6.2.1 and loaded into the left hand side of the Pyrex boat within the evacuated counting cell as described in 6.2.2. The furnace was heated to the required temperature of the reaction by setting the Variac to the voltage required to obtain that temperature as determined from the furnace calibration. The left hand side of the boat, containing the catalyst, was positioned in the centre of the heated area and a pressure (10 Torr) of [^{36}Cl] - chlorine labelled CF_3CH_2Cl was admitted to the counting cell as described in 6.2.2. After 40 min the boat was moved from the heated area and the fluorinated chromia in the left hand side was positioned under G.M.2. Counting of the gas phase and surface count plus gas phase began simultaneously until counts > 10,000 were obtained. When counting was complete, the boat was moved to position the fluorinated chromia within the centre of the heated area and the pressure of [^{36}Cl] - chlorine labelled CF_3CH_2Cl was increased as described in 6.2.2.

6.2.4 STUDIES OF RETAINED [^{36}Cl] - CHLORINE ON FLUORINATED CHROMIAS.

Following experiments to determine the interaction of various pressures of [^{36}Cl] - chlorine labelled CF_3CH_2Cl with fluorinated chromias at differing temperatures, count rates of retained material on the chromia were determined. When the maximum reaction pressure of 100 Torr [^{36}Cl] - chlorine labelled CF_3CH_2Cl count rates were measured in all reactions, [^{36}Cl] - chlorine labelled CF_3CH_2Cl was vacuum distilled back into the Monel bomb. The bomb was sealed and the manifold and counting cell were opened to the vacuum. Evacuation of the counting cell proceeded for 40 min and during this period fluorinated chromia, which had been allowed to interact with [^{36}Cl] - CF_3CH_2Cl, in experiments performed above room temperature, was positioned in the centre of the heated area at the required reaction temperature. Following evacuation the counting cell was isolated from the pump and the boat was moved to position the fluorinated chromia under G.M.1 and the empty right hand side under G.M.2. When counts > 10,000 were accumulated counting was ended and the retained [^{36}Cl] - chlorine count on the evacuated fluorinated chromia was calculated.

6.3 RESULTS.

Medium crystallinity fluorinated chromias were allowed to interact with [^{36}Cl] - chlorine labelled CF_3CH_2Cl at various temperatures. Undoped, 0.25 w/w % zinc doped and 4 w/w % zinc doped chromias were examined to determine the effect of zinc doping on the interaction. These studies were performed to obtain absorption isotherms of CF_3CH_2Cl on chromias, however limitations of the experiment prevented isotherms from being obtained. The results were used to obtain information about the interaction of CF_3CH_2Cl with fluorinated chromia surfaces as gas and surface count rates were obtained from the system. These results are reported in Tables 6.1 to 6.9 and Figs 6.1 to 6.9. Table 6.10 reports the

highest gas count rate at various temperatures for differing fluorinated chromias and Table 6.11 reports the retained count rate from the surface of various fluorinated chromias following interaction of CF_3CH_2Cl at differing temperatures.

Table 6.1 Counts Obtained From the Room Temperature Interaction of [^{36}Cl] - Chlorine Labelled CF_3CH_2Cl With Medium Crystallinity Fluorinated Chromia (Undoped).

Gas Count Rate (count min^{-1})	Surface Count Rate (count min^{-1})
0	0
493	257
970	521
981	494
1367	636
1723	750
1765	801
2244	969
2440	1015
2526	1140
3284	1583

FIGURE 6.1 Plot of Surface Count vs. Gas Count for Interaction of [^{36}Cl] - CF_3CH_2Cl With Undoped Mid Crystalline Chromia at Room Temperature

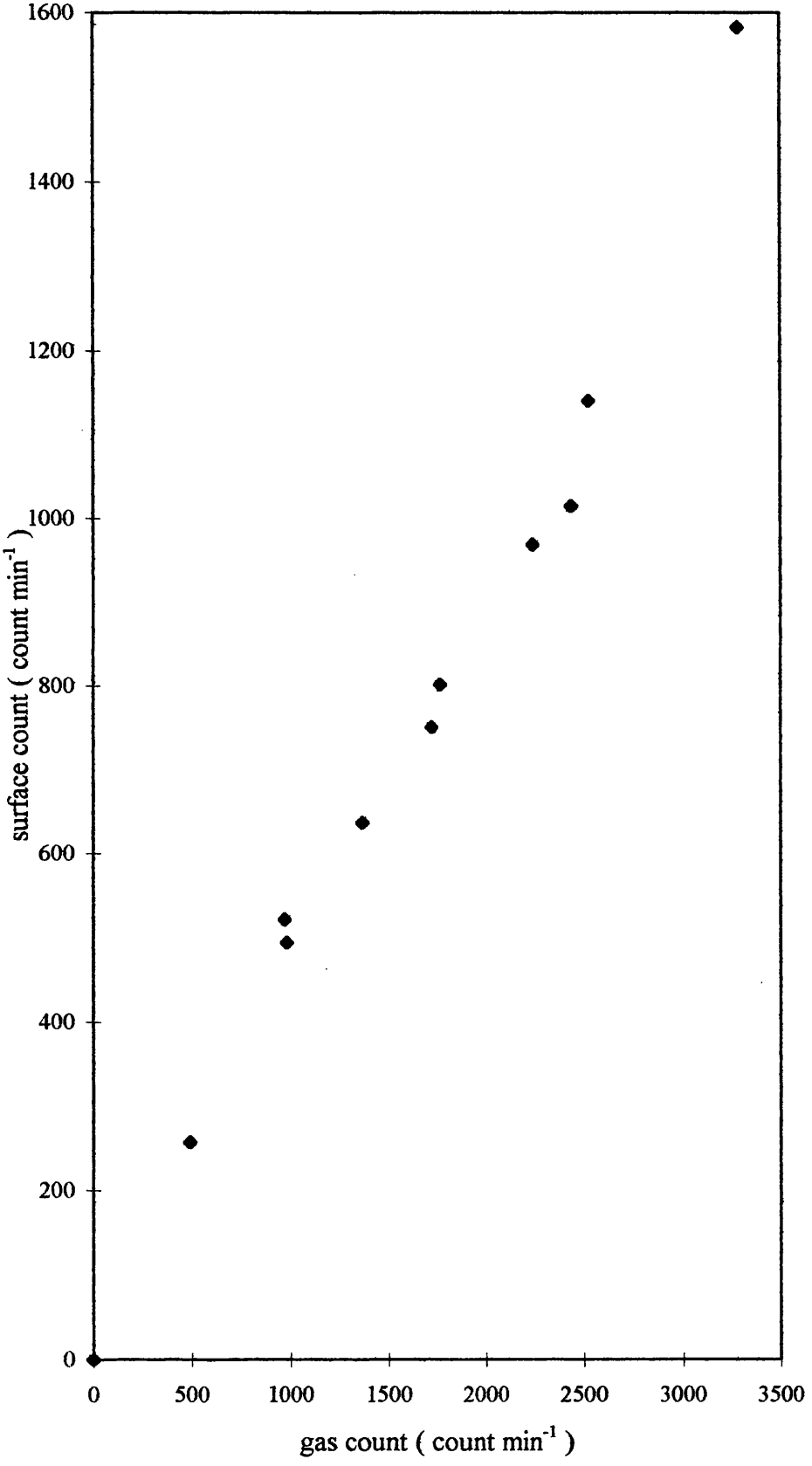

Table 6.2 Counts Obtained From the Room Temperature Interaction of [^{36}Cl] - Chlorine Labelled CF_3CH_2Cl With Medium Crystallinity Fluorinated Chromia (0.25 w/w % Zn doped).

Gas Count Rate (count min^{-1})	Surface Count Rate (count min^{-1})
0	0
93	35
665	178
926	508
1361	611
1753	1068
2290	1000
2576	1183
2871	1206
3247	1408
3513	1331

FIGURE 6.2 Plot of Surface Count vs. Gas Count for Interaction of [^{36}Cl] - CF_3CH_2Cl With 0.25% w/w Zinc Doped Mid Crystalline Chromia at Room Temperature

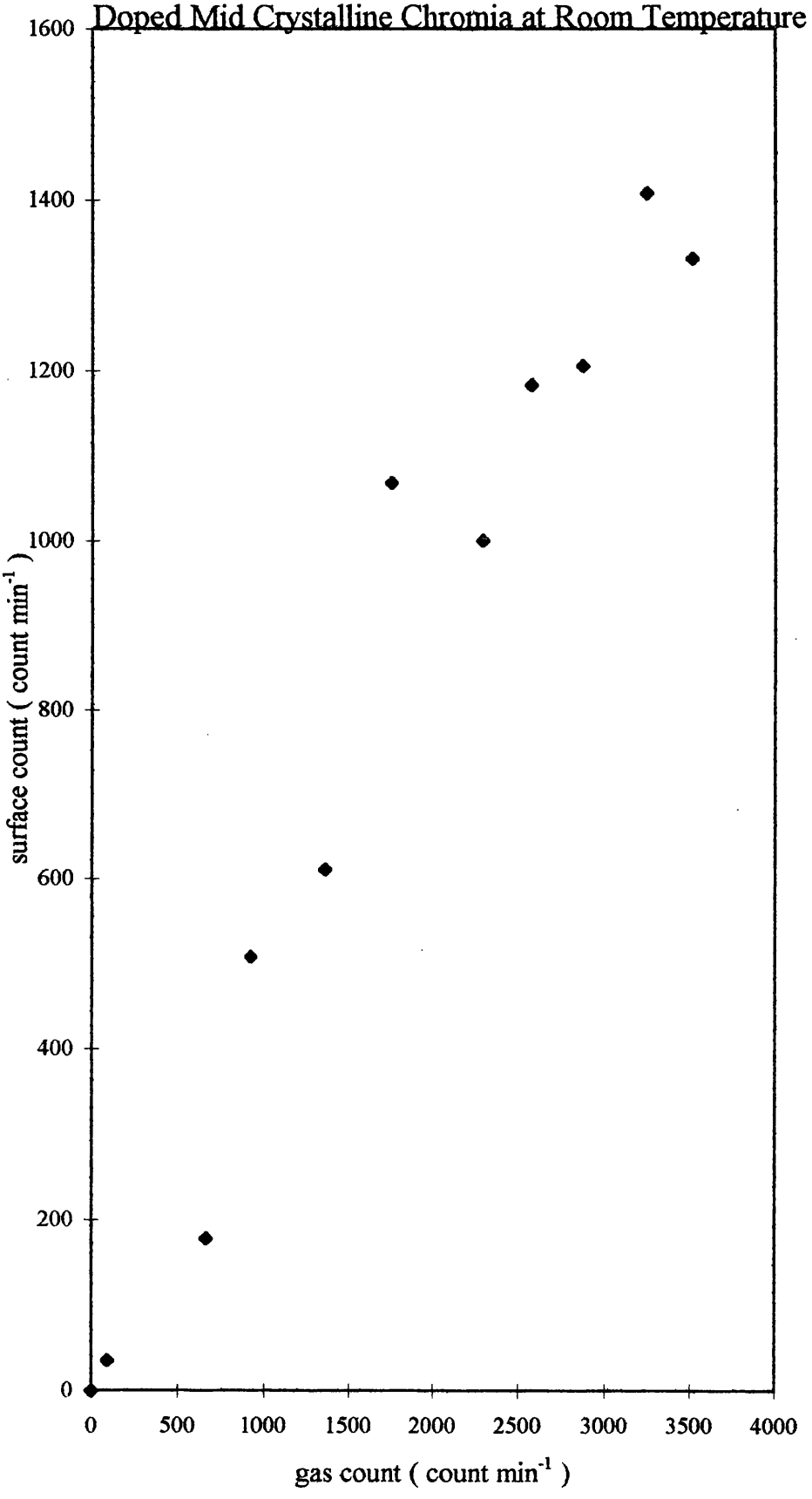

Table 6.3 Counts Obtained From the Room Temperature Interaction of [^{36}Cl] - Chlorine Labelled CF_3CH_2Cl With Medium Crystallinity Fluorinated Chromia (4 w/w % Zn doped).

Gas Count Rate (count min^{-1})	Surface Count Rate (count min^{-1})
0	0
414	239
634	412
991	748
1429	1150
1595	1345
2122	1684
2747	2061
3412	2279

Table 6.4 Counts Obtained From the Interaction of [^{36}Cl] - Chlorine Labelled CF_3CH_2Cl With Medium Crystalline Fluorinated Chromia (Undoped) at 423K.

Gas Count Rate (count min^{-1})	Surface Count Rate (count min^{-1})
0	0
668	250
739	444
999	416
1099	575
2190	658
3030	665

FIGURE 6.3 Plot of Surface Count vs. Gas Count for Interaction of [^{36}Cl] - CF_3CH_2Cl With 4% w/w Zinc Doped Mid Crystalline Chromia at Room Temperature

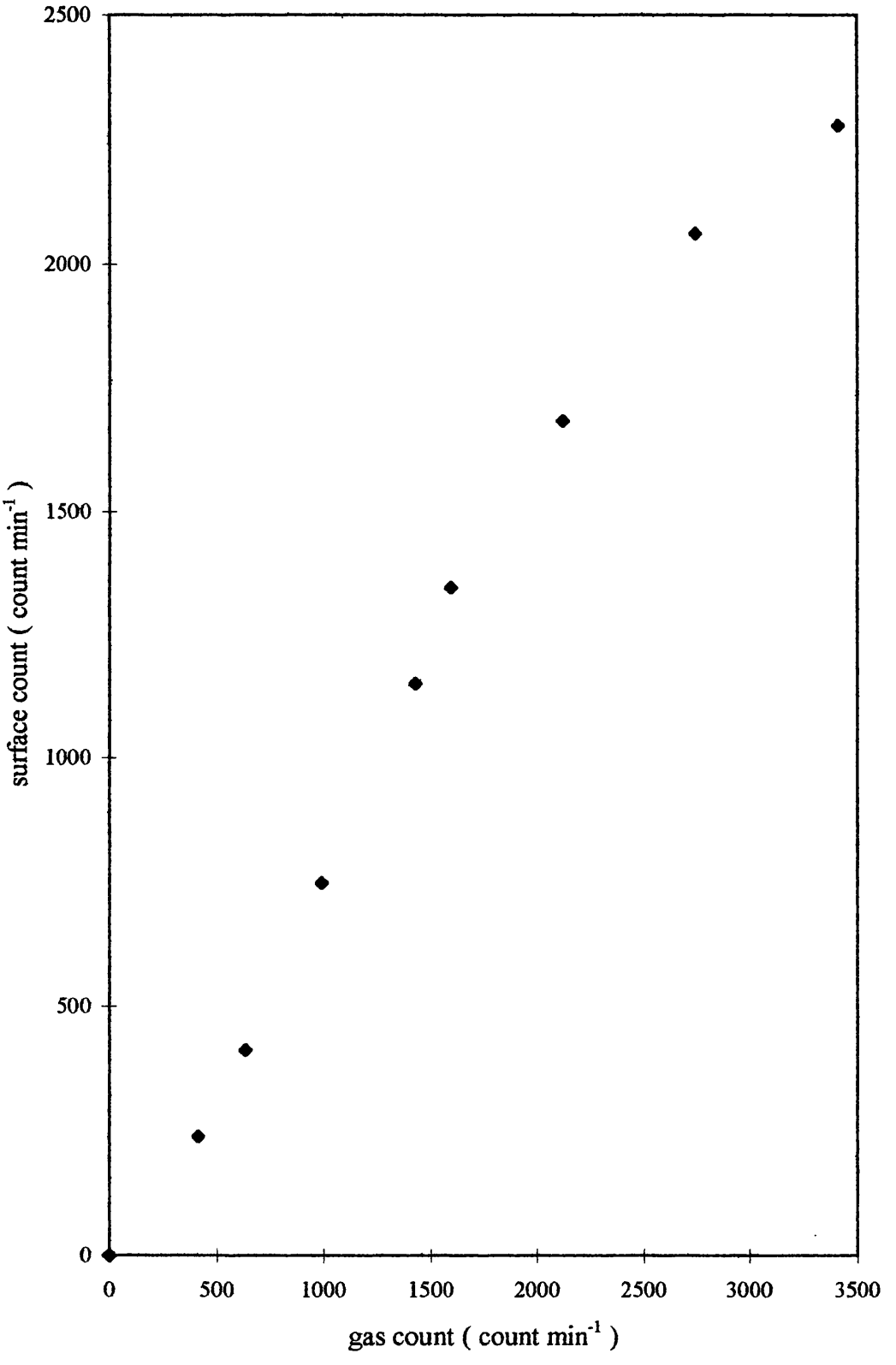

FIGURE 6.4 Plot of Surface Count vs. Gas Count for Interaction of [^{36}Cl] - CF_3CH_2Cl With Undoped Mid Crystalline Chromia at 423K

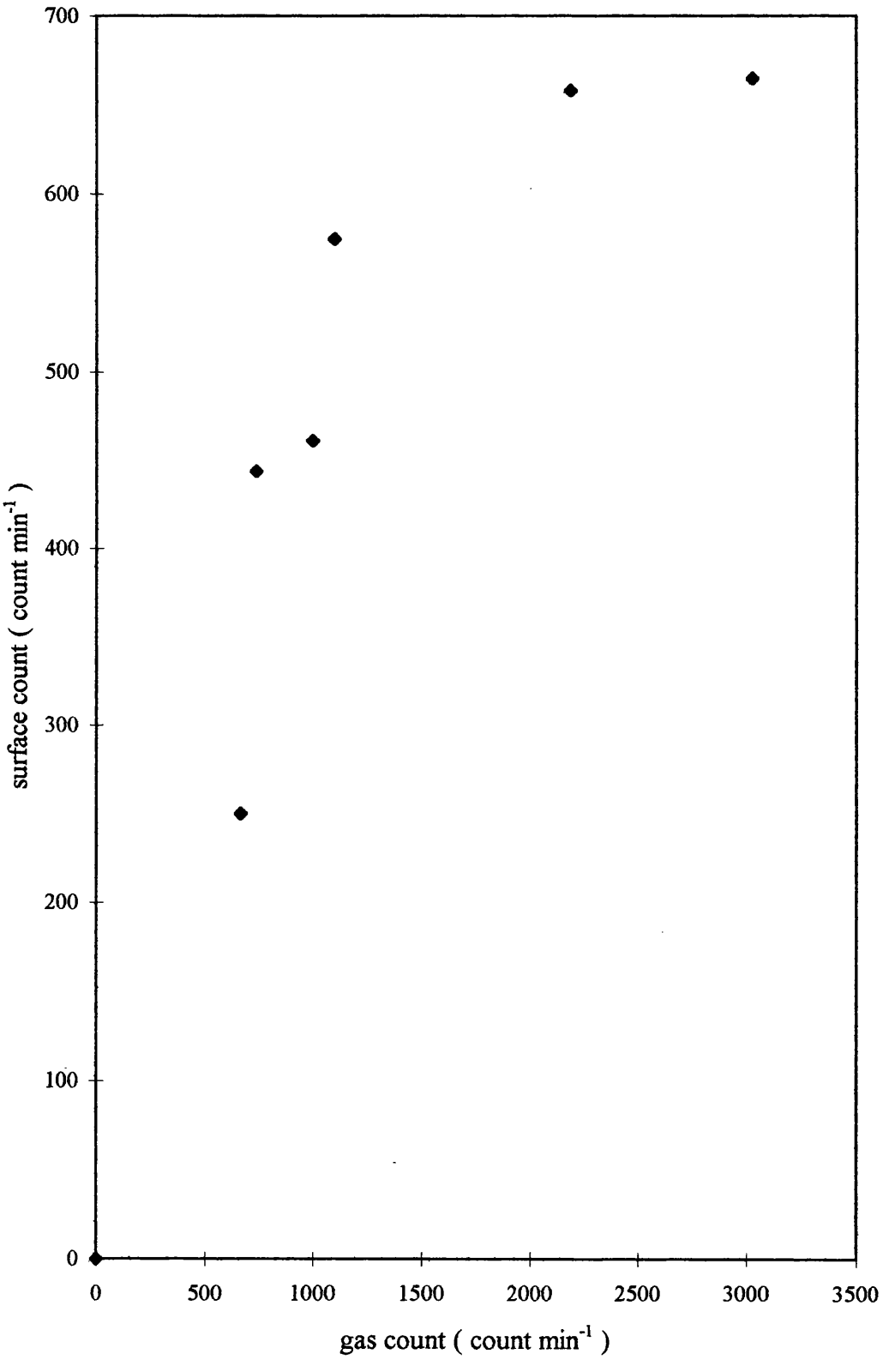

Table 6.5 Counts Obtained From the Interaction of [^{36}Cl] - Chlorine Labelled CF_3CH_2Cl With Medium Crystalline Fluorinated Chromia (0.25 w/w % Zn doped) at 423K.

Gas Count Rate (count min^{-1})	Surface Count Rate (count min^{-1})
0	0
202	128
452	151
773	367
921	447
1161	494
1305	590
1528	699
1927	761
2656	935
2837	1259

FIGURE 6.5 Plot of Surface Count vs. Gas Count for Interaction of [^{36}Cl] - CF_3CH_2Cl With 0.25% w/w Zinc Doped Mid Crystalline Chromia at 423K

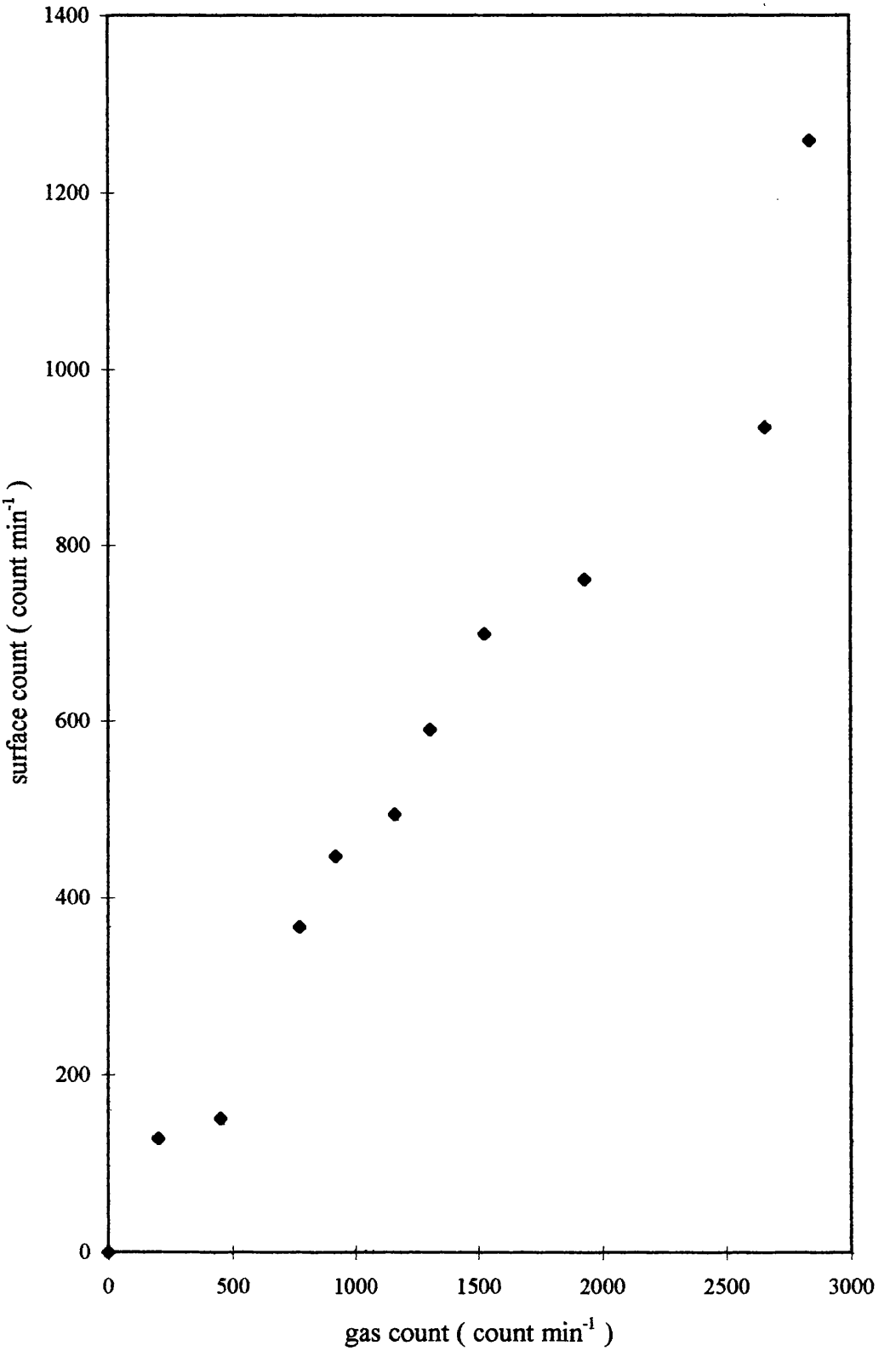

Table 6.6 Counts Obtained From the Interaction of [^{36}Cl] - Chlorine Labelled CF_3CH_2Cl With Medium Crystalline Fluorinated Chromia (4 w/w % Zn doped) at 423K.

Gas Count Rate (count min^{-1})	Surface Count Rate (count min^{-1})
0	0
548	600
628	843
696	967
1165	1435
1365	1474
1521	2077
2050	3223

Table 6.7 Counts Obtained From the Interaction of [^{36}Cl] - Chlorine Labelled CF_3CH_2Cl With Medium Crystallinity Fluorinated Chromia (undoped) at 503K.

Gas Count Rate (count min^{-1})	Surface Count Rate (count min^{-1})
0	0
245	251
656	278
1057	314
1237	369
1405	395
2434	583
3104	838
4135	940

FIGURE 6.6 Plot of Surface Count vs. Gas Count for Interaction of [^{36}Cl] - CF_3CH_2Cl With 4% w/w Zinc Doped Mid Crystalline Chromia at 423K

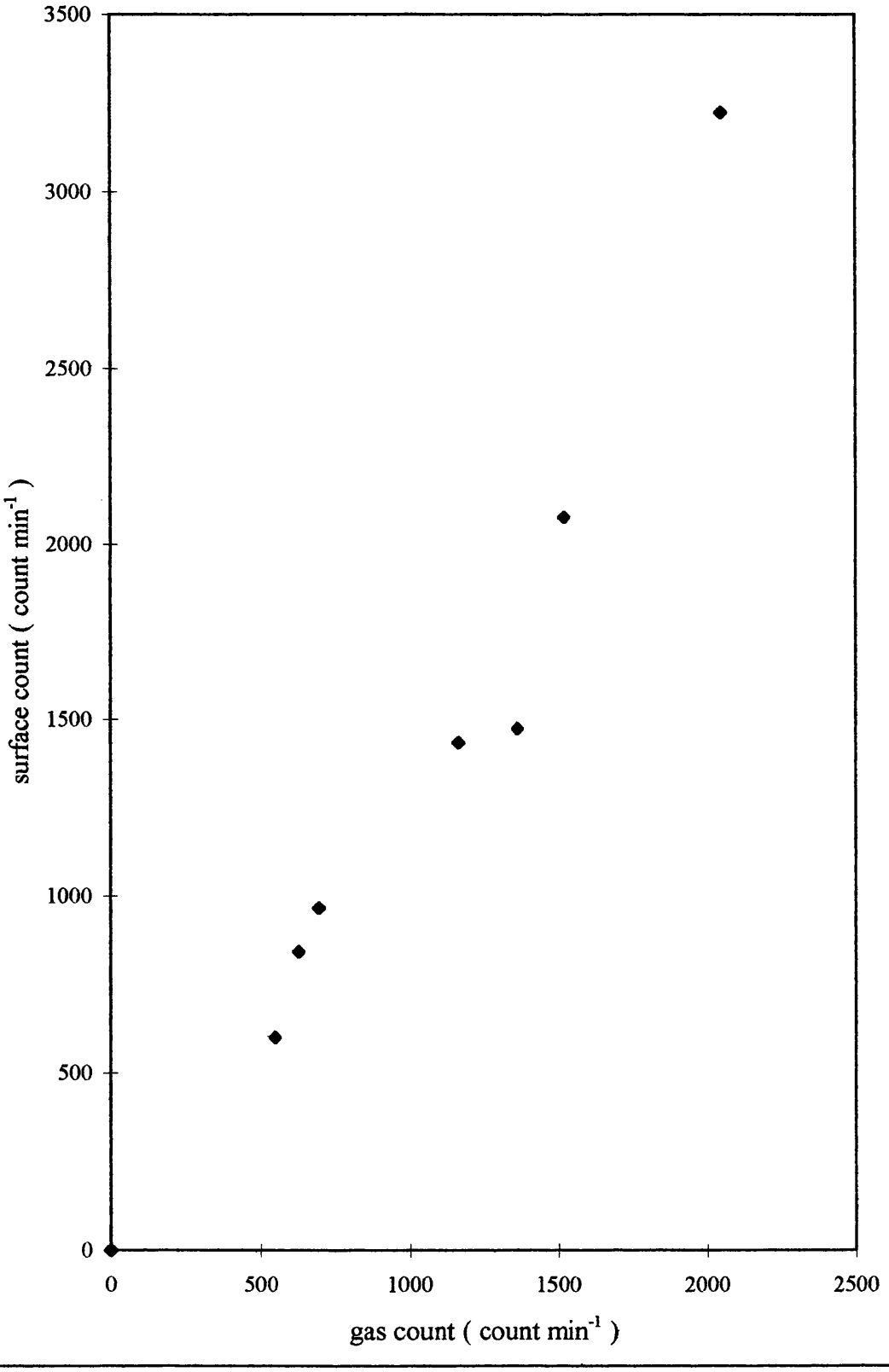

FIGURE 6.7 Plot of Surface Count vs. Gas Count for Interaction of [^{36}Cl] - CF_3CH_2Cl With Undoped Mid Crystalline Chromia at 503K

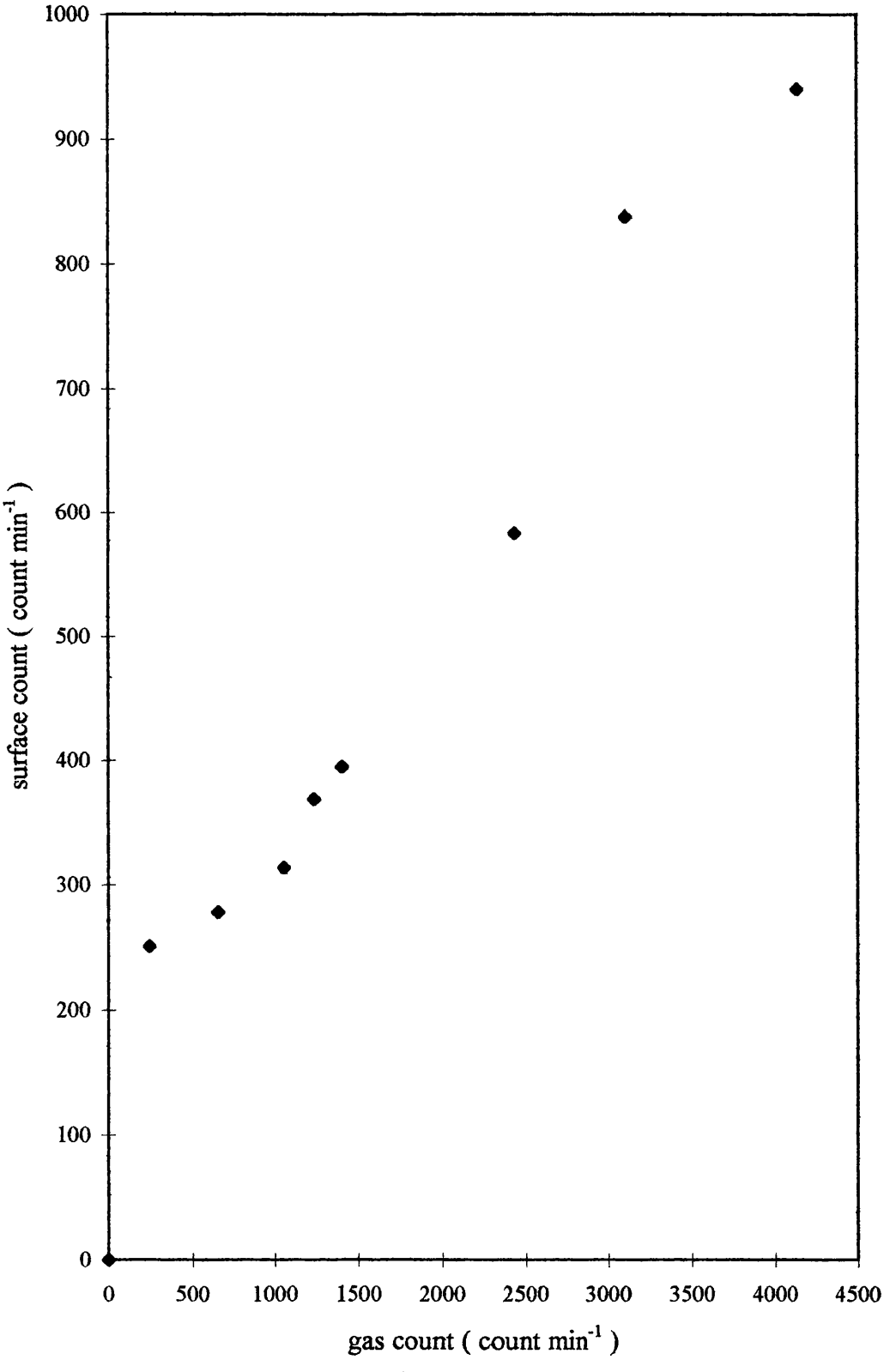

Table 6.8 Counts Obtained From the Interaction of [^{36}Cl] - Chlorine Labelled CF_3CH_2Cl With Medium Crystallinity Fluorinated Chromia (0.25 w/w % Zn doped) at 503K.

Gas Count Rate (count min^{-1})	Surface Count Rate (count min^{-1})
0	0
192	171
352	197
632	254
987	326
1926	646
2463	904
2808	1176
4048	1356

Table 6.9 Counts Obtained From the Interaction of [^{36}Cl] - Chlorine Labelled CF_3CH_2Cl With Medium Crystallinity Fluorinated Chromia (4 w/w % Zn doped) at 503K.

Gas Count Rate(count min^{-1})	Surface Count Rate (count min^{-1})
0	0
447	1352
604	1426
685	2925
840	3570
886	4182
943	4587
961	4812

FIGURE 6.8 Plot of Surface Count vs. Gas Count for Interaction of [^{36}Cl] - CF_3CH_2Cl With 0.25% w/w Zinc Doped Mid Crystalline Chromia at 503K

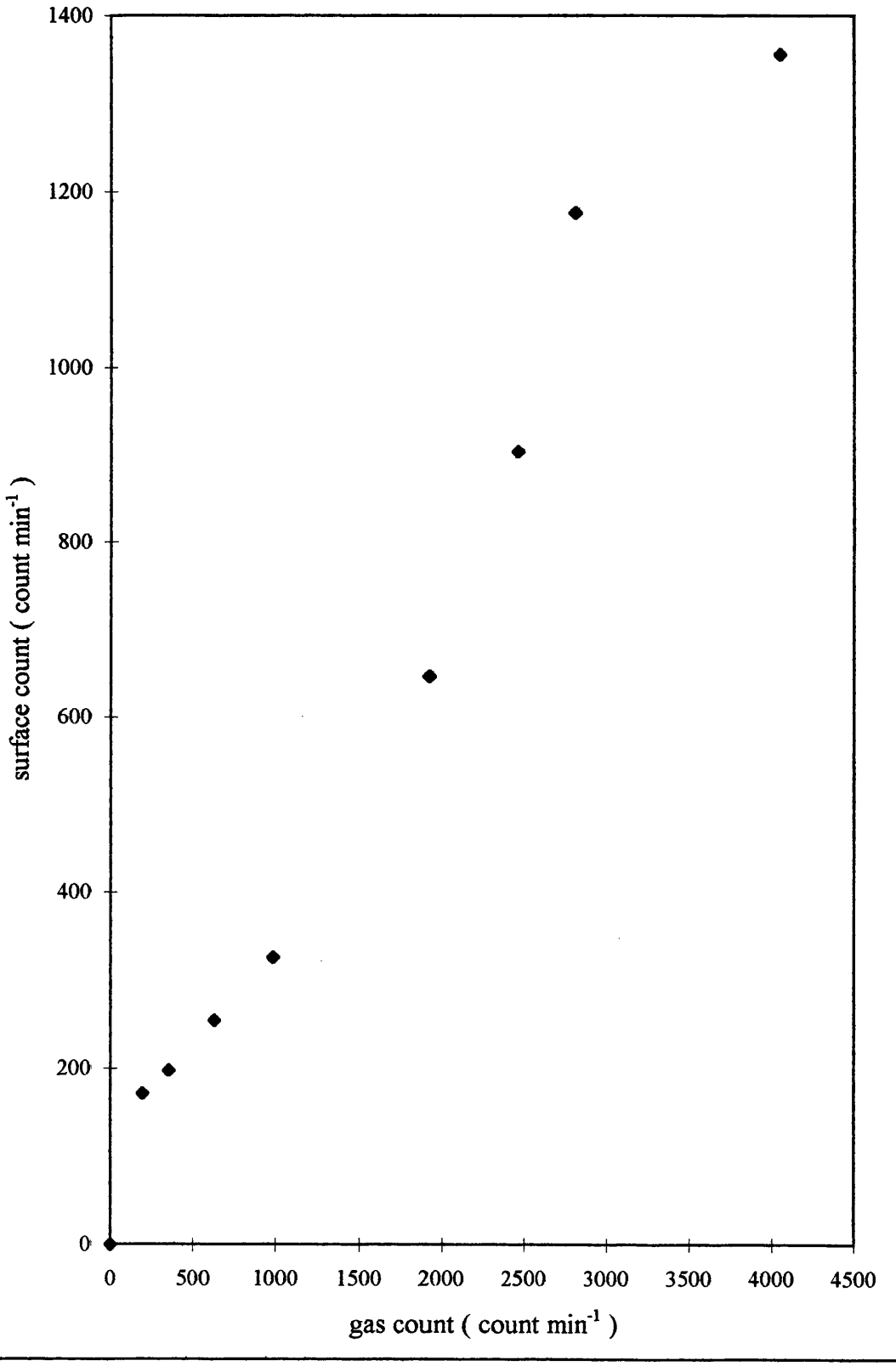

FIGURE 6.9 Plot of Surface Count vs. Gas Count for Interaction of [36Cl] - CF3CH2Cl With 4% w/w Zinc Doped Mid Crystalline Chromia at 503K

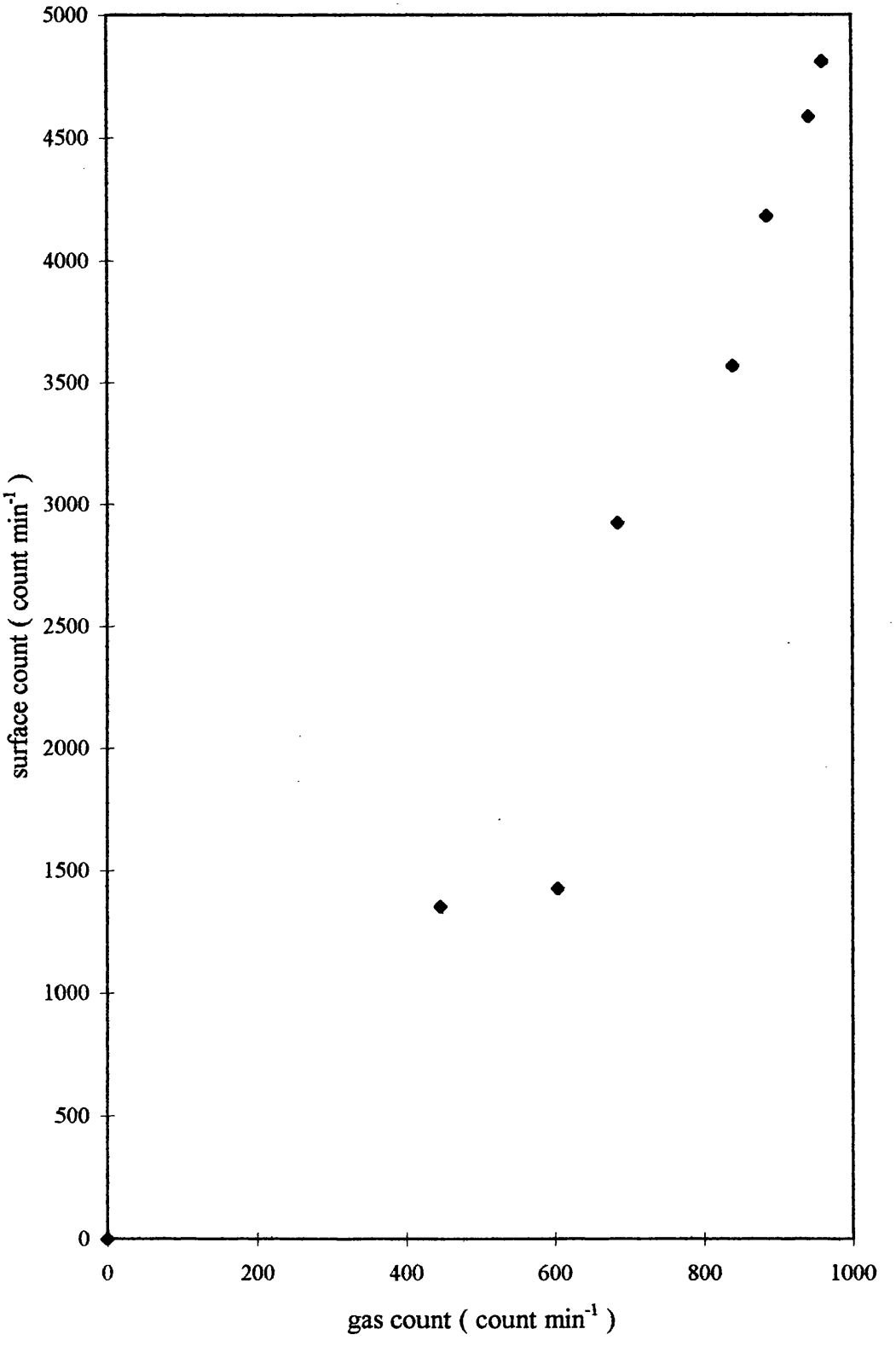

Interpretation of these results relies upon an understanding of the limitations of the system. As the chromias used in the reaction of CF_3CH_2Cl with HF to form CF_3CH_2F and HCl were fluorinated, it was necessary to use fluorinated chromia in this study to determine the interaction of CF_3CH_2Cl with the catalyst. As shown in Chapter 5, this fluorinated chromia has labile fluoride species present on the surface. An interaction between [^{36}Cl] - CF_3CH_2Cl and fluorinated chromia could lead to reaction forming CF_3CH_2F, leaving [^{36}Cl] - chloride species on the surface of the fluorinated chromia. Distinguishing between the absorbed state of [^{36}Cl] - CF_3CH_2Cl and [^{36}Cl] - chloride retained on chromia following reaction is difficult. This prevents the accumulation of data to form an adsorption isotherm as a 'true' surface [^{36}Cl] - CF_3CH_2Cl count would not be obtained. This interaction also prevents the development of a relationship between the gas pressure and gas count rate. Gas count rates obtained from this work are a true reflection of the partial pressure of [^{36}Cl] - CF_3CH_2Cl gas within the system. However, this count rate is unlikely to be a reflection of the gas pressure admitted into the counting cell at various stages of the reaction. Infrared analysis of gas phase samples indicates the presence of CF_3CH_2F and CF_3CH_2Cl. 1,1,1,2-tetrafluoroethane was present in the gas phase as a result of the interaction of [^{36}Cl] - CF_3CH_2Cl with the fluorinated chromia and therefore the gas count rate would represent the partial pressure of [^{36}Cl] - CF_3CH_2Cl.

Other possibilities exist to explain surface [^{36}Cl] - chloride species. Dehydrofluorination, significant in the reactions of other workers, will contribute to the surface [^{36}Cl] - chloride count rate if [^{36}Cl] - CF_2CHCl adsorbs strongly on the fluorinated chromia surface. Studies by Blanchard *et al* (35) indicate that this is not the case and CF_2CHCl does desorb from fluorinated chromia surfaces. This compound is not a significant reaction product, as discussed in chapter 3, forming less than 2 % of reaction products in catalyst microreactor studies. Conditions in these studies were different from those of the microreactor studies as no constant flow of HF was refluorinating the chromia throughout the experiment and heavy

fluorination conditions retarded the dehydrofluorination reaction, therefore [^{36}Cl] - CF_2CHCl may well have been a more significant product in these experiments. Other possibilities exist as sources of [^{36}Cl] - chlorine count rates such as the breakdown of [^{36}Cl] - CF_3CH_2Cl to C_1 compounds, strongly adsorbed [^{36}Cl] - CF_3CH_2Cl and dehydrochlorination which is likely to result in retained chloride species. However, all of the possibilities mentioned cannot be distinguished as the Geiger - Müller direct monitoring method does not allow for compound identification.

Examination of the results reveals a considerable amount of scatter in the data particularly amongst undoped and low zinc doped chromias at lower temperatures. Values obtained as surface count were mostly below 1500 count min^{-1}, the lower limit for observing an event of significance. In order to increase observed count rates the specific count rate of the [^{36}Cl] - CF_3CH_2Cl would require a considerable increase. This would prove both expensive and increase the radiochemical hazards associated with this work. Therefore, low surface count rates were inevitable unless [^{36}Cl] - CF_3CH_2Cl adsorbed onto the surface in large quantities.

Scatter in data was aided by the stock of [^{36}Cl] - CF_3CH_2Cl being produced from different reactions to manufacture [^{36}Cl] - CF_3CH_2Cl. This was unavoidable and each reaction was monitored to attain as great a degree of reproducibility of reaction conditions as was possible. Batches of [^{36}Cl] - CF_3CH_2Cl were examined by infrared spectroscopic analysis of samples of [^{36}Cl] - CF_3CH_2Cl from each batch before being added to the stock.

Allowing for these limitations, some interesting data can be obtained from this work. Undoped and lightly zinc doped chromias demonstrate little significant difference between count rates. As gas count rates can be used to indicate partial pressures of [^{36}Cl] - CF_3CH_2Cl in each system when examining similar gas count rates for both chromias similar surface count rates were observed. This occurs in most cases, accounting for scatter as a result of the insignificance of the counts.

When the reaction temperature and partial pressure of [^{36}Cl] - CF_3CH_2Cl were increased, lightly zinc doped chromia surface count rates were appreciably larger than the surface count rate from undoped fluorinated chromia.

Heavier zinc doped chromia has an appreciably larger surface count rate in comparison to undoped and lightly zinc doped chromia over a range of similar partial pressures of [^{36}Cl] - CF_3CH_2Cl and temperatures. Increased partial pressure of [^{36}Cl] - CF_3CH_2Cl and increased temperature serve to exaggerate the difference in surface count rate between heavier zinc doped and lighter doped and undoped chromia. At higher temperatures and partial pressures many of the fluorinated chromia surface count rates are significant.

Table 6.10 Highest Gas Count Rate at Various Temperatures for Differing Fluorinated Chromias

Temperature (K)	Undoped	0.25 w/w % Zn	4 w/w % Zn
R. Temp	3284	3513	3412
423	3030	2837	2050
503	4135	4048	961

Table 6.11 Count From [^{36}Cl] - Chlorine Containing Species Retained on Fluorinated Medium Crystallinity Chromias

w/w % Zn	Temp. Of Reaction (K)	Retained Count Rate (count min^{-1})	Surface Count Rate at Highest Gas Count Rate (count min^{-1})
0	293	158 ± 1.58	1583
0	423	251 ± 2.51	665
0	503	274 ± 2.74	940
0.25	293	126 ± 1.26	1331
0.25	423	184 ± 1.84	1259
0.25	503	285 ± 2.85	1356
4	293	406 ± 4.06	2279
4	423	1229 ± 12.29	3223
4	503	1475 ± 14.76	4812

Table 6.10 shows gas count rates indicative of the partial pressure of gas obtained when the highest pressure of gas was admitted into the system. It is clear that gas count rates decrease as zinc doping increases. This is the reverse of one of the trends observed when surface count rates are considered. Table 6.11 describes surface count rates retained after evacuation of the system following admission of the highest gas pressure during an experimental run. These retained counts are low in both undoped and lightly zinc doped chromias and temperature does not appear to have any dramatic effect to increase retained count rates. Heavier zinc doped chromias have retained count rates which become more significant as the temperature of the experiment increases.

By comparison of retained count rates with surface count rates at the highest gas pressure admitted into the system, it was clear that the adsorption of [^{36}Cl] - CF_3CH_2Cl on the surface of fluorinated chromias was weak. In each case,

retained count rates were a fraction of the surface count rate at the highest gas pressure suggesting that the adsorption strength of [^{36}Cl] - CF_3CH_2Cl was not strong. This also suggested that the retained count rate was the result of [^{36}Cl] - chlorine left on the surface of the fluorinated chromia as a result of reaction. Tables 6.10 and 6.11 are complementary to each other as gas count rates decrease with increasing surface count rate for various chromias at differing temperatures.

This work has established that the adsorption of [^{36}Cl] - CF_3CH_2Cl with fluorinated chromia was very weak and that the largest portion of the surface count rate was the result of weakly adsorbed [^{36}Cl] - CF_3CH_2Cl. The smaller portion of the surface count rate was a more strongly adsorbed [^{36}Cl] - chlorine species which was retained on the surface of the fluorinated chromia, following evacuation of the counting cell. This was believed to be the result of the reaction of [^{36}Cl] - CF_3CH_2Cl with the surface although other possibilities exist. The extent of this retained surface count rate was influenced by the amount of zinc doped onto the chromia, increasing amounts of zinc resulting in increasing surface count rates.

7 DISCUSSION

Several aspects of fluorinated chromia catalysts used for the production of CF_3CH_2Cl, were under investigation in this work. The properties of the catalysts are related to the pretreatment which they have undergone and this is discussed. Common catalyst pretreatments in this work differed significantly from those of other workers and resulted in catalysts with differing properties. Differences and similarities between catalysts of other workers and those used in this work are discussed. The results of these investigations have led to proposals regarding the nature of the active site and possible reaction mechanisms.

7.1 FACTORS AFFECTING CATALYST ACTIVITY

The percentage of crystalline α - chromia phase which is present on the surface has a heavy influence on the performance of the chromia catalyst. This has been shown by microreactor studies of chromias containing very different levels of α - chromia (crystallinity). Chromias containing lower levels of crystallinity have superior conversion of CF_3CH_2Cl to CF_3CH_2F than chromias with higher levels of crystallinity. This can be explained by higher surface areas characteristic of chromias of lower crystallinity. Higher surface area chromias will have more active sites which will result in increased conversion of CF_3CH_2Cl.

The degree of crystallinity also effects doped chromias by altering the amounts of zinc(II) required to induce differing effects during microreactor studies. Impregnating chromias with zinc(II) chloride produces differing effects on catalyst performance during microreactor studies. Lightly zinc(II) doped chromias have superior catalytic activities to undoped chromias and heavily zinc(II) doped chromias have inferior catalytic activities to undoped chromias. Designation of 'light' and 'heavy' doping of chromias is dependent upon the degree of crystallinity of the chromia. Catalysts with high crystallinity require less zinc(II) to produce inferior activity to undoped chromia than catalysts with lower crystallinity. This is

largely due to the differences in surface area between chromias. Chromias with lower surface areas and , consequently, lower numbers of active sites, will require less zinc(II) to induce improved catalytic activity to undoped chromias. Less zinc(II) is also required to 'poison' chromias with lower surface areas. Zinc(II) 'promotion' and 'poisoning' is very marked throughout the range of chromias tested. For each different crystallinity of chromia light zinc(II) doping results in increased activity and the promotional effects on catalytic activity of impregnation of low levels of zinc(II) on chromia is beyond doubt. When the catalytic activity of lightly zinc(II) doped chromias is compared with undoped chromia, conversion of CF_3CH_2Cl to products, in the temperature range 573 - 553K, is often 3 - 4 times greater. For example, in the medium crystallinity chromia catalyst series, lightly zinc(II) doped chromia has a conversion of CF_3CH_2Cl which is four times greater than that of undoped chromia at 563K. Catalyst relative reaction rates, indicative of the performance of a catalyst , have determined that light zinc(II) doping can increase the relative reaction rate of chromia by almost 50 %.

Studies of other transition metal dopants in the 2+ oxidation state have failed to produce any promotional effect to match that of zinc(II) observed during this work. Landon (132), has studied chromia catalysts using exactly the same methods as described in this work. In Landon's study, nickel(II) and magnesium(II) were used as dopants employing a coprecipitation method of metal doping and similar calcination temperatures to those used in this study. Only one chromia examined by Landon had an increased conversion to CF_3CH_2F to undoped chromia. This catalyst was 5% nickel(II) doped chromia calcined at 823K, however the increase in conversion in comparison to undoped chromia was minimal. Materials containing 11 or 33 atom % nickel are all significantly more inactive than undoped chromia. Magnesium(II) doped chromias were less active or, at best, as active as, undoped chromias. In this instance the behaviour of 5 atom % Mg(II) doped amorphous chromia was indistinguishable from undoped chromia in activity, while 33 atom % Mg(II) doped chromia shows little or no activity at all. In all cases

increasing calcination temperatures produce poorer catalysts such that the best doped chromias of both the Ni(II) and Mg(II) series are both amorphous.

Brunet *et al* (133) have examined Ni(II) doped chromias made via a coprecipitation method, fluorinated to both a lesser and greater degree than chromias in both this study and the work of Landon. The gas phase flow reactor system used differing ratios of CF_3CH_2Cl and HF and the reaction was performed at a higher temperature. Results obtained for Ni(II) doped chromias in comparison with undoped chromias indicated a slight improvement in conversion of CF_3CH_2Cl. Selectivity of these chromia catalysts is poorer than selectivity of catalysts in this work and the work of Landon. This is probably not the result of the doping level and coprecipitation method and it is more likely the result of reaction conditions in particular the ratio of reactants. Kim *et al* (37) used Mg(II) as a dopant and this work indicated that Mg(II) lightly doped chromias had inferior conversion of CF_3CH_2Cl, however catalyst lifetime studies indicate that chromia doped with Mg(II) had longer lifetimes than chromias which were undoped. This improved lifetime was attributed to a reduction in the percentage of CF_2CHCl present in the reaction products as CF_2CHCl was believed to contribute to catalyst coking and thus deactivation.

No lifetime studies were performed in this work, however, if a reduction in the percentage of CF_2CHCl in products is a criteria for the improvement of catalyst lifetimes then Zn(II) doped chromias, under the reaction conditions employed during this work, should have increased catalytic lifetimes as CF_2CHCl is present as $< 2\%$ of the reaction products in this work. In all studies of doped chromias which can be compared with this work, no M(II) doping displays improvement in catalytic activity which compare favourably to zinc(II) doping in this work. The relationship between M(II) doping and chromia crystallinity was also examined by Landon. In that study, however, increasing calcination temperature and hence increasing crystallinity resulted in catalysts which were distinctly poorer than undoped chromias.

The effects of crystallinity on the catalytic activity of chromia during the reaction of CF_3CH_2Cl and HF was not examined by Brunet and Kim. Landon has examined chromias of differing crystallinity. The activity of chromias prepared during this work in comparison to those of Landon indicate that, in both cases, trends in catalytic activity in relation to chromia crystallinity were the same. Reductions in crystallinity, in both sets of work, give rise to improved catalytic activity.

The presence of only small quantities of $CF_2 = CHCl$ in the reaction products, during this work, is the result of a large HF : CF_3CH_2Cl ratio of 4 : 1. This forces the reaction towards the fluorination of CF_3CH_2Cl as opposed to the dehydrofluorination reaction. The same HF : CF_3CH_2Cl ratio is also employed in the work of Landon and similar $CF_2 = CHCl$ percentages appear in the reaction products during that study. This is not true in the work of Blanchard, Brunet *et al* (134, 35, 71, 133) and Kemnitz *et al* (34, 135). These workers use reaction systems which have lower HF : CF_3CH_2Cl ratios than those employed in this work. Therefore, the fluorination reaction to form CF_3CH_2F is less favoured and the formation of $CF_2 = CHCl$ becomes more favourable. Blanchard, Brunet *et al* have studied the effects of introducing increasing quantities of HF into the reaction system. The result is a reduction in the amount of $CF_2 = CHCl$ in the reaction products as the ratio of HF : CF_3CH_2Cl is increased.

X - ray diffraction of zinc(II) doped and undoped chromias was performed to determine the effects of zinc(II) doping on the bulk structure of chromia. Zinc(II) doping, whether as a light doping or a heavy doping, does not alter the bulk structure of chromia. Therefore, zinc(II) promotion via an interaction with the bulk structure of the chromia catalyst is unlikely. X - ray diffraction of Ni(II) and Mg(II) doped chromias prepared via coprecipitation by Landon, results in the inhibition of crystallisation when 33 atom % doping levels are used. Five atom % doping with Ni(II) and Mg(II) does not inhibit the formation of crystalline chromia phase to the extent where disruption of crystalline chromia can be detected by X - ray

diffraction. Fluorination of chromias from the work of Landon indicated that the bulk structure is relatively unaffected in comparison with unfluorinated chromias.

Surface area analysis of chromias from this work have determined that fluorination results in reduced surface areas. There is no evidence for chromium halide formation as a result of chromia fluorination, however in every case the surface area of chromia is reduced by fluorination. The size of the reduction in surface area is related to the crystallinity of the chromia. Amorphous chromias, having large surface areas, have larger reductions in surface area. This is true for both the actual surface area loss and the relative percentage of surface area lost in comparison with chromias of higher crystallinity. In general, further reductions in surface area occur after catalytic use but these reductions are smaller than reductions observed during fluorination. Similar trends in surface area data for chromias were also noted by Landon.

Exceptions to the trends in surface area are heavily zinc(II) doped chromias. Small increases in surface area were noted upon fluorination of heavily zinc(II) doped chromias in comparison with unfluorinated heavily zinc(II) doped chromia, which had the lowest surface areas of all chromias examined. Mercury pore volume analysis has shown that heavily zinc(II) doped chromia, both unfluorinated and fluorinated, had the same pore volume. Partial blockage of the pore structure on unfluorinated heavily zinc(II) doped chromia were indicated by mercury extrusion curves. This effect is not observed on fluorinated chromias. The reason for this change in the pore blockage material is possibly a change in the zinc(II) environment of zinc(II) species which block the pore opening, for example, zinc(II) chloride reacting with HF to form zinc(II) fluoride. Such a change may also occur with other zinc(II) species on the surface of the chromia.

The effect of zinc(II) doping on the apparent activation energies of catalysts is dramatic. Small quantities of zinc(II) reduce the apparent activation energies of chromia catalysts by a large amount and larger quantities of zinc(II) reduce the apparent activation energy of chromia by slightly larger amounts. For example,

medium crystallinity chromia has an apparent activation energy of 179.17kJmol^{-1}. With 0.25 w/w % zinc(II) doping on this same chromia, the apparent activation energy is reduced to 113.154 kJmol^{-1} and 4 w/w % zinc(II) doping reduces the apparent activation energy to 91.720kJmol^{-1}. Thus the effect of zinc(II) doping on apparent activation energy is not a linear one and larger levels of zinc(II) doping on chromias will not reduce the apparent activation energy by a proportionally large amount, but will result in a further, smaller decrease in activation energy. The decrease in activation energy can account for the effect of improved activity in lightly zinc(II) doped chromias, however it does not account for the poisoning of heavily zinc(II) doped chromias and indeed it would seem contradictory to observed experimental results. The most plausible explanation for zinc(II) poisoning is the masking of active sites by zinc(II) species on chromia. Thus zinc(II) doping lowers activation energies, however, it leads to active site blockage if zinc(II) dispersal is too high.

Landon has performed activation energy studies on nickel(II) and Mg(II) doped chromias. These studies have determined that nickel(II) doping lowers the activation energy of chromias for the reaction of HF and CF_3CH_2Cl. Large quantities of nickel(II) give rise to a substantial reduction in activation energy. However the decrease in activation energy with increasing nickel(II) also does not appear to be proportional, similar to zinc(II) doping in this work. Nickel(II) doping does not lower the activation energy of chromia to the same extent as zinc(II) doping in this work, but the relationship between nickel(II) doping levels and decreases in activation energy is similar to that of zinc(II). Magnesium(II) doping has the opposite effect from both nickel(II) doping and zinc(II) doping. At low levels of magnesium(II) doping little or no effect on activation energy is observed. At larger levels of magnesium(II) doping an increase in activation energy is observed. The results from both this work and that of Landon indicate that the lowering of activation energy is not simply dependant upon the presence of a first row transition metal in the 2+ oxidation state. A larger decrease in activation energy

by zinc(II) doping in comparison with nickel(II) doping complements the findings of microreactor studies when this work and that of Landon are compared. This also suggests that the effects of dopant promotion for catalysts in this reaction are primarily concerned with a lowering of activation energy. Magnesium(II) effects on activity are also complemented by microreactor studies. Comparisons between this work and that of Landon underline the unique position of zinc(II) as a promoter of chromia.

7.2 SURFACE SPECIES ON WORKING CATALYSTS

In the present work studies of the surface species indicate that chromia is in a partially fluorinated state. X - ray photoelectron spectroscopy indicates that chromium 2p binding energies for catalysts which fall between the fully fluorinated CrF_3 and unfluorinated Cr_2O_3. This raises possibilities of a chromium oxy - fluoro phase or partial formation of CrF_3 on the catalyst surface with Cr_2O_3 as the remaining surface species. Kemnitz *et al* (136) reported similar Cr 2p spectra for chromia catalysts fluorinated by fluorine containing haloalkanes. The formation of ether α - CrF_3 or β - CrF_3 on the chromia surface would result in considerable surface disruption as both α - CrF_3, β - CrF_3 and Cr_2O_3 have very different structures although the formation of β - CrF_3 on a chromia surface is possible. It is known that α - CrF_3 is catalytically inactive for the reaction of CF_3CH_2Cl and HF and it was speculated previously by Webb, Winfield *et al* (28) that chromia catalyst deactivation by HF was the result of the formation of α - CrF_3 phases on the chromia surface. The study undertaken by Kemnitz, postulated that, as β - CrF_3 is catalytically active for this reaction, this phase or a fluorinated chromia phase very similar to β - CrF_3 was the active phase on the chromia.

Work by Landon (132) on X - ray photoelectron Cr 2p spectra of nickel(II) and magnesium(II) doped fluorinated chromias reveals similar results to the Cr 2p X - ray photoelectron spectra of zinc(II) doped fluorinated chromias. In this work, the work of Kemnitz and that of Landon, fluorinated chromia samples all

have X - ray photoelectron spectra binding energies which fall in between the binding energies of α - Cr_2O_3 and α - and β - CrF_3 phases. As stated, Kemnitz postulates that the active phase on fluorinated chromias is similar to β - CrF_3. This is based upon the catalytic activity of this phase. No definitive evidence for β - CrF_3 on the surface of these fluorinated chromias can be gained from X - ray photoelectron spectra from any of these studies. It should be noted that in the case of the Kemnitz work, a greater degree of fluorination of chromia results in a higher binding energy, closer to that of both α - CrF_3 and β - CrF_3 . However, even at the highest levels of fluorination, Cr 2p spectra binding energies of fluorinated chromias are closer to that of Cr_2O_3 than β - CrF_3.

Transmission electron microscopy did not reveal any evidence for α - Cr_2O_3 or α - CrF_3. A very few 'uncertain' assignments of 'd' spacings could be attributed to α - Cr_2O_3 or α - CrF_3. As no chromium oxyfluoride powder Diffraction File data was available for comparison the existence of such a phase was a matter of speculation. Chromium(III) fluoride Powder Diffraction File data was for α - CrF_3 only, no data on β - CrF_3 'd' spacings was found. Landon also performed transmission electron microscopy on nickel(II) doped chromias. In this case no evidence for α - Cr_2O_3 or α - CrF_3 was found and it was speculated that a CrOF phase or a Cr(III) in a disordered oxyfluoride environment may be present.

Fluorination of chromias results in dramatic changes to the chromia surface as in this work and all comparative studies X - ray photoelectron spectroscopy and transmission electron microscopy data indicates that chromia is no longer present as a predominant phase on the surface. Assigning a heavily fluorinated chromium compound to be the major surface phase is not possible as results indicate that this is not present. The speculation of Kemnitz that β - CrF_3 or a similar phase may be the active phase on fluorinated chromia is based upon the fact that β - CrF_3 or a similar phase is an active catalyst for this reaction, without the need for a prior fluorination. No structural evidence from this work was obtained to support this

theory. All evidence obtained from this work indicates that a chromium phase which is between α - Cr_2O_3 and CrF_3 is present on the surface. It could be suggested that a CrOF phase may be present but no CrOF standard is available to make comparison with. Therefore, the suggestion of a CrOF phase is, as in the case of β - CrF_3 phase assignment from the work of Kemnitz, purely speculative.

Zinc(II) on the surface of these chromias is in a highly fluorinated state. Within the errors of the experiment, Zn 2p binding energies of zinc(II) containing chromias indicate that all of the zinc on the surface of these catalysts is present as ZnF_2. This assignment is more certain on heavily zinc(II) doped chromia, particularly as doping of zinc(II) on the more lightly doped chromia is so little that the spectrum is less clearly resolved. The evidence for ZnF_2 is not supported well by transmission electron microscopy data. Powder Diffraction File 'd' spacings for ZnF_2 and ZnO are very similar. The resultant of this is that few clear assignments can be made. X - ray photoelectron spectroscopy evidence for zinc(II) species indicates that Zn 2p spectra of chromia samples are the same as the ZnF_2 standard and that this is distinctly different from ZnO. From this evidence it is less likely that 'd' spacing assignments made to both ZnO and ZnF_2 are, infact ZnO.

Landon's X - ray photoelectron spectroscopy and transmission electron microscopy analysis of nickel(II) doped chromias concluded that the only clear assignments which could be made from microscopy were of NiF_2. Evidence for NiF_2 on nickel(II) doped chromias from X - ray photoelectron spectroscopy was very strong and assigning nickel(II) species as NiF_2 was performed with some certainty. From evidence in this work and Landon's work it appears that dopant atoms undergo a radical change in their chemical environment upon fluorination. Unlike chromia itself transition metal(II) dopant species become fully fluorinated on the surface of the catalyst. This suggests that the dopant forms a distinct phase on fluorinated chromia surfaces as opposed to becoming integrated into the partially fluorinated chromia surface structure. Transmission electron microscopy studies from this work indicate the presence of Zn - Cr - O species. This conflicts with X -

ray photoelectron spectroscopy studies which indicate that both Cr 2p and Zn 2p spectra of a $ZnCr_2O_4$ standard are distinctly different from those of the chromias under study. It may be the case that a Zn - Cr - O species may link the ZnF_2 species to the surface of the fluorinated chromia. Transmission electron microscopy studies by Landon give no evidence for $NiCr_2O_4$ and this is supported by X - ray photoelectron spectroscopy studies on Landon's nickel(II) doped chromias.

X- ray photoelectron F 1s spectra of zinc(II) doped and undoped chromias in this work give binding energies for F 1s in each chromia which are the same, within the errors on the experimental binding energy data. These F 1s binding energies also match those of CrF_3 and ZnF_2 and therefore this information does not clarify speculative proposals made on the basis of Cr 2p spectra and transmission electron microscopy. One interesting observation is the lack of difference in Cr 2p and F 1s spectra of undoped and doped chromias. This lack of difference supports the idea that the zinc(II) species on doped fluorinated chromias does not become integrated into the surface structure of the fluorinated chromia and is, in fact, a distinct phase in its own right on the surface.

Cr 2p spectra of catalysts used in Landon's work reveal differences in binding energy values. These chromia catalysts were prepared by a different method from chromias from this work. Higher dopant levels were used and chromia calcination was performed at various temperatures following doping. The largest differences in binding energies between chromias occurred where distinctly different calcination parameters were used. In this work, unlike that of Landon, chromias which underwent surface analysis were all calcined using the same parameters. Different dopant levels on chromias calcined at the same temperature from Landon's work gave little difference in binding energy. Within the errors of the experiment, binding energies of chromias of the same calcination temperature, but different dopant level were the same. Thus differences in Cr 2p spectra binding energies of catalysts are most likely to be dependant upon the crystallinity of chromias examined as opposed to the amounts of dopant present. This is further

evidence for the structural independence of dopant metals on these fluorinated chromias.

7.3 FLUORIDE LABILITY

All of the fluorinated chromias examined have a percentage of fluoride species which are labile to reaction with HF and/or HF and CF_3CH_2Cl. At least two distinct types of labile fluoride species have been identified. These are fluoride labile to HF alone and fluoride labile to both HF and CF_3CH_2Cl. Each fluorinated chromia has an uptake of labile fluoride and this uptake is dependant upon two factors. First, the degree of crystallinity of the chromia, prefluorinated for these experiments, is important and second, the percentage of zinc(II) doped onto the chromia is important. Uptakes of labelled fluoride on chromia will be the result of exchange with labile fluoride on the prefluorinated chromia. Uptake of fluoride increases with decreasing crystallinity, as a result of largely increased surface area. The presence of chromium in oxidation states other than chromium(III), such as chromium(IV) and (VI), could also give rise to increased uptakes as these higher oxidation state chromium ions are known to be present on less crystalline chromias from TPR studies.

Work by Landon on uptakes using the same system has revealed that unfluorinated chromias have large uptakes equivalent to 8.37 mmol g^{-1} on amorphous chromia which reduce to 1 - 2 mmol g^{-1} on higher crystalline chromias. In this work uptakes on fluorinated amorphous chromias are in the region of 1 - 2 mmol g^{-1} and for higher crystallinity chromias of 0.2 - 0.3 mmol g^{-1}. It is apparent, therefore, that some uptake of fluoride on fluorinated chromias is the result of exchange as this uptake is a small percentage of the amount of fluoride uptake on chromia in an unfluorinated state. In this work small amounts of zinc(II) doping have no effect upon the uptake of fluoride, however large amounts of zinc(II) do effect the uptake of fluoride species on fluorinated chromias. The cause of this anomaly could be the pore structure of heavily zinc(II) doped chromias. As

discussed earlier, mercury extrusion curves from the process clearly indicate that a pore blockage is occouring on the unfluorinated chromia structure and this is present to a much lesser extent on the fluorinated chromia. It is postulated that zinc(II) species is blocking the pores of chromia on the surface and reaction of this species with HF results in an unblocking of the pores. Another explanation for the larger HF uptake is the exchange involving zinc(II) fluoride which is more facile than chromium fluoride species and this would only become apparent with large amounts of zinc(II).

The percentage of fluoride uptake which is labile to exchange with HF is dependant upon zinc(II) doping and crystallinity. High levels of zinc doping, which cause large fluoride uptake, give rise to small percentages of labile fluoride. Low levels and undoped chromias have larger percentages of fluoride labile to reaction with HF and CF_3CH_2Cl. The amounts of labile fluoride on one crystallinity of chromia are similar regardless of zinc(II) doping. However, as high zinc(II) doping gives rise to larger uptakes, the percentage of labile fluoride on zinc(II) highly doped chromia appears to be lower. Less crystalline chromias have larger uptakes of fluoride species, however they also have lower percentages of labile fluoride than higher crystalline chromias. For comparison, lower crystalline chromias tend to have approximately 50% of fluoride uptake labile to exchange with HF and higher crystalline chromias tend to have 70% of fluoride labile to exchange with HF. Therefore, the amount of fluoride labile to exchange with HF on lower crystalline chromias is larger than on higher crystalline chromias, however the relative percentage is lower.

Work performed by Landon on nickel(II) doped fluorinated chromias indicates similar uptakes and percentages of fluoride lability to that reported in this work. Similar trends such as increases in the relative percentages of fluoride uptake which is labile to exchange with HF is considerably larger on lower crystalline chromias. From this work and that of Landon, it is clear that in each catalyst examined a considerable pool of fluoride is labile to exchange with HF. The size of

that pool is effected by the crystallinity of the chromia from which the fluorinated chromia is prepared. Zinc(II) doping, however does not effect the amounts of fluoride labile to exchange with HF.

A certain percentage of fluoride labile to exchange with HF is also labile to exchange with CF_3CH_2Cl. This fluoride forms around 70% of the total fluoride labile to exchange with HF and this relative percentage of labile fluoride also labile to reaction with CF_3CH_2Cl is consistent regardless of the degree of crystallinity of the chromia. The fluoride in this category will be the amount of fluoride available for reaction with CF_3CH_2Cl. Similar results using the same system were found by Landon using nickel(II) and magnesium(II) doped chromias. This work and the work of Landon has led to the discovery of more than one type of strongly held labile fluoride. These types of labile fluoride can be described as 'reactive' - fluoride which partakes in an exchange with HF and CF_3CH_2Cl and 'non - reactive' - fluoride which is labile to reaction with HF alone.

This work and that of Landon is consistent with work previously performed by Webb, Winfield *et al* (27, 28, 73). By employing the radiotracer ^{18}F and fluorinating chromias using the same system described for radiotracer experiments, followed by unlabelling of labelled chromias by HF, these workers identified different fluoride species on fluorinated chromia. By purging labelled chromias with nitrogen flow, a small percentage of labelled fluoride was removed from the surface. This was attributed to weakly adsorbed HF molecules and / or oligomers associated with the fluorinated chromia surface. In fluoride lability experiments on fluorinated chromias, performed during the course of this work, this weakly bound type of labile fluoride species was not detected as labelled chromias were purged with nitrogen before determination of fluoride uptakes and this type of fluoride would be lost. The second type of fluoride identified by Webb and Winfield was inert to exchange with HF. The percentage of fluoride which was in this category increased over the lifetime of the catalyst. This type of fluoride was also identified from the work of Landon and from studies performed during this work. No catalyst

lifetime studies of chromias were performed, however increases in the percentage of non - exchangeable fluoride over the catalyst lifetime is not surprising as the work of Webb and Winfield determined that HF poisons chromias over prolonged use.

The third type of fluoride identified by Webb and Winfield was fluoride labile to exchange with HF. This fluoride is was not removed by nitrogen purging and is therefore held more tenaciously on the chromia. It was believed that this was the source of fluoride incorporated into chlorofluorocarbons which were reacted over these fluorinated chromias. The work of Landon and this work has suggested that only a percentage of this labile fluoride will be incorporated into halocarbon reactants. This work has described the subdivision of a fluoride type previously described in earlier work by Webb, Winfield *et al.* Possible reasons for the subdivision of this category of fluoride into the 'reactive' and 'non - reactive' types is concerned with the relative size of the two reactant molecules HF and CF_3CH_2Cl. As HF is a very small molecule it can react with labile fluoride which is located in areas in which CF_3CH_2Cl may be sterically hindered. An example could be labile fluoride species located within the pore structure of chromia which may hinder the entry of CF_3CH_2Cl molecules if the pore diameter is narrow. It was suggested by Webb and Winfield that this labile fluoride may be bonded to Cr(VI) which was shown to be present in their chromias by TPR studies. This possibility cannot be ruled out, however, the relative percentage of fluoride uptaken by fluorinated chromias examined in this study which is labile to reaction with HF, increases with increasing crystallinity. Higher crystalline chromias are likely to have more Cr(III) present on the surface than less crystalline chromias, which conversely are likely to have a higher proportion of other chromium atoms in higher oxidation states.

The non - exchangeable fluoride species described in this work and other studies mentioned, was attributed to the slow conversion of Cr(III) - O bonds to Cr(III) - F bonds, according to Webb and Winfield. Thus the formation of inactive CrF_3 over a period of catalyst usage from the partially fluorinated state of the working catalyst was described as the reason for catalyst deactivation by HF. The

work of Kemnitz would predict that this inactive CrF_3 was α - CrF_3, which is catalytically inactive as opposed to the catalytically active β - CrF_3. A change from partially fluorinated chromia to α - CrF_3 would result in considerable surface disruption. However, as the formation of the partially fluorinated chromia is a surface disruption in itself and the fluorinated chromia catalysts slowly deactivates with usage, this cannot be ruled out. In this work no catalyst lifetime studies were performed and a determination of this hypothesis was not possible.

7.4 INTERACTION OF CF_3CH_2Cl ON FLUORINATED CHROMIA SURFACES AND RETENTION OF THE ASSOCIATED CHLORIDE

The interaction of CF_3CH_2Cl on the surface of fluorinated chromias is a weak adsorption. Removal by dynamic vacuum of [^{36}Cl] - chloride species from the surface of fluorinated chromias which has been interacted with [^{36}Cl] - CF_3CH_2Cl and examination of the material removed confirms the weak nature of the interaction. The uptake of [^{36}Cl] - CF_3CH_2Cl by fluorinated chromia is affected by the temperature at which the interaction was performed and the doping level of zinc(II) on the chromia. The total amount of chloride species uptaken on the fluorinated chromia is divided into two major types. Chloride which is weakly interacted and chloride which is more strongly interacted. Infrared spectroscopy analysis of the material removed by dynamic vacuum revealed this to be [^{36}Cl] - CF_3CH_2Cl. More strongly adsorbed chloride was retained on the surface of the fluorinated chromias. The percentage of chloride which was of the strongly adsorbed type increased with experimental temperature and zinc(II) doping.

The exact nature of this retained chloride is open to speculation, however, a few possibilities can be considered. The probability of this chloride being CF_3CH_2Cl is remote as this would pose the question as to why only some of the CF_3CH_2Cl was retained on the fluorinated chromia surface and the remainder has a weak interaction. The chloride species retained on the chromia surface is more likely to be the result of a reaction between the CF_3CH_2Cl and the fluorinated chromia. A

number of possible reactions can be considered. The most likely of these is a halogen exchange reaction between the labile fluoride species on the fluorinated chromia surface and the CF_3CH_2Cl molecule. These fluorinated chromias have labile fluoride species on the surface, as determined by fluoride lability studies discussed previously, and so such a reaction can take place. As the temperature during the interaction is increased, the amount of chloride which is retained increases and this would correspond with an increase in the extent of reaction. This would also be predicted from microreactor studies on these catalysts.

Webb, Winfield *et al* (29, 73, 137) have used [^{36}Cl] - chlorine as a radiotracer to examine fluorinated chromias using the Geiger - Müller direct monitoring system. Labelled CCl_2FCF_3 flow over fluorinated chromia at 623K resulted in the deposition of [^{36}Cl] - chloride activity on fluorinated chromia surfaces. Subsequent flow of HF over this surface removes 75 - 85% of this chloride. By passing other haloorganics, which were non - labelled, over the surface of the [^{36}Cl] - chloride labelled chromia catalyst incorporation of [^{36}Cl] - chlorine into reaction products was observed. This work, incorporating [^{36}Cl] - chloride into reaction products, requires the breaking of C - Cl bonds in the CCl_2FCF_3 molecule. These bonds are most likely to be broken on the catalyst surface. Labelled [^{18}F] - fluorine radiotracer studies by these same workers, using fluorinated chromias, gave rise to chloride species on the fluorinated chromia surface which could, in turn, react with other haloorganic compounds. It was suggested that labile fluoride exchanges with chloride on the surface of the fluorinated chromia depositing chloride species which would be labile to reaction with HF, HCl or other haloorganic compounds, but not with inert gas flow.

Such a mechanism would explain the observations of this work with regard to the source of the retained chloride species. In these experiments, work was not performed to remove retained chloride from fluorinated chromia surfaces by passing other haloorganic compounds over the chromia or by passing HF or HCl. It is

interesting however, that the features common to both the [^{36}Cl] - chloride labelling experiments performed by Webb and Winfield and this work, yield similar results.

Another possible reaction mechanism which is plausible, is the formation of CF_2CHCl and HF in an olefination process. The conditions used in these experiments are similar to some of the reaction conditions used by Blanchard, Brunet *et al* (35, 71, 133). The common link between these experiments and those of Blanchard and Brunet is the lack of HF in the reactant system. In their work, chromias which had undergone extensive (70h) fluorination processes were reacted with CF_3CH_2Cl and the reaction products were found to contain large quantities of $CF_2 = CHCl$. The quantity of $CF_2 = CHCl$ in the reaction product was often in excess of CF_3CH_2Cl in the product distribution. The results obtained by these workers suggest that, in the experiments to determine the interaction of CF_3CH_2Cl with the catalysts in this work in which no HF is present in the gas phase, some $CF_2 = CHCl$ will be formed. If this is the case the formation of $CF_2 = CHCl$ is unlikely to contribute to the retained chloride. In microreactor studies, performed during the course of this work, $CF_2 = CHCl$ is present as a minor product in the reactor effluent under the reaction conditions employed, suggesting that it does not adsorb strongly onto the surface of the catalyst. The work of Blanchard and Brunet also shows that $CF_2 = CHCl$ appears in the reactor effluent. It is, however, known that $CF_2 = CHCl$ leads to catalyst deactivation via a coking process (37). This would imply that the adsorption or reaction of $CF_2 = CHCl$ could take place on the catalyst and this may lead to retained chloride. There is no direct evidence of this in this work.

The most heavy influence on the amount of retained chloride on the catalyst surface is the quantity of zinc(II) doped onto the chromia. Surface studies have revealed that zinc(II) species on the surface of these fluorinated chromias is present as ZnF_2. Heavily zinc(II) doped chromias have large quantities of retained [^{36}Cl] - chloride. Lightly zinc(II) doped chromias and undoped chromias have similar, smaller, amounts of retained [^{36}Cl] - chloride, lightly zinc(II) doped chromia having

slightly more [^{36}Cl] - chloride. The influence of zinc(II) is clear and the relative amounts of retained chloride on progressively more heavily doped zinc(II) increases with temperature. The relationship between zinc(II) doping and chloride retention may be the result of a lowering of activation energy by zinc(II) on chromia active sites, as discussed earlier in this chapter. Such a lowering of activation energy would promote the exchange reaction on the fluorinated chromia surface resulting in retained chloride following exchange. However, as was postulated earlier, the poisoning of chromia by heavy zinc doping is believed to be the result of active site masking. More active site masking would result in less chloride for fluoride exchange and so less retained chloride should be noted. Another possibility for chloride retention increase with zinc(II) doping is the reaction of ZnF_2 with CF_3CH_2Cl to form $ZnCl_2$ This reaction could occur directly on the ZnF_2 or it could occur indirectly by reaction of CF_3CH_2Cl with the few active sites available and subsequent reaction of the retained chloride with ZnF_2 to form $ZnCl_2$. These possibilities are discussed further in 7.5.

Most of the available evidence from other experiments involved in this work and that of Webb and Winfield suggests that this retained chloride is derived from the halogen exchange reaction. The formation of [^{36}Cl] - chloride labelled CF_3CH_2Cl occurs via the reaction of [^{36}Cl] - HCl and CF_3CH_2F over chromia. This reaction is clearly a halogen exchange with chloride from the HCl exchange with fluoride from CF_3CH_2F. As it is a surface reaction it is clear that chloride can be a labile species on chromia surfaces and so the exchange mechanism can provide a source for this chloride. The reaction involved in the preparation of [^{36}Cl] - CF_3CH_2Cl, if allowed to proceed for a sufficient length of time, will result in the reformation of CF_3CH_2F. This implies that the fluoride lost in the formation of [^{36}Cl] - CF_3CH_2Cl is retained as a labile fluoride on the chromia surface and can participate in the reverse reaction. This further supports the findings of Webb and Winfield (73) and it is a strong indication of the nature of the retained chloride species. This retained chloride may react with ZnF_2 on the surface which could lead

to chloride containing zinc(II) halide species as the permanently retained chloride on doped chromias.

7.5 PROPOSALS CONCERNING THE NATURE OF THE ACTIVE SITE AND CATALYTIC MECHANISM

The mechanism of halogen exchange is the most probable for the chromia catalysts used in this work. The predominance of the fluorinated product CF_3CH_2F over all other reaction products strongly suggests that a dehydrochlorination / hydrofluorination reaction is not occouring. The work of Kavanagh *et al* (36) using DF as a fluorinating agent for the reaction of C_2Cl_4 and C_2Cl_3H on chromia suggests that, with the haloalkane reactants, further fluorination reactions are via a halogen exchange mechanism. The absence of significant amounts of deuterium in the reaction products as well as a lack of reaction intermediate compounds which would be necessary for a dehydrochlorination / hydrofluorination to occur indicate halogen exchange. No detectable amounts of dehydrochlorination / hydrofluorination reaction intermediates were observed in this work.

Based upon the findings of these studies and those of other workers mentioned previously in this chapter, a picture of the general reaction mechanism of CF_3CH_2Cl on chromias can be envisaged. In the absence of heavy fluorination and HF in the reactant gases, the competing reaction of dehydrofluorination to form CF_2CHCl occurs. The HF produced from this reaction fluorinates the chromia surface and following a minimum critical level of fluorination a halogen exchange process begins to form CF_3CH_2F. This dehydrofluorination is not predominant and can be kept to a minimum of less than 2% of reaction products if the chromia is heavily fluorinated and there are sufficient amounts of HF in the reactant gases. The presence of HF retards the dehydrofluorination reaction and promotes the fluorination reaction via a halogen exchange.

The nature of the active site of the chromias in this reaction should fulfil the following obvious criteria. First, the active site should have a labile fluoride

available for reaction. Second, the active site should be sufficiently accessible thus preventing the steric hindrance of the CF_3CH_2Cl molecule participating in the exchange reaction. This would seem to rule out reaction within the pore structure, unless the pore diameter is sufficiently wide enough to allow a CF_3CH_2Cl molecule to enter comfortably into the pore for reaction and then exit the pore following reaction. The reaction proceeds regardless of the presence of zinc(II) fluoride. As the molecule of CF_3CH_2Cl adsorbs only weakly on the surface of the fluorinated chromia it is probable that the adsorption is through the chloride species which is undergoing exchange and the labile fluoride on the catalyst attacks the carbon centre of the CF_3CH_2Cl molecule via a nucleophilic substitution reaction. This would require only a one centre active site, the single centre holding the labile fluoride species.

Other more complex adsorption sites can be envisaged involving more than one centre . Electropositive atoms such as the terminal hydrogen of an HF molecule or oligomer could serve as an adsorption site. For example, the delta negative charge of the fluoride atoms on the CF_3CH_2Cl molecule being attracted to the delta positive charge of the terminal hydrogen. Similarly chromium(III), (IV), (V) or (VI) atoms of the chromia could also exert a similar influence on the CF_3CH_2Cl molecule. Chromium atoms of oxidation states higher than (III) could be the centre from which labile fluoride originates, however, increased percentages in fluoride lability with increases in α - Cr_2O_3 would seem to contradict this. A higher oxidation state chromium atom with a fluoride directly attached could act as a one centre site or as part of a two centre site. The attraction of the chloride of CF_3CH_2Cl for exchange to the site would be more hindered sterically.

These ideas do not incorporate zinc(II) fluoride within the active site. The role of this zinc(II) fluoride is almost certainly concerned with fluorination as fluoride is clearly associated with the zinc(II) species. Zinc(II) may also enhance the attraction of the adsorption site. Zinc(II) fluoride is not incorporated into the fluorinated chromia surface structure, this is apparent from surface studies

performed. Attaining a degree of independence from the surface reduces the probability that zinc(II) has a direct influence on the chromia surface. It seems unlikely that CF_3CH_2Cl will adsorb on the ZnF_2 regions of the surface preferentially over chromium sites and this suggests a fluorination supporting role of ZnF_2 as opposed to it being a distinct part of the active site.

The promotional effects of zinc are clearly connected to the apparent activation energy change which zinc doping imparts to these chromias. This does not effect the adsorption of CF_3CH_2Cl on the surface of these fluorinated chromias as this work has shown. Nor does it effect the amounts of fluoride for exchange. Therefore, some other explanation is required to explain this promotional effect. Results from X - ray photoelectron spectroscopy analysis have shown that the zinc on the surface of these chromias is in a zinc(II) fluoride environment. X - ray diffraction work has shown that the zinc does not alter the bulk nor the surface structures of these chromias. Therefore, it can be concluded that zinc(II) is not integrated into the chromia structure in any way but is however present on the surface as, for example, islands associated with, but not strongly bonded to, the fluorinated chromia surface. A possible explanation as to how this zinc(II) fluoride influences the activation energy of the active sites on fluorinated chromia is the provision of fluoride species on active sites to act as labile fluoride for reaction. Undoped chromias contain sites which are active for this catalytic fluorination and therefore labile fluoride species will be present on these sites for exchange. These active sites require a source of fluoride to replenish labile fluoride incorporated into a CF_3CH_2F molecule as a result of halogen exchange with CF_3CH_2Cl and labile fluoride species on the active site. The most likely source of this fluoride species is HF gas which is present during the reactive process. In order to replenish active fluoride species HF gas must dissociate its hydrogen and fluoride components with the fluoride becoming the labile fluoride species. This dissociation is very difficult as HF has a very large bond strength of 569.87 +/- 0.06 $kJmol^{-1}$ (146). In order to overcome this difficult stage in the replenishment of labile fluoride species, this

zinc(II) fluoride can act as a source for replacement fluoride for labile species lost from active sites. Thus easier replenishment of chromia active sites lowers the activation energy of these zinc doped chromias which have apparent activation energies which are approximately half that of undoped chromias.

When fluoride from zinc has replenished the active site, chloride on the active site could be uptaken by the depleted zinc(II) atom from which the fluoride was lost. A halogen exchange could then occur between HF in the gas phase and the chloride on the ZnF_2 island. The halogen exchange need not occur on the ZnF_2 atom onto which the chloride attached itself and a system in which the chloride passed from zinc(II) atom to zinc(II) atom by replacement of the chloride attached to one zinc(II) atom by fluoride from its neighbour can be envisaged. Such a system of chloride 'migration' could account for large quantities of chloride retained on the surface of poisoned chromias. As no HF was present in the gas phase, replenishment of fluoride on zinc(II) fluoride islands would not occur. Replenishment of fluoride on the few active sites on these chromias could still continue until the zinc(II) halide island was largely $ZnCl_2$. Therefore, large quantities of chloride could be detected on the surface of heavily zinc(II) doped chromias. This idea and other mechanistic and active site proposals are illustrated in Fig. 7.1.

The active site for this reaction is unlikely to be centred upon a zinc atom and zinc(II) fluoride is not catalytically active for this reaction. The fact that the catalysis occurs on undoped chromia suggests that the active site is centred on chromia and probably a chromium atom on the chromia surface. Another possible system for the catalytic mechanism is a two atom active site model in which the fluorided zinc species is directly involved in the catalysis as opposed to the more indirect fluoride 'feeder' system described above. This system would involve the adsorption of CF_3CH_2Cl on one site, probably a chromium atom and the labile fluoride species would be on the other site, this being a zinc atom. This model would have more substance if the fluoride lability of this heavily fluorided zinc

species were examined. Fluoride lability of this species would open the possibility of this occouring. Zinc 'poisoning' would again be dependent upon blockage with more than one fluorided zinc species present over an active site, the possibility of blocking the chromium adsorption site would arise. An more facile exchange of fluoride on fluorided zinc as opposed to a chromium site would produce a promotional effect lowering the activation energy of active sites. Alternatively, if HF adsorption is more active on ZnF_2 than on chromium(III) this would also potentially produce a more favourable labile fluoride centre.

In both of these possible cases described above there lies one potential problem which may be contradicted by experimental evidence. Both scenarios rely upon the mobility or lability of fluoride species associated with zinc on the surface of the chromia. Clearly this dictates that reaction can only occur on active sites associated with zinc species accounting for promotion. However, this does not allow for the possibility of larger quantities of labile fluoride which cannot participate in the exchange reaction as it is not associated with active sites. Such fluoride almost certainly exists and can be accounted for by the two types of labile fluoride species observed from this work, namely fluoride which is labile to reaction with HF alone and fluoride which is labile to reaction with HF and CF_3CH_2Cl. If zinc(II) fluoride has labile fluoride, as it would require to be for these two mechanisms to work, then it would be predicted that these two chromias containing more zinc species would have more labile fluoride species over all, a greater percentage of this being fluoride labile to reaction with HF as opposed to undoped chromias. Experimental evidence discounts this as chromias had similar amounts of labile fluoride regardless of zinc(II) fluoride content. Thus, for these mechanisms to occur a more subtle reaction must be in place. One possible explanation is that the interaction between chromium based active sites and zinc would induce the lability of fluoride species associated with the active site. This would allow the number of labile fluoride species to remain constant throughout a chromia series at the same time as increasing the lability of fluoride.

FIGURE 7.1 Possible Active Sites and Mechanisms

One Centre Active Site Models

(I) Undoped Fluorinated Chromias

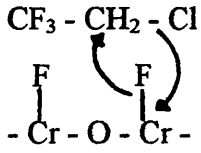

(a) Halogen exchange with CF_3CH_2Cl

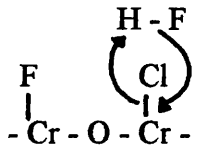

(b) Replacement of lost labile fluoride by HF

(II) Zinc(II) Doped Fluorinated Chromias

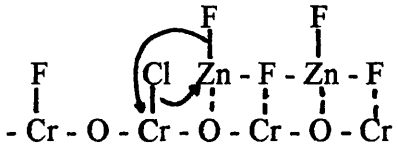

Two Centre Active Site Models

(I) Undoped Fluorinated Chromia

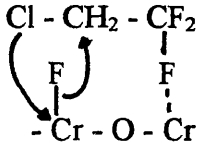

(a) Halogen exchange

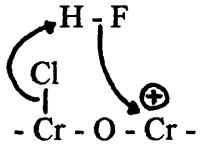

(b) Replacement of lost labile fluoride

(II) Doped fluorinated chromias same as above with fluoride replacement model as detailed in one centre active site model

Chloride Migration On Zinc(II) Fluoride

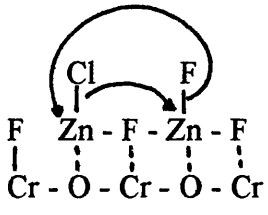

(a)Zn(II) picks up Cl

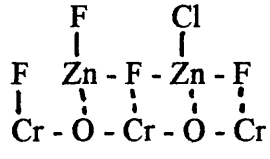

(b)Cl moves to next Zn(II)

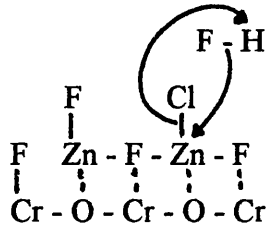

(c)Cl replaced by F from HF

The unknown interaction between the fluorided zinc species and the chromia surface could give rise to another possible model for halogen exchange. The relationship between zinc and the chromia surface could be a subtle electronic interaction which increased the lability of fluoride species on a chromia active site. As zinc is a d10 transition metal and chromium is d4, a zinc atom, in the immediate environment of the chromium based active site, could serve to weaken the chromium - fluoride linkage on labile fluoride species resulting in increased fluoride lability. It is known that zinc species are not incorporated into the lattice structure of these chromia catalysts but are however, associated with the surface of the chromia. Such an arrangement would not cause a large disruption to the chromia and would be unlikely to give rise to 'new sites' which are catalytically active. The possibility of a subtle interaction, such as an electronic influence, cannot be dismissed.

Future work could show whether these mechanistic and active site proposals have substance. The chloride migration mechanism described could be proven by exhaustive reaction of a heavily zinc(II) doped fluorinated chromia with CF_3CH_2Cl alone. Examination of the reaction effluent to detect the presence of CF_3CH_2F over time, would determine if the reaction has continued as would be predicted if this mechanism was occurring. Analysis of the catalyst, following this reaction, by X - ray photoelectron spectroscopy will be to obtain the Zn 2p spectra. Examination of the Zn 2p spectra of the catalyst in comparison to those of $ZnCl_2$ and ZnF_2 standards will determine the zinc(II) halide present.

A two centre active site model, involving a Lewis acid CF_3CH_2Cl adsorption centre, could be proven by pyridine adsorption studies on fluorinated chromias. Following pyridine adsorption catalyst microreactor studies will determine whether the chromia has become inactive and fluoride lability studies with [^{18}F] - HF will determine whether labile fluoride is still present. If pyridine adsorption occurs resulting in inactivity of the chromia catalyst, then it is likely that Lewis acid centres are involved in the reaction. However, if the amount of labile fluoride is the same

both before and after pyridine adsorption, then this would suggest that a separate Lewis acid adsorption centre exists and a two centre active site is probable. These experiments would further advance the findings of this study and bring greater understanding to the nature of the active site and mechanism.

8 CONCLUSIONS.

This work has established that anhydrous HF fluorinated chromia has a large pool of labile fluoride species on its surface which readily undergoes exchange with CF_3CH_2Cl, in the presence of gaseous HF at 573K, to form CF_3CH_2F. The reaction conditions employed strongly promote the fluorination reaction of CF_3CH_2Cl on fluorinated chromia as opposed to the competing dehydrofluorination reaction forming CF_2CHCl. This is a mass balance effect as the ratio of HF to CF_3CH_2Cl employed is 4 : 1 thus the fluorination is promoted as the dehydrofluorination is retarded. The reaction mechanism is a halogen exchange. This is determined by the fact that the reaction is over 98% selective towards CF_3CH_2F and reaction intermediates, characteristic of other potential mechanisms, are not observed.

The ability of the chromia to act as a catalyst for this reaction is heavily dependent on the crystallinity of the chromia. Poorly crystalline chromias, with higher surface areas and subsequently more active sites, have a superior catalytic activity to highly crystalline chromias. The activity of these chromia catalysts is also effected by wet impregnation of $ZnCl_2$ onto the chromia before fluorination. Small amounts of zinc(II) species can induce increases the catalytic activity up to four times that of undoped chromias. Larger amounts of zinc(II) induce decreases in catalytic activity in comparison with undoped chromia.

The amounts of zinc(II) required to effect the activity of chromia are dependent upon the crystallinity of the chromia. Highly crystalline chromias require less zinc(II) to induce increases in catalytic activity than less crystalline chromias. Thus, some crystallinity of the chromia is beneficial as it reduces the amount of zinc(II) required to obtain a promotion of the catalytic activity. In all cases, however, zinc(II) impregnation lowers the activation energy of the catalyst. The activation energy of these chromium catalysts is unaffected by the crystallinity of the chromia. The correlation between lowering activation energy and increasing zinc(II) doping is not linear as only small amounts of zinc(II) are required to induce

a large decrease in activation energy and increasing zinc doping does not produce a decrease in activation energy proportional to the increase in zinc(II) doping.

Zinc(II) doping does not alter the bulk structure of the chromia catalyst in any way. Fluorination by HF of the zinc(II) impregnated chromia causes the reaction of $ZnCl_2$ with HF to form ZnF_2 on the surface of the chromia. This fluorination also effects the chromia by reaction forming a partially fluorinated surface. The exact nature of this fluorinated chromia surface is unknown, but it may be speculated that a Cr - O - F phase may be present. This fluorinated chromia forms the working catalyst for the reaction, having labile fluoride species.

The surface of these doped and undoped chromias have differing fluoride species present. Three types of fluoride have been identified by this work. The first is non - exchangeable with respect to reaction with HF or CF_3CH_2Cl. The second is exchangeable with respect to reaction with HF alone and this type of labile fluoride is termed 'non - reactive'. The third type of fluoride is exchangeable with respect to reaction with both HF and CF_3CH_2Cl. This type of fluoride is termed 'reactive' and is believed to be the fluoride incorporated into CF_3CH_2F following reaction of the catalyst with CF_3CH_2Cl. One more type of fluoride is likely to be present on the surface of the chromia. This is weakly bound HF molecules and oligomers which can be removed by inert gas flow. Experiments to determine the quantities of this type of fluoride present on the chromia surface were not undertaken during the course of this work. The relative amounts of both 'reactive' and 'non - reactive' labile fluoride species are not effected by zinc(II) doping. Increases in fluoride uptake do occur on heavily zinc(II) doped chromias, possibly as a result of partial pore blockage of the pore opening on heavily zinc(II) doped chromias by zinc(II) fluoride.

The interaction of CF_3CH_2Cl on fluorinated chromias is weak in all cases and CF_3CH_2Cl can be removed by dynamic vacuum. Reaction of CF_3CH_2Cl on fluorinated chromias, in a static system in the absence of HF, increases with temperature and zinc(II) doping leaving chloride species which are permanently

retained on the surface of the chromia. The nature of the reaction and the retained chloride species is open to speculation. The most plausible explanation is the reaction of the CF_3CH_2Cl with labile fluoride species to form CF_3CH_2F, leaving chloride retained on the chromia surface. Increases in the amount of retained chloride with zinc(II) doping could be due to the reaction of ZnF_2 with the chloride forming a chloride containing zinc(II) halide.

REFERENCES

1. M. Hudlicky. Chemistry of Organic Fluorine Compounds. 2nd Edn. Prentice Hall Organic Chemistry Series. New York. 1992.
2. A. L. Henne and E. C. Ladd, J. Am. Chem. Soc. 58 (1936) 402.
3. R. P. Wayne. Chemistry of Atmospheres. Oxford Press. Oxford. 1985. p10.
4. A. L. Henne and E. P. Plueddeman, J. Am. Chem. Soc. 65 (1943) 1271.
5. A. L. Henne and R. C. Arnold, J. Am. Chem. Soc. 70 (1948) 758.
6. J. Lovelock, R. J. Maggs and R. J. Webb, Nature 214 (1973) 194.
7. M. J. Molina and F. S. Rowland, Nature 249 (1974) 810.
8. P. P. Bemand, M. A. A. Clyne and R. T. Watson, J. Chem. Soc., Faraday Trans. 69 (1973) 1356.
9. T. G. Spiro and W. M. Stigiani. Chemistry of the Environment. Prentice Hall. New Jersey. 1996.
10. A. A. Woolf, J. Fluorine Chem. 75 (1995) 187.
11. G. Webb and J. M. Winfield, Chem. Brit. 28 (1992) 996.
12. A. McCulloch, Renewable Energy 5 (1994) 1262.
13. K. C. Waugh, J. Chromatog. 155 (1978) 83.
14. E. Kemnitz, D. Hass, W. Metzgen, A. Kohne, N. Noak and J. Janchen, Z. Phys. Chem. 271 (1990) 515.
15. J. C. Stakebake, J. Colloid Interface Sci. 113 (1986) 308.
16. T. H. Ballinger and J. T. Yates Jr., J. Phys. Chem. 96 (1992) 1417.
17. J. Kvicaka, O. Paleta and V. Dedek, J. Fluorine Chem. 43 (1989) 155.
18. L. Kolditz and S. Schultz, J. Fluorine Chem. 5 (1975) 141.
19. H. S. Booth and C. F. Swinehart, J. Am. Chem. Soc. 57 (1935) 1333.
20. E. Santacesaria, M. Diserio, G. Basile and S. Carra, J. Fluorine Chem. 44 (1989) 87.
21. S. Brunet, C. Batiot, J. Barrault and M. Blanchard, J. Fluorine Chem. 59 (1992) 33.
22. S. Brunet, C. Batiot, J. Barrault, M. Blanchard and J. M. Coustard J. Fluorine Chem. 63 (1993) 227.
23. M. Blanchard and S. Brunet, J. Mol. Catal. 62 (1990) L.33.

24. W. W. Dukat, J. H. Holloway, E. G. Hope, M. Rieland, P. J. Townson and R. L. Powell, Eur. Pat. Appl. 503, 792.
25. A. Lantz and B. Cheminal, U. S. Patent 5,055,624.
26. A. J. Wismer, Eur. Pat. Appl. 402,626.
27. J. Kijowski, G. Webb and J. M. Winfield, J. Fluorine Chem. 27 (1985) 213.
28. J. KiJowski, G. Webb and J. M. Winfield, Appl. Catal. 27 (1986) 181.
29. L. Rowley, G. Webb, J. M. Winfield and A. McCulloch, Appl. Catal. 52 (1989) 69.
30. L. Kolditz, G. Kaushka and W. Schmidt, Z. Anorg. Allg. Chem. 434 (1977) 41.
31. A. Hess and E. Kemnitz, Appl. Catal. A 82 (1992) 247.
32. E. Kemnitz, D. Hass and B. Grimm, Z. Anorg. Allg. Chem. 589 (1990) 228.
33. A. Hess and E. Kemnitz, J. Fluorine Chem. 74 (1995) 27.
34. A. Kohne and E. Kemnitz, J. Fluorine Chem. 75 (1995) 103.
35. S. Brunet, B. Requieme, E. Colnay, J. Barrault and M. Blanchard Appl. Catal. B 5 (1995) 305.
36. D. M. C. Kavanagh, T. A. Ryan and B. Mile, J. Fluorine Chem. 64 (1993) 167.
37. H. Kim, H. S. Kim, B. G. Lee, H. Lee and S. Kim, J. Chem. Soc. Chem. Comm. (1995) 2383.
38. A. Venugopal, K. S. Rama Rao, P. S. Sai Prasad and P. Kanta Rao J. Chem. Soc. Chem. Comm. (1995) 2377.
39. T. Shibanuma, Y. Yamada, T. Yoshimura and H. Momota, Int. Pat. Appl. 9,413,610.
40. H. W. Swiderski, R. Werner and T. Born, Ger. Patent 4,041,771.
41. J. Thompson, G. Webb and J. M. Winfield, Eur. Pat. Appl. 0,439,338.
42. J. D. Scott and M. J. Watson, Int. Pat. Appl. 9,316,798.
43. S. Okazaki and A. Kurosaki, Bull. Chem. Soc. Jpn. 60 (1987) 2833.
44. S. Kurosawa, T. Yamada, A. Sekiya and T. Armura, J. Fluorine Chem. 62 (1993) 69.
45. A. F. Benning and J. D. Park, U. S. Patent 2,407,129.
46. F. J. Christoph Jnr., Ger. Patent 1,903,556.
47. C. Woolf and C. B. Miller, U. S. Patent 2,673,139.
48. M. Vecchio, G. Groppelli and V. Fattore, S. African Patent 6,905,139.

49. M. Vecchio and L. Lodi, U. S. Patent 3,442,962.

50. S. Hub, F. Figuéras and D. Tournigant, Appl. Catal. A 101 (1993) 41.

51. Y. Takita, H. Yamada, M. Hashida and T. Ishihara, Chem. Let. (1990) 715.

52. T. Yamada and Y. Mitsuda, Int. Pat. Appl. 9,407,829.

53. M. Shinsuke, Y. Masaru and T. Shin, Jap. Pat. Appl. 01,319,441.

54. I. Yamagami, H. Ono, Y. Ishimura and H. Nakayama, Jap. Patent 03,163,033.

55. R. W. Johnson, W. C. Moeller, M. van der Puy, M. Kaiser and L. Wang Int. Pat. Appl. 9,505,353.

56. M. Shinsuke, Y. Masaru and T. Shin, Jap. Pat. Appl. 01,319,440.

57. N. Vanlautem, V. Wilmet, J. Pirotton and L. Lerot, Eur. Pat. Appl. 556,893.

58. M. Shinsuke, S. Shunichi, Y. Masaru and T. Shin, Eur. Pat. Appl. 347,830.

59. G. J. Moore and J. O'Kell, Braz. Patent 9,201,323.

60. F. Wöhler and F. Mahla, Ann. Chem. 81 (1852) 255.

61. R. Burwell Jnr., G. L. Haller, K. C. Taylor and J. F. Read, Adv. Catal. 20 (1969) 1.

62. D. R. Coulson, P. W. J. G. Wijnen, J. J. Lerou and L. E. Manzer, J. Catal. 140 (1993) 103.

63. K. Jagannathan, A. Srinivasan and C. N. R. Rao, J. Catal. 69 (1981) 418.

64. A. Zecchina, F. Coluccia, E. Guglielminotti and G. Ghiotti, J. Phys. Chem. 75 (1971) 2774.

65. S. W. Weller and S. E. Voltz, J. Am. Chem. Soc. 76 (1954) 4695.

66. Burwell R. L. Jnr. and C. J. Loner, Proc. 3rd. Int. Cong. Catal. Amsterdam (1964) 804.

67. Burwell R. L. Jnr., A. B. Littlewood, M. Cardrew, G. Pass and C. T. H. Stoddart, J. Am. Chem. Soc. 82 (1960) 6272.

68. S. E. Voltz and S. W. Weller, J. Am. Chem. Soc. 75 (1953) 5227.

69. N. E. Cross and H. F. Leach, J. Catal. 21 (1971) 239.

70. S. R. Dyne, J. B. Butt and G. Haller, J. Catal. 25 (1972) 391.

71. J. Barrault, S. Brunet, B. Requieme and M. Blanchard, J. Chem. Soc. Chem. Comm. (1993) 374.

72. L. Marangoni, C. Gervasutti and L. Conte, J. Fluorine Chem. 19 (1981) 21.

73. J. Kijowski, J. M. Winfield and G. Webb, J. Fluorine Chem. 24 (1984) 133.

74. J. Kijowski, G. Webb and J. M. Winfield, J. Fluorine Chem. 27 (1985) 213.

75. L. Kolditz, V. Nitzsche, G. Heller and S. Stosser, Z. Anorg. Allg. Chem. 23 (1981) 476.

76. M. Blanchard, D. Bechadergue and P. Canesson, Het. Catal. Fine Chem. 41 (1988) 257.

77. D. W. Bonnieface, J. D. Scott and M. J. Watson, Int. Pat. Appl. 9,421,579.

78. J. D. Scott and J. G. Ramsbottom, U. K. Pat. Appl. 2,275,924.

79. J. D. Scott, C. J. Shields and P. N. Ewing, Int. Pat. Appl. 9,516,654.

80. M. V. Felix, W. H. Gumprecht and B. A. Mahler, Int. Pat. Appl. 9,219,576.

81. J. J. Lerou, Eur. Pat. Appl. 403,108.

82. F. Garcia, E. Lacroix, A. Lerch and A. Rousset, Eur. Pat. Appl. 657,409.

83. S. Karmakar and H. L. Greene, J. Catal. 151 (1995) 394.

84. A. Hess, E. Kemnitz, A. Lippitz, W. E. S. Unger and D. H. Menz, J. Catal. 149 (1994) 449.

85. A. Corma, V. Fornes and E. Ortega, 92 (1985) 284.

86. J. Thomson, G. Webb and J. M. Winfield, J. Mol. Catal. 67 (1991) 117.

87. J. Thomson, G. Webb and J. M. Winfield, J. Chem. Soc. Chem. Comm. (1991) 323.

88. J. Thomson, G. Webb, J. M. Winfield, D. Bonnieface, C. Shortman and N. Winterton, Appl. Catal. A: General 97 (1993) 67.

89. I. Mochida and Y. Yoneda, J. Org. Chem. 33 (1968) 2163.

90. F. Janssens, P. Gilbeau and P. Pennetreau, Eur. Pat. Appl. 462,645.

91. I. Sobolev, Eur. Pat. Appl. 259,885.

92. C. Luo, J. Li and S. Wu, Chinese Patent 1,099,375.

93. C. Luo, J. Li and S. Wu, Chinese Patent 1,099,314.

94. D. Carmallo and G. Guglielmo, Eur. Pat. Appl. 282,005.

95. P. Cuzzato and A. Masiero, Eur. Pat. Appl. 408,004.

96. H. S. Tung and A. M. Smith, U. S. Patent 5,155,082.

97. P. Cuzzato and A. Masiero, Eur. Pat. Appl. 408,005.

98. K. Yanagii, S. Yoshikawa and K. Murata, Jap. Patent 02,157,235.

99. Y. Lin and Y. Liang, Chinese Patent 1,075,708.

100. Y. Motohiko and Y. Yukya, Jap. Patent 01,228,925.

101. H. Ohno, M. Miyamura, T. Arai, K. Muramaki and T. Ohi, Eur. Pat. Appl. 582,156.
102. D. R. Corbin and V. N. M. Rao, Int. Pat. Appl. 9,216,481.
103. L. E. Manzer, Eur. Pat. Appl. 331,991.
104. D. R. Corbin and V. N. M. Rao, Int. Pat. Appl. 9,216,479.
105. L. E. Manzer and V. N. M. Rao, U. S. Patent 4,766,260.
106. B. Cheminal, E. Lacroix and A. Lantz, Eur. Pat. Appl. 486,333.
107. K. Tsuji, S. Tomota, M. Hotsuta, T. Nakajo and H. Nakayama, Jap. Patent 06,228,022.
108. K. Tsuji, S. Tomota, N. Sasaki and T. Nakajo, Jap. Patent 06,298,682.
109. K. Tsuji, K. Oshiro and T. Nakajo, Eur. Pat. Appl. 629,440.
110. J. D. Scott and M. J. Watson, Eur. Pat.Appl. 502,605.
111. F. Garcia, E. Lacroix, A. Lerch and A. Rousset, Eur. Pat. Appl. 657,409.
112. B. Cheminal, E. Lacroix and A. Lantz, Eur. Pat. Appl. 456,552.
113. T. Shibananuma, Y. Iwai and S. Koyama, Eur. Pat. Appl. 514,932.
114. T. Sibanuma, T. Kanemura and S. Koyama, Eur. Pat. Appl. 516,000.
115. M. H. Lucy, J. S. Bass and H. S. Tung, Int. Pat. Appl. 9,325,507.
116. F. Fairbrother and J. F. Nixon, J. Chem. Soc. (1958) 3224.
117. C. R. C. Handbook of Chemistry and Physics, 75th Edn. 11-37.
118. C. R. C. Handbook of Chemistry and Physics, 75th Edn. 11-40.
119. L. Rowley, PhD. Thesis, University of Glasgow. 1987.
120. R. N. Maxon, Inor. Synth. 1 (1939) 147.
121. A. J. Vogel, "Textbook of Practical Inorganic Chemistry", Longmans, London. (1962) p.179.
122. R. L. Burwell Jnr., A. B. Littlewood, M. Cardew, G. Pass and C. T. H. Stoddart, J. Am. Chem. Soc. 82 (1960) 6273.
123. D. J. Malcome - Lawes, "Introduction to Radiochemistry", MacMillan Press Ltd. London. (1979).
124. G. Friedlander, J. W. Kennedy, E. S. Macias and J. M. Miller, "Nuclear and Radiochemistry", J. Wiley, New York (1981).
125. A. S. Al - Ammar and G. Webb, J. Chem. Soc. Faraday Trans. 74 (1978) 195.
126. G. A. Kolta, G. Webb and J. M. Winfield, Appl. Catal. 2 (1982) 257.

127. K. A. Brownlee, "Statistical Theory and Methodology in Science and Engineering", J. Wiley, New York. (1960).

128. C. A. Bennet and N. L. Franklin, "Stasticical Analysis in Chemistry", J. Wiley, New York, (1954).

129. E. Breitnberger, "Scintillation Spectrometer Stastistics Progress in Nuclear Physics", Perammon Press, London. (1955).

130. P. W. Atkins, "Physical Chemistry" 4th Edn., Oxford University Press, Oxford. (1992) p. 148.

131. C. Lamonier, A. Bennani, A. D'Huysser, A. Aboukais and G. Wrobel, J. Chem. Soc. Faraday Trans. 92 (1996) 131.

132. P. Landon, unpublished work.

133. S. Brunet, B. Boussand and J. Barrault, Proc. 11th. Int. Cong. Catal. Baltimore (1996) 433.

134. S. Brunet, B. Requieme, E. Matouba, J. Barrault and M. Blanchard, J. Catal. 152 (1995) 70.

135. E. Kemnitz and K. U. Niedersen, J. Fluorine Chem. 79 (1996) 111.

136. E. Kemnitz, A. Kohne, I. Grohmann, A. Lippitz and W. E. S. Unger, J. Catal. 159 (1996) 270.

137. L. Rowley, J. Thomson, G. Webb, J. M. Winfield and A. McCulloch, Appl. Catal. 79 (1991) 89.